

neutron scattering

by

Roger Pynn

Los Alamos
National Laboratory

LECTURE 1: Introduction & Neutron Scattering “Theory”

Overview

1. Introduction and theory of neutron scattering
 1. Advantages/disadvantages of neutrons
 2. Comparison with other structural probes
 3. Elastic scattering and definition of the structure factor, $S(Q)$
 4. Coherent & incoherent scattering
 5. Inelastic scattering
 6. Magnetic scattering
 7. Overview of science studied by neutron scattering
 8. References
2. Neutron scattering facilities and instrumentation
3. Diffraction
4. Reflectometry
5. Small angle neutron scattering
6. Inelastic scattering

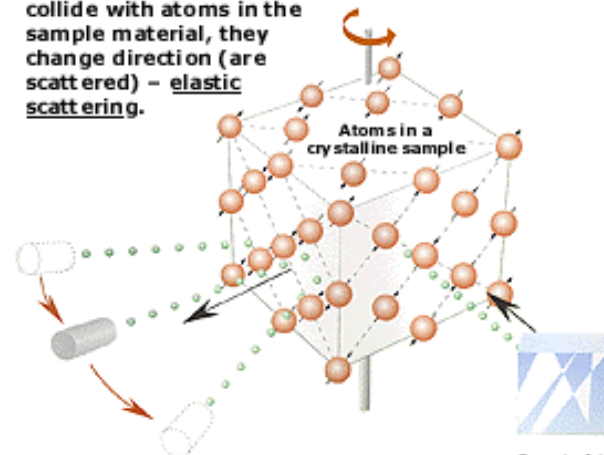
Why do Neutron Scattering?

- To determine the positions and motions of atoms in condensed matter
 - 1994 Nobel Prize to Shull and Brockhouse cited these areas
(see <http://www.nobel.se/physics/educational/poster/1994/neutrons.html>)
- Neutron advantages:
 - Wavelength comparable with interatomic spacings
 - Kinetic energy comparable with that of atoms in a solid
 - Penetrating => bulk properties are measured & sample can be contained
 - Weak interaction with matter aids interpretation of scattering data
 - Isotopic sensitivity allows contrast variation
 - Neutron magnetic moment couples to \mathbf{B} => neutron “sees” unpaired electron spins
- Neutron Disadvantages
 - Neutron sources are weak => low signals, need for large samples etc
 - Some elements (e.g. Cd, B, Gd) absorb strongly
 - Kinematic restrictions (can’t access all energy & momentum transfers)

The 1994 Nobel Prize in Physics – Shull & Brockhouse

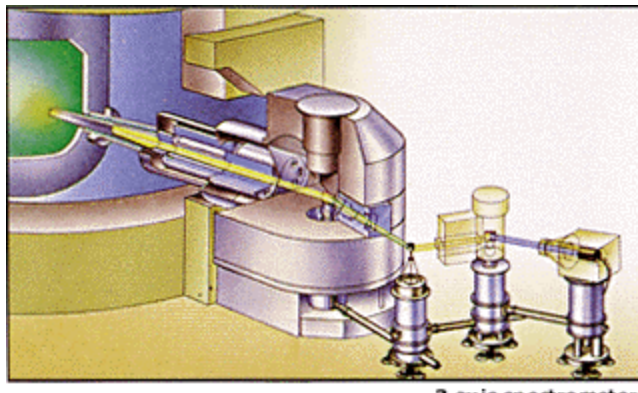
Neutrons show where the atoms are....

When the neutrons collide with atoms in the sample material, they change direction (are scattered) – elastic scattering.



Detectors record the directions of the neutrons and a diffraction pattern is obtained.

The pattern shows the positions of the atoms relative to one another.



Research reactor

Neutron beam

...and what the atoms do.



Crystal that sorts and forwards neutrons of a certain wavelength (energy) – mono-chromatized neutrons

3-axis spectrometer with rotatable crystals and rotatable sample

Atoms in a crystalline sample

When the neutrons penetrate the sample they start or cancel oscillations in the atoms. If the neutrons create phonons or magnons they themselves lose the energy these absorb – inelastic scattering

Changes in the energy of the neutrons are first analysed in an analyser crystal...

...and the neutrons then counted in a detector.

The Neutron has Both Particle-Like and Wave-Like Properties

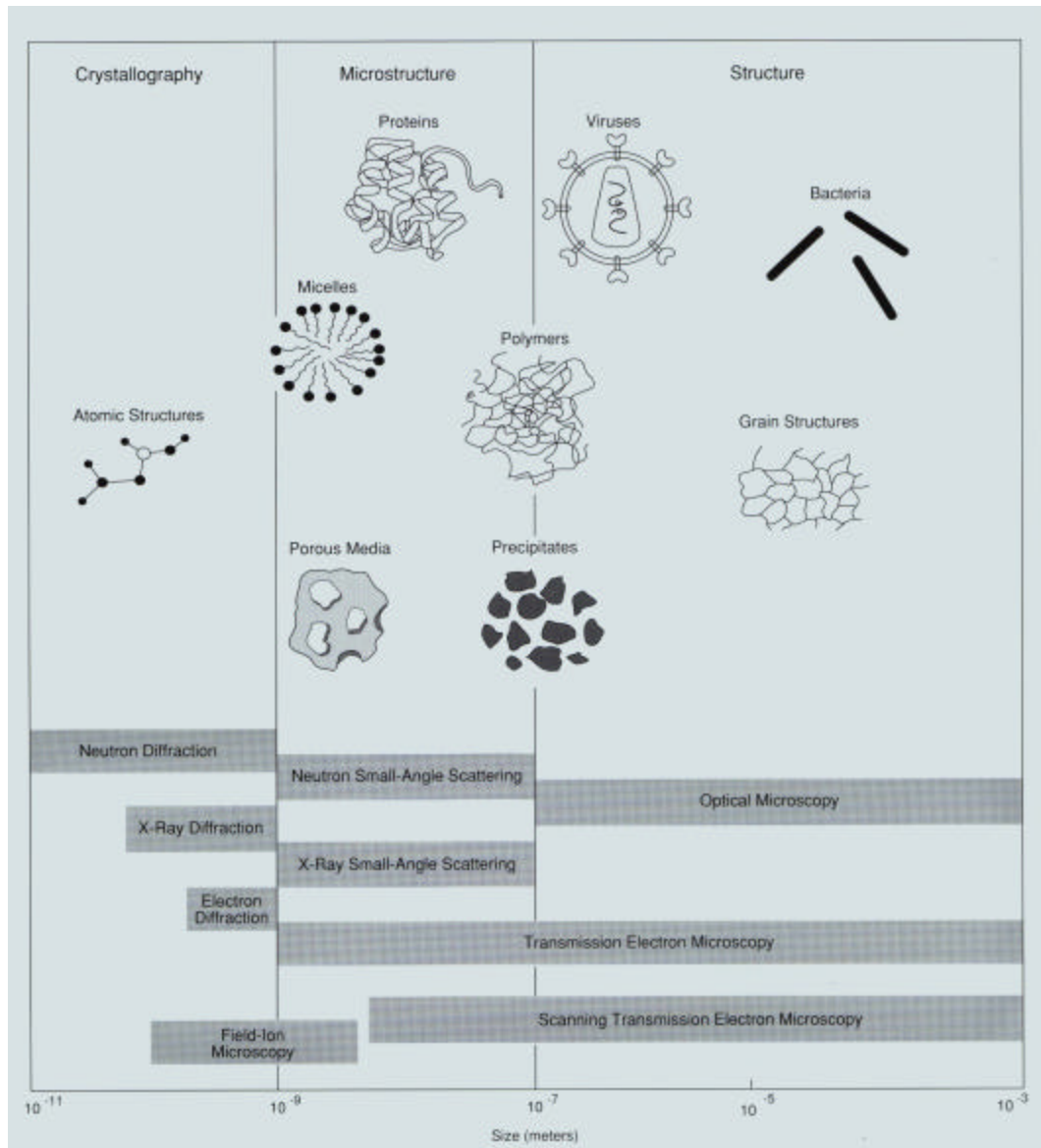
- Mass: $m_n = 1.675 \times 10^{-27} \text{ kg}$
- Charge = 0; Spin = $\frac{1}{2}$
- Magnetic dipole moment: $\mu_n = -1.913 \mu_N$
- Nuclear magneton: $\mu_N = eh/4\pi m_p = 5.051 \times 10^{-27} \text{ J T}^{-1}$
- Velocity (v), kinetic energy (E), wavevector (k), wavelength (λ), temperature (T).
- $E = m_n v^2/2 = k_B T = (h k / 2\pi)^2 / 2m_n$; $k = 2\pi/\lambda = m_n v / (h/2\pi)$

	<u>Energy (meV)</u>	<u>Temp (K)</u>	<u>Wavelength (nm)</u>
Cold	0.1 – 10	1 – 120	0.4 – 3
Thermal	5 – 100	60 – 1000	0.1 – 0.4
Hot	100 – 500	1000 – 6000	0.04 – 0.1

$$\lambda \text{ (nm)} = 395.6 / v \text{ (m/s)}$$

$$E \text{ (meV)} = 0.02072 k^2 \text{ (k in nm}^{-1}\text{)}$$

Comparison of Structural Probes



Note that scattering methods provide statistically averaged information on structure rather than real-space pictures of particular instances

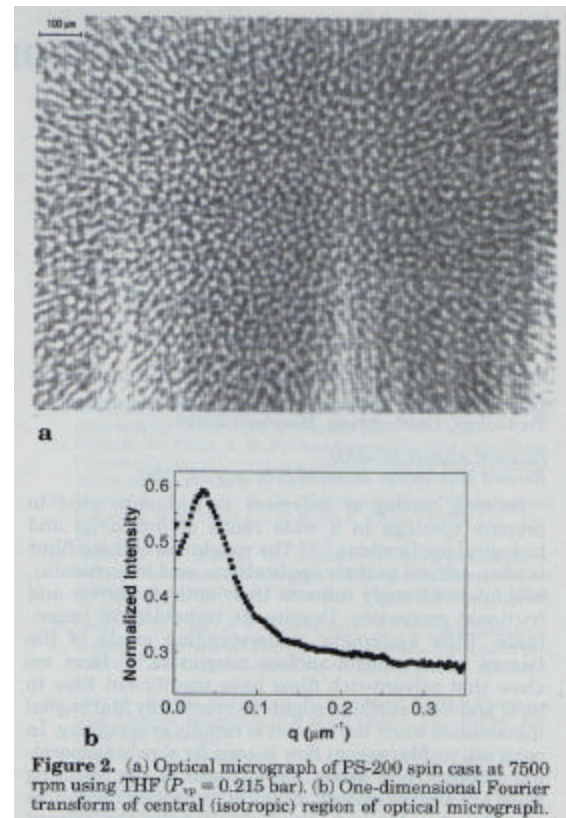
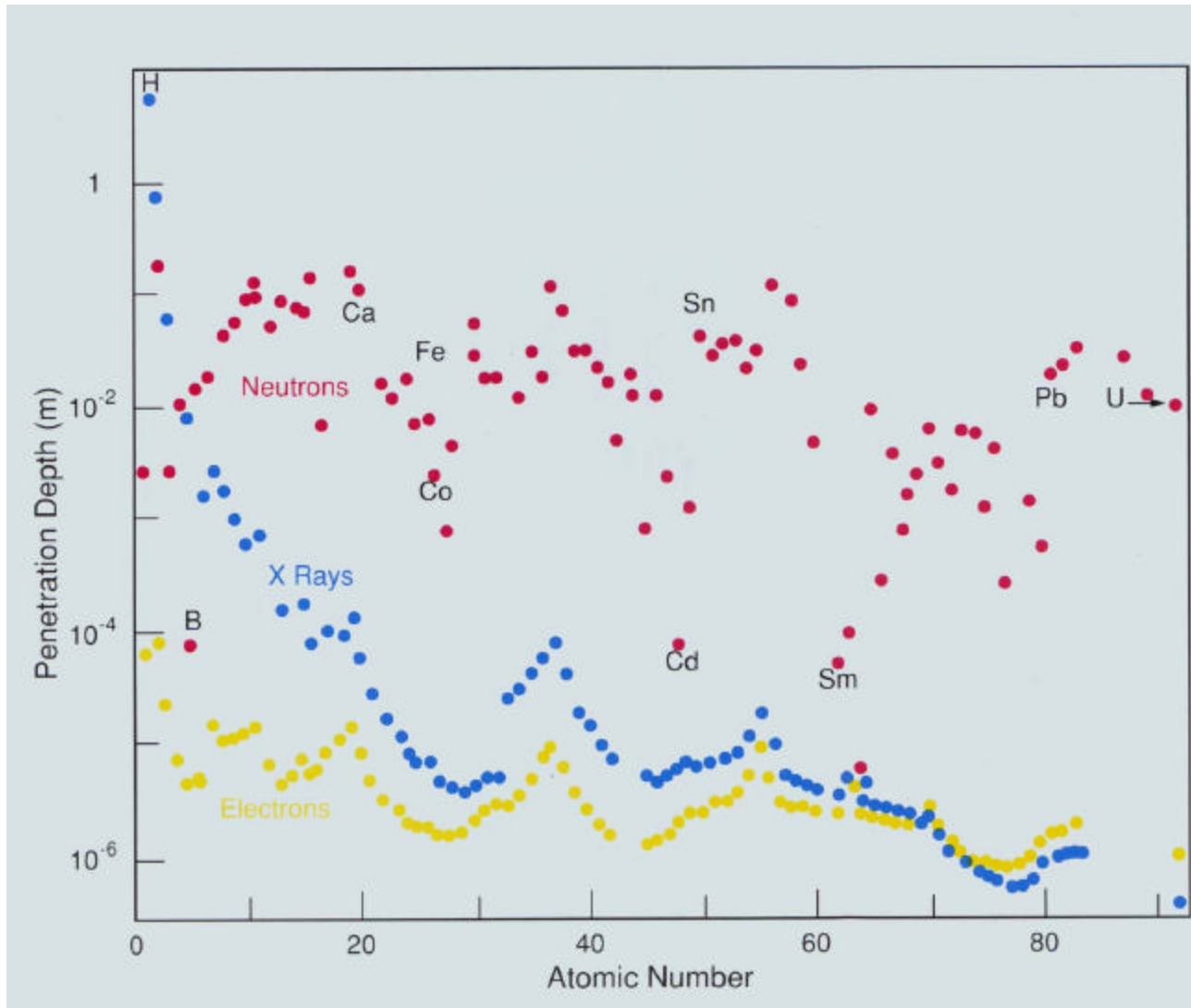


Figure 2. (a) Optical micrograph of PS-200 spin cast at 7500 rpm using THF ($P_{vp} = 0.215$ bar). (b) One-dimensional Fourier transform of central (isotropic) region of optical micrograph.

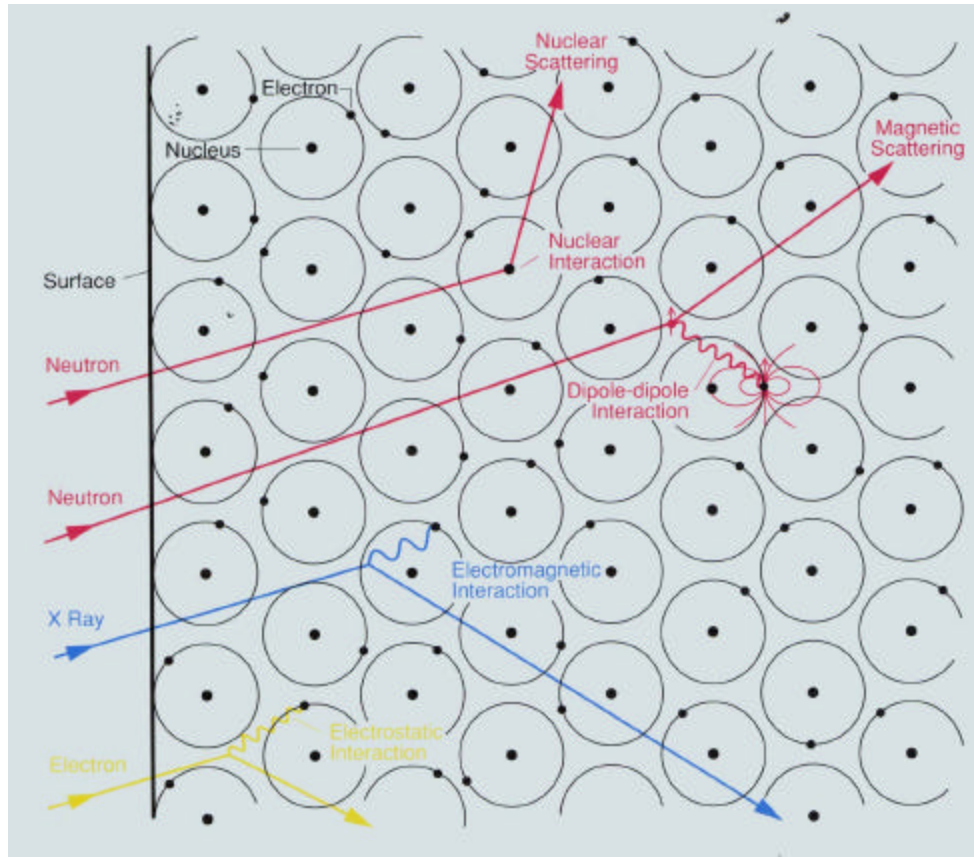
Thermal Neutrons, 8 keV X-Rays & Low Energy Electrons:- Absorption by Matter



Note for neutrons:

- H/D difference
- Cd, B, Sm
- no systematic A dependence

Interaction Mechanisms

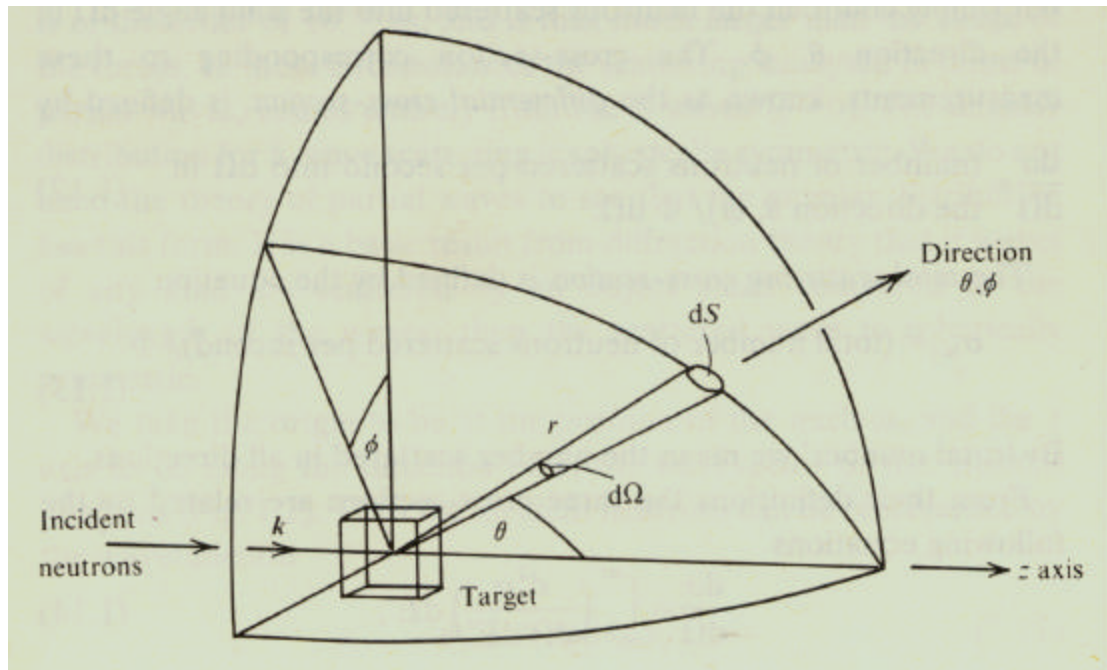


- Neutrons interact with atomic nuclei via very short range (\sim fm) forces.
- Neutrons also interact with unpaired electrons via a magnetic dipole interaction.

Brightness & Fluxes for Neutron & X-Ray Sources

	<i>Brightness</i> ($s^{-1} m^{-2} ster^{-1}$)	dE/E (%)	<i>Divergence</i> (mrad 2)	<i>Flux</i> ($s^{-1} m^{-2}$)
Neutrons	10^{15}	2	10×10	10^{11}
Rotating Anode	10^{16}	3	0.5×10	5×10^{10}
Bending Magnet	10^{24}	0.01	0.1×5	5×10^{17}
Wiggler	10^{26}	0.01	0.1×1	10^{19}
Undulator (APS)	10^{33}	0.01	0.01×0.1	10^{24}

Cross Sections

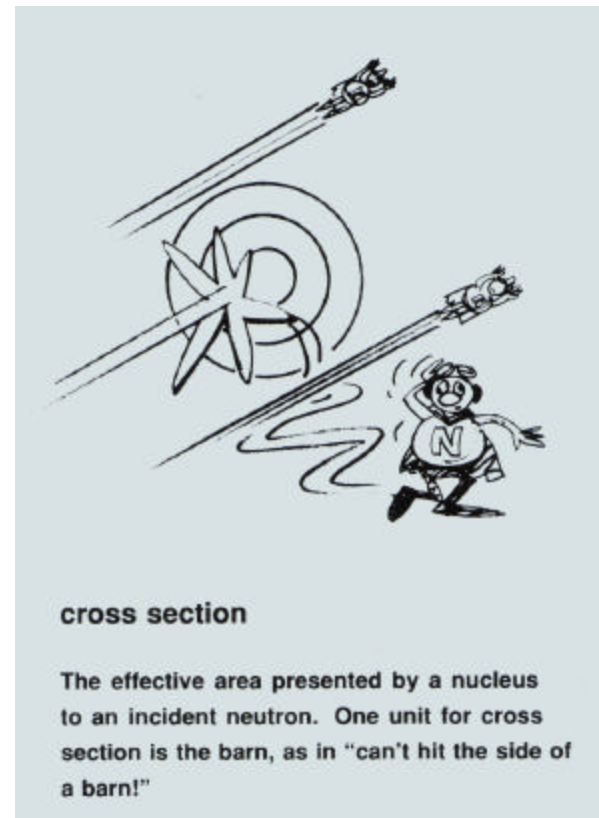


Φ = number of incident neutrons per cm^2 per second

s = total number of neutrons scattered per second / Φ

$$\frac{ds}{d\Omega} = \frac{\text{number of neutrons scattered per second into } d\Omega}{\Phi d\Omega}$$

$$\frac{d^2s}{d\Omega dE} = \frac{\text{number of neutrons scattered per second into } d\Omega \text{ & } dE}{\Phi d\Omega dE}$$



σ measured in barns:

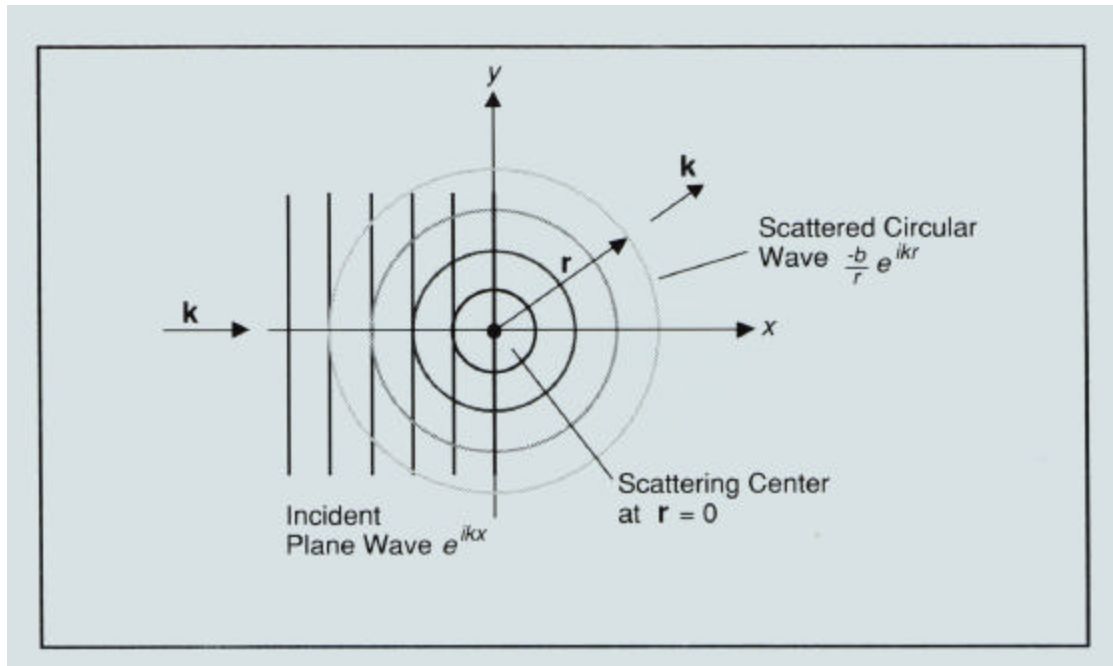
$$1 \text{ barn} = 10^{-24} \text{ cm}^2$$

$$\text{Attenuation} = \exp(-N\sigma t)$$

N = # of atoms/unit volume

t = thickness

Scattering by a Single (fixed) Nucleus



- range of nuclear force ($\sim 1\text{fm}$) is \ll neutron wavelength so scattering is “point-like”
- energy of neutron is too small to change energy of nucleus & neutron cannot transfer KE to a fixed nucleus \Rightarrow scattering is elastic
- we consider only scattering far from nuclear resonances where neutron absorption is negligible

If v is the velocity of the neutron (same before and after scattering), the number of neutrons passing through an area dS per second after scattering is :

$$v dS |\mathbf{y}_{\text{scat}}|^2 = v dS b^2/r^2 = v b^2 d\Omega$$

Since the number of incident neutrons passing through unit area is : $\Phi = v |\mathbf{y}_{\text{incident}}|^2 = v$

$$\frac{dS}{d\Omega} = \frac{v b^2 d\Omega}{\Phi d\Omega} = b^2 \quad \text{so } S_{\text{total}} = 4pb^2$$

Adding up Neutrons Scattered by Many Nuclei

At a nucleus located at \vec{R}_i the incident wave is $e^{i\vec{k}_0 \cdot \vec{R}_i}$

so the scattered wave is $\mathbf{y}_{\text{scat}} = \sum e^{i\vec{k}_0 \cdot \vec{R}_i} \left[\frac{-\mathbf{b}_i}{|\vec{\mathbf{r}} - \vec{\mathbf{R}}_i|} e^{i\vec{k}' \cdot (\vec{\mathbf{r}} - \vec{\mathbf{R}}_i)} \right]$

$$\therefore \frac{d\mathbf{S}}{d\Omega} = \frac{vdS|\mathbf{y}_{\text{scat}}|^2}{vd\Omega} = \frac{dS}{d\Omega} \left| b_i e^{i\vec{k}' \cdot \vec{r}} \sum \frac{1}{|\vec{\mathbf{r}} - \vec{\mathbf{R}}_i|} e^{i(\vec{k}_0 - \vec{k}') \cdot \vec{R}_i} \right|^2$$

If we measure far enough away so that $r \gg R_i$ we can use $d\Omega = dS/r^2$ to get

$$\frac{d\mathbf{S}}{d\Omega} = \sum_{i,j} b_i b_j e^{i(\vec{k}_0 - \vec{k}') \cdot (\vec{R}_i - \vec{R}_j)} = \sum_{i,j} b_i b_j e^{-i\vec{Q} \cdot (\vec{R}_i - \vec{R}_j)}$$

where the wavevector transfer \mathbf{Q} is defined by $\vec{Q} = \vec{k}' - \vec{k}_0$

Coherent and Incoherent Scattering

The scattering length, b_i , depends on the nuclear isotope, spin relative to the neutron & nuclear eigenstate. For a single nucleus:

$$b_i = \langle b \rangle + \mathbf{d}b_i \quad \text{where } \mathbf{d}b \text{ averages to zero}$$

$$b_i b_j = \langle b \rangle^2 + \langle b \rangle (\mathbf{d}b_i + \mathbf{d}b_j) + \mathbf{d}b_i \mathbf{d}b_j$$

but $\langle \mathbf{d}b \rangle = 0$ and $\langle \mathbf{d}b_i \mathbf{d}b_j \rangle$ vanishes unless $i = j$

$$\langle \mathbf{d}b_i^2 \rangle = \langle b_i - \langle b \rangle \rangle^2 = \langle b^2 \rangle - \langle b \rangle^2$$

$$\therefore \frac{d\mathbf{S}}{d\Omega} = \langle b \rangle^2 \sum_{i,j} e^{-i\vec{Q} \cdot (\vec{R}_i - \vec{R}_j)} + (\langle b^2 \rangle - \langle b \rangle^2) N$$


Coherent Scattering

(scattering depends on the direction of \mathbf{Q})

Incoherent Scattering

(scattering is uniform in all directions)

Note: N = number of atoms in scattering system

Values of σ_{coh} and σ_{inc}

Nuclide	S_{coh}	S_{inc}	Nuclide	S_{coh}	S_{inc}
1H	1.8	80.2	V	0.02	5.0
2H	5.6	2.0	Fe	11.5	0.4
C	5.6	0.0	Co	1.0	5.2
O	4.2	0.0	Cu	7.5	0.5
Al	1.5	0.0	^{36}Ar	24.9	0.0

- Difference between H and D used in experiments with soft matter (contrast variation)
- Al used for windows
- V used for sample containers in diffraction experiments and as calibration for energy resolution
- Fe and Co have nuclear cross sections similar to the values of their magnetic cross sections
- Find scattering cross sections at the NIST web site at:
<http://webster.ncnr.nist.gov/resources/n-lengths/>

Coherent Elastic Scattering measures the Structure Factor S(Q) i.e. correlations of atomic positions

$$\frac{d\mathbf{s}}{d\Omega} = \langle b \rangle^2 N \cdot S(\vec{Q}) \quad \text{for an assembly of similar atoms where } S(\vec{Q}) = \frac{1}{N} \left\langle \sum_{i,j} e^{-i\vec{Q} \cdot (\vec{R}_i - \vec{R}_j)} \right\rangle_{\text{ensemble}}$$

Now $\sum_i e^{-i\vec{Q} \cdot \vec{R}_i} = \int d\vec{r} \cdot e^{-i\vec{Q} \cdot \vec{r}} \sum_i \mathbf{d}(\vec{r} - \vec{R}_i) = \int d\vec{r} \cdot e^{-i\vec{Q} \cdot \vec{r}} \mathbf{r}_N(\vec{r})$ where \mathbf{r}_N is the nuclear number density

so

$$S(\vec{Q}) = \frac{1}{N} \left\langle \left| \int d\vec{r} \cdot e^{-i\vec{Q} \cdot \vec{r}} \mathbf{r}_N(\vec{r}) \right|^2 \right\rangle$$

$$\text{or } S(\vec{Q}) = \frac{1}{N} \int d\vec{r}' \int d\vec{r} \cdot e^{-i\vec{Q} \cdot (\vec{r} - \vec{r}')} \langle \mathbf{r}_N(\vec{r}) \mathbf{r}_N(\vec{r}') \rangle = \frac{1}{N} \int d\vec{R} \int d\vec{r} e^{-i\vec{Q} \cdot \vec{R}} \langle \mathbf{r}_N(\vec{r}) \mathbf{r}_N(\vec{r} - \vec{R}) \rangle$$

ie

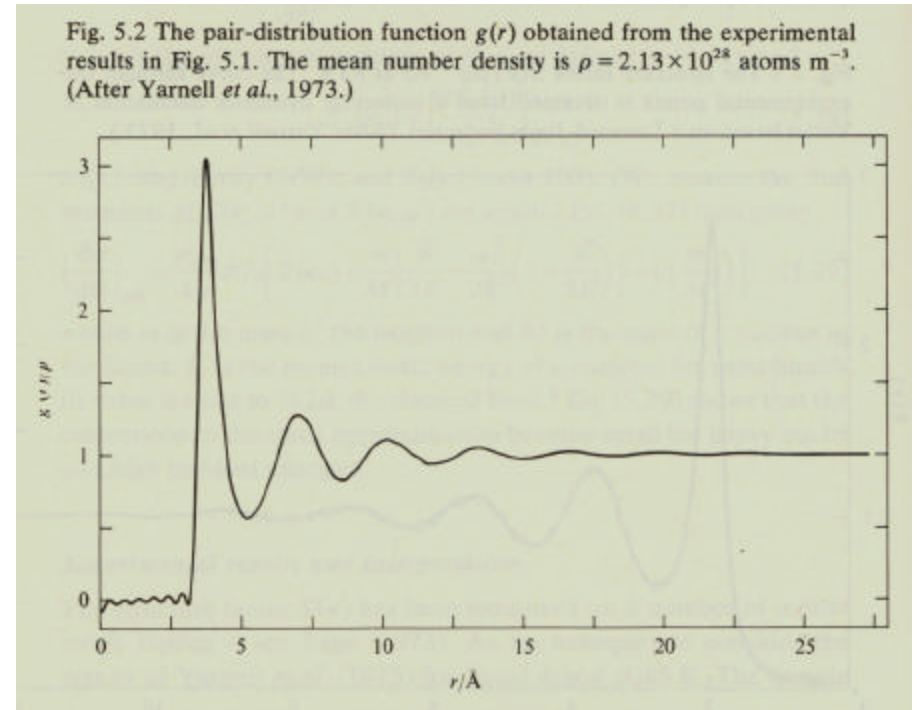
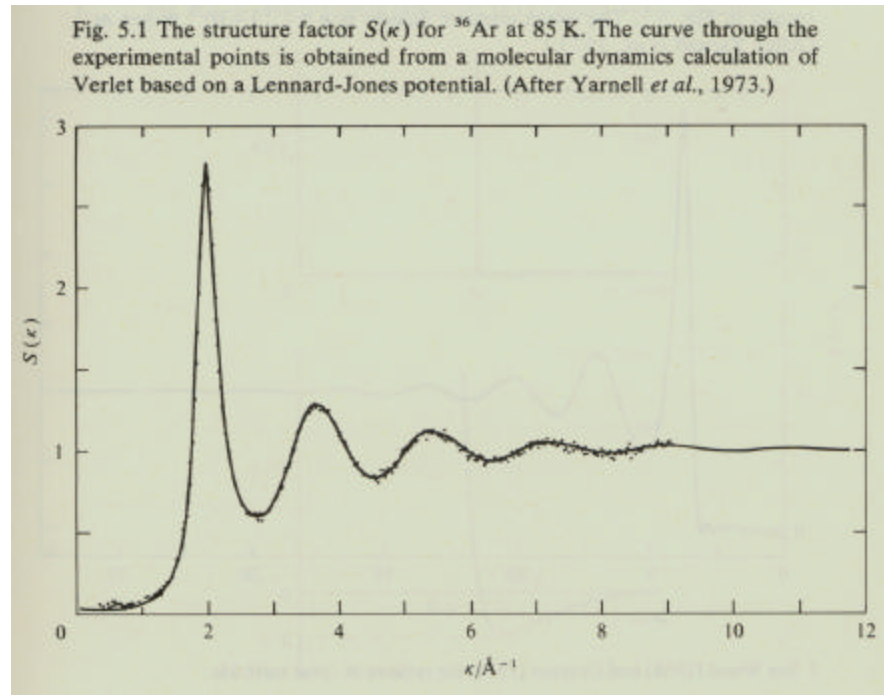
$$S(\vec{Q}) = 1 + \int d\vec{R} \cdot g(\vec{R}) \cdot e^{-i\vec{Q} \cdot \vec{R}}$$

where $g(\vec{R}) = \sum_{i \neq 0} \langle \mathbf{d}(\vec{R} - \vec{R}_i + \vec{R}_0) \rangle$ is a function of \vec{R} only.

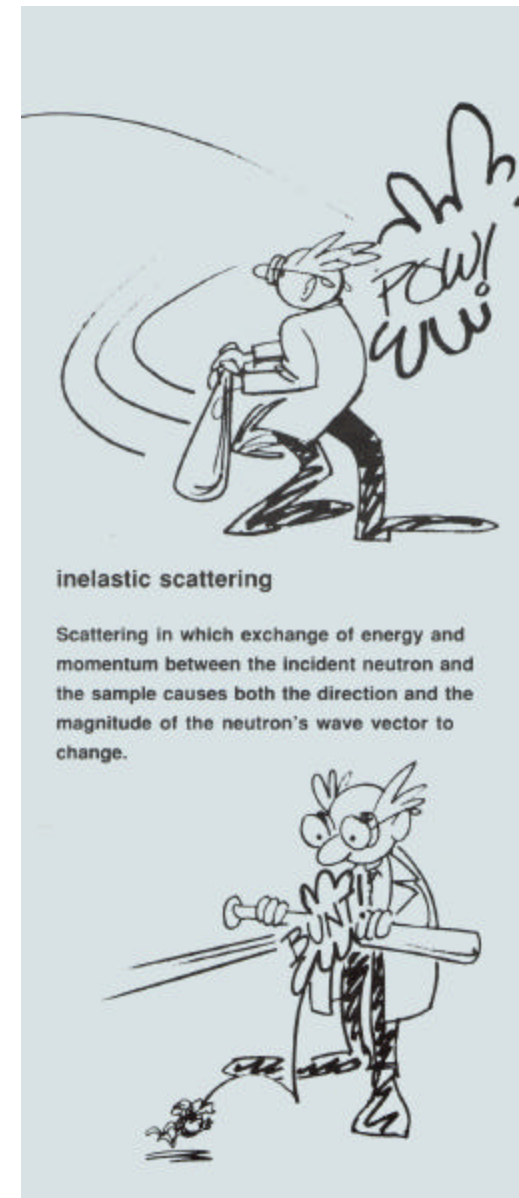
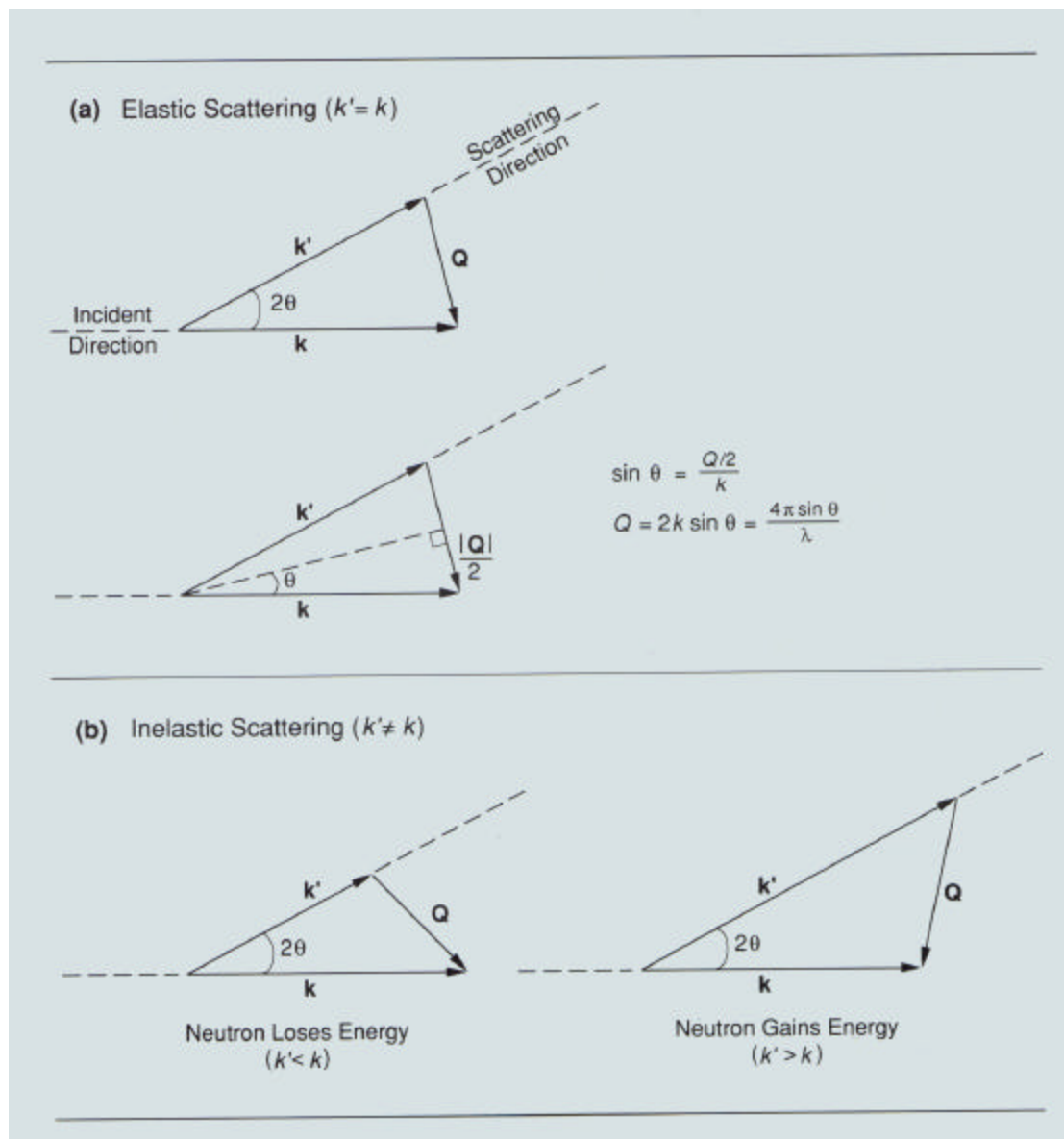
$g(\vec{R})$ is known as the **static pair correlation function**. It gives the probability that there is an atom, i , at distance R from the origin of a coordinate system at time t , given that there is also a (different) atom at the origin of the coordinate system

$S(Q)$ and $g(r)$ for Simple Liquids

- Note that $S(Q)$ and $g(r)/\rho$ both tend to unity at large values of their arguments
- The peaks in $g(r)$ represent atoms in “coordination shells”
- $g(r)$ is expected to be zero for $r <$ particle diameter – ripples are truncation errors from Fourier transform of $S(Q)$



Neutrons can also gain or lose energy in the scattering process: this is called inelastic scattering



Inelastic neutron scattering measures atomic motions

The concept of a pair correlation function can be generalized:

$G(r,t)$ = probability of finding a nucleus at (r,t) given that there is one at $r=0$ at $t=0$

$G_s(r,t)$ = probability of finding a nucleus at (r,t) if the *same* nucleus was at $r=0$ at $t=0$

Then one finds:

$$\left(\frac{d^2\mathbf{S}}{d\Omega.dE} \right)_{coh} = b_{coh}^2 \frac{k'}{k} NS(\vec{Q}, \mathbf{w})$$

$$\left(\frac{d^2\mathbf{S}}{d\Omega.dE} \right)_{inc} = b_{inc}^2 \frac{k'}{k} NS_i(\vec{Q}, \mathbf{w})$$

$(h/2\pi)\mathbf{Q}$ & $(h/2\pi)\omega$ are the momentum & energy transferred to the neutron during the scattering process

where

$$S(\vec{Q}, \mathbf{w}) = \frac{1}{2p\hbar} \iint G(\vec{r}, t) e^{i(\vec{Q} \cdot \vec{r} - \mathbf{w}t)} d\vec{r} dt \text{ and } S_i(\vec{Q}, \mathbf{w}) = \frac{1}{2p\hbar} \iint G_s(\vec{r}, t) e^{i(\vec{Q} \cdot \vec{r} - \mathbf{w}t)} d\vec{r} dt$$

Inelastic coherent scattering measures *correlated* motions of atoms

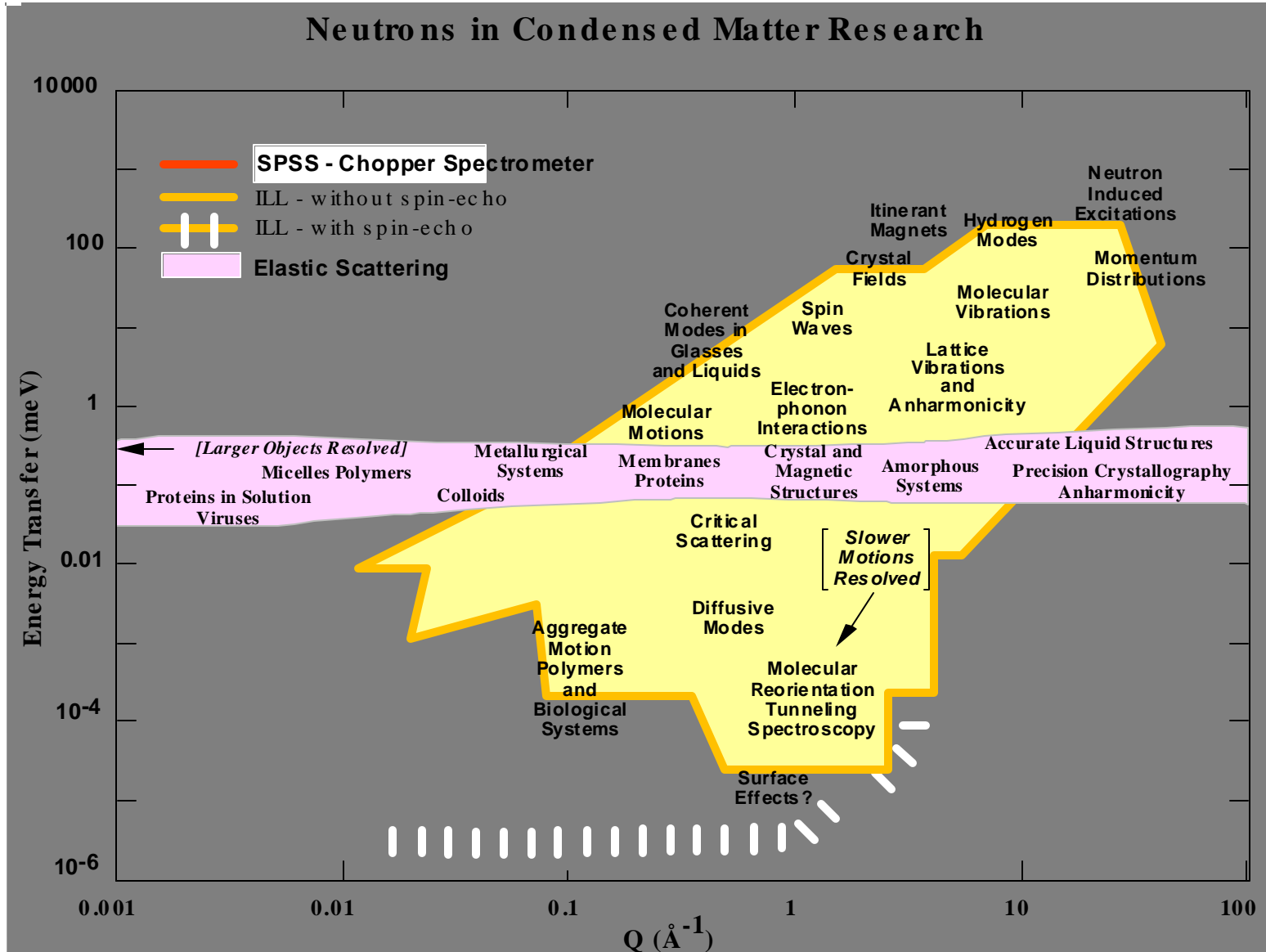
Inelastic incoherent scattering measures *self-correlations* e.g. diffusion

Magnetic Scattering

- The magnetic moment of the neutron interacts with B fields caused, for example, by unpaired electron spins in a material
 - Both spin and orbital angular momentum of electrons contribute to B
 - Expressions for cross sections are more complex than for nuclear scattering
 - Magnetic interactions are long range and non-central
 - Nuclear and magnetic scattering have similar magnitudes
 - Magnetic scattering involves a form factor – FT of electron spatial distribution
 - Electrons are distributed in space over distances comparable to neutron wavelength
 - Elastic magnetic scattering of neutrons can be used to probe electron distributions
 - Magnetic scattering depends *only* on component of B perpendicular to Q
 - For neutrons spin polarized along a direction z (defined by applied H field):
 - Correlations involving B_z do not cause neutron spin flip
 - Correlations involving B_x or B_y cause neutron spin flip
 - Coherent & incoherent nuclear scattering affects spin polarized neutrons
 - Coherent nuclear scattering is non-spin-flip
 - Nuclear spin-incoherent nuclear scattering is 2/3 spin-flip
 - Isotopic incoherent scattering is non-spin-flip

Magnetic Neutron Scattering is a Powerful Tool

- In early work Shull and his collaborators:
 - Provided the first direct evidence of antiferromagnetic ordering
 - Confirmed the Neel model of ferrimagnetism in magnetite (Fe_3O_4)
 - Obtained the first magnetic form factor (spatial distribution of magnetic electrons) by measuring paramagnetic scattering in Mn compounds
 - Produced polarized neutrons by Bragg reflection (where nuclear and magnetic scattering scattering cancelled for one neutron spin state)
 - Determined the distribution of magnetic moments in 3d alloys by measuring diffuse magnetic scattering
 - Measured the magnetic critical scattering at the Curie point in Fe
- More recent work using polarized neutrons has:
 - Discriminated between longitudinal & transverse magnetic fluctuations
 - Provided evidence of magnetic solitons in 1-d magnets
 - Quantified electron spin fluctuations in correlated-electron materials
 - Provided the basis for measuring slow dynamics using the neutron spin-echo technique....etc



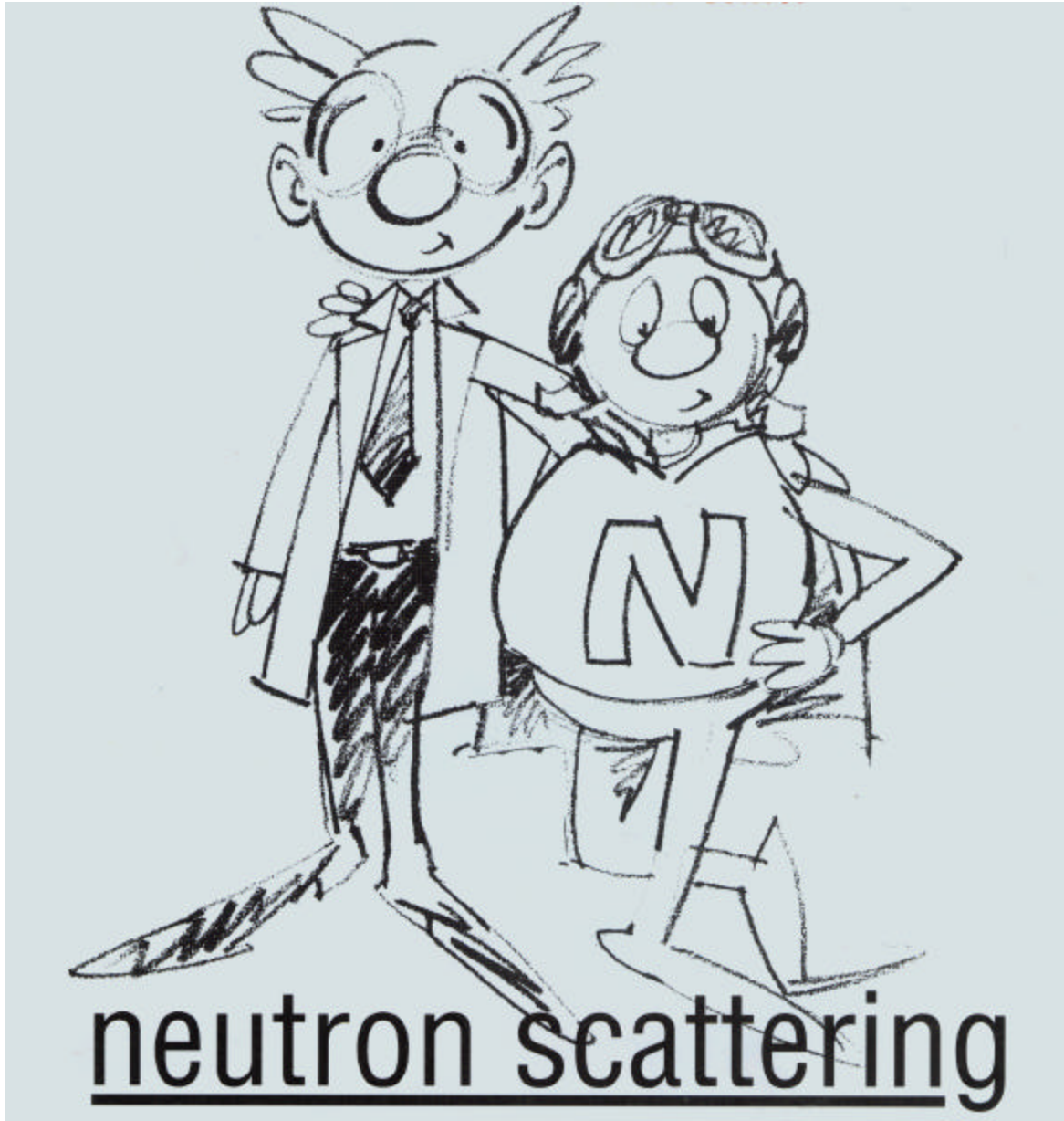
Neutron scattering experiments measure the number of neutrons scattered at different values of the wavevector and energy transferred to the neutron, denoted Q and E . The phenomena probed depend on the values of Q and E accessed.

Next Lecture

2. Neutron Scattering Instrumentation and Facilities – how is neutron scattering measured?
 1. Sources of neutrons for scattering – reactors & spallation sources
 1. Neutron spectra
 2. Monochromatic-beam and time-of-flight methods
 2. Instrument components
 1. Crystal monochromators and analysers
 2. Neutron guides
 3. Neutron detectors
 4. Neutron spin manipulation
 5. Choppers
 6. etc
 3. A zoo of specialized neutron spectrometers

References

- Introduction to the Theory of Thermal Neutron Scattering
by G. L. Squires
Reprint edition (February 1997)
Dover Publications
ISBN 048669447
- Neutron Scattering: A Primer
by Roger Pynn
Los Alamos Science (1990)
(see www.mrl.ucsb.edu/~pynn)



neutron scattering

by

Roger Pynn

Los Alamos
National Laboratory

LECTURE 2: Neutron Scattering Instrumentation & Facilities

Overview

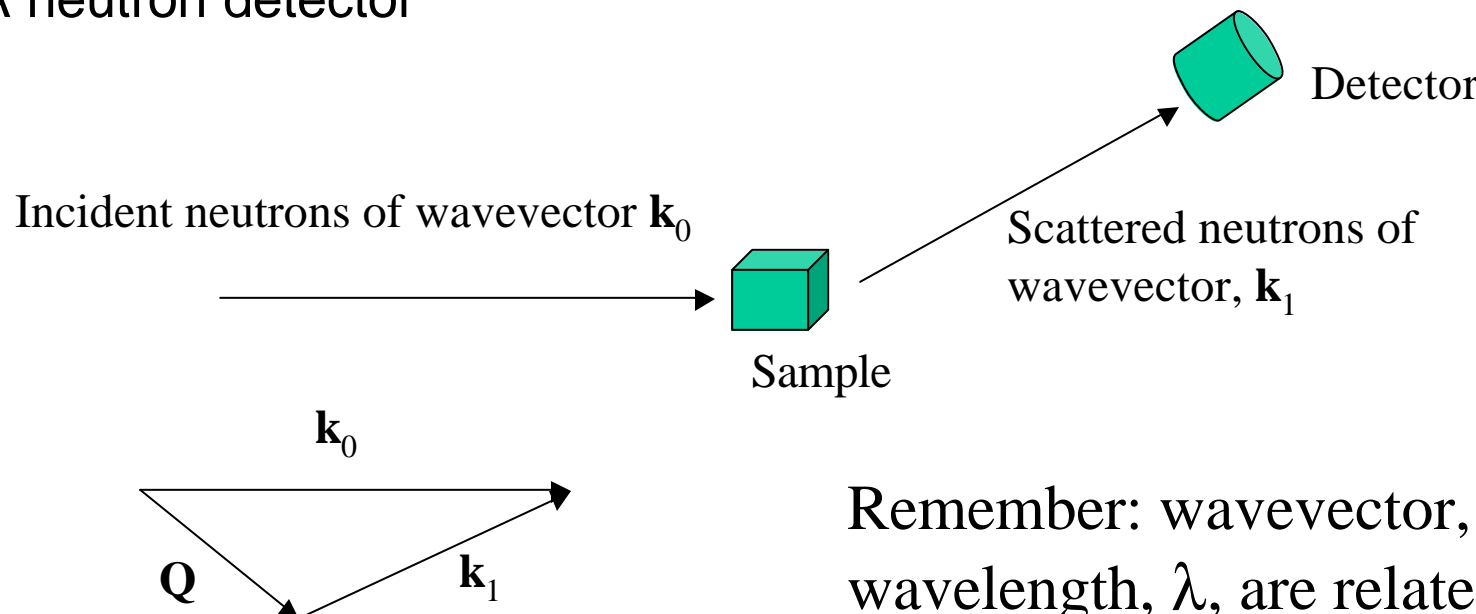
1. Essential messages from Lecture #1
2. Neutron Scattering Instrumentation and Facilities – how is neutron scattering measured?
 1. Sources of neutrons for scattering – reactors & spallation sources
 1. Neutron spectra
 2. Monochromatic-beam and time-of-flight methods
 2. Instrument components
 3. A “zoo” of specialized neutron spectrometers

Recapitulation of Key Messages From Lecture #1

- Neutron scattering experiments measure the number of neutrons scattered by a sample as a function of the wavevector change (Q) and the energy change (E) of the neutron
- Expressions for the scattered neutron intensity involve the positions and motions of atomic nuclei or unpaired electron spins in the scattering sample
- The scattered neutron intensity as a function of Q and E is proportional to the space and time Fourier Transform of the probability of finding two atoms separated by a particular distance at a particular time
- Sometimes the change in the spin state of the neutron during scattering is also measured to give information about the locations and orientations of unpaired electron spins in the sample

What Do We Need to Do a Basic Neutron Scattering Experiment?

- A source of neutrons
- A method to prescribe the wavevector of the neutrons incident on the sample
- (An interesting sample)
- A method to determine the wavevector of the scattered neutrons
 - Not needed for elastic scattering
- A neutron detector

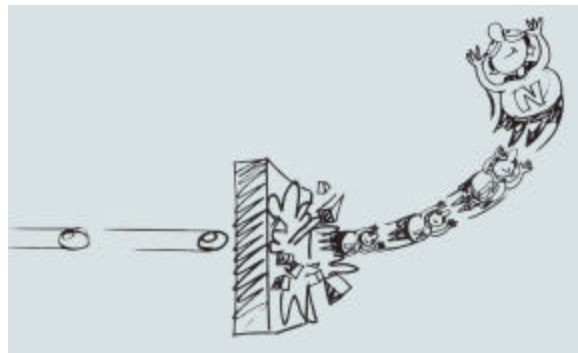


Remember: wavevector, k , & wavelength, λ , are related by:
$$k = m_n v / (h/2\pi) = 2\pi/\lambda$$

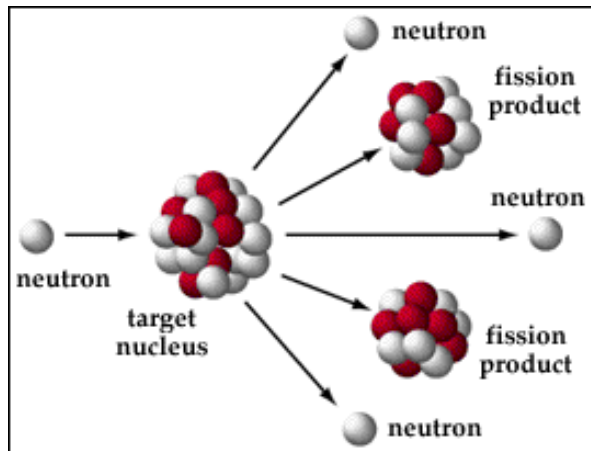
Neutron Scattering Requires Intense Sources of Neutrons

- Neutrons for scattering experiments can be produced either by nuclear fission in a reactor or by spallation when high-energy protons strike a heavy metal target (W, Ta, or U).
 - In general, reactors produce continuous neutron beams and spallation sources produce beams that are pulsed between 20 Hz and 60 Hz
 - The energy spectra of neutrons produced by reactors and spallation sources are different, with spallation sources producing more high-energy neutrons
 - Neutron spectra for scattering experiments are tailored by moderators – solids or liquids maintained at a particular temperature – although neutrons are not in thermal equilibrium with moderators at a short-pulse spallation sources
- Both reactors and spallation sources are expensive to build and require sophisticated operation.
 - SNS at ORNL will cost about \$1.5B to construct & ~\$140M per year to operate
- Either type of source can provide neutrons for 30-50 neutron spectrometers
 - Small science at large facilities

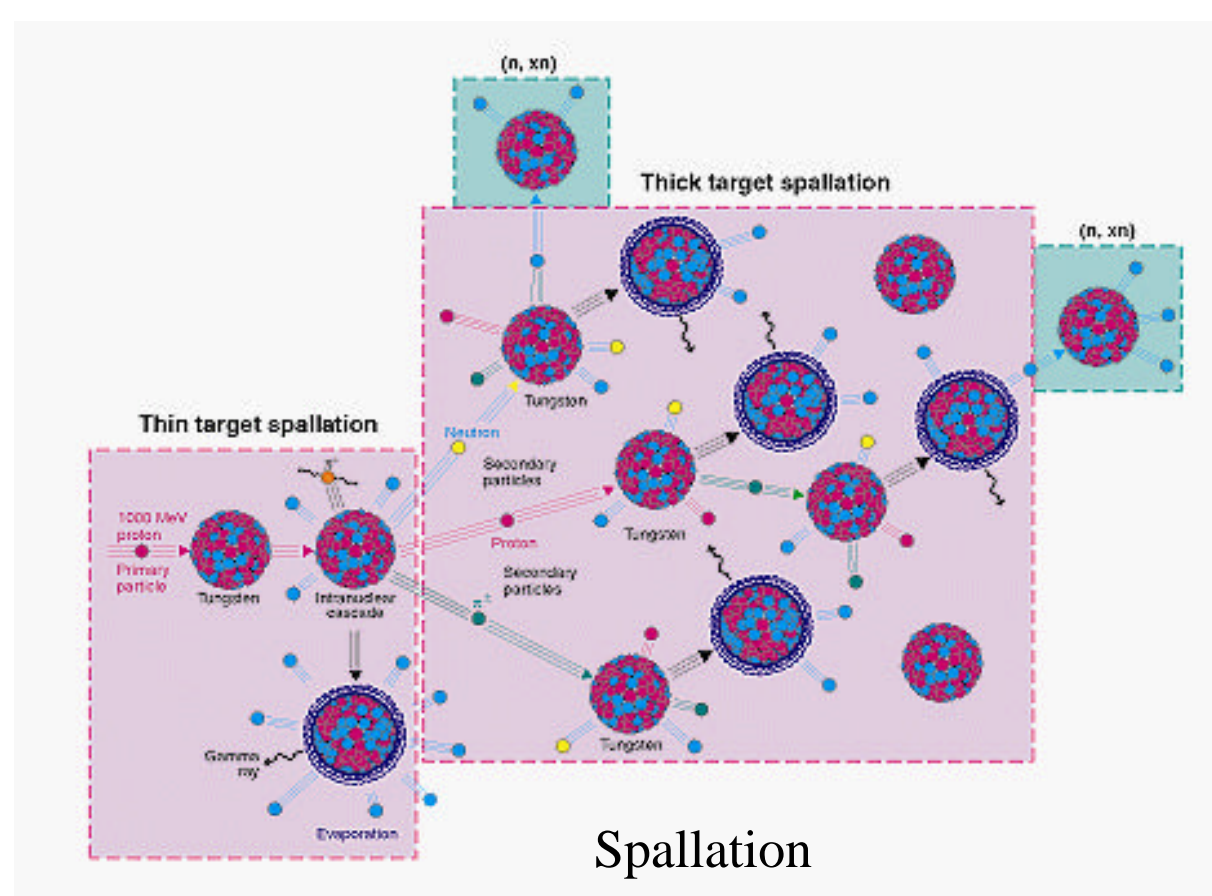
About 1.5 Useful Neutrons Are Produced by Each Fission Event in a Nuclear Reactor Whereas About 25 Neutrons Are Produced by spallation for Each 1-GeV Proton Incident on a Tungsten Target



Artist's view of spallation



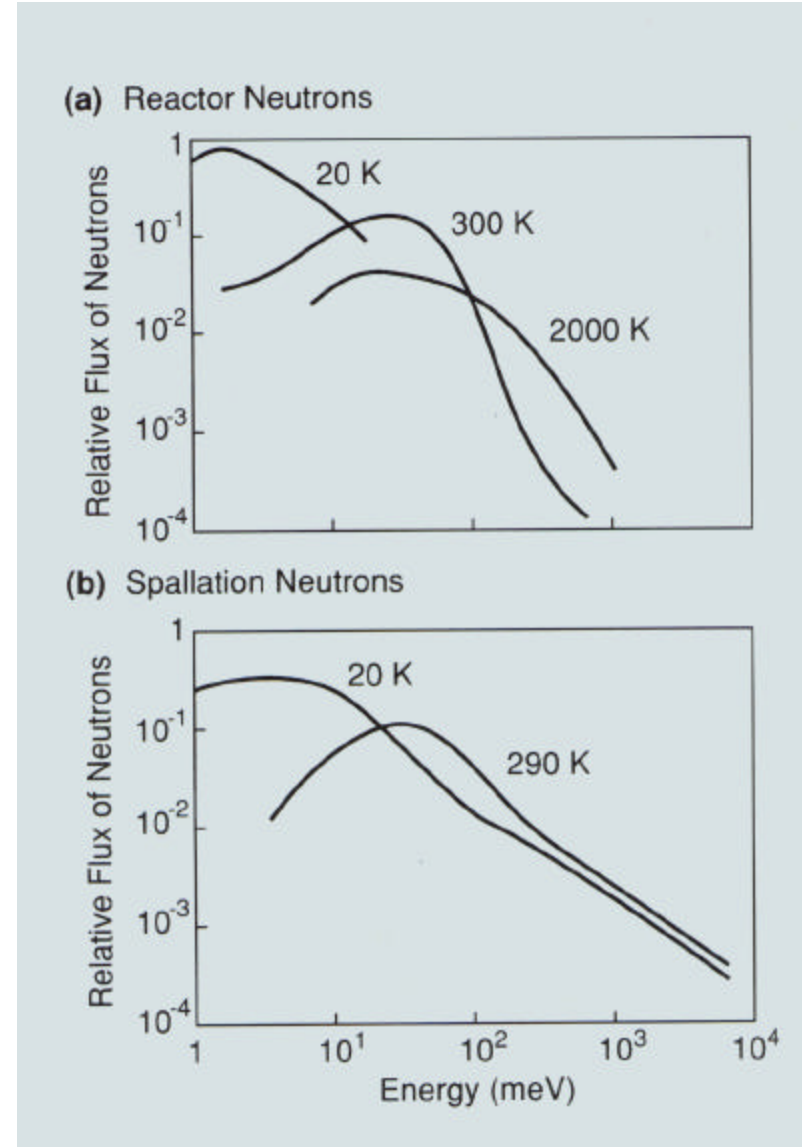
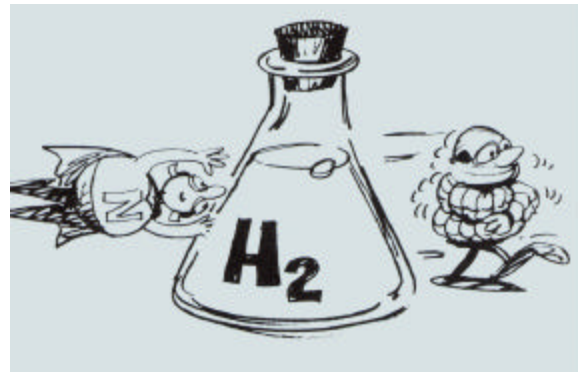
Nuclear Fission



Spallation

Neutrons From Reactors and Spallation Sources Must Be Moderated Before Being Used for Scattering Experiments

- Reactor spectra are Maxwellian
- Intensity and peak-width $\sim 1/(E)^{1/2}$ at high neutron energies at spallation sources
- Cold sources are usually liquid hydrogen (though deuterium is also used at reactors & methane is sometimes used at spallation sources)
- Hot source at ILL (only one in the world) is graphite, radiation heated.



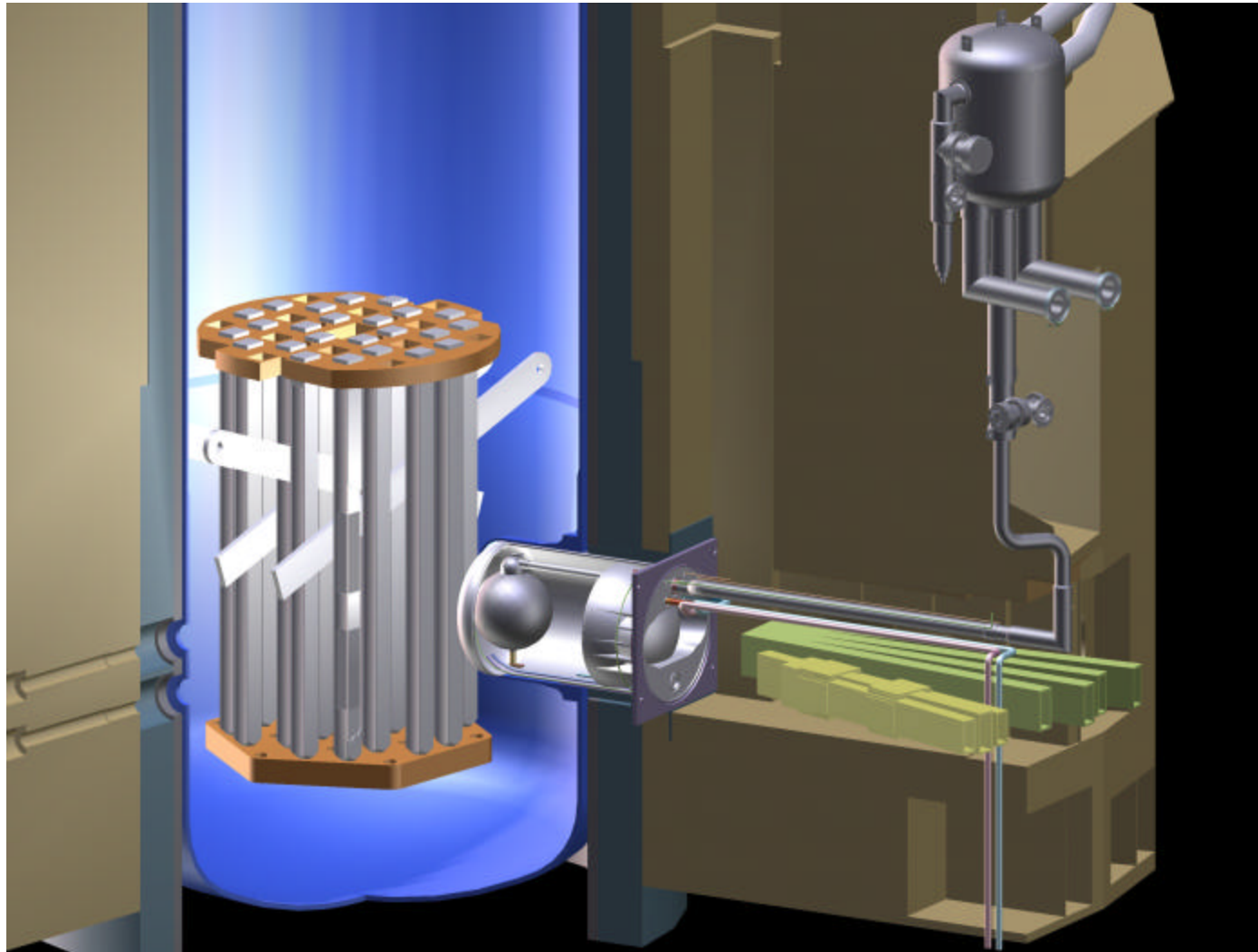
The ESRF* & ILL* With Grenoble & the Beldonne Mountains



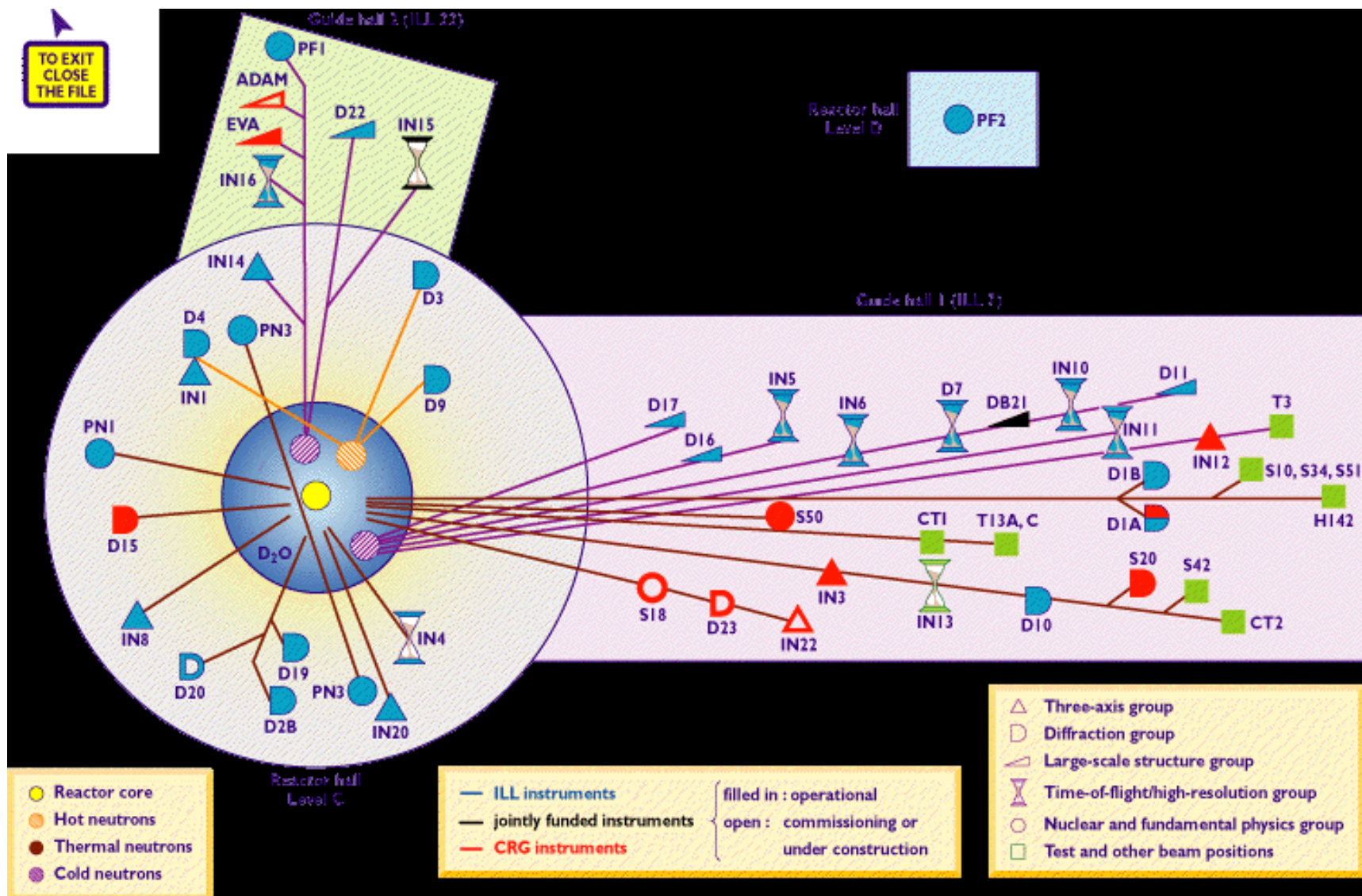
Photo ESRF/Studio de la Revirée

*ESRF = European Synchrotron Radiation Facility; ILL = Institut Laue-Langevin

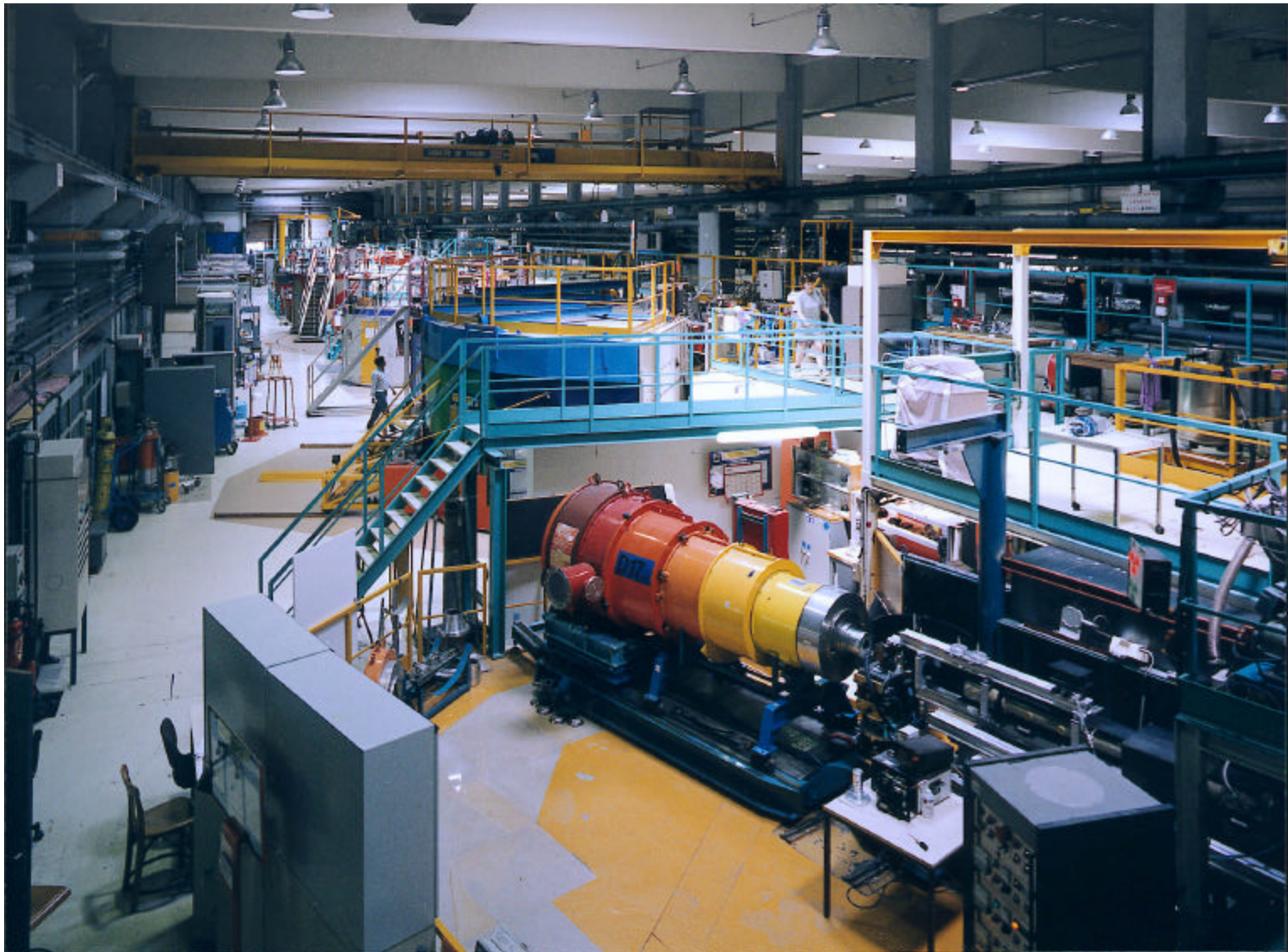
The National Institute of Standards and Technology (NIST) Reactor Is a 20 MW Research Reactor With a Peak Thermal Flux of 4×10^{14} N/sec. It Is Equipped With a Unique Liquid-hydrogen Moderator That Provides Neutrons for Seven Neutron Guides



Neutron Sources Provide Neutrons for Many Spectrometers: Schematic Plan of the ILL Facility



A $\sim 30 \times 20 \text{ m}^2$ Hall at the ILL Houses About 30 Spectrometers.
Neutrons Are Provided Through Guide Tubes

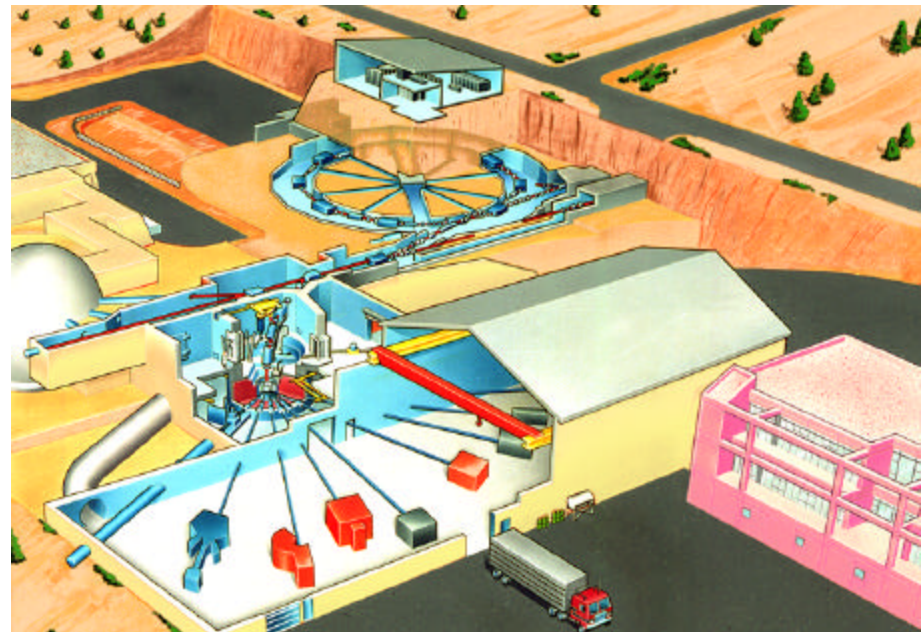
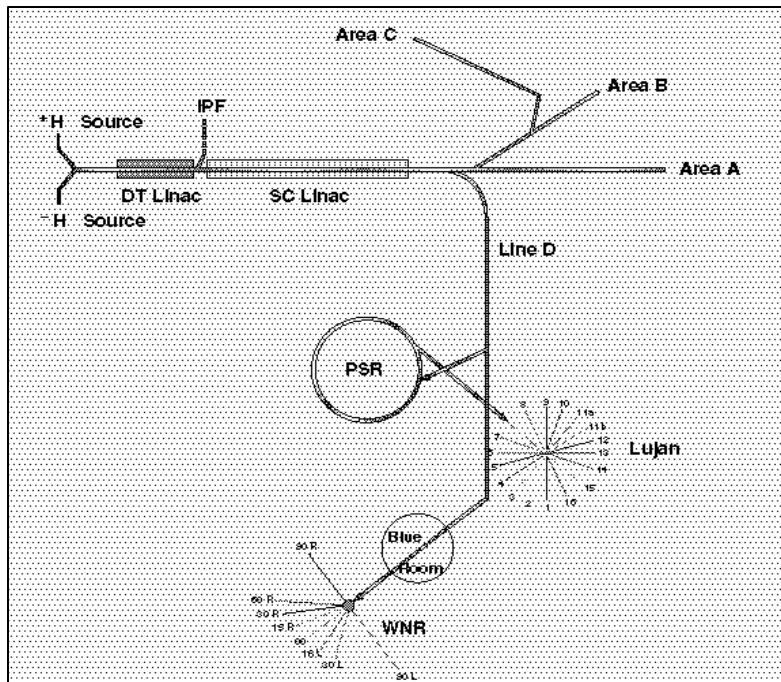


Los Alamos Neutron Science Center

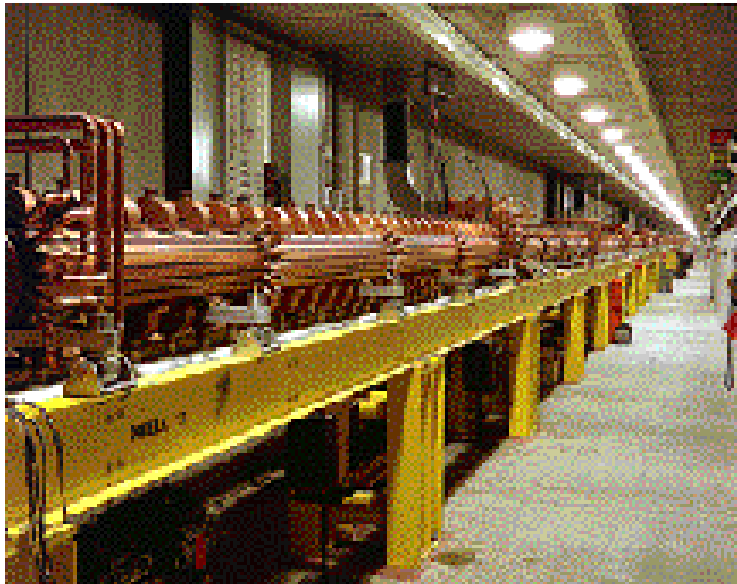


Neutron Production at LANSCE

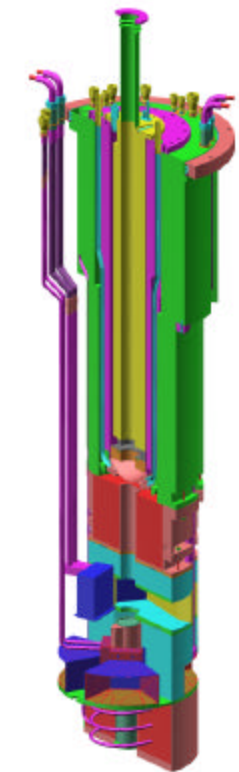
- Linac produces 20 H⁻ (a proton + 2 electrons) pulses per second
 - 800 MeV, ~800 μsec long pulses, average current ~100 μA
- Each pulse consists of repetitions of 270 nsec on, 90 nsec off
- Pulses are injected into a Proton Storage Ring with a period of 360 nsec
 - Thin carbon foil strips electrons to convert H⁻ to H⁺ (I.e. a proton)
 - ~3 x 10¹³ protons/pulse ejected onto neutron production target



Components of a Spallation Source



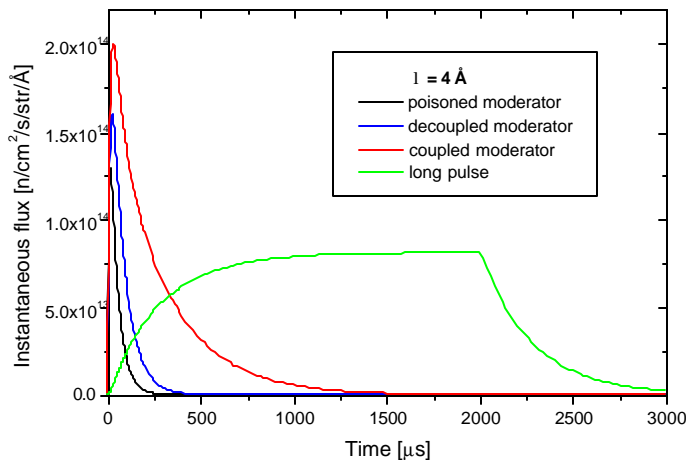
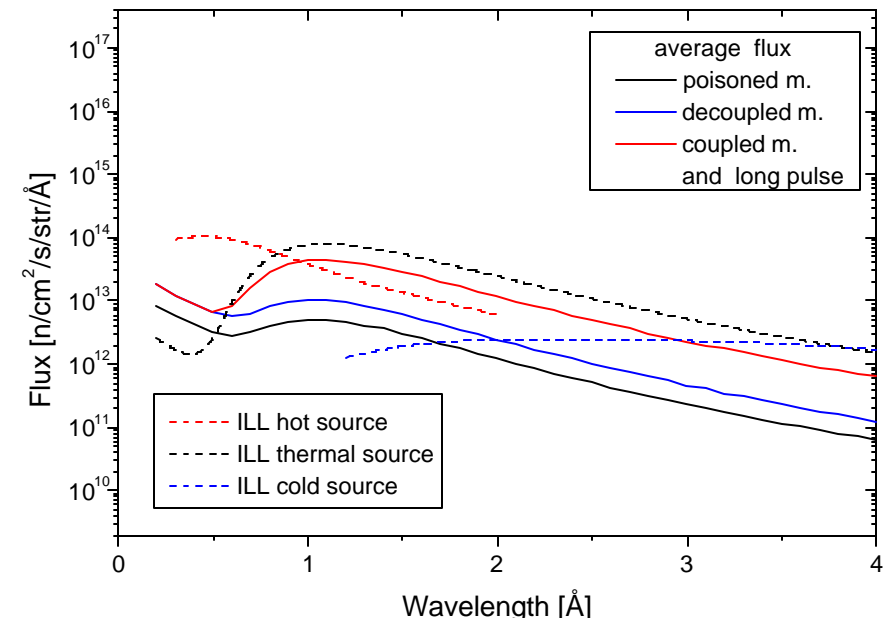
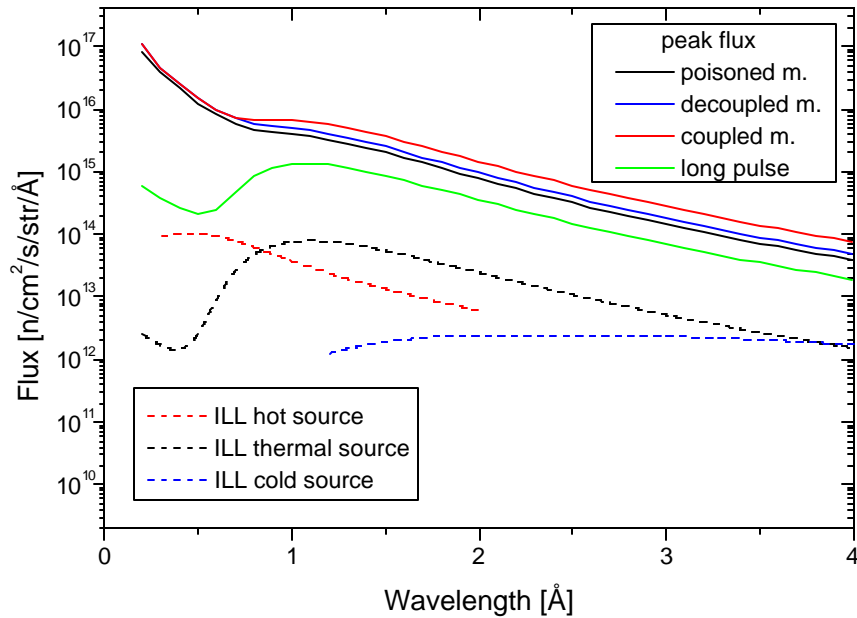
A half-mile long proton linac...



...and a neutron production target

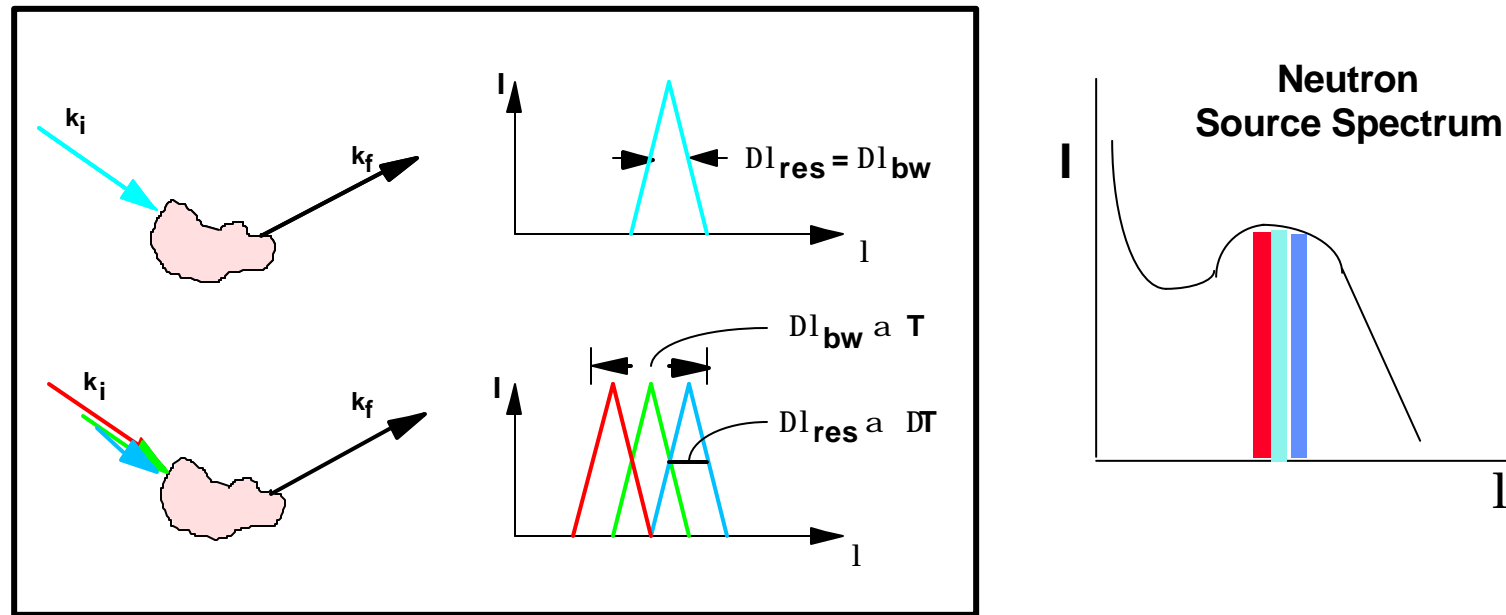
....a proton accumulation ring....

A Comparison of Neutron Flux Calculations for the ESS SPSS (50 Hz, 5 MW) & LPSS (16 Hz, 5W) With Measured Neutron Fluxes at the ILL



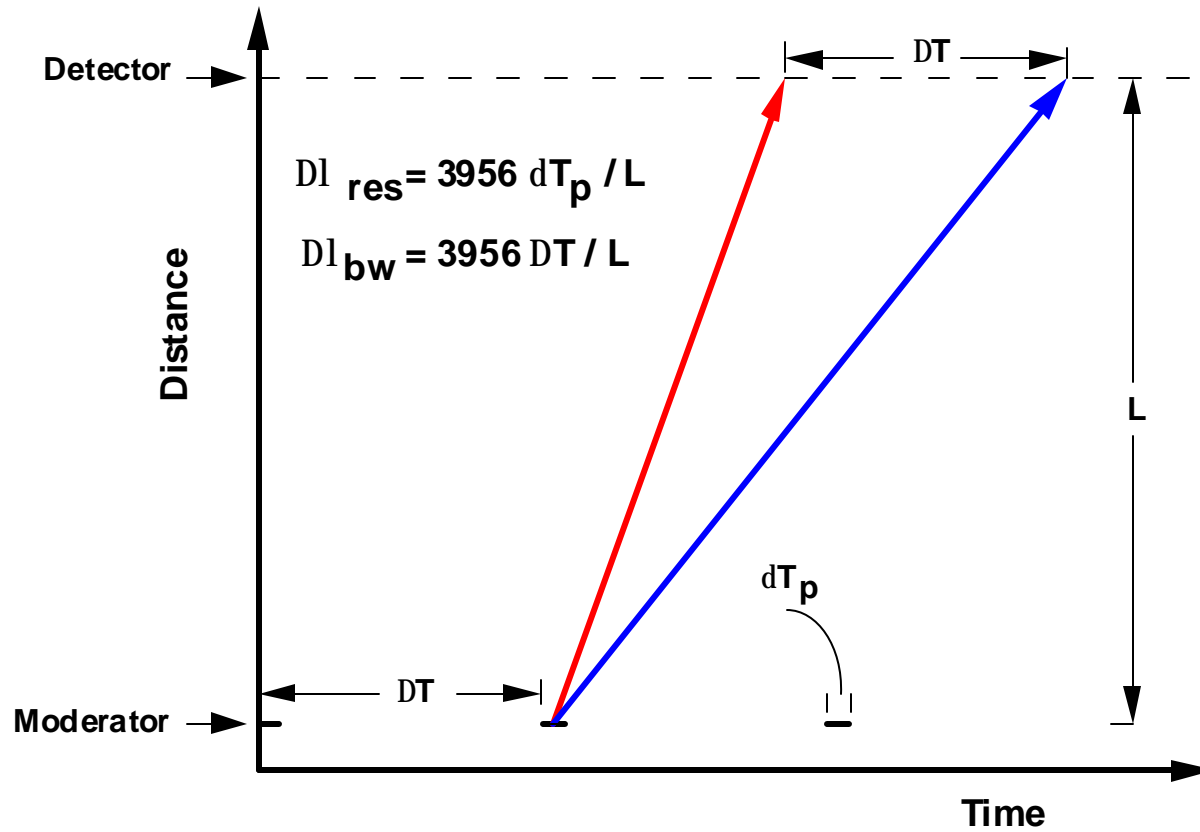
Pulsed sources only make sense if one can make effective use of the flux in each pulse, rather than the average neutron flux

Simultaneously Using Neutrons With Many Different Wavelengths Enhances the Efficiency of Neutron Scattering Experiments



Potential Performance Gain relative to use of a Single Wavelength
is the Number of Different Wavelength Slices used

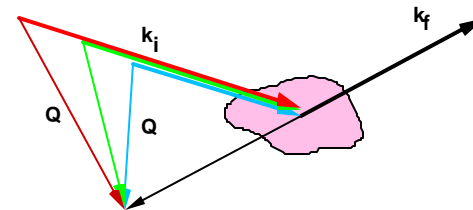
The Time-of-flight Method Uses Multiple Wavelength Slices at a Reactor or a Pulsed Spallation Source



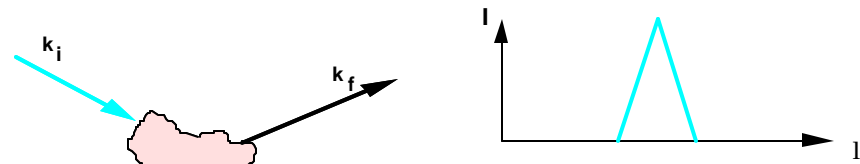
When the neutron wavelength is determined by time-of-flight, $\Delta T/\delta\tau_p$ different wavelength slices can be used simultaneously.

The Actual ToF Gain From Source Pulsing Often Does Not Scale Linearly With Peak Neutron Flux

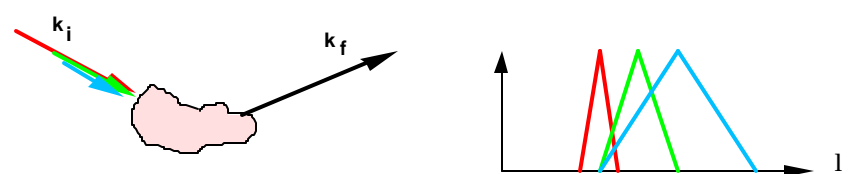
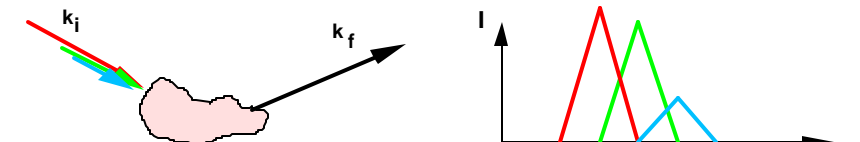
low rep. rate => large dynamic range
short pulse => good resolution —
neither may be necessary or useful



large dynamic range may result in intensity changes across the spectrum



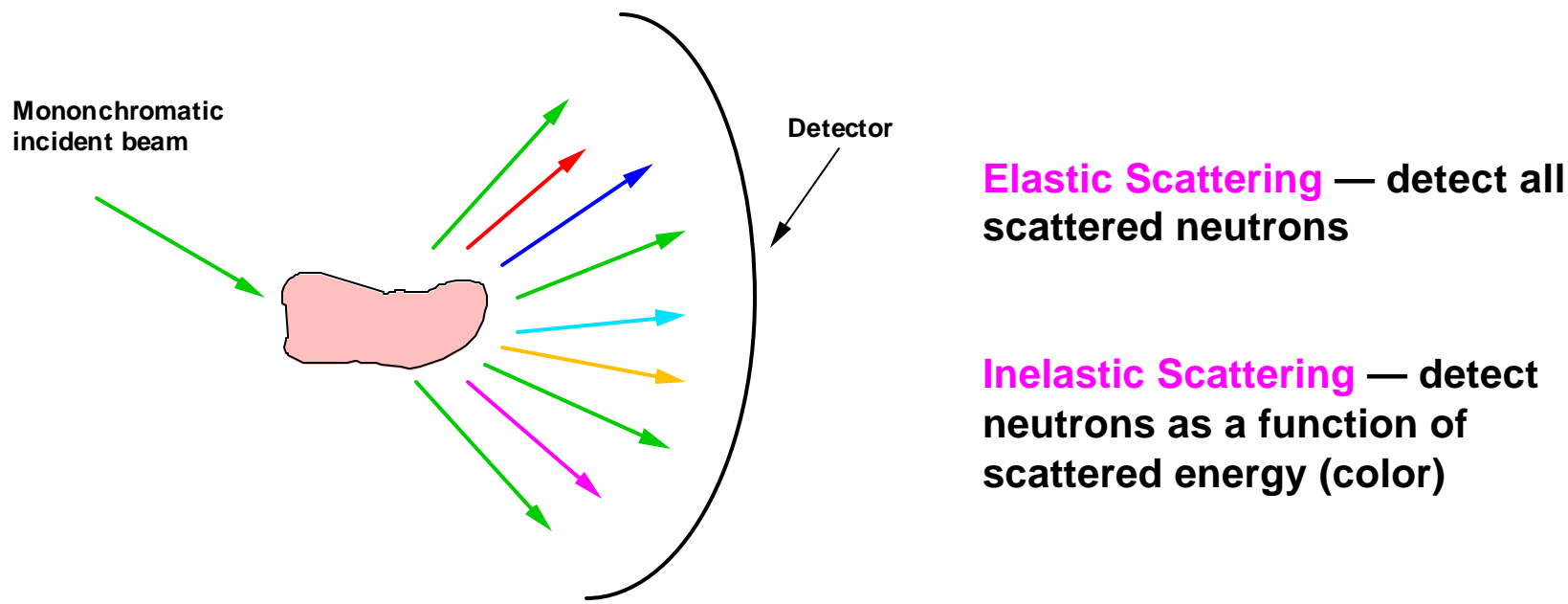
at a traditional short-pulse source the wavelength resolution changes with wavelength



A Comparison of Reactors & Spallation Sources

Short Pulse Spallation Source	Reactor
Energy deposited per useful neutron is ~20 MeV	Energy deposited per useful neutron is ~ 180 MeV
Neutron spectrum is “slowing down” spectrum – preserves short pulses	Neutron spectrum is Maxwellian
Constant, small $\delta\lambda/\lambda$ at large neutron energy => excellent resolution especially at large Q and E	Resolution can be more easily tailored to experimental requirements, except for hot neutrons where monochromator crystals and choppers are less effective
Copious “hot” neutrons=> very good for measurements at large Q and E	Large flux of cold neutrons => very good for measuring large objects and slow dynamics
Low background between pulses => good signal to noise	Pulse rate for TOF can be optimized independently for different spectrometers
Single pulse experiments possible	Neutron polarization easier

Why Isn't There a Universal Neutron Scattering Spectrometer?



- Conservation of momentum $\Rightarrow \underline{Q} = \underline{k}_f - \underline{k}_i$
- Conservation of energy $\Rightarrow E = (\ h^2 m / 8 p^2) (k_f^2 - k_i^2)$
- Scattering properties of sample depend only on Q and E, not on neutron l

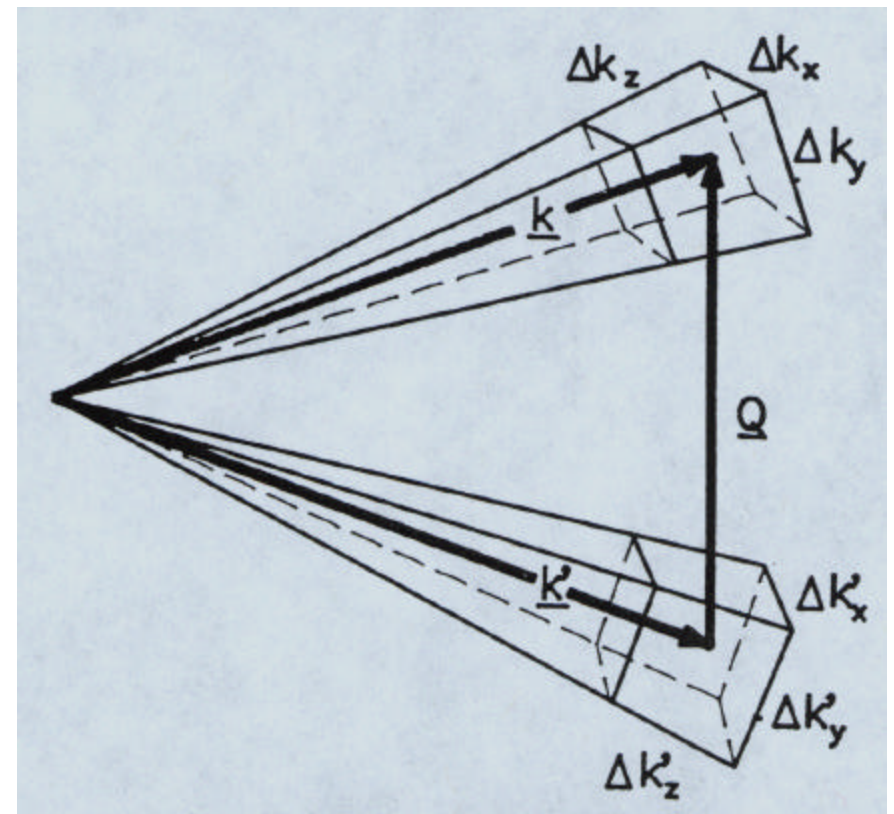
Many types of neutron scattering spectrometer are required because the accessible Q and E depend on neutron energy and because resolution and detector coverage have to be tailored to the science for such a signal-limited technique.

Brightness & Fluxes for Neutron & X-ray Sources

	<i>Brightness</i> ($s^{-1} m^{-2} ster^{-1}$)	<i>dE/E</i> (%)	<i>Divergence</i> (mrad 2)	<i>Flux</i> ($s^{-1} m^{-2}$)
Neutrons	10^{15}	2	10×10	10^{11}
Rotating Anode	10^{16}	3	0.5×10	5×10^{10}
Bending Magnet	10^{24}	0.01	0.1×5	5×10^{17}
Wiggler	10^{26}	0.01	0.1×1	10^{19}
Undulator (APS)	10^{33}	0.01	0.01×0.1	10^{24}

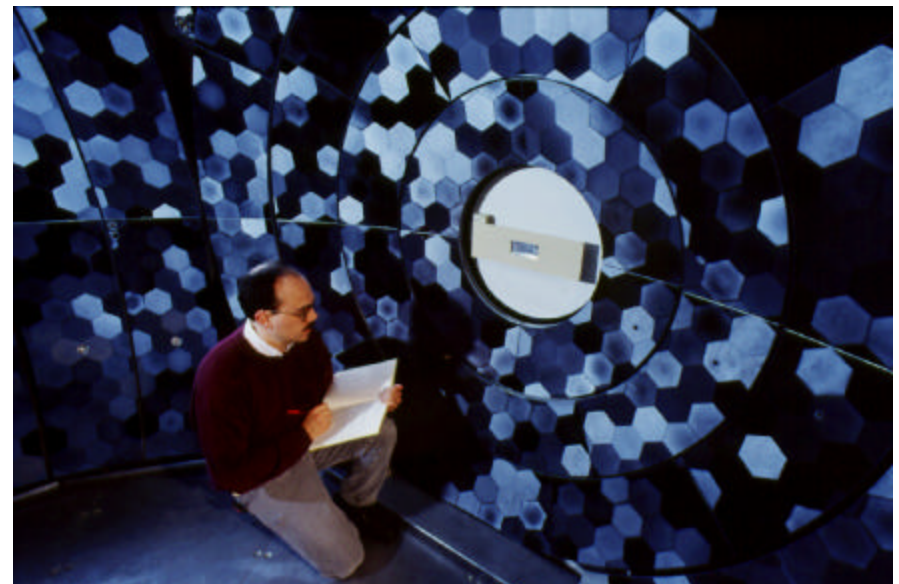
Instrumental Resolution

- Uncertainties in the neutron wavelength & direction of travel imply that Q and E can only be defined with a certain precision
- When the box-like resolution volumes in the figure are convolved, the overall resolution is Gaussian (central limit theorem) and has an elliptical shape in (Q, E) space
- The total signal in a scattering experiment is proportional to the phase space volume within the elliptical resolution volume – the better the resolution, the lower the count rate

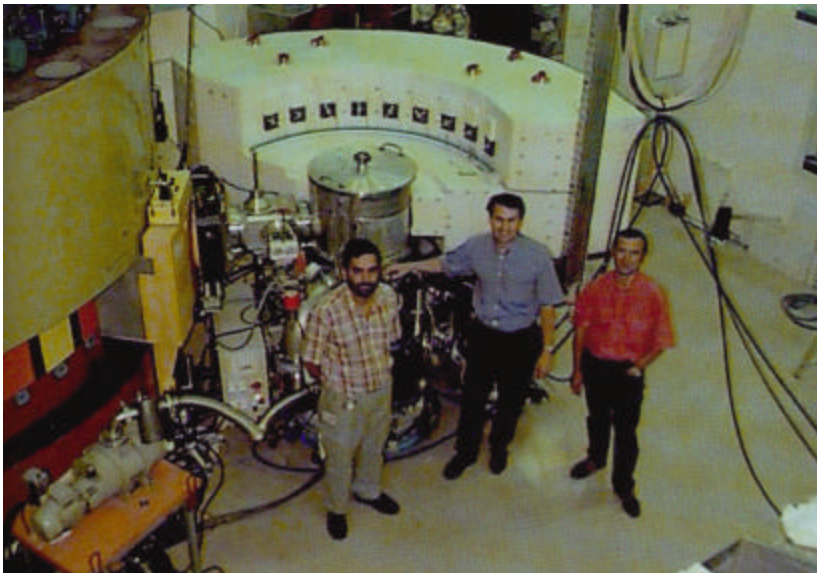


Examples of Specialization of Spectrometers: Optimizing the Signal for the Science

- **Small angle scattering** [$Q = 4\pi \sin\theta/\lambda$; $(\delta Q/Q)^2 = (\delta\lambda/\lambda)^2 + (\cot\theta \delta\theta)^2$]
 - Small diffraction angles to observe large objects => long (20 m) instrument
 - poor monochromatization ($\delta\lambda/\lambda \sim 10\%$) sufficient to match obtainable angular resolution (1 cm² pixels on 1 m² detector at 10 m => $\delta\theta \sim 10^{-3}$ at $\theta \sim 10^{-2}$)
- **Back scattering** [$\theta = \pi/2$; $\lambda = 2 d \sin \theta$; $\delta\lambda/\lambda = \cot \theta + \dots$]
 - very good energy resolution (\sim neV) => perfect crystal analyzer at $\theta \sim \pi/2$
 - poor Q resolution => analyzer crystal is very large (several m²)



Typical Neutron Scattering Instruments



Note: relatively massive shielding; long flight paths for time-of-flight spectrometers; many or multi-detectors

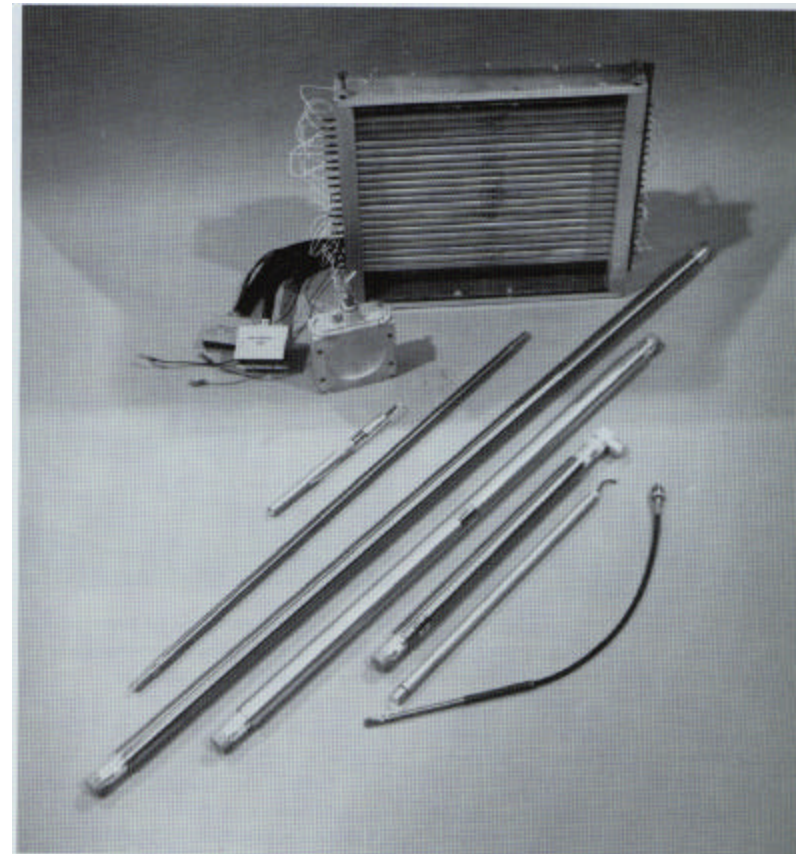
but... small science at a large facility

Components of Neutron Scattering Instruments

- **Monochromators**
 - Monochromate or analyze the energy of a neutron beam using Bragg's law
- **Collimators**
 - Define the direction of travel of the neutron
- **Guides**
 - Allow neutrons to travel large distances without suffering intensity loss
- **Detectors**
 - Neutron is absorbed by ^3He and gas ionization caused by recoiling particles is detected
- **Choppers**
 - Define a short pulse or pick out a small band of neutron energies
- **Spin turn coils**
 - Manipulate the neutron spin using Lamor precession
- **Shielding**
 - Minimize background and radiation exposure to users

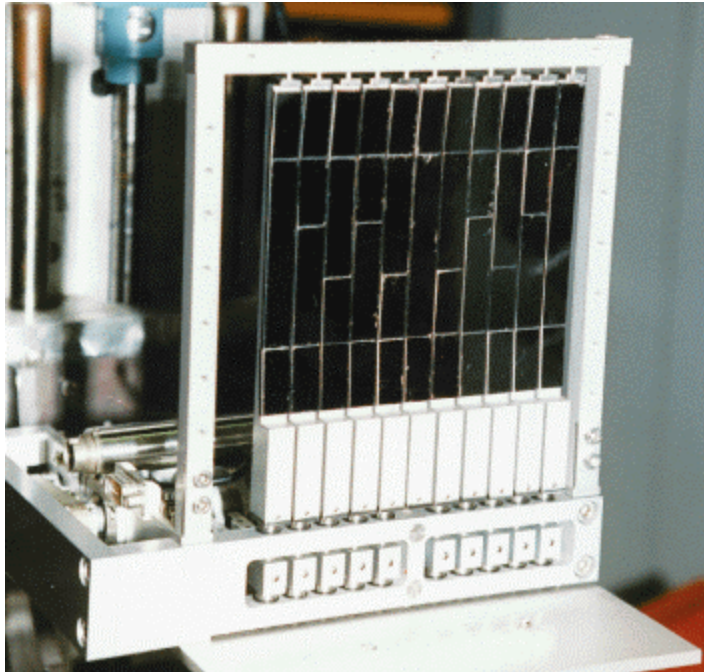
Most Neutron Detectors Use ${}^3\text{He}$

- ${}^3\text{He} + n \rightarrow {}^3\text{H} + p + 0.764 \text{ MeV}$
- Ionization caused by triton and proton is collected on an electrode
- 70% of neutrons are absorbed when the product of gas pressure \times thickness \times neutron wavelength is 16 atm. cm. Å
- Modern detectors are often “position sensitive” – charge division is used to determine where the ionization cloud reached the cathode.



A selection of neutron detectors – thin-walled stainless steel tubes filled with high-pressure ${}^3\text{He}$.

Essential Components of Modern Neutron Scattering Spectrometers



Horizontally & vertically focusing monochromator (about $15 \times 15 \text{ cm}^2$)



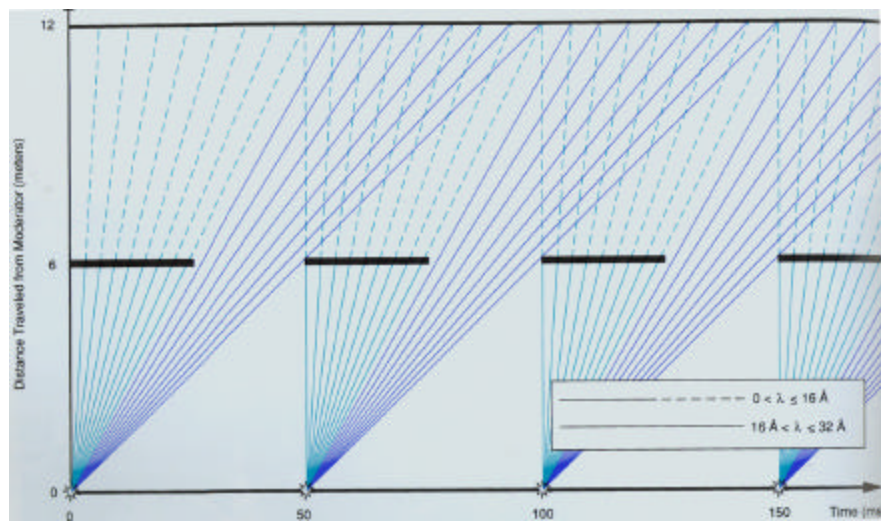
Pixelated detector covering a wide range of scattering angles (vertical & horizontal)



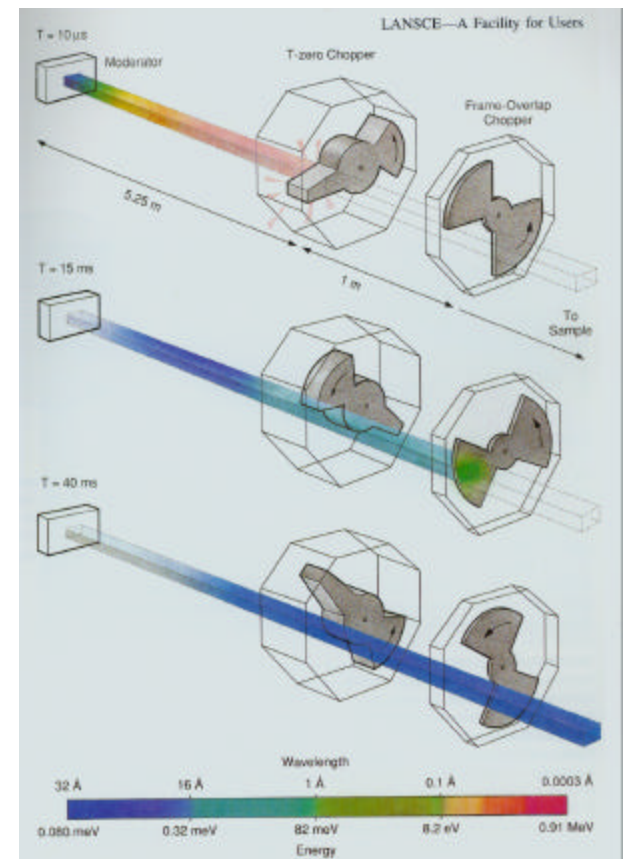
Neutron guide (glass coated either with Ni or “supermirror”)

Rotating Choppers Are Used to Tailor Neutron Pulses at Reactors and Spallation Sources

- T-zero choppers made of Fe-Co are used at spallation sources to absorb the prompt high-energy pulse of neutrons
- Cd is used in frame overlap choppers to absorb slower neutrons



Fast neutrons from one pulse can catch-up with slower neutrons from a succeeding pulse and spoil the measurement if they are not removed. This is called “frame-overlap”



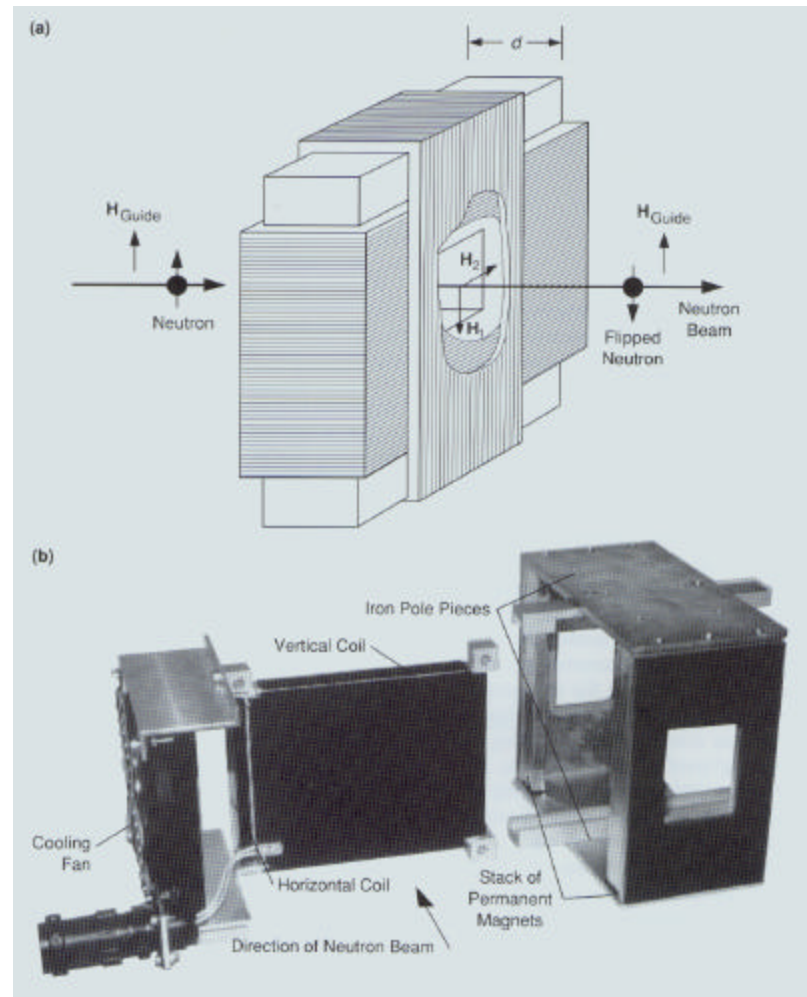
Larmor Precession & Manipulation of the Neutron Spin

- In a magnetic field, H , the neutron spin precesses at a rate

$$u_L = -gH / 2p = -2916.4H \text{ Hz}$$

where γ is the neutron's gyromagnetic ratio & H is in Oesteds

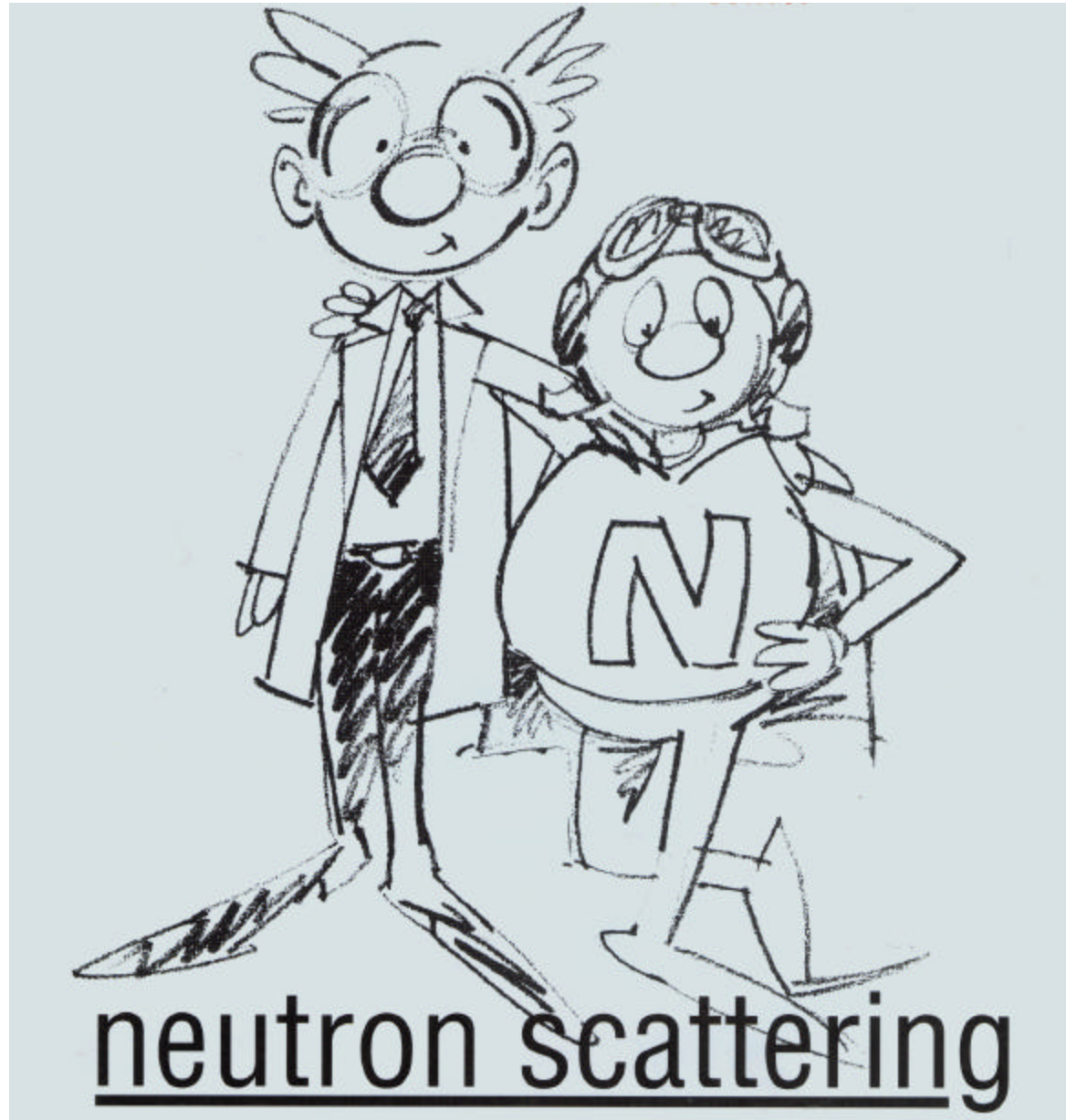
- This effect can be used to manipulate the neutron spin
- A “spin flipper” – which turns the spin through 180 degrees is illustrated
- The spin is usually referred to as “up” when the spin (not the magnetic moment) is parallel to a (weak ~ 10 – 50 Oe) magnetic guide field



Next Lecture

3. Diffraction

1. Diffraction by a lattice
2. Single-crystal diffraction and powder diffraction
3. Use of monochromatic beams and time-of-flight to measure powder diffraction
4. Rietveld refinement of powder patterns
5. Examples of science with powder diffraction
 - Refinement of structures of new materials
 - Materials texture
 - Strain measurements
 - Structures at high pressure
 - Microstrain peak broadening
 - Pair distribution functions (PDF)



by

Roger Pynn

Los Alamos
National Laboratory

LECTURE 3: Diffraction

This Lecture

2. Diffraction

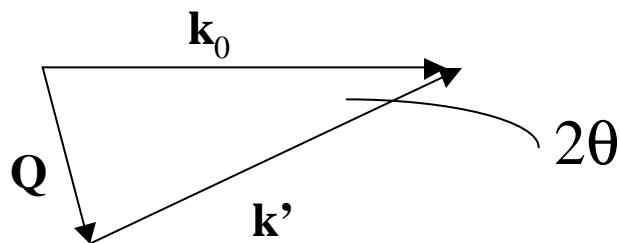
1. Diffraction by a lattice
2. Single-crystal compared with powder diffraction
3. Use of monochromatic beams and time-of-flight to measure powder diffraction
4. Rietveld refinement of powder patterns
5. Examples of science with powder diffraction
 - Refinement of structures of new materials
 - Materials texture
 - Strain measurements
 - Pair distribution functions (PDF)

From Lecture 1:

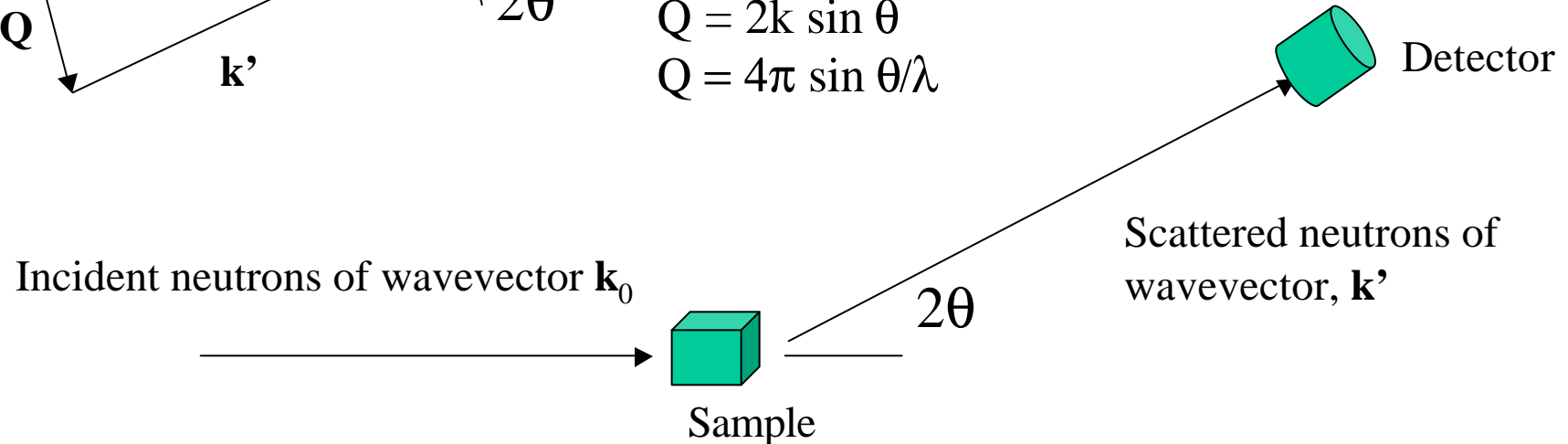
$$\frac{d\mathbf{s}}{d\Omega} = \frac{\text{number of neutrons scattered through angle } 2\mathbf{q} \text{ per second into } d\Omega}{\text{number of incident neutrons per square cm per second}}$$

$$\left(\frac{d\mathbf{s}}{d\Omega} \right)_{coh} = \sum_{i,j} b_i^{coh} b_j^{coh} e^{i(\vec{k}_0 - \vec{k}').(\vec{R}_i - \vec{R}_j)} = \sum_{i,j} b_i^{coh} b_j^{coh} e^{-i\vec{Q}.(\vec{R}_i - \vec{R}_j)}$$

where the wavevector transfer \vec{Q} is defined by $\vec{Q} = \vec{k}' - \vec{k}_0$

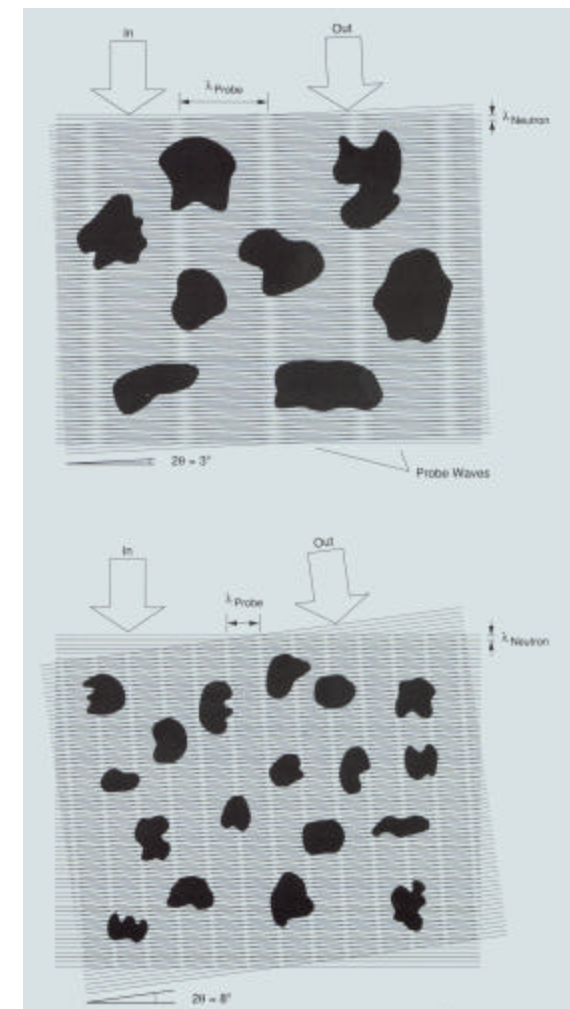


For elastic scattering $\mathbf{k}_0 = \mathbf{k}' = \mathbf{k}$:
 $Q = 2k \sin \theta$
 $Q = 4\pi \sin \theta / \lambda$



Neutron Diffraction

- Neutron diffraction is used to measure the differential cross section, $d\sigma/d\Omega$ and hence the static structure of materials
 - Crystalline solids
 - Liquids and amorphous materials
 - Large scale structures
 - Depending on the scattering angle, structure on different length scales, d , is measured:
- $$2p/Q = d = \lambda / 2\sin(q)$$
- For crystalline solids & liquids, use wide angle diffraction. For large structures, e.g. polymers, colloids, micelles, etc. use small-angle neutron scattering



Diffraction by a Lattice of Atoms

$$S(\vec{Q}) = \frac{1}{N} \left\langle \sum_{i,j} e^{-i\vec{Q} \cdot (\vec{R}_i - \vec{R}_j)} \right\rangle \quad \text{with } \vec{R}_i = \vec{i} + \vec{u}_i \text{ where } \vec{i} \text{ is the equilibrium position}$$

of atomi and \vec{u}_i is any displacement (e.g. thermal) from the equilibrium position.

Ignoring thermal vibrations, $S(Q)$ is only non - zero for Q 's such that $\vec{Q} \cdot (\vec{i} - \vec{j}) = 2Mp$.

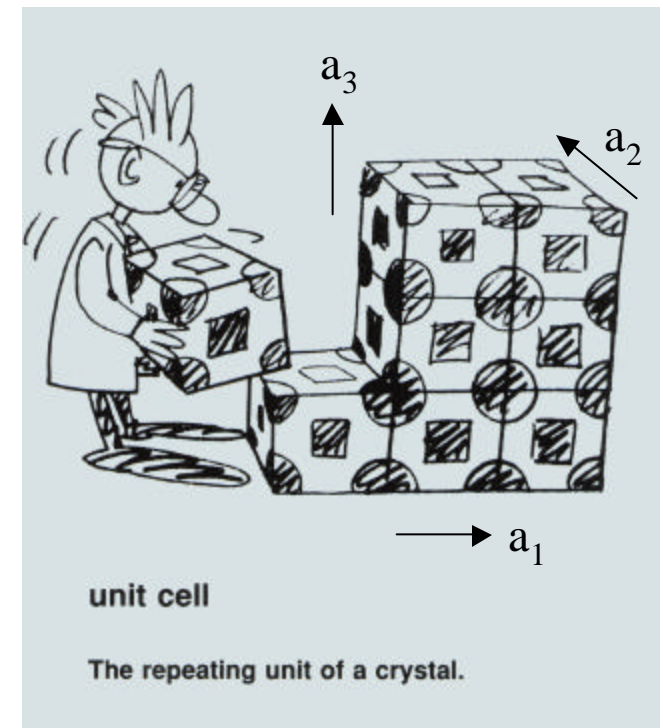
In a Bravais lattice, we can write $\vec{i} = m_{1i}\vec{a}_1 + m_{2i}\vec{a}_2 + m_{3i}\vec{a}_3$ where $\vec{a}_1, \vec{a}_2, \vec{a}_3$ are the primitive translation vectors of the unit cell.

Define $\vec{a}_1^* = \frac{2p}{V_0} \vec{a}_2 \wedge \vec{a}_3$ and cyclic permutations.

Then $\vec{a}_i^* \cdot \vec{a}_j = 2pd_{ij}$.

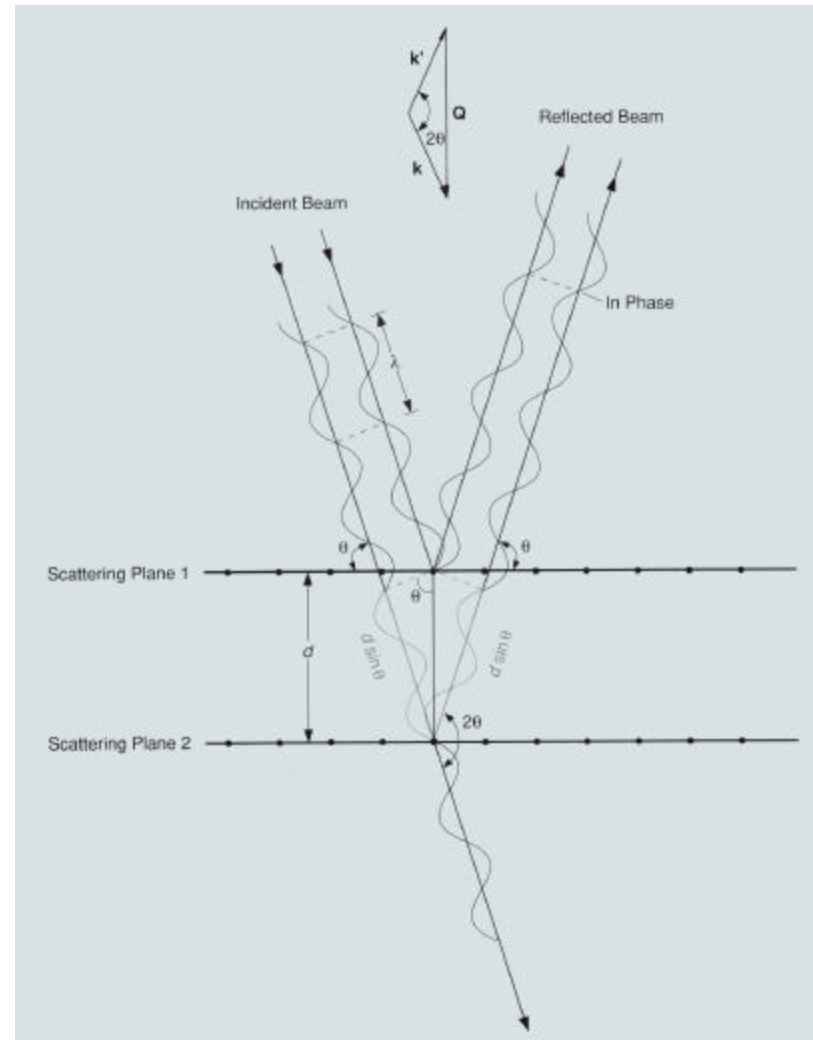
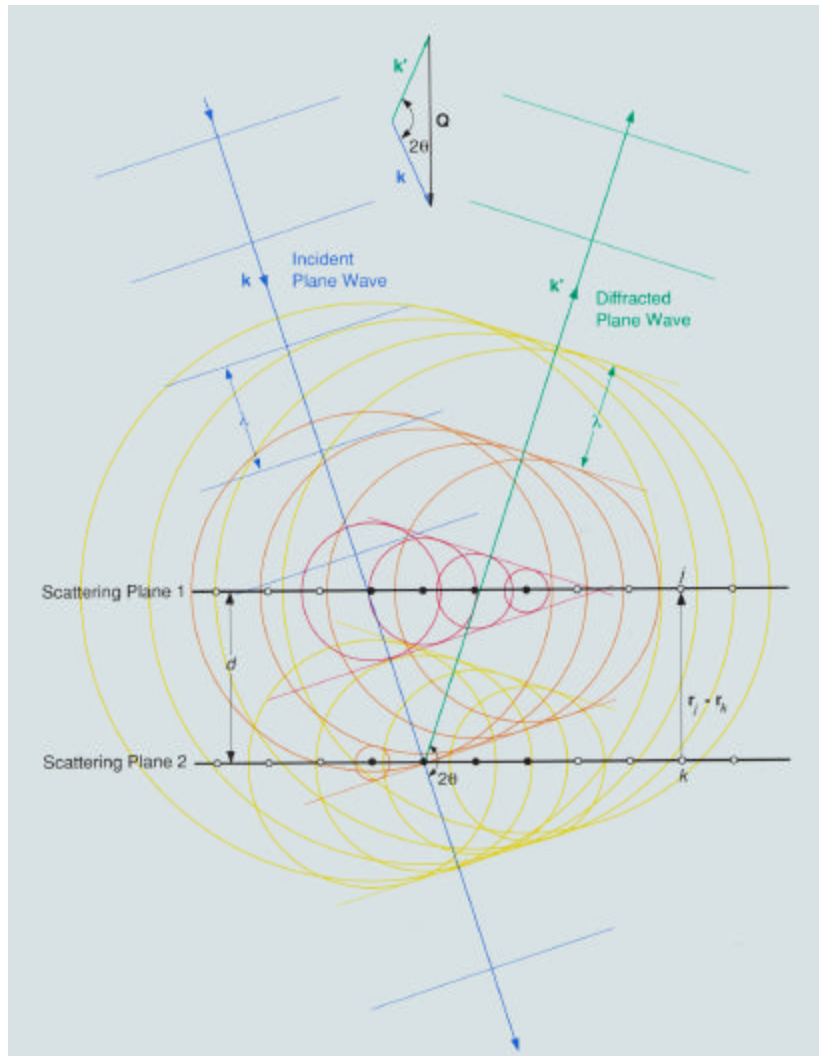
If $\vec{Q} = \vec{G}_{hkl} = h\vec{a}_1^* + k\vec{a}_2^* + l\vec{a}_3^*$ then $\vec{Q} \cdot (\vec{i} - \vec{j}) = 2Mp$.

So scattering from a (frozen) lattice only occurs when the scattering wavevector, Q , is equal to a reciprocal lattice vector, G_{hkl} .



For Periodic Arrays of Nuclei, Coherent Scattering Is Reinforced Only in Specific Directions Corresponding to the Bragg Condition:

$$\lambda = 2 d_{hkl} \sin(\theta) \text{ or } 2 k \sin(\theta) = G_{hkl}$$



Bragg Scattering from Crystals

Working through the math (see, for example, Squires' book), we find :

$$\left(\frac{d\mathbf{s}}{d\Omega} \right)_{Bragg} = N \frac{(2\mathbf{p})^3}{V_0} \sum_{hkl} \mathbf{d}(\vec{Q} - \vec{G}_{hkl}) |F_{hkl}(\vec{Q})|^2$$

where the unit - cell structure factor is given by

$$F_{hkl}(\vec{Q}) = \sum_d \bar{b}_d e^{i\vec{Q} \cdot \vec{d}} e^{-W_d}$$

and W_d is the Debye - Waller factor that accounts for thermal motions of atoms

- Using either single crystals or powders, neutron diffraction can be used to measure F^2 (which is proportional to the intensity of a Bragg peak) for various values of (hkl) .
- Direct Fourier inversion of diffraction data to yield crystal structures is not possible because we only measure the magnitude of F , and not its phase => models must be fit to the data
- Neutron powder diffraction has been particularly successful at determining structures of new materials, e.g. high T_c materials

We would be better off if diffraction measured phase of scattering rather than amplitude!
Unfortunately, nature did not oblige us.

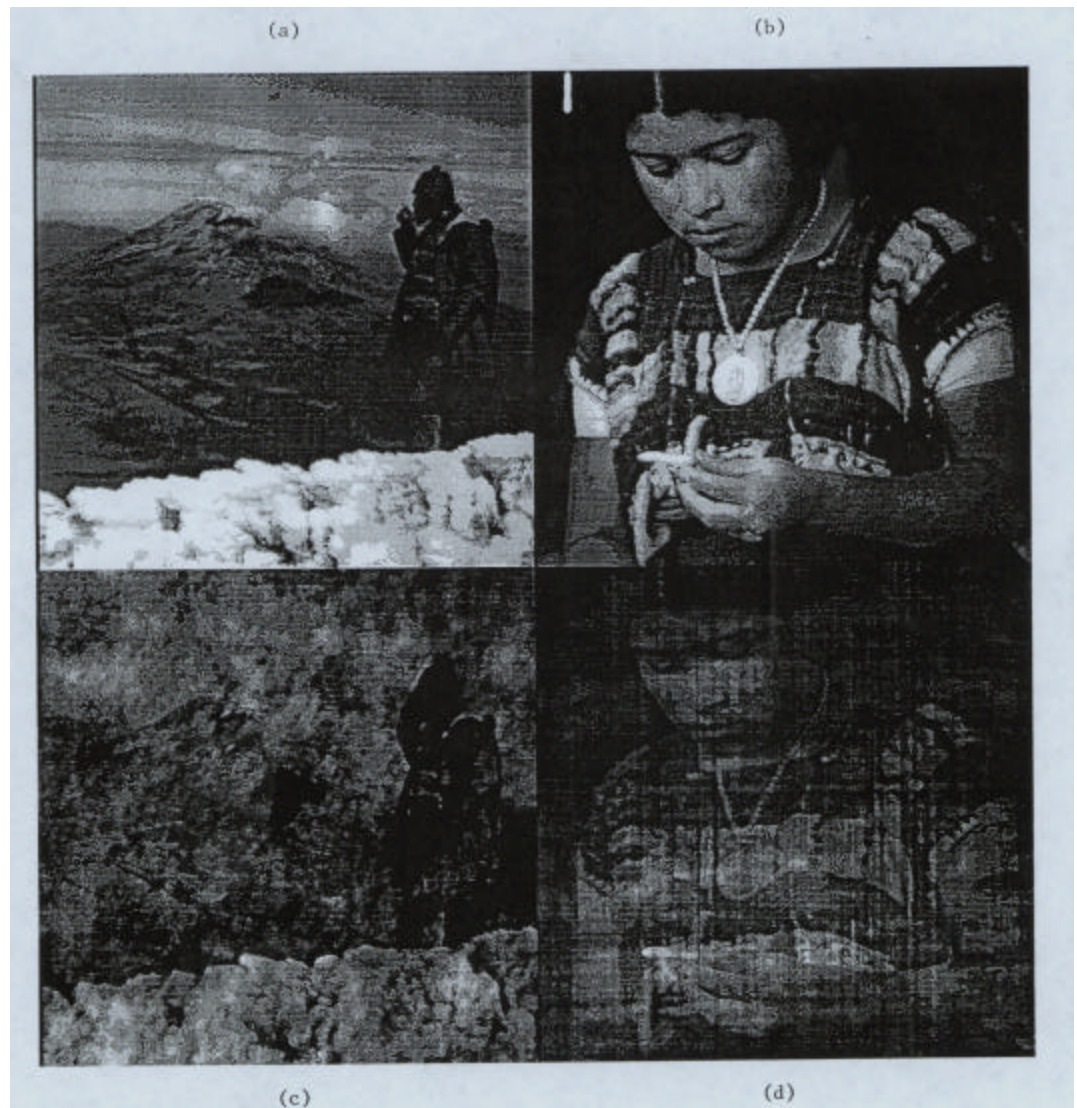
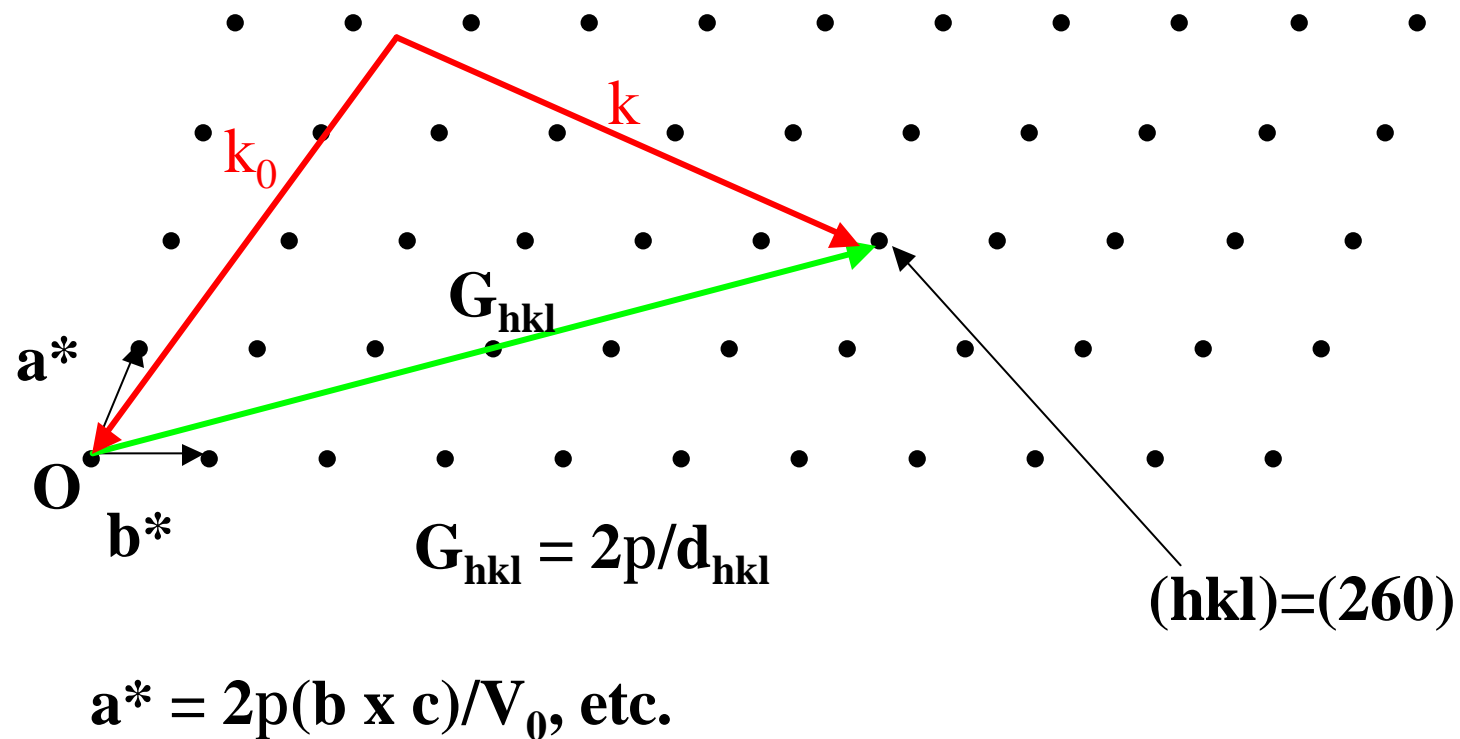


Figure 1.2

A graphic illustration of the phase problem: (a) and (b) are the original images. (c) is the (Fourier) reconstruction which has the Fourier phases of (a) and Fourier amplitudes of (b); (d) is the reconstruction with the phases of (b) and the amplitudes of (a).

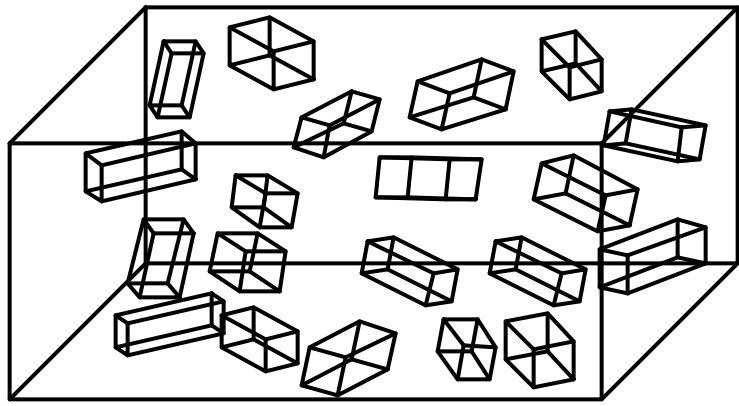
Picture by courtesy of D. Sivia

Reciprocal Space – An Array of Points (hkl) that is Precisely Related to the Crystal Lattice



A single crystal has to be aligned precisely to record Bragg scattering

Powder – A Polycrystalline Mass



**All orientations of
crystallites possible**

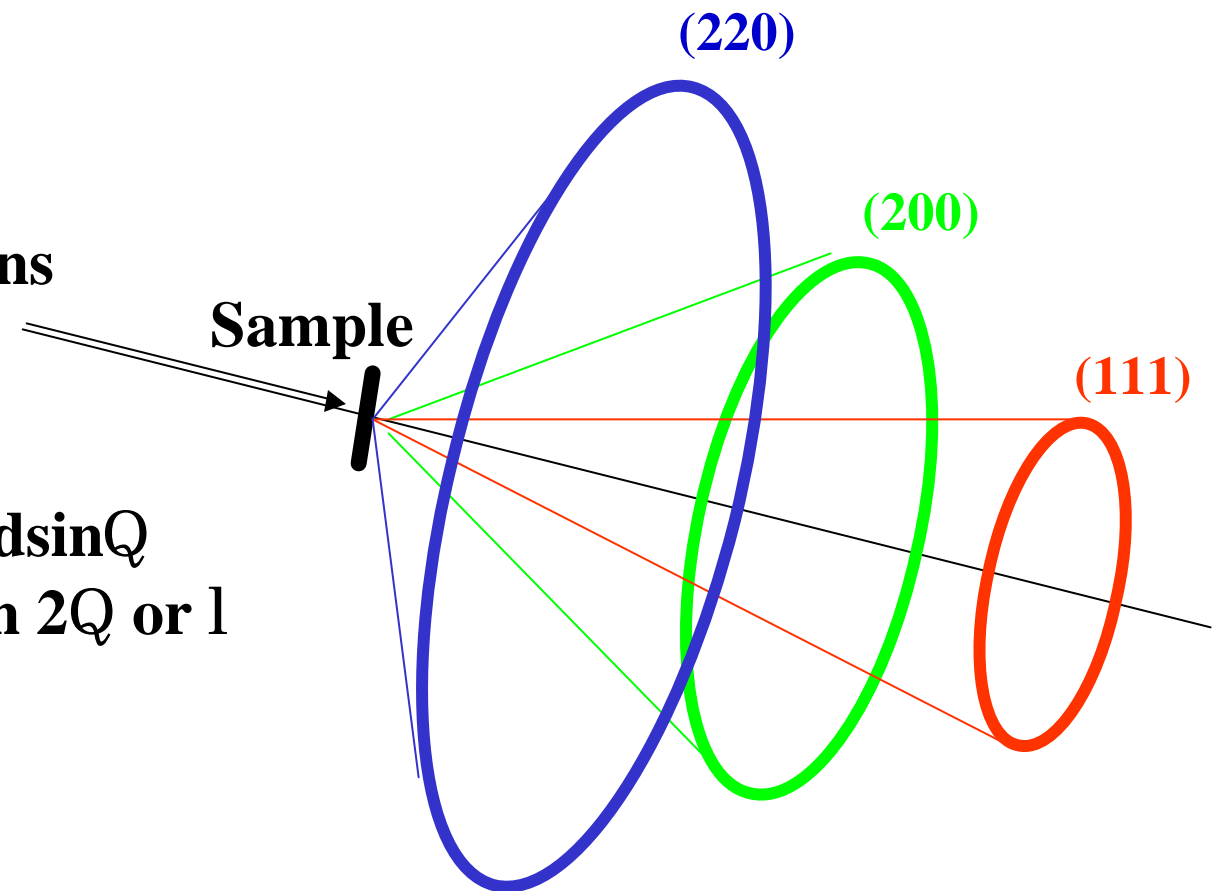
**Typical Sample: 1cc powder of
10mm crystallites - 10^9 particles
if 1mm crystallites - 10^{12} particles**

**Single crystal reciprocal lattice
- smeared into spherical shells**

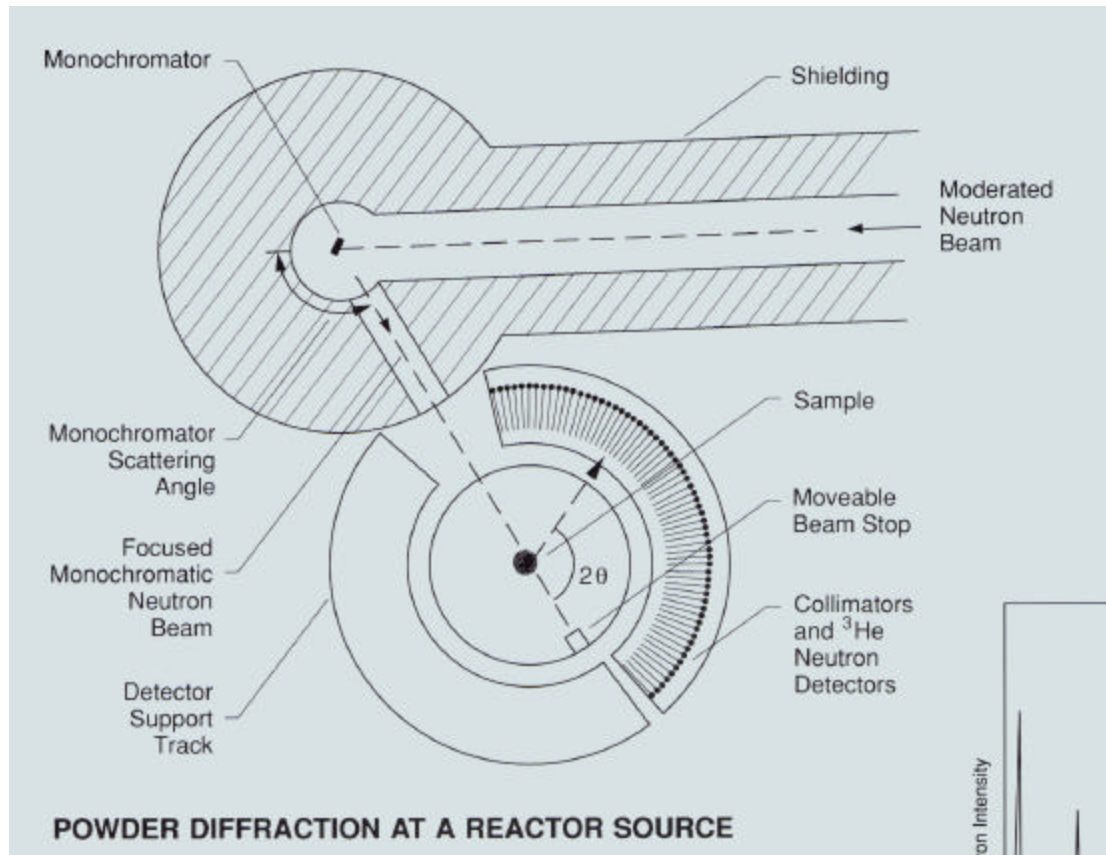
Powder Diffraction gives Scattering on Debye-Scherrer Cones

Incident beam
x-rays or neutrons

Bragg's Law $l = 2d \sin Q$
Powder pattern – scan $2Q$ or l

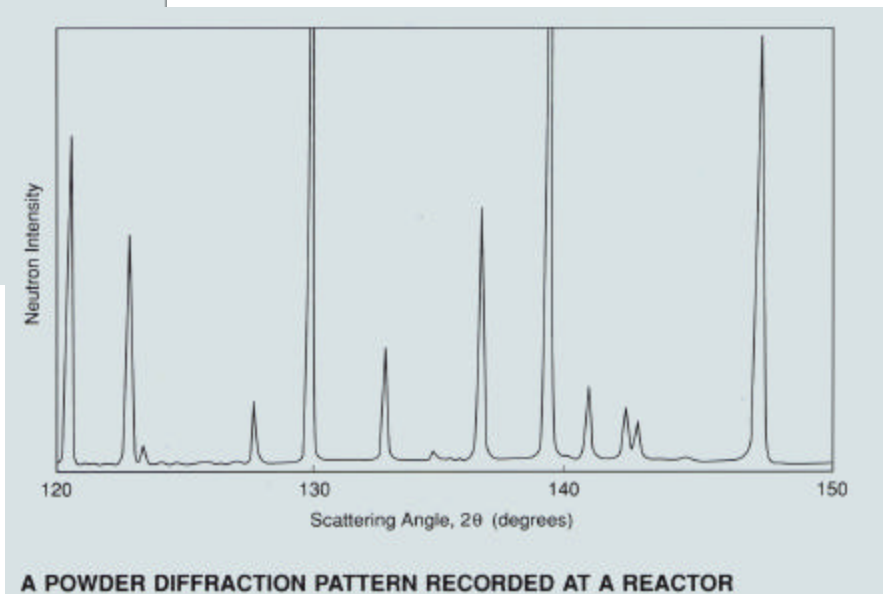


Measuring Neutron Diffraction Patterns with a Monochromatic Neutron Beam

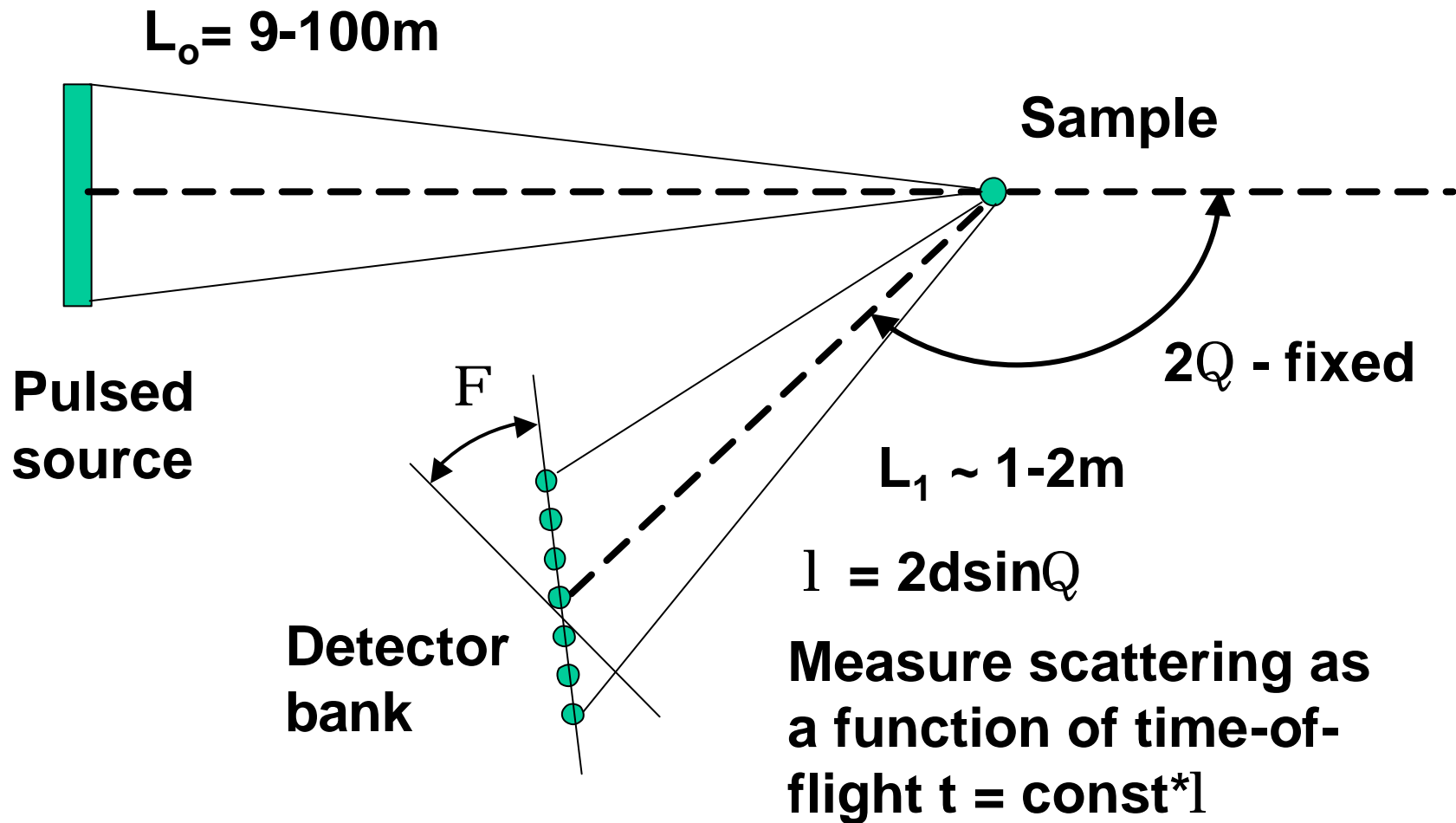


Since we know the neutron wavevector, k , the scattering angle gives G_{hkl} directly:
$$G_{hkl} = 2 k \sin \theta$$

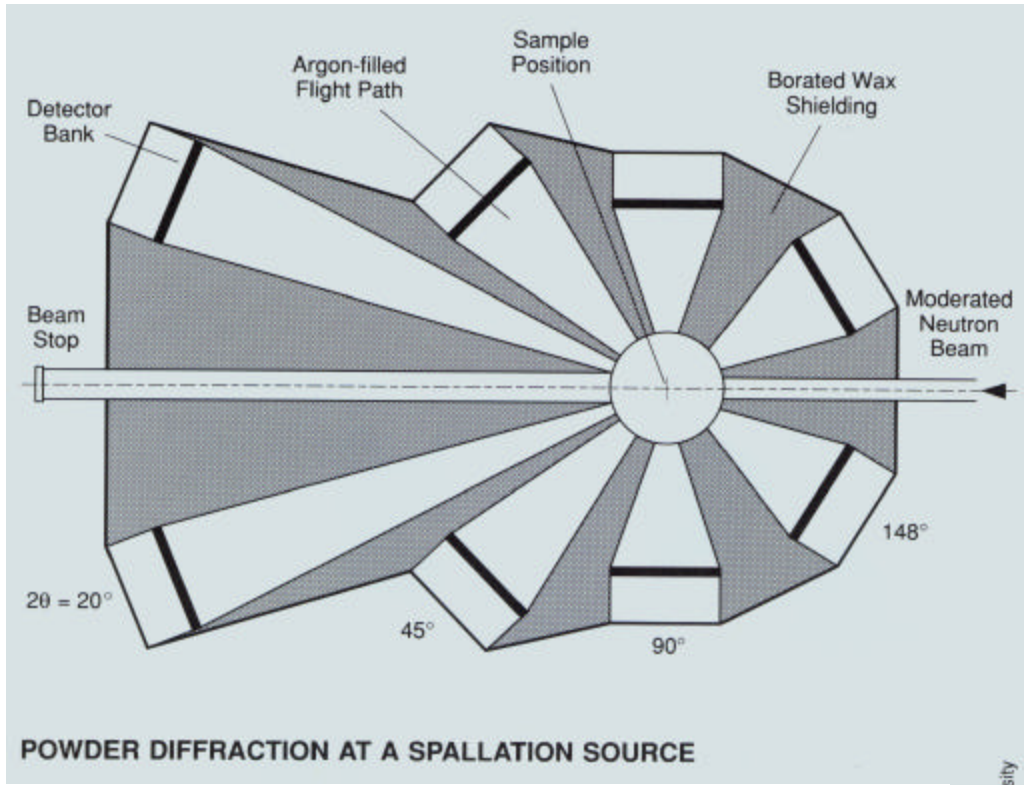
Use a continuous beam of mono-energetic neutrons.



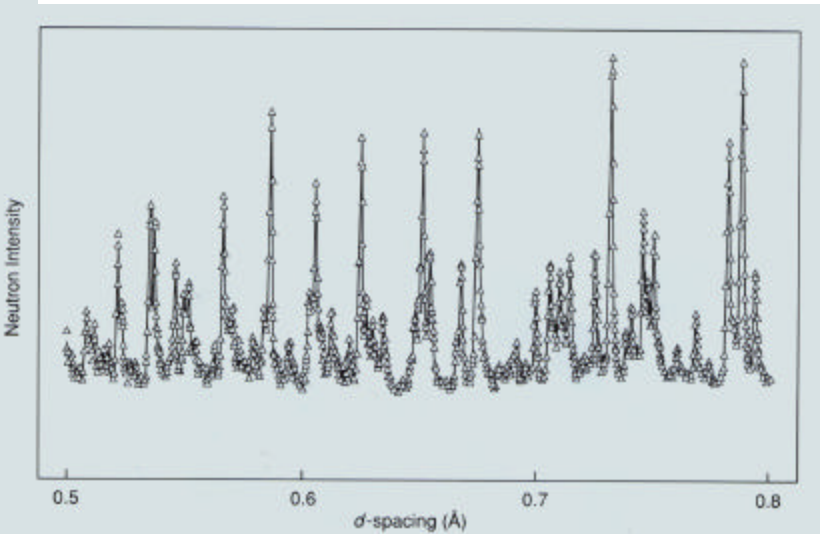
Neutron Powder Diffraction using Time-of-Flight



Time-of-Flight Powder Diffraction



Use a pulsed beam with a broad spectrum of neutron energies and separate different energies (velocities) by time of flight.

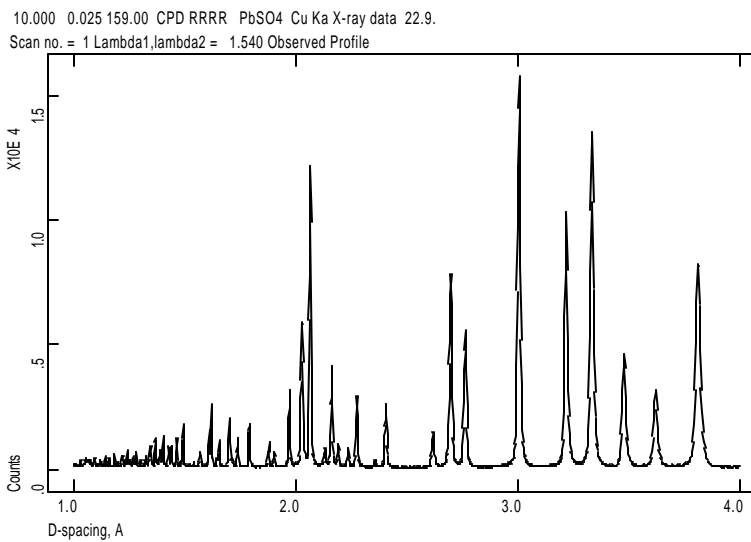
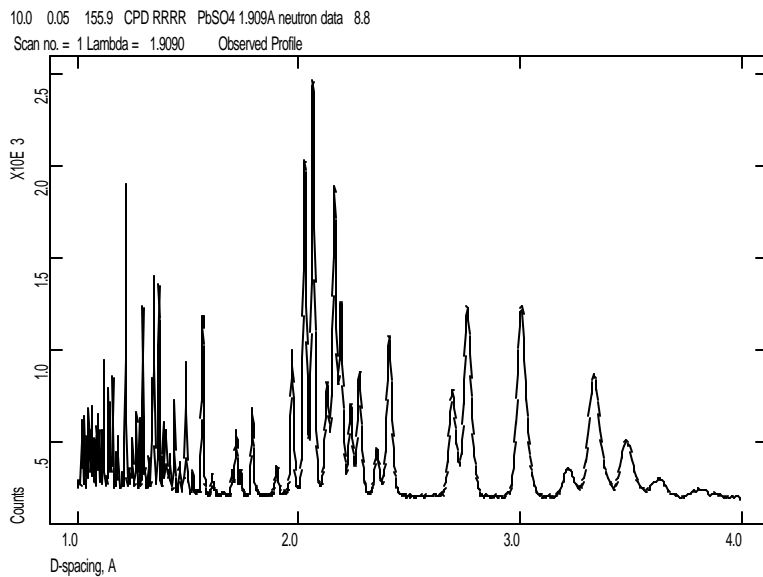


A POWDER DIFFRACTION PATTERN RECORDED AT A SPALLATION SOURCE

Compare X-ray & Neutron Powder Patterns

X-ray Diffraction - CuKa Phillips PW1710

- Higher resolution
- Intensity fall-off at small d spacings
- Better at resolving small lattice distortions



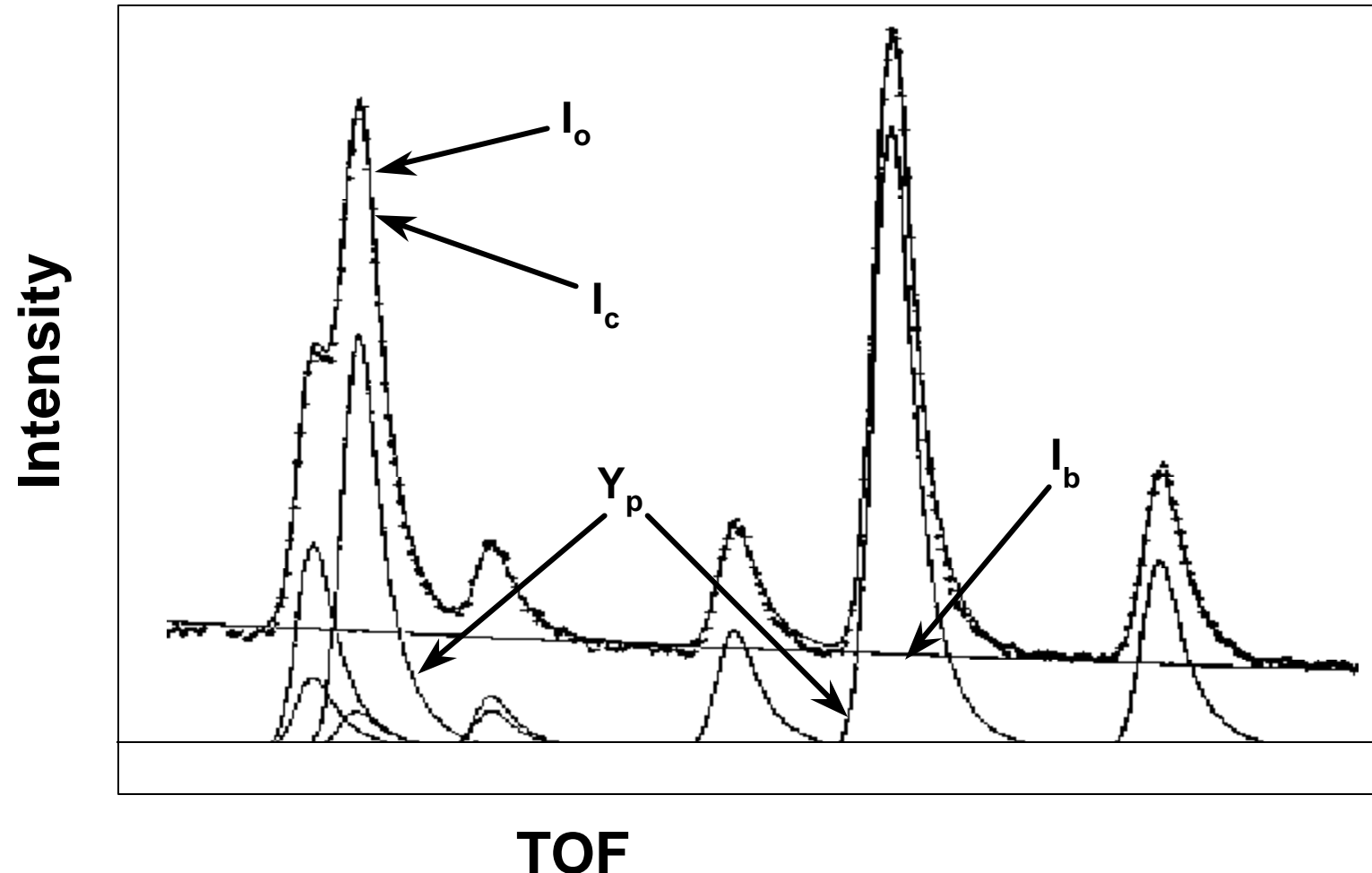
Neutron Diffraction - D1a, ILL
 $\lambda = 1.909 \text{ \AA}$

- Lower resolution
- Much higher intensity at small d-spacings
- Better atomic positions/thermal parameters



There's more than meets the eye in a powder pattern*

Rietveld Model $I_c = I_b + S Y_p$



*Discussion of Rietveld method adapted from viewgraphs by R. Vondreele (LANSCE)

The Rietveld Model for Refining Powder Patterns

$$I_c = I_o \{ S k_h F^2_h m_h L_h P(D_h) + I_b \}$$

I_o - incident intensity - variable for fixed $2Q$

k_h - scale factor for particular phase

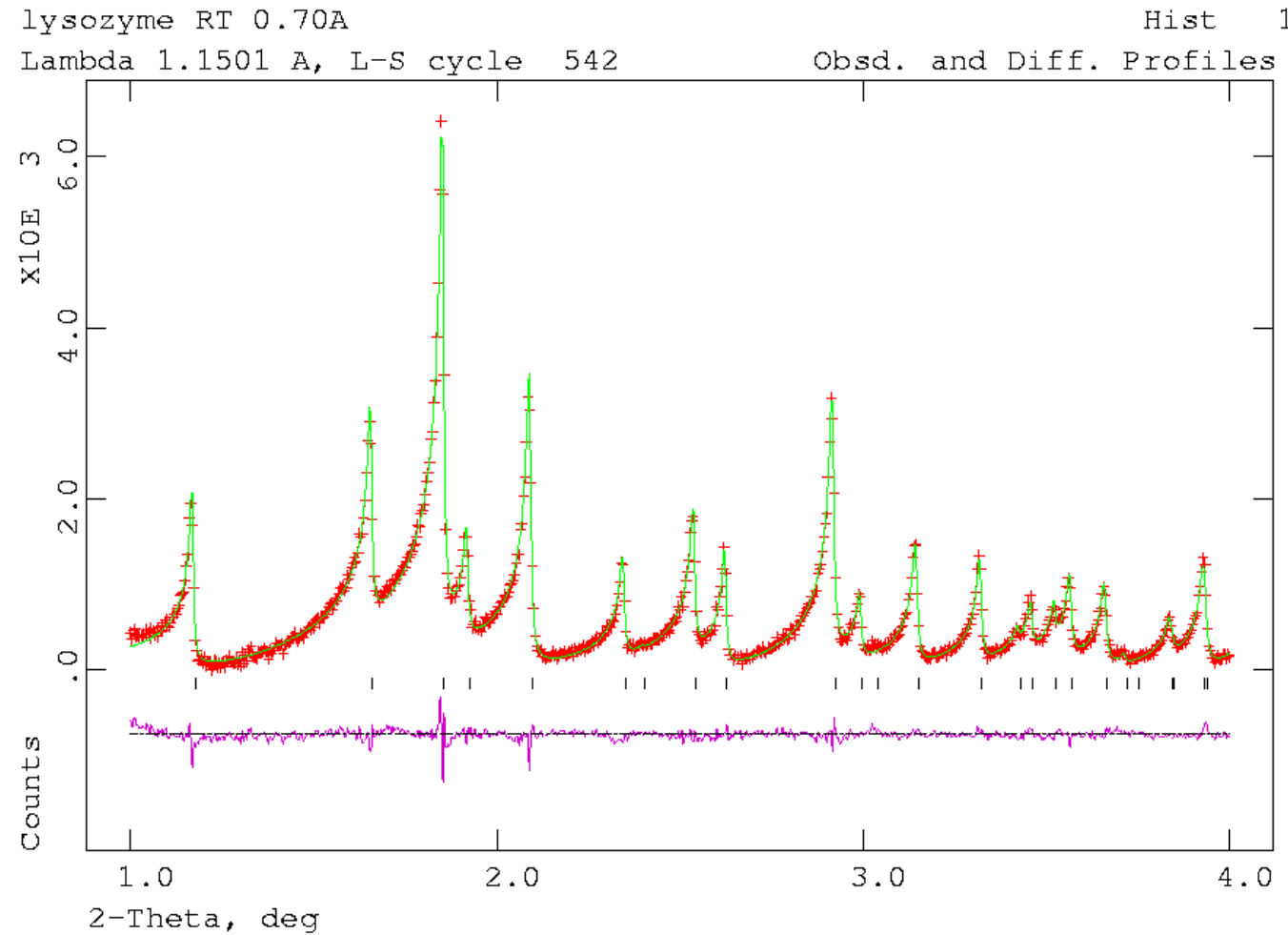
F^2_h - structure factor for particular reflection

m_h - reflection multiplicity

L_h - correction factors on intensity - texture, etc.

$P(D_h)$ - peak shape function – includes instrumental resolution, crystallite size, microstrain, etc.

How good is this function?



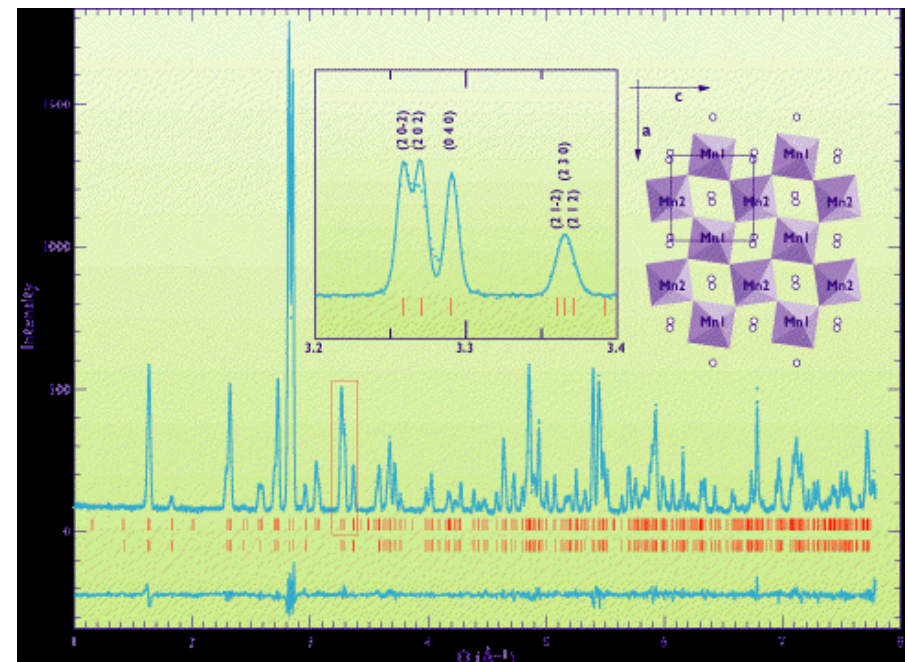
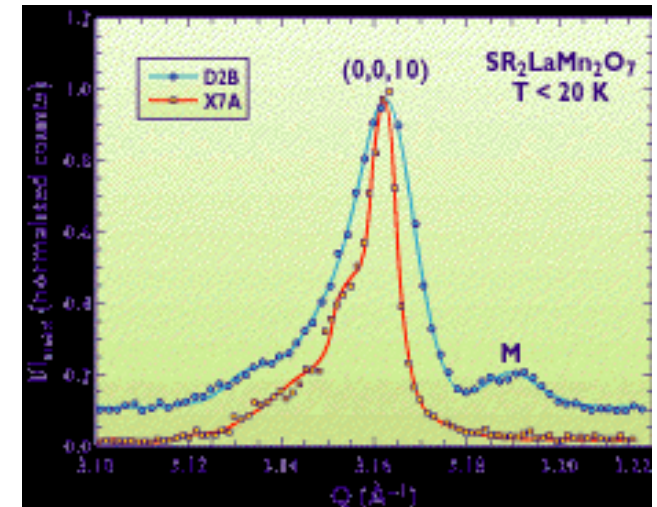
**Protein Rietveld refinement - Very low angle fit
1.0-4.0° peaks - strong asymmetry
“perfect” fit to shape**

Examples of Science using Powder Diffraction

- Refinement of structures of new materials
- Materials texture
- Strain measurements
- Pair distribution functions (PDF)

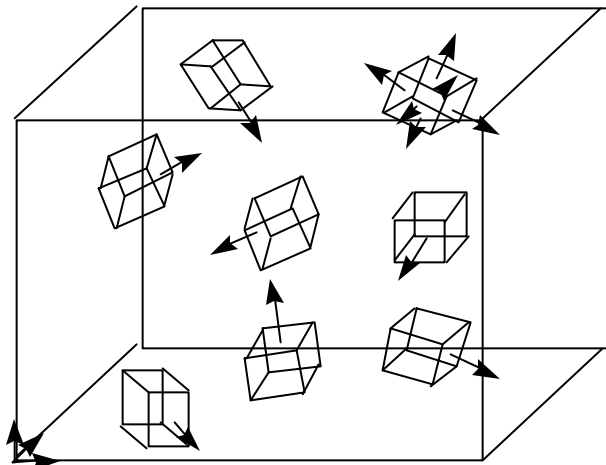
High-resolution Neutron Powder Diffraction in CMR manganates*

- In $\text{Sr}_2\text{LaMn}_2\text{O}_7$ – synchrotron data indicated two phases at low temperature. Simultaneous refinement of neutron powder data at 2 λ 's allowed two almost-isostructural phases (one FM the other AFM) to be refined. Only neutrons see the magnetic reflections
- High resolution powder diffraction with $\text{Nd}_{0.7}\text{Ca}_{0.3}\text{MnO}_3$ showed splitting of (202) peak due to a transition to a previously unknown monoclinic phase. The data showed the existence of 2 Mn sites with different Mn-O distances. The different sites are likely occupied by Mn^{3+} and Mn^{4+} respectively

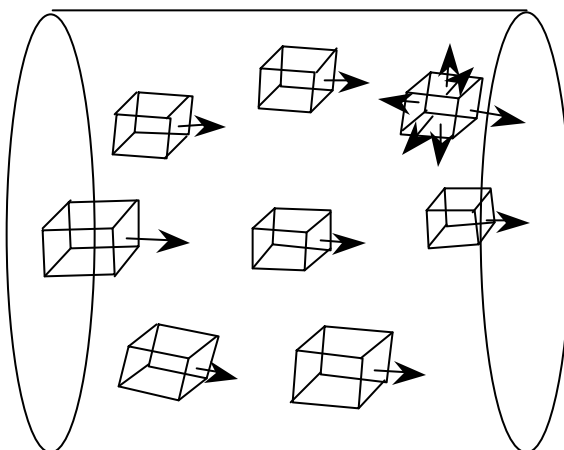


* E. Suard & P. G. Radaelli (ILL)

Texture: “Interesting Preferred Orientation”



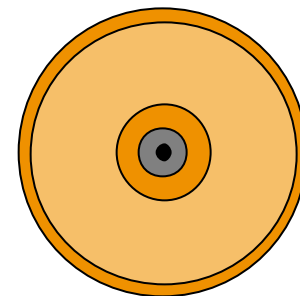
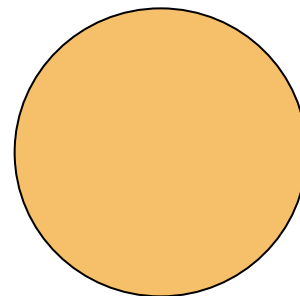
Loose powder



Metal wire

Random powder - all crystallite orientations equally probable - flat pole figure

Pole figure - stereographic projection of a crystal axis down some sample direction



(100) random texture

(100) wire texture

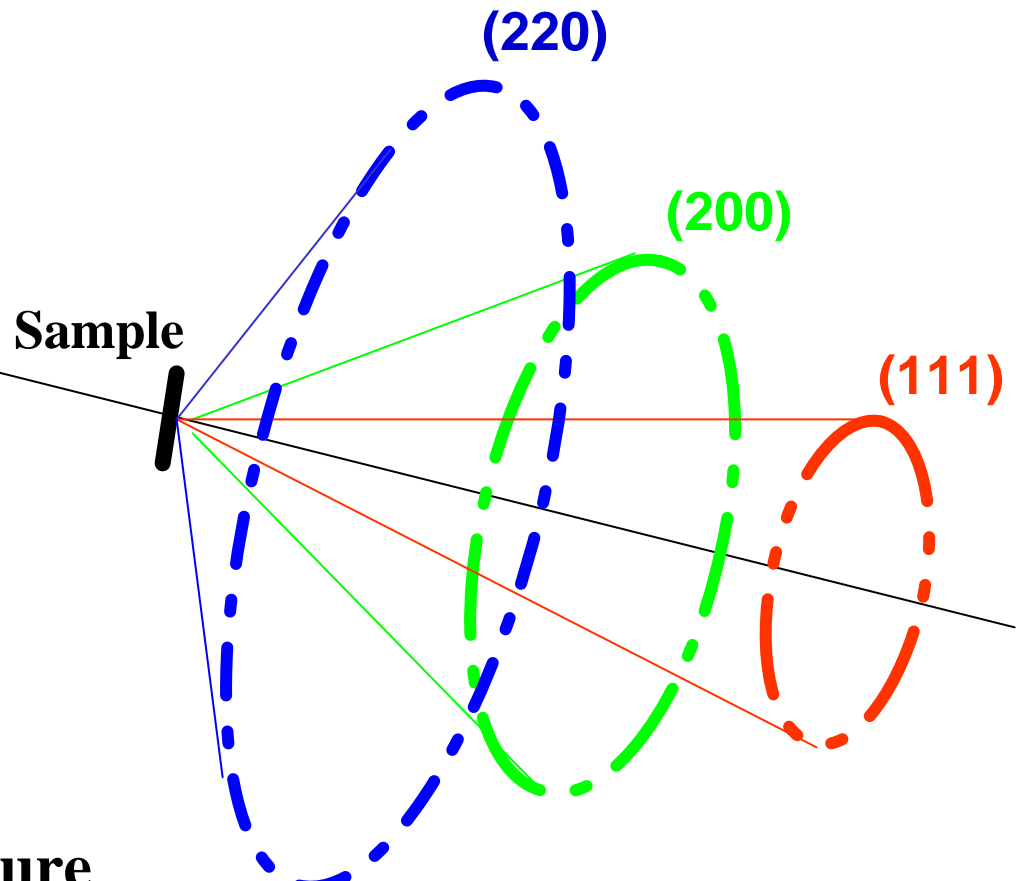
Crystallites oriented along wire axis - pole figure peaked in center and at the rim (100's are 90° apart)

Orientation Distribution Function - probability function for texture

Texture Measurement by Diffraction

Non-random crystallite orientations in sample

**Incident beam
x-rays or neutrons**



Debye-Scherrer cones

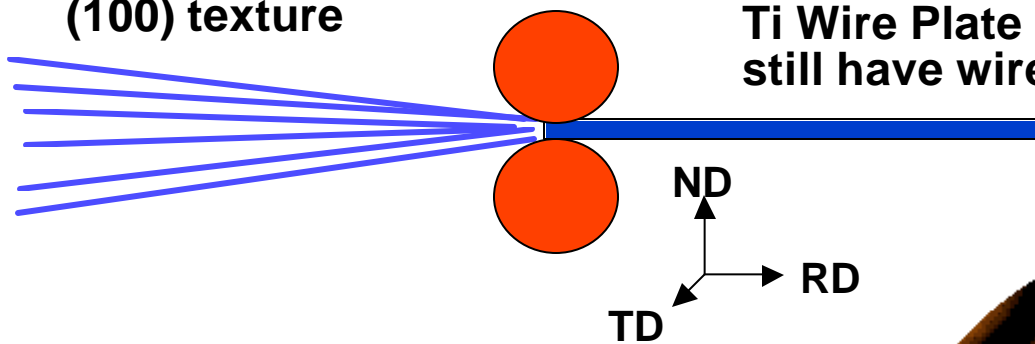
- uneven intensity due to texture
- different pattern of unevenness for different hkl's
- intensity pattern changes as sample is turned

Texture Determination of Titanium Wire Plate

(Wright-Patterson AFB/LANSCE Collaboration)

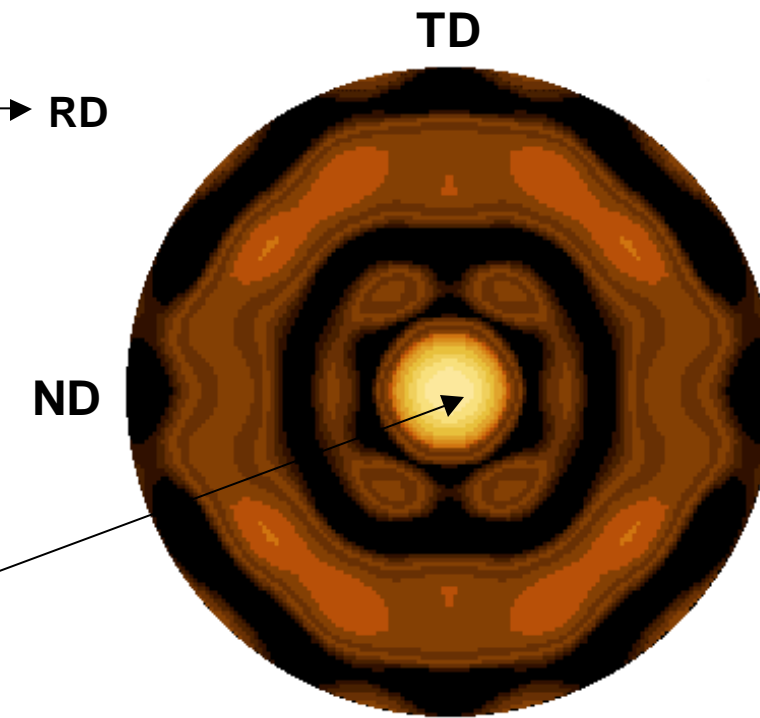
Possible “pseudo-single crystal” turbine blade material

Ti Wire -
(100) texture



Ti Wire Plate - does it
still have wire texture?

- Bulk measurement
- Neutron time-of-flight data
- Rietveld refinement of texture
- Spherical harmonics to $L_{\max} = 16$
- Very strong wire texture in plate



reconstructed (100) pole figure

Definitions of Stress and Strain

- Macroscopic strain – total strain measured by an extensometer
- Elastic lattice strain – response of lattice planes to applied stress, measured by diffraction

$$e_{hkl} = \frac{d_{hkl} - d_0}{d_0}$$

- Intergranular strain – deviation of elastic lattice strain from linear behavior

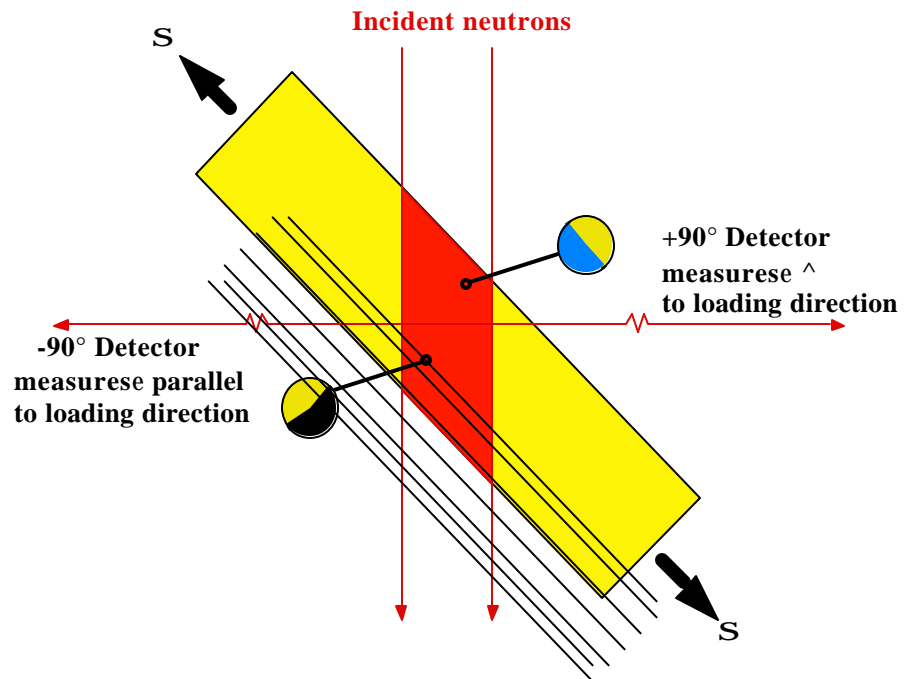
$$e_I = e_{hkl} - \frac{S_{\text{applied}}}{E_{hkl}}$$

- Residual strains – internal strains present with no applied force
- Thermal residual strains – strains that develop on cooling from processing temperature due to anisotropic coefficients of thermal expansion

Neutron Diffraction Measurements of Lattice Strain*



The Neutron Powder
Diffractometer at LANSCE



Neutron measurements :-

- **Non destructive, bulk, phase sensitive**
- **Time consuming, Limited spatial resolution**

* Discussion of residual strain adapted from viewgraphs by M. Bourke (LANSCE)

Why use Metal Matrix Composites ?



↑ F117 (JSF)
↓ Landing Gear



Higher Pay Loads
High temperatures
High pressures
Reduced Engine Weights
Reduced Fuel Consumption
Better Engine Performance



National AeroSpace Plane
Engine

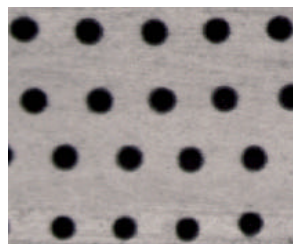
MMC Applications

Rotors
Fan Blades
Structural Rods
Impellers
Landing Gears

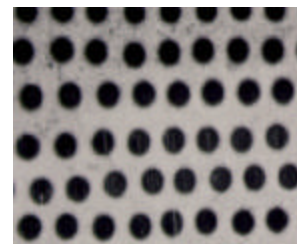


W-Fe :- Fabrication, Microstructure & Composition

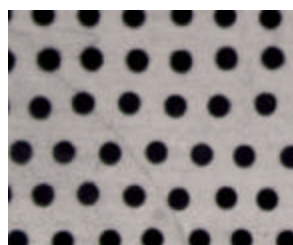
- **200 mm diameter continuous Tungsten fibers,**
- **Hot pressed at 1338 K for 1 hour into Kanthal (73 Fe, 21 Cr, 6 Al wt%) – leads to residual strains after cooling**
- **Specimens :- 200 * 25 * 2.5 mm³**



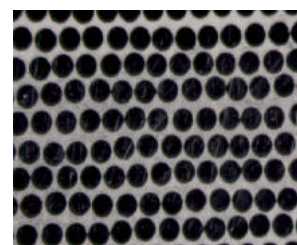
10 vol.%



30 vol.%

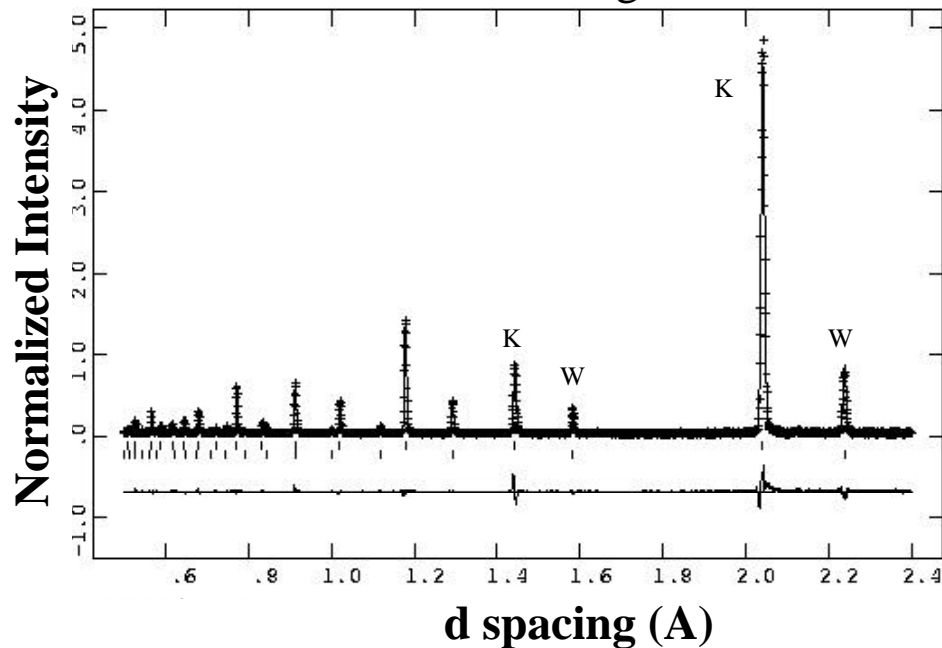


20 vol.%

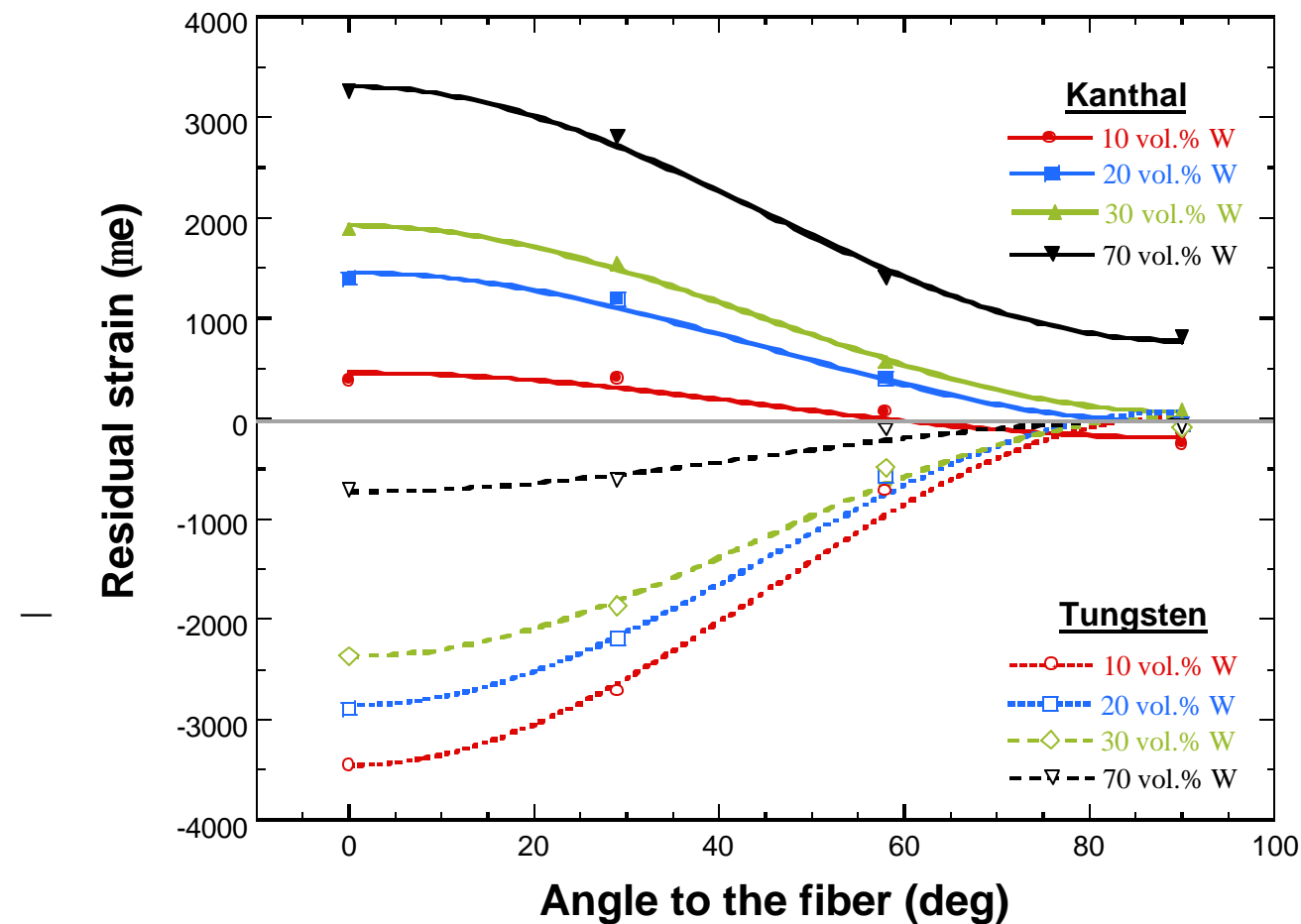


70 vol.%

Powder diffraction data includes Bragg peaks from both Kanthal and Tungsten.



Neutron Diffraction Measures Mean Residual Phase Strains when Results for a MMC are compared to an Undeformed Standard

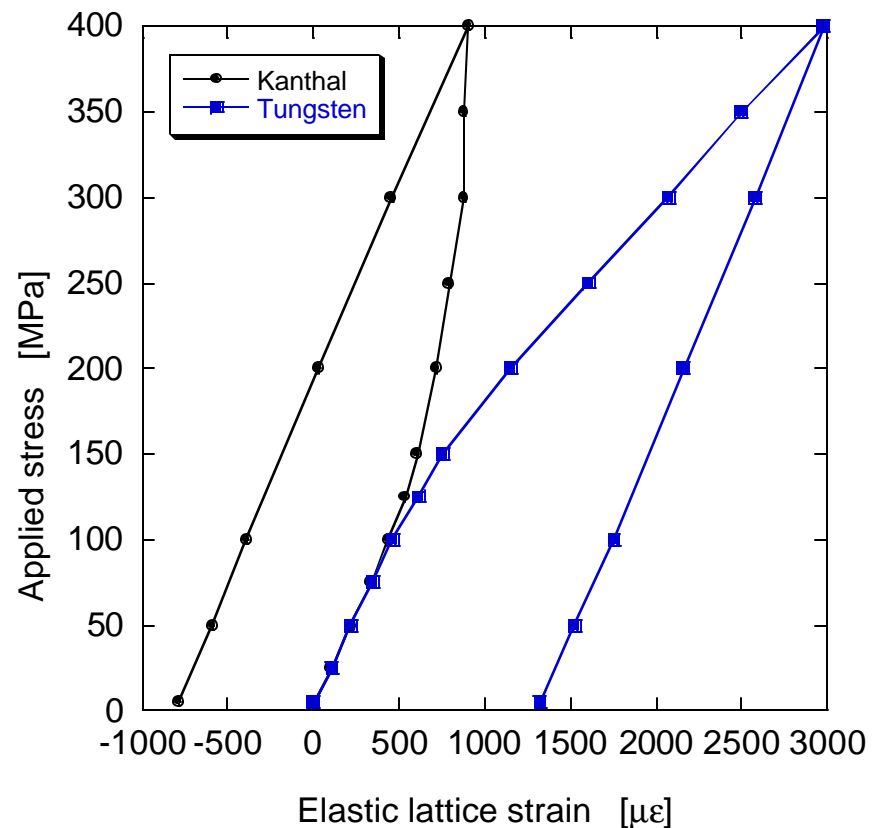


Symbols show data points

Curves are fits of the form $\langle e \rangle = \langle e_{11} \rangle \cos^2 a + \langle e_{22} \rangle \sin^2 a$

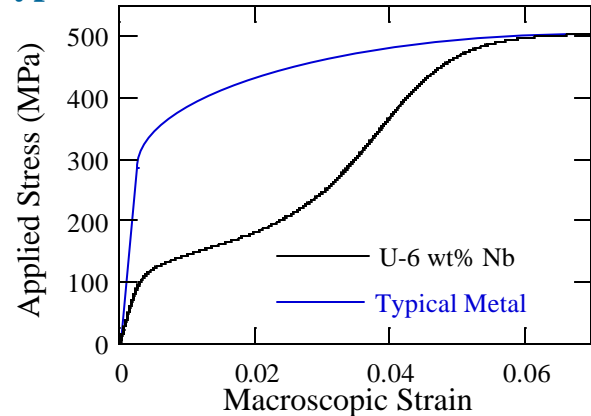
Load Sharing in MMCs can also be Measured by Neutron Diffraction

- Initial co-deformation results from confinement of W fibers by the Kanthal matrix
- Change of slope (125 MPa) is the typical load sharing behavior of MMCs:
 - Kanthal yields and ceases to bear further load
 - Tungsten fibers reinforce and strengthen the composite

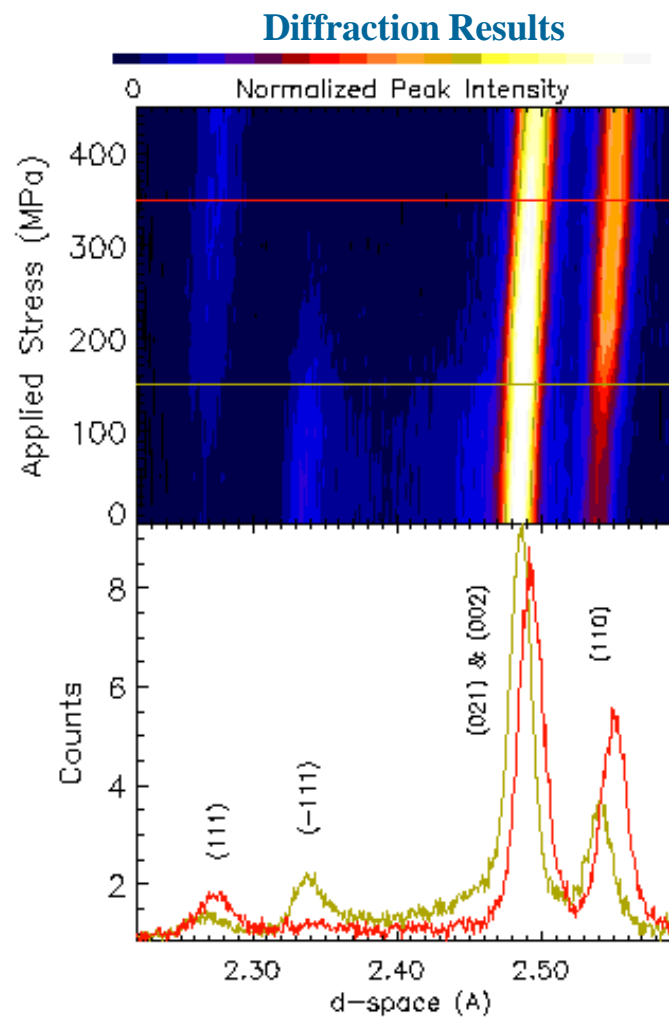
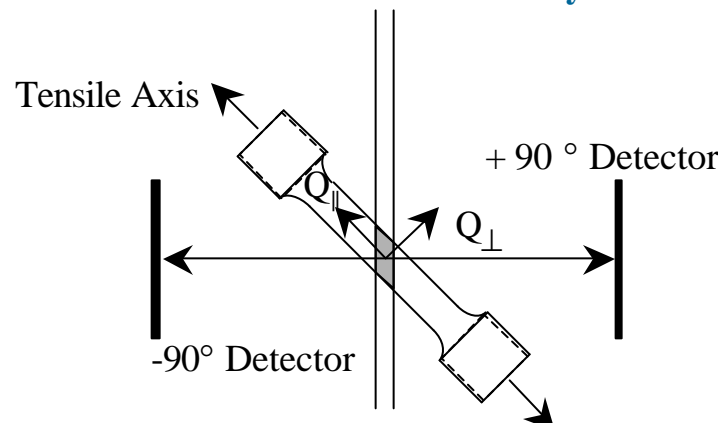


Deformation Mechanism in U/Nb Alloys

Atypical “Double Plateau Stress Strain Curve.



NPD Diffraction Geometry



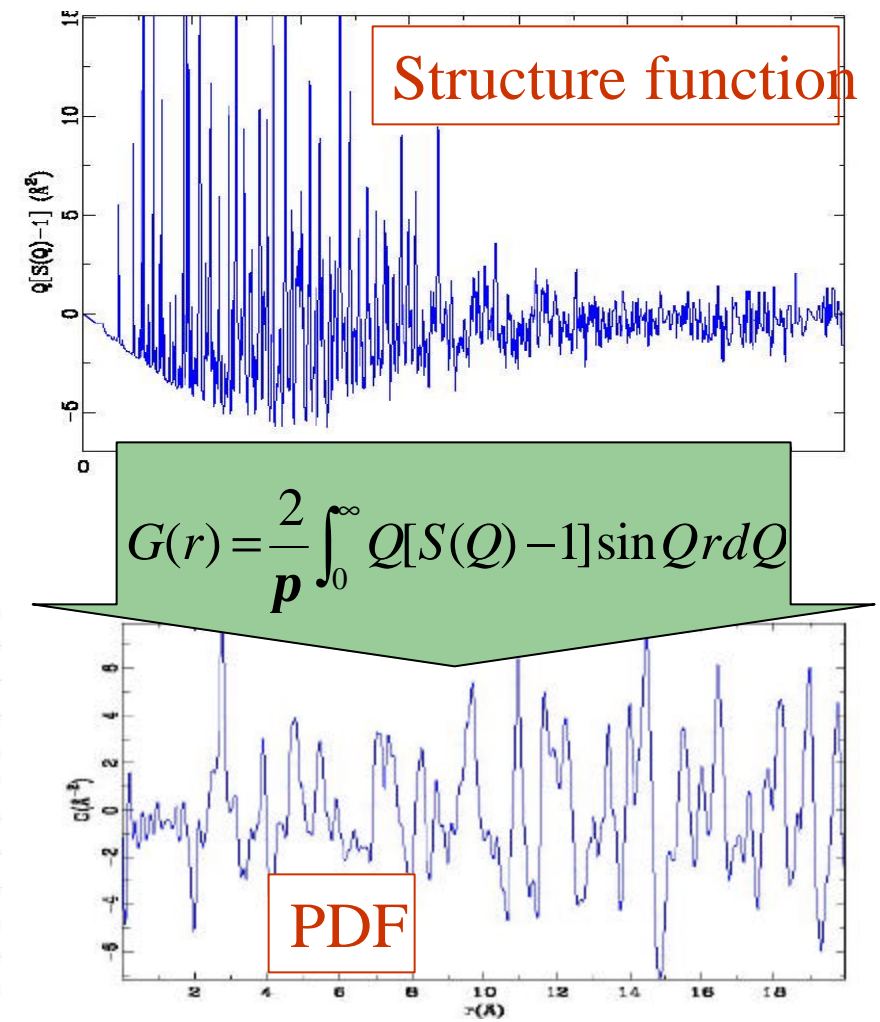
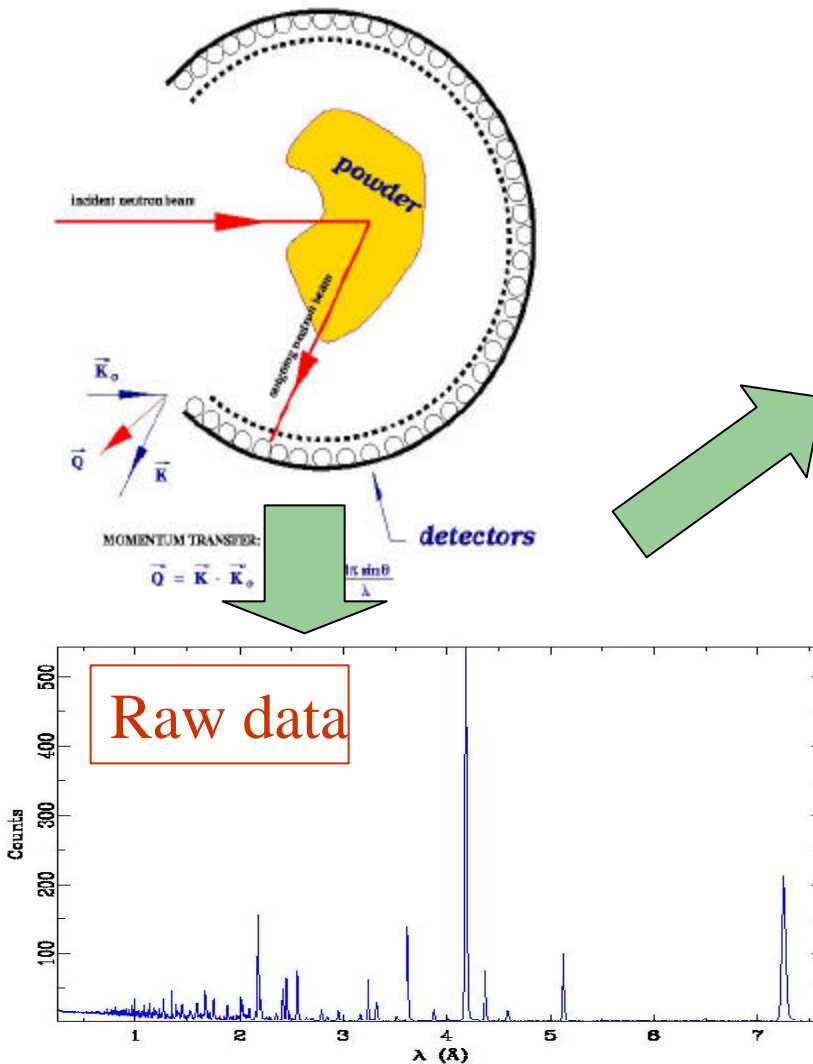
- Important Programmatic Answers.

1. Material is Single Phase Monoclinic (a'').
2. Lack of New Peaks Rules out Stress Induced Phase Transition.
3. Changes in Peak Intensity Indicate That Twinning is the Deformation Mechanism.

Pair Distribution Functions

- Modern materials are often disordered.
- Standard crystallographic methods lose the aperiodic (disorder) information.
- We would like to be able to **sit on an atom and look at our neighborhood**.
- The **PDF method** allows us to do that (see next slide):
 - First we do a neutron or x-ray diffraction experiment
 - Then we correct the data for experimental effects
 - Then we Fourier transform the data to real-space

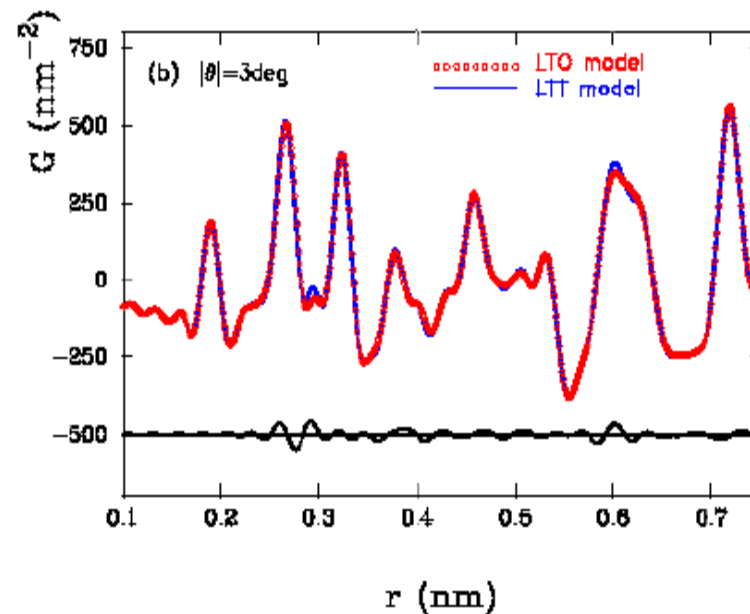
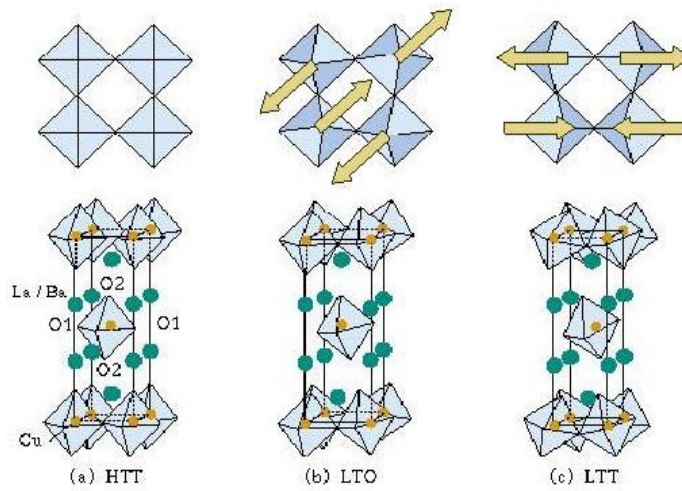
Obtaining the Pair Distribution Function*



* See <http://www.pa.msu.edu/cmp/billinge-group/>

Structure and PDF of a High Temperature Superconductor

The structure of $\text{La}_{2-x}\text{Sr}_x\text{CuO}_4$ looks like this: (copper [orange] sits in the middle of octahedra of oxygen ions [shown shaded with pale blue].)

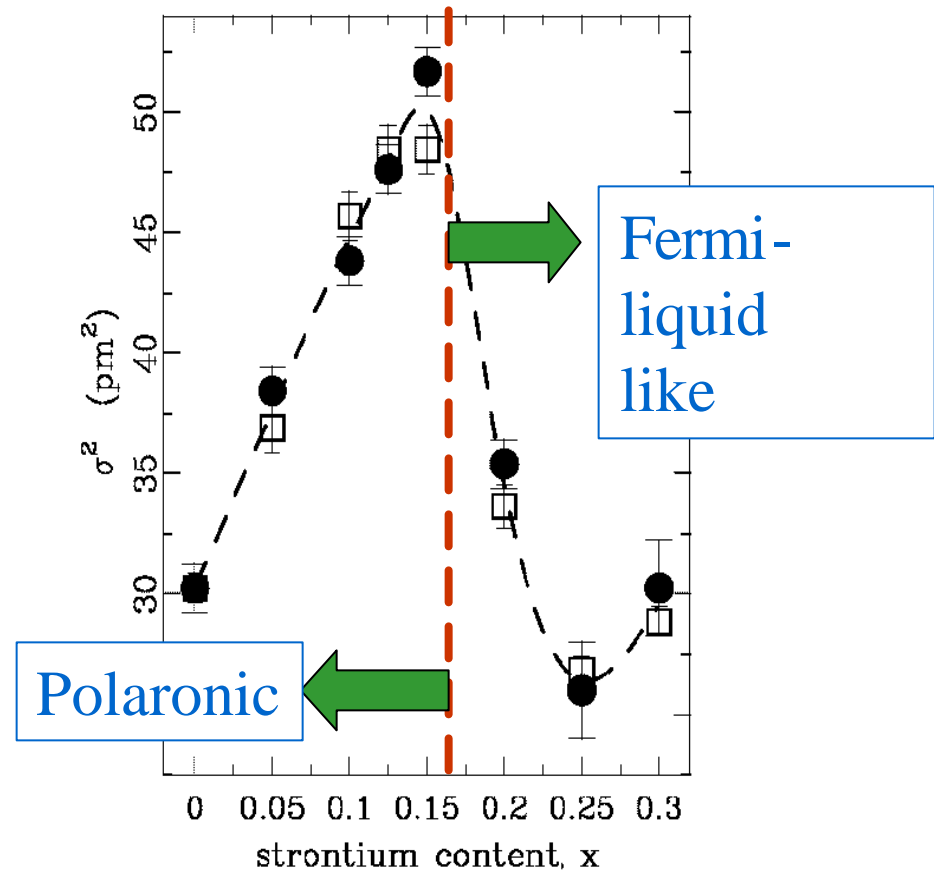


The resulting PDFs look like this.
The peak at 1.9\AA is the Cu-O bond.

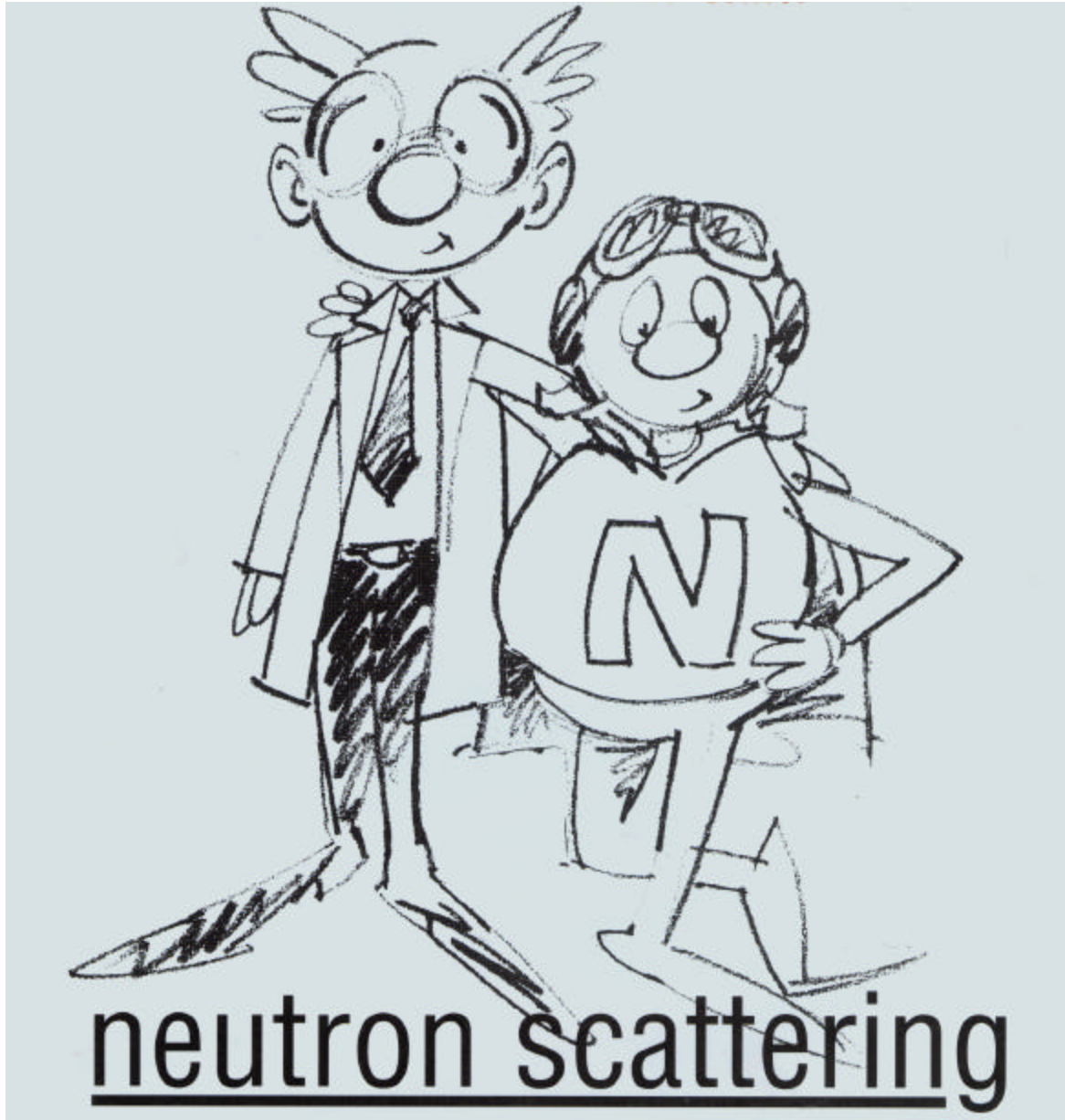
So what can we learn about charge-stripes from the PDF?

Effect of Doping on the Octahedra

- Doping holes (positive charges) by adding Sr shortens Cu-O bonds
- Localized holes in stripes implies a coexistence of short and long Cu-O in-plane bonds => increase in Cu-O bond distribution width with doping.
- We see this in the PDF: σ^2 is the **width of the CuO bond distribution** which increases with doping then decreases beyond optimal doping



Bozin *et al.* Phys. Rev. Lett. Submitted;
cond-mat/9907017



neutron scattering

LECTURE 3: Surface Reflection

by

Roger Pynn

Los Alamos
National Laboratory

Surface Reflection Is Very Different From Most Neutron Scattering

- We worked out the neutron cross section by adding scattering from different nuclei
 - We ignored double scattering processes because these are usually very weak
- This approximation is called the Born Approximation
- Below an angle of incidence called the critical angle, neutrons are perfectly reflected from a smooth surface
 - This is NOT weak scattering and the Born Approximation is not applicable to this case
- Specular reflection is used:
 - In neutron guides
 - In multilayer monochromators and polarizers
 - To probe surface and interface structure in layered systems

This Lecture

- Reflectivity measurements
 - Neutron wavevector inside a medium
 - Reflection by a smooth surface
 - Reflection by a film
 - The kinematic approximation
 - Graded interface
 - Science examples
 - Polymers & vesicles on a surface
 - Lipids at the liquid air interface
 - Boron self-diffusion
 - Iron on MgO
 - Rough surfaces
 - Shear aligned worm-like micelles

What Is the Neutron Wavevector Inside a Medium?

Comparing our expression for $S(Q)$ with that given by Fermi's Golden Rule, the

nucleus - neutron potential is given by : $V(\vec{r}) = \frac{2\mathbf{p}\hbar^2}{m} b\mathbf{d}(\vec{r})$ for a single nucleus.

So the average potential inside the medium is : $\bar{V} = \frac{2\mathbf{p}\hbar^2}{m} \mathbf{r}$ where $\mathbf{r} = \frac{1}{volume} \sum_i b_i$

\mathbf{r} is called the nuclear Scattering Length Density (SLD)

The neutron obeys Schrodinger's equation :

$$[\nabla^2 + 2m(E - \bar{V})/\hbar^2] \mathbf{y}(r) = 0$$

in *vacuo* $\mathbf{y}(r) = e^{i\vec{k}_0 \cdot \vec{r}}$ so $k_0^2 = 2mE/\hbar^2$. Similarly $k^2 = 2m(E - \bar{V})/\hbar^2 = k_0^2 - 4\mathbf{p}\mathbf{r}$

where k_0 is neutron wavevector in *vacuo* and k is the wavevector in a material

Since $k/k_0 = n$ = refractive index (by definition), and \mathbf{r} is very small ($\sim 10^{-6} \text{ A}^{-2}$) we get :

$$n = 1 - \mathbf{I}^2 \mathbf{r} / 2\mathbf{p}$$

Since generally $n < 1$, neutrons are externally reflected from most materials.

Typical Values

- Let us calculate the scattering length density for quartz – SiO_2
- Density is 2.66 gm.cm^{-3} ; Molecular weight is $60.08 \text{ gm. mole}^{-1}$
- Number of molecules per $\text{\AA}^3 = N = 10^{-24}(2.66/60.08)*N_{\text{avagadro}}$
 $= 0.0267 \text{ molecules per } \text{\AA}^3$
- $\rho = \Sigma b/\text{volume} = N(b_{\text{Si}} + 2b_{\text{O}}) = 0.0267(4.15 + 11.6) 10^{-5} \text{\AA}^{-2} = 4.21 \times 10^{-6} \text{\AA}^{-2}$
- This means that the refractive index $n = 1 - \lambda^2 2.13 \times 10^{-7}$ for quartz
- To make a neutron “bottle” out of quartz we require $k= 0$ i.e.
 $k_0^2 = 4\pi\rho$ or $\lambda = (\pi/\rho)^{1/2}$.
- Plugging in the numbers -- $\lambda = 864 \text{\AA}$ or a neutron velocity of
4.6 m/s (you could out-run it!)

Only Those Thermal or Cold Neutrons With Very Low Velocities Perpendicular to a Surface Are Reflected

$$k / k_0 = n$$

The surface cannot change the neutron velocity parallel to the surface so :

$$k_0 \cos \mathbf{a} = k \cos \mathbf{a}' = k_0 n \cos \mathbf{a}' \quad \text{i.e. } n = \cos \mathbf{a} / \cos \mathbf{a}'$$

Neutrons obey Snell's Law

Since $k^2 = k_0^2 - 4pr$ $k^2(\cos^2 \mathbf{a}' + \sin^2 \mathbf{a}') = k_0^2(\cos^2 \mathbf{a} + \sin^2 \mathbf{a}) - 4pr$

i.e. $k^2 \sin^2 \mathbf{a}' = k_0^2 \sin^2 \mathbf{a} - 4pr$ or $k_z^2 = k_{0z}^2 - 4pr$

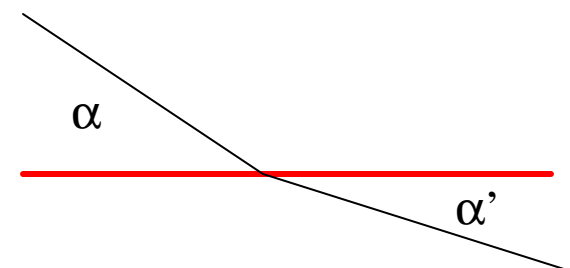
The critical value of k_{0z} for total external reflection is $k_{0z} = \sqrt{4pr}$

For quartz $k_{0z}^{critical} = 2.05 \times 10^{-3} \text{ \AA}^{-1}$

$$(2p / I) \sin \mathbf{a}_{critical} = k_{0z}^{critical} \Rightarrow$$

$$\mathbf{a}_{critical} (^\circ) \approx 0.02I (A) \text{ for quartz}$$

Note : $\mathbf{a}_{critical} (^\circ) \approx 0.1I (A)$ for nickel



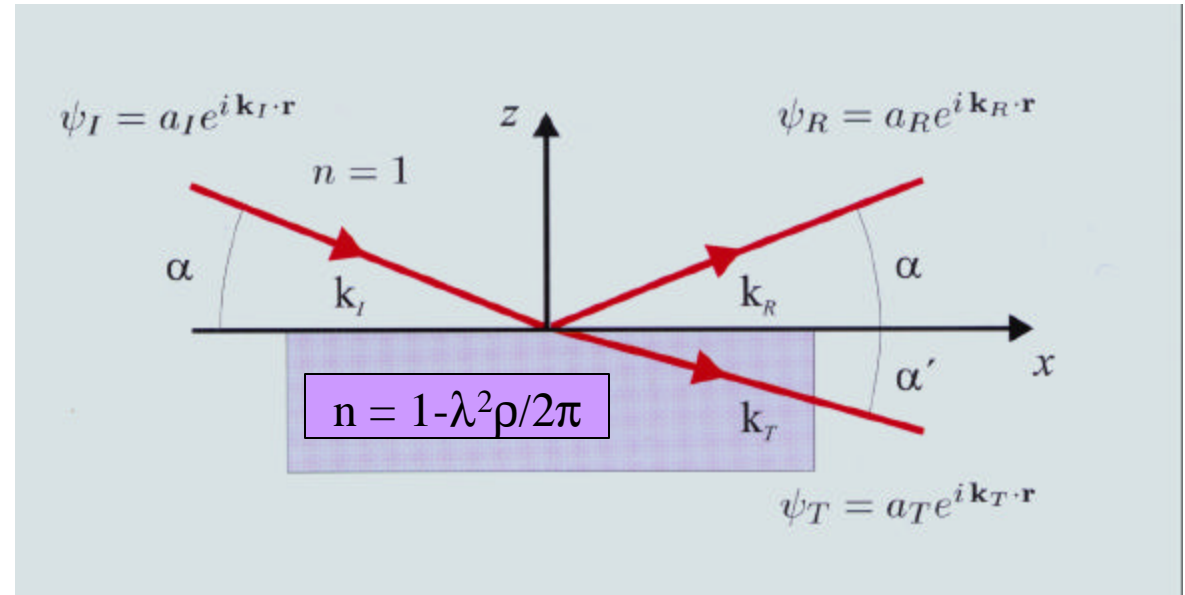
Reflection of Neutrons by a Smooth Surface: Fresnel's Law

continuity

of \mathbf{y} & $\dot{\mathbf{y}}$ at $z = 0 \Rightarrow$

$$a_I + a_R = a_T \quad (1)$$

$$a_I \vec{k}_I + a_R \vec{k}_R = a_T \vec{k}_T$$



components perpendicular and parallel to the surface :

$$a_I k \cos \mathbf{a} + a_R k \cos \mathbf{a} = a_T n k \cos \mathbf{a}' \quad (2)$$

$$-(a_I - a_R) k \sin \mathbf{a} = -a_T n k \sin \mathbf{a}' \quad (3)$$

(1) & (2) \Rightarrow Snell's Law : $\boxed{\cos \mathbf{a} = n \cos \mathbf{a}'}$

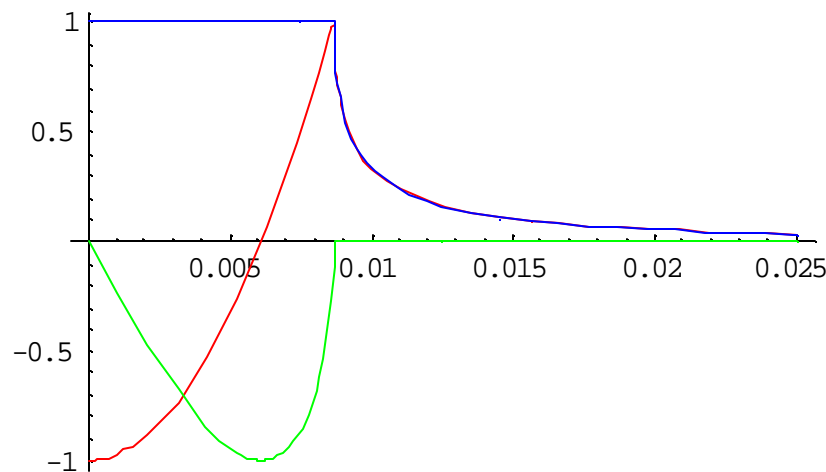
$$(1) \& (3) \Rightarrow \frac{(a_I - a_R)}{(a_I + a_R)} = n \frac{\sin \mathbf{a}'}{\sin \mathbf{a}} \approx \frac{\sin \mathbf{a}'}{\sin \mathbf{a}} = \frac{k_{Tz}}{k_{Iz}}$$

so reflectance is given by

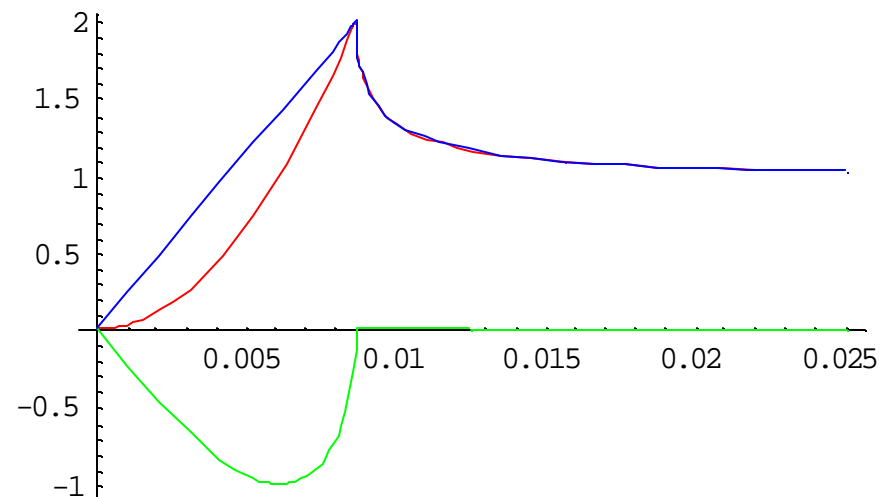
$$\boxed{r = a_R / a_I = (k_{Iz} - k_{Tz}) / (k_{Iz} + k_{Tz})}$$

What do the Amplitudes a_R and a_T Look Like?

- For reflection from a flat substrate, both a_R and a_T are complex when $k_0 < 4\pi\rho$ i.e. below the critical edge. For $a_i = 1$, we find:

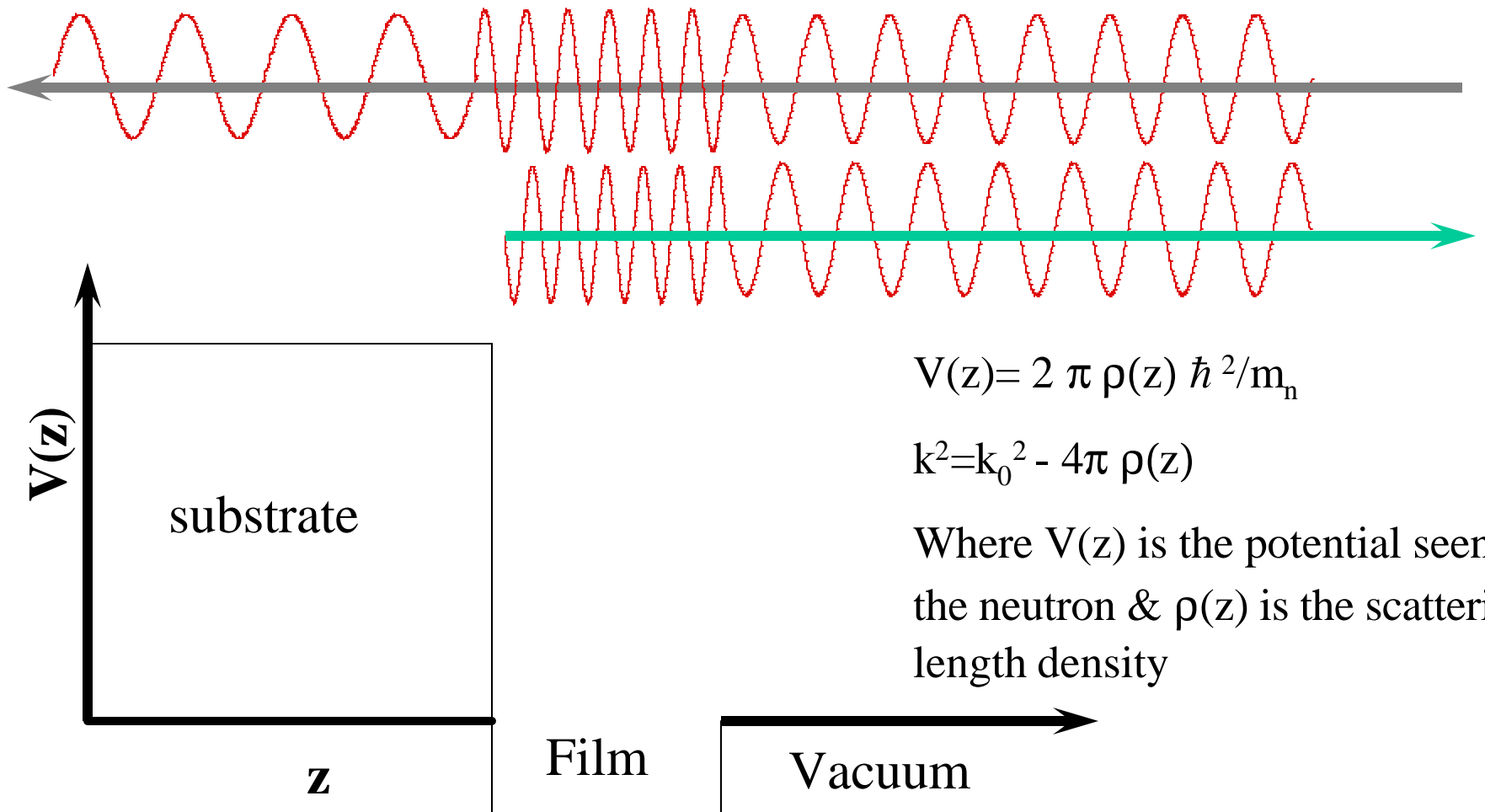


Real (red) & imaginary (green) parts of a_R plotted against k_0 . The modulus of a_R is plotted in blue. The critical edge is at $k_0 \sim 0.009 \text{ \AA}^{-1}$. Note that the reflected wave is completely out of phase with the incident wave at $k_0 = 0$



Real (red) and imaginary (green) parts of a_T . The modulus of a_T is plotted in blue. Note that a_T tends to unity at large values of k_0 as one would expect

One can also think about Neutron Reflection from a Surface as a 1-d Problem

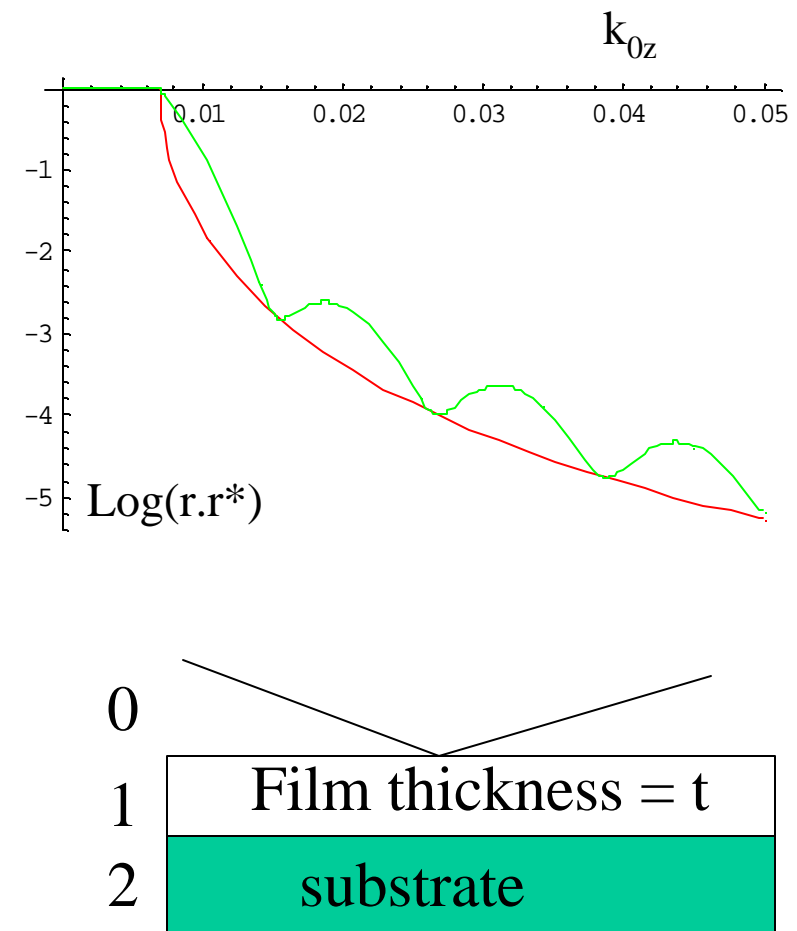


Fresnel's Law for a Thin Film

- $r = (k_{1z} - k_{0z}) / (k_{1z} + k_{0z})$ is Fresnel's law
- Evaluate with $\rho = 4.10^{-6} \text{ A}^{-2}$ gives the red curve with critical wavevector given by $k_{0z} = (4\pi\rho)^{1/2}$
- If we add a thin layer on top of the substrate we get interference fringes & the reflectance is given by:

$$r = \frac{r_{01} + r_{12} e^{i2k_{1z}t}}{1 + r_{01} r_{12} e^{i2k_{1z}t}}$$

and we measure the reflectivity $R = r.r^*$



- If the film has a higher scattering length density than the substrate we get the green curve (if the film scattering is weaker than the substance, the green curve is below the red one)
- The fringe spacing at large k_{0z} is $\sim \pi/t$ (a 250 Å film was used for the figure)

Kinematic (Born) Approximation

- We defined the scattering cross section in terms of an incident plane wave & a **weakly** scattered spherical wave (called the Born Approximation)
- This picture is not correct for surface reflection, except at large values of Q_z
- For large Q_z , one may use the definition of the scattering cross section to calculate R for a flat surface (in the Born Approximation) as follows:

$$R = \frac{\text{number of neutrons reflected by a sample of size } L_x L_y}{\text{number of neutrons incident on sample } (= \Phi L_x L_y \sin a)}$$

$$= \frac{s}{L_x L_y \sin a} = \frac{1}{L_x L_y \sin a} \int \frac{dS}{d\Omega} d\Omega = \frac{1}{L_x L_y \sin a} \int \frac{ds}{d\Omega} \frac{dk_x dk_y}{k_0^2 \sin a}$$

because $k_x = k_0 \cos a$ so $dk_x = -k_0 \sin a da$.

From the definition of a cross section we get for a smooth substrate :

$$\frac{dS}{d\Omega} = \mathbf{r}^2 \int d\vec{r} \int d\vec{r}' e^{i\vec{Q} \cdot (\vec{r} - \vec{r}')} = \mathbf{r}^2 \frac{4\mathbf{p}^2}{Q_z^2} L_x L_y \mathbf{d}(Q_x) \mathbf{d}(Q_y) \text{ so } R = 16\mathbf{p}^2 \mathbf{r}^2 / Q_z^4$$

It is easy to show that this is the same as the Fresnel form at large Q_z

Reflection by a Graded Interface

Repeating the bottom line of the previous viewgraph but keeping the z - dependence

$$\text{of } \mathbf{r} \text{ gives : } R = \frac{16\mathbf{p}^2}{Q_z^2} \left| \int \mathbf{r}(z) e^{iQ_z z} dz \right|^2 = \frac{16\mathbf{p}^2}{Q_z^4} \left| \int \frac{d\mathbf{r}(z)}{dz} e^{iQ_z z} dz \right|^2 \text{ where the second}$$

equality follows after intergrating by parts.

If we replace the prefactor by the Fresnel reflectivity R_F , we get the right answer for a smooth interface, as well as the correct form at large Q_z

$$R = R_F \left| \int \frac{d\mathbf{r}(z)}{dz} e^{iQ_z z} dz \right|^2$$

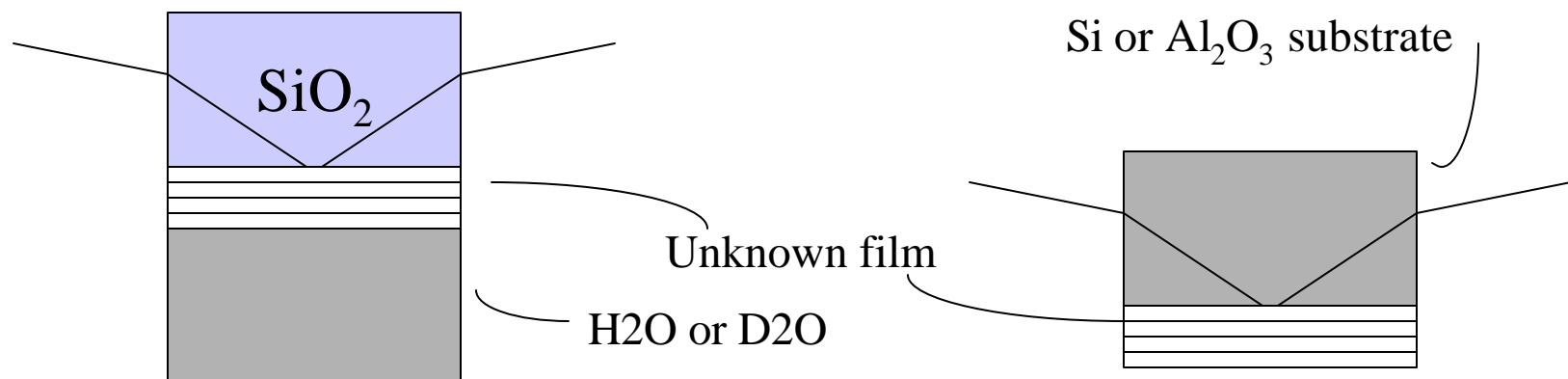
This can be solved analytically for several convenient forms of $d\mathbf{r}/dz$ such as $1/\cosh^2(z)$. This approximate equation illustrates an important point : reflectivity data cannot be inverted uniquely to obtain $\mathbf{r}(z)$, because we generally lack important phase information. This means that models refined to fit refelctivity data must have good physical justification.

The Goal of Reflectivity Measurements Is to Infer a Density Profile Perpendicular to a Flat Interface

- In general the results are not unique, but independent knowledge of the system often makes them very reliable
- Frequently, layer models are used to fit the data
- Advantages of neutrons include:
 - Contrast variation (using H and D, for example)
 - Low absorption – probe buried interfaces, solid/liquid interfaces etc
 - Non-destructive
 - Sensitive to magnetism
 - Thickness length scale 10 – 5000 Å

Direct Inversion of Reflectivity Data is Possible*

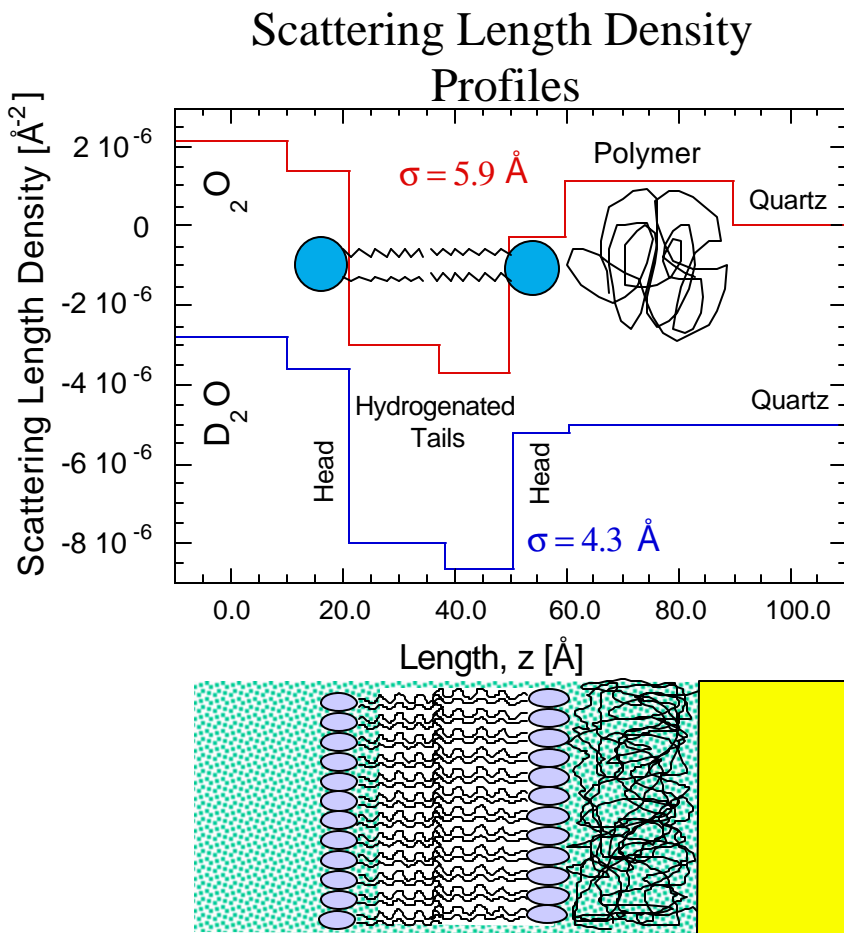
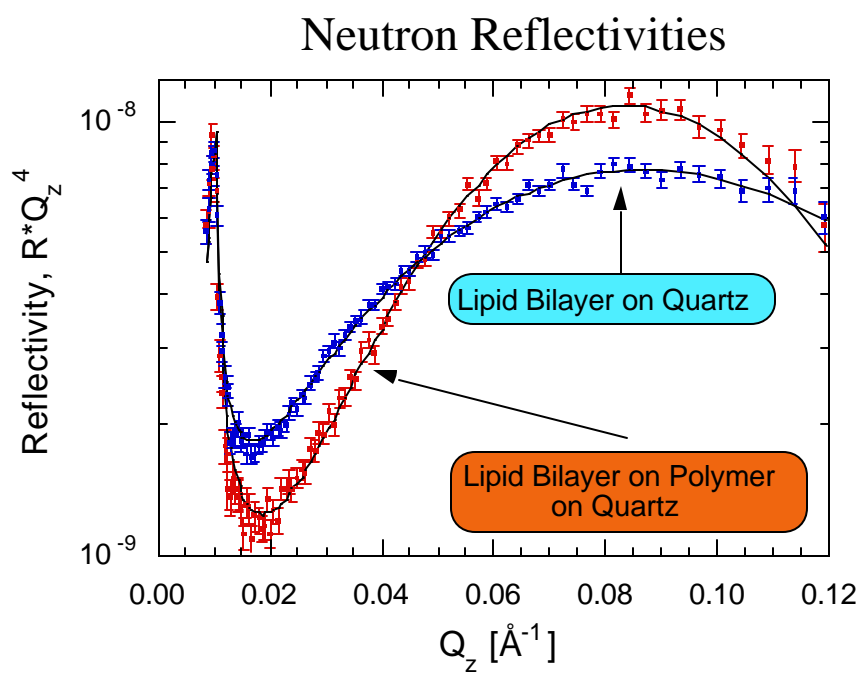
- Use different “fronting” or “backing” materials for two measurement of the same unknown film
 - E.g. D₂O and H₂O “backings” for an unknown film deposited on a quartz substrate or Si & Al₂O₃ as substrates for the same unknown sample
 - Allows Re(R) to be obtained from two simultaneous equations for $|R_1|^2$ and $|R_2|^2$
 - Re(R) can be Fourier inverted to yield a unique SLD profile
- Another possibility is to use a magnetic “backing” and polarized neutrons



* Majkrzak et al Biophys Journal, 79,3330 (2000)

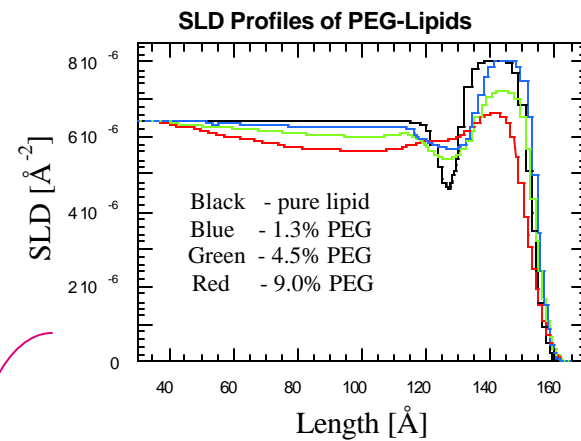
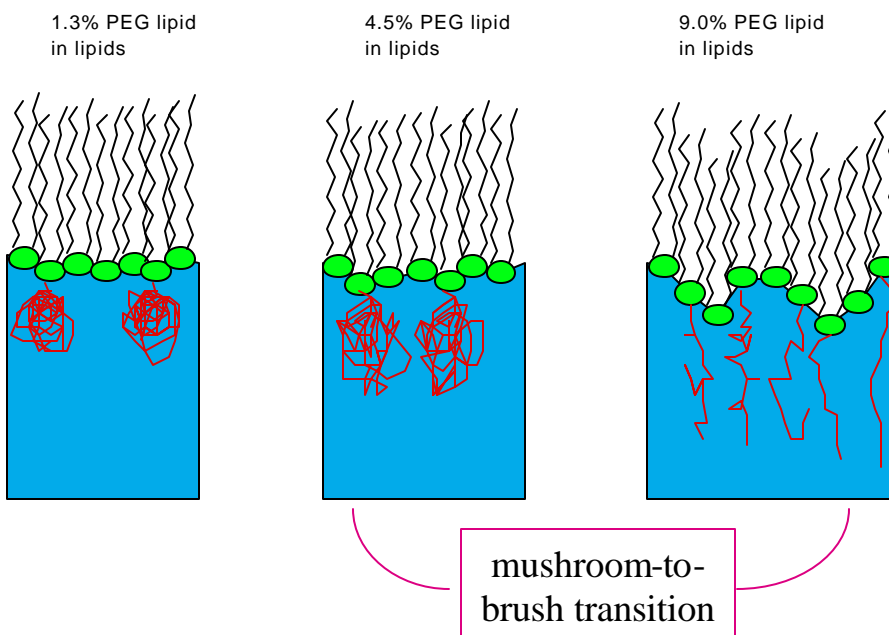
Vesicles composed of DMPC molecules fuse creating almost a perfect lipid bilayer when deposited on the pure, uncoated quartz block*
 (blue curves)

When PEI polymer was added only after quartz was covered by the lipid bilayer, the PEI appeared to diffuse under the bilayer (red curves)

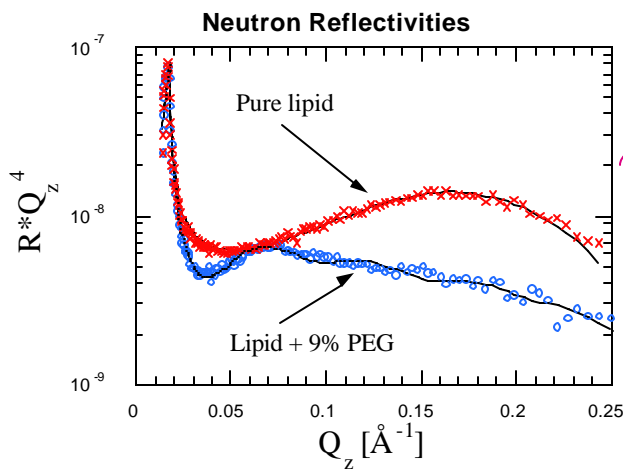


* Data courtesy of G. Smith (LANSCE)

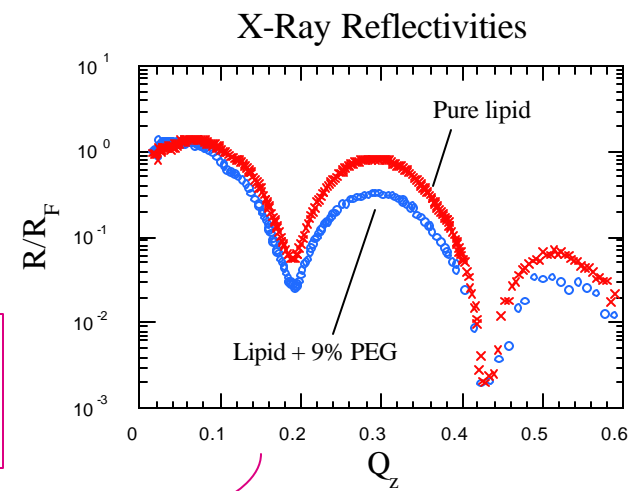
Polymer-Decorated Lipids at a Liquid-Air Interface*



Interface broadens as PEG concentration increases - this is main effect seen with x-rays



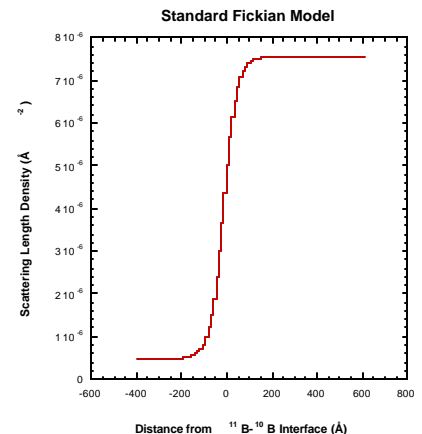
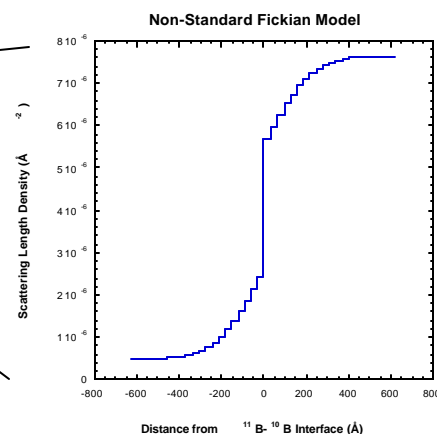
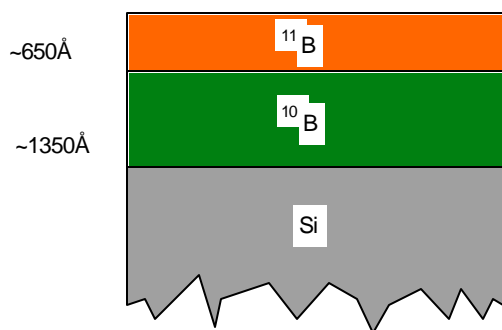
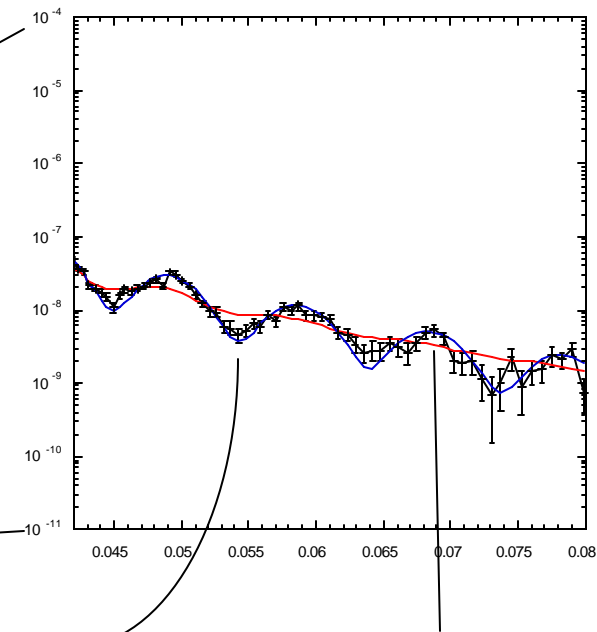
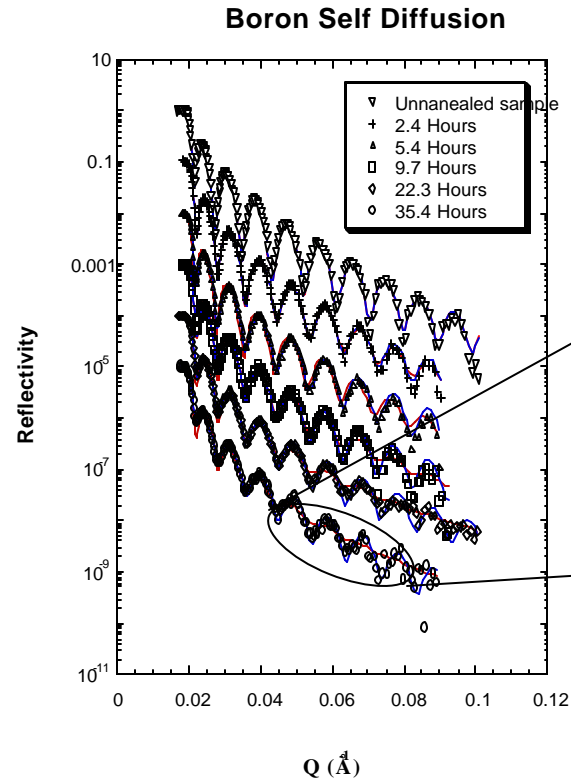
neutrons see contrast between heads (2.6), tails (-0.4), D₂O (6.4) & PEG (0.24)



x-rays see heads (0.65), but all else has same electron density within 10% (-0.33)

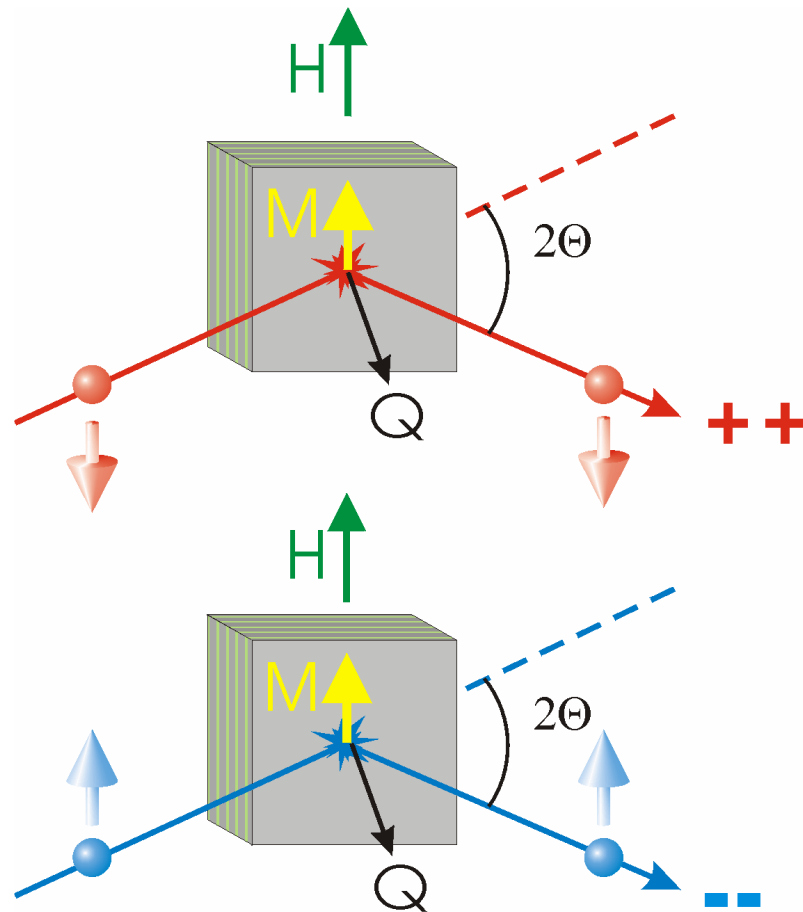
*Data courtesy of G. Smith (LANSCE)

Non-Fickian Boron Self-Diffusion at an Interface*



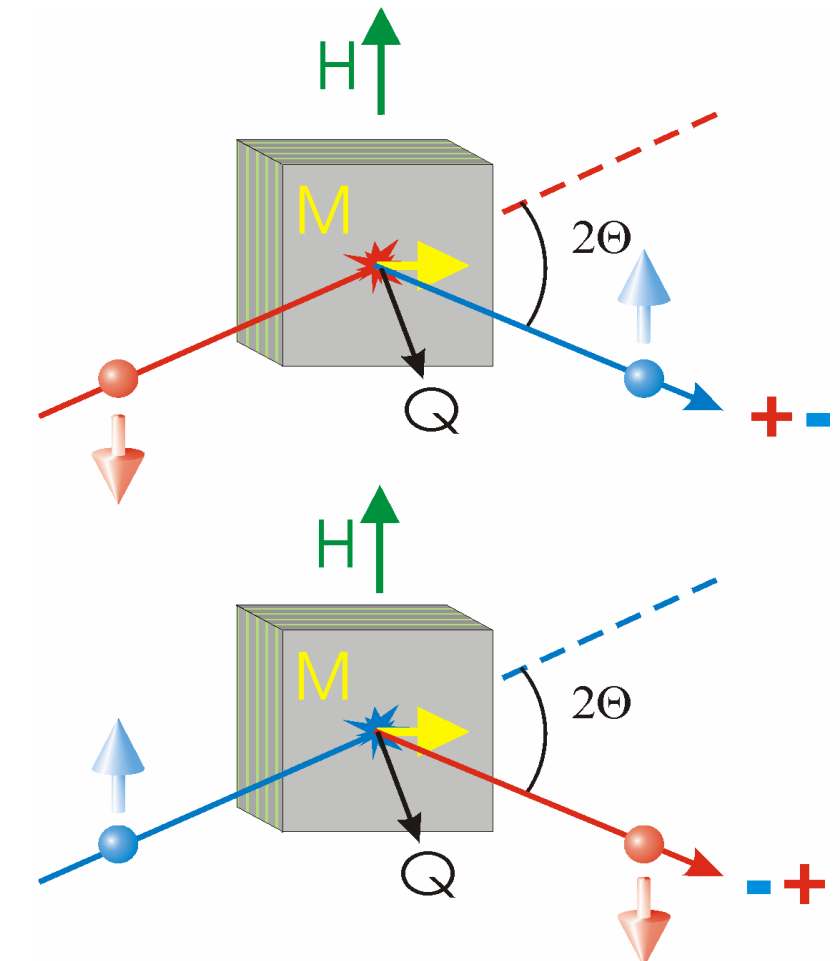
*Data courtesy of G. Smith (LANSCE)

Polarized Neutron Reflectometry (PNR)



Non-Spin-Flip

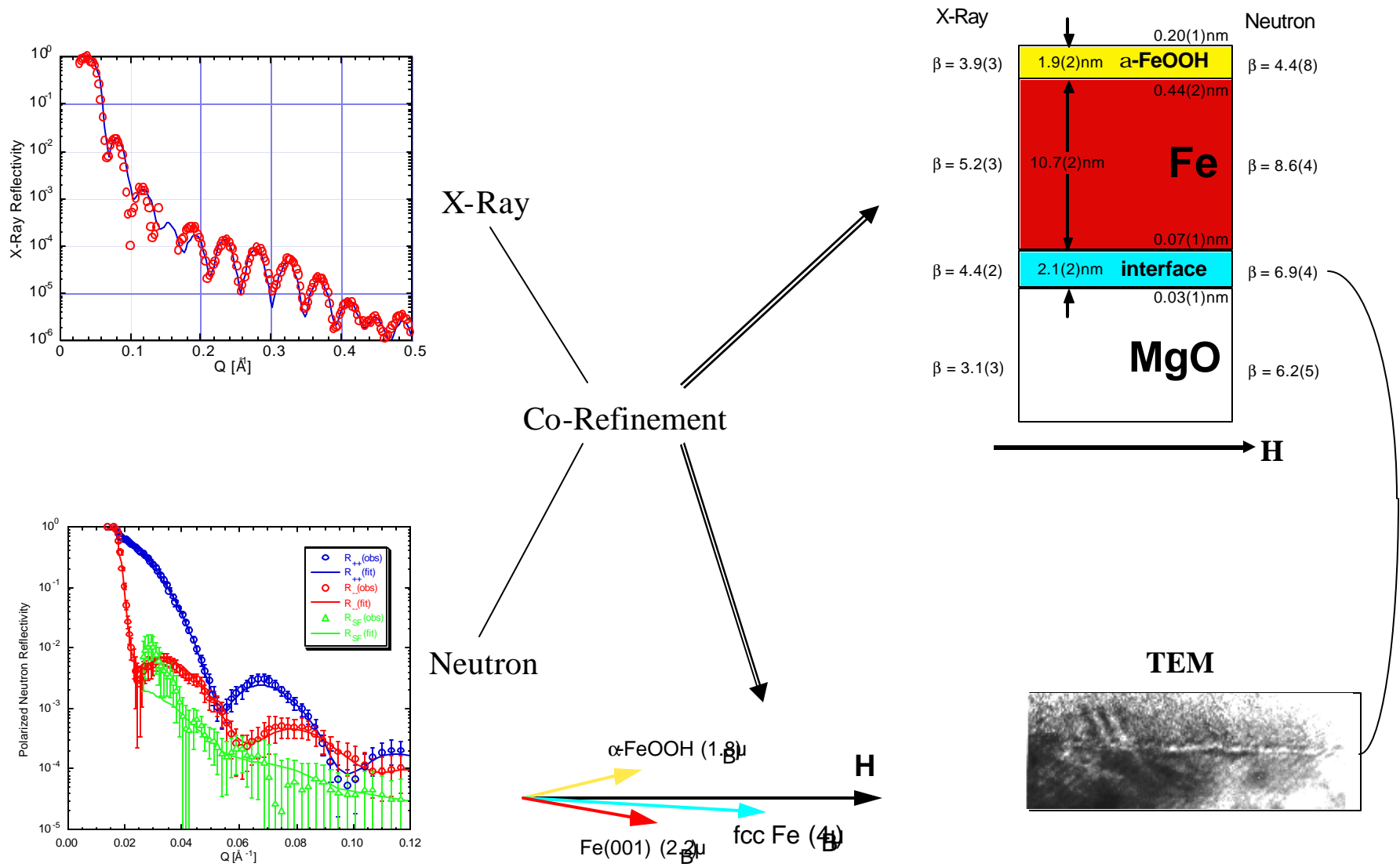
++ measures $b + M_z$
-- measures $b - M_z$



Spin-Flip

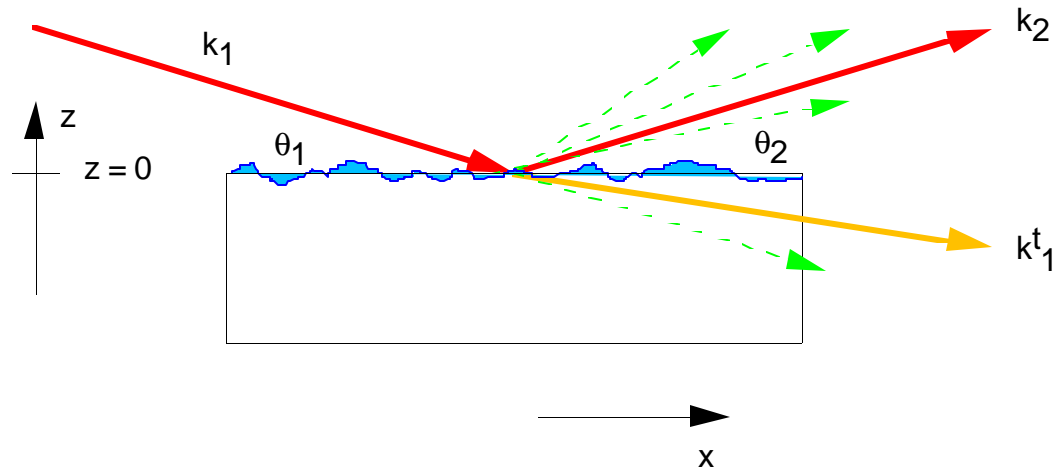
+ - measures $M_x + i M_y$
- + measures $M_x - i M_y$
-- measures $b - M_z$

Structure, Chemistry & Magnetism of Fe(001) on MgO(001)*



*Data courtesy of M. Fitzsimmons (LANSCE)

Reflection from Rough Surfaces

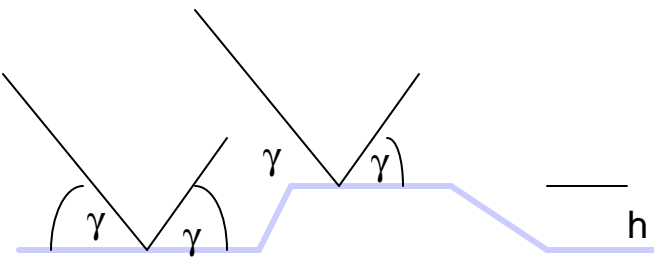


- diffuse scattering is caused by surface roughness or inhomogeneities in the reflecting medium
- a smooth surface reflects radiation in a single (specular) direction
- a rough surface scatters in various directions
- specular scattering is damped by surface roughness – treat as graded interface. For a single surface with r.m.s roughness σ :

$$R = R_F e^{-2k_{Iz} k_{1z}^t s^2}$$

When Does a “Rough” Surface Scatter Diffusely?

- Rayleigh criterion

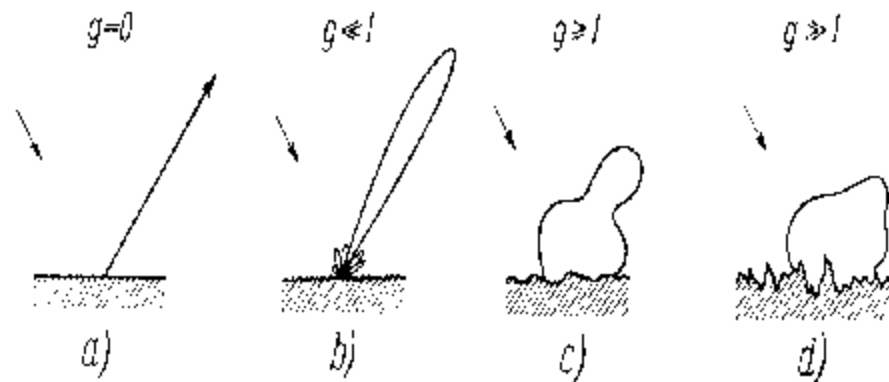


path difference: $D_r = 2 h \sin g$

phase difference: $D_f = (4ph/l) \sin g$

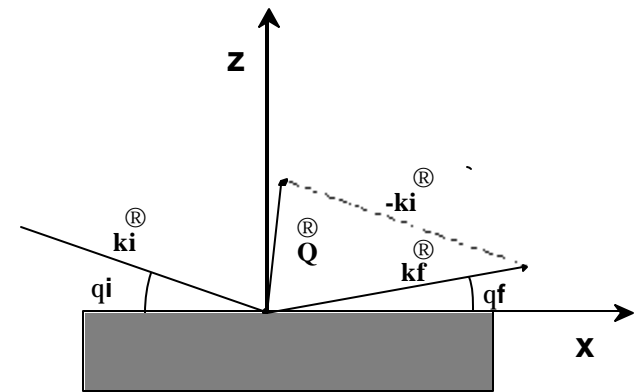
boundary between rough and smooth: $Df = p/2$

that is $h < l/(8\sin g)$ for a smooth surface



where $g = 4 p h \sin g / l = Q_z h$

Time-of-Flight, Energy-Dispersive Neutron Reflectometry

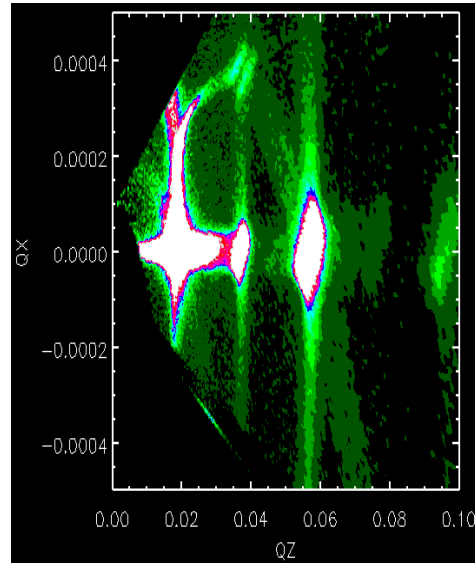
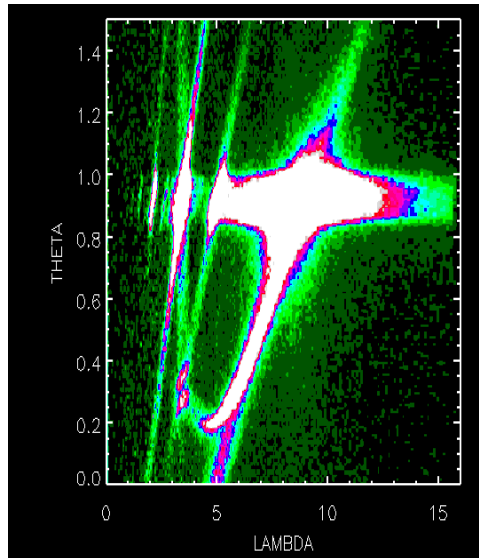


$$Q = \sqrt{k_f^2 - k_i^2}$$

where

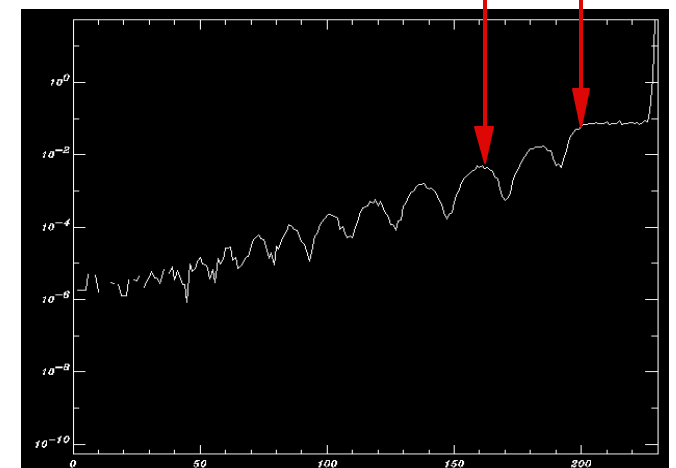
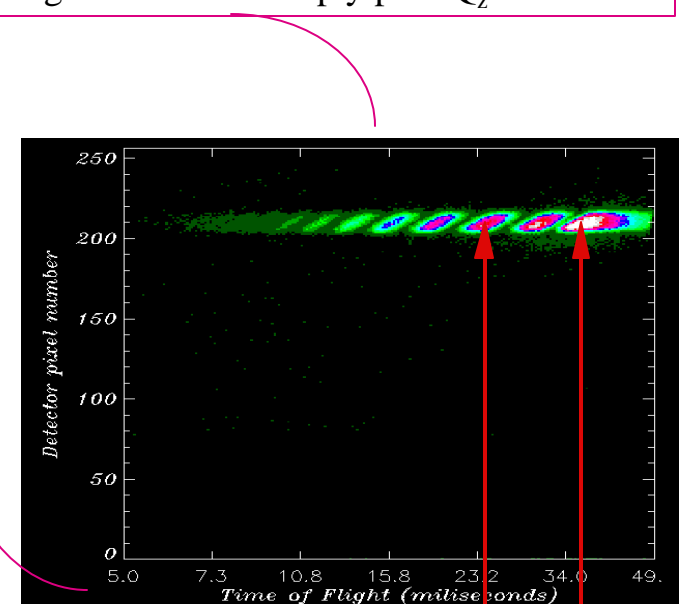
$$Q_x = \frac{2}{\lambda} p^* (\cos q_f - \cos q_i)$$

$$Q_z = \frac{2}{\lambda} p^* (\sin q_f + \sin q_i)$$



Raw data in θ_f -TOF space for a single layer.
Note that large divergence does not imply poor Q_z resolution

TOF - 1 . L / 4

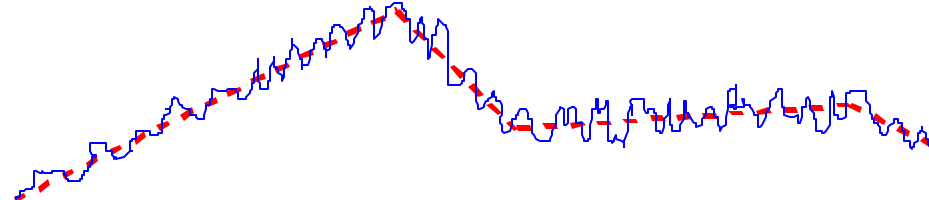


Vandium-Carbon Multilayer — specular & diffuse scattering
in θ_f -TOF space and transformed to Q_x - Q_z

The Study of Diffuse Scattering From Rough Surfaces Has Not Made Much Headway Because Interpretation Is Difficult

The theory (Distorted Wave Born Approximation) used to describe scattering from a rough surface, works in some cases but breaks down when $xk_z^2/k^2 \gg 1$, where x is the range of correlations in the surface

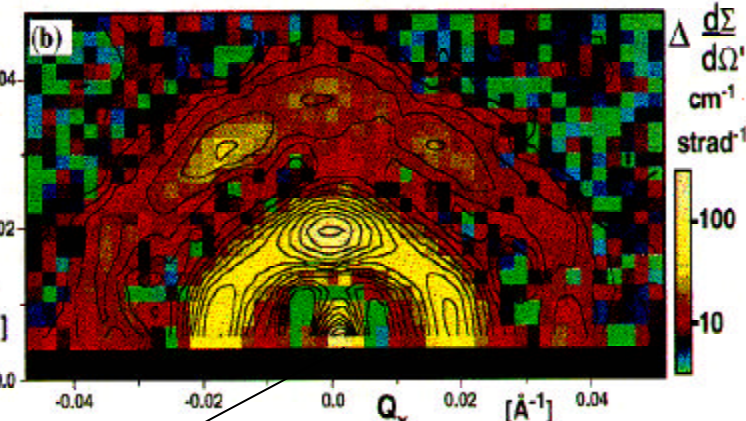
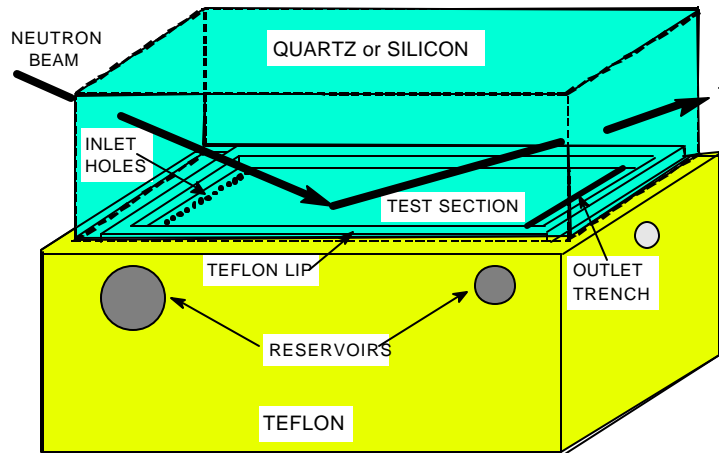
In some cases (e.g. faceted surfaces) one would also expect the approximation of using an "average surface" wavefunction for perturbation theory to break down.



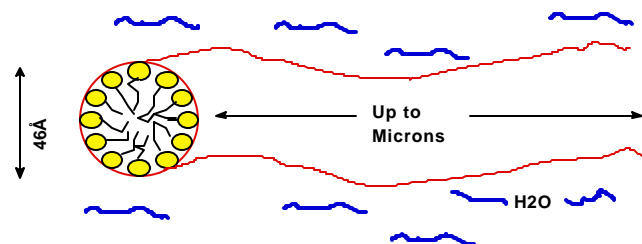
$$R_{\text{micro-rough}} = R_{\text{smooth}} e^{-2k_0 k_1 s^2}$$

$$R_{\text{facet}} = R_{\text{smooth}} e^{-2k_0^2 s^2}$$

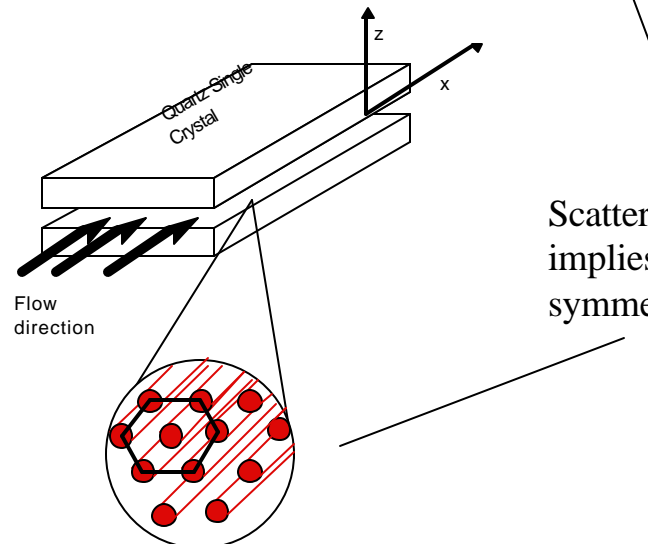
Observation of Hexagonal Packing of Thread-like Micelles Under Shear: Scattering From Lateral Inhomogeneities



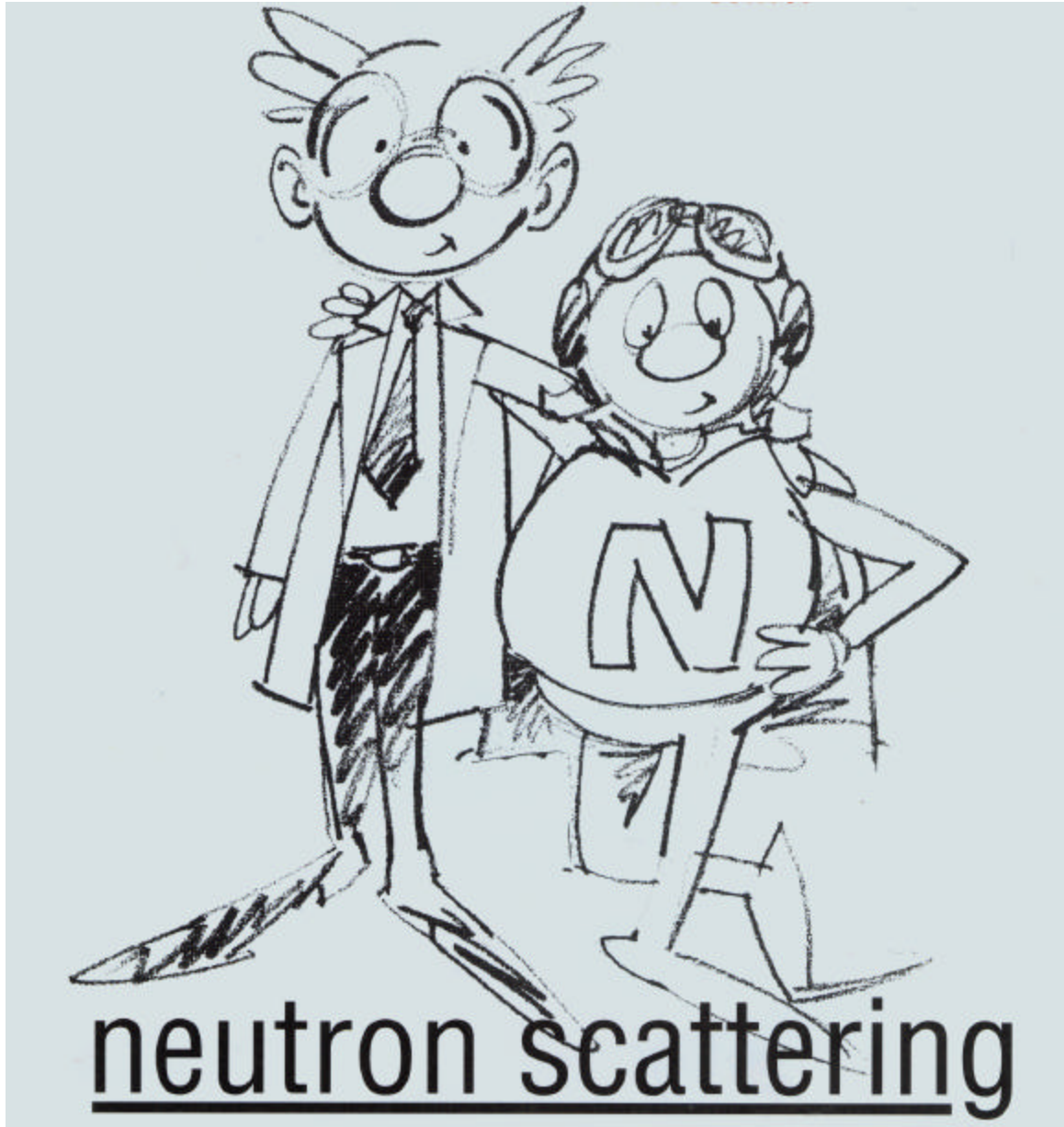
Specularly reflected beam



Thread-like micelle



Scattering pattern implies hexagonal symmetry



neutron scattering

by

Roger Pynn

Los Alamos
National Laboratory

LECTURE 5: Small Angle Scattering

This Lecture

5. Small Angle Neutron Scattering (SANS)

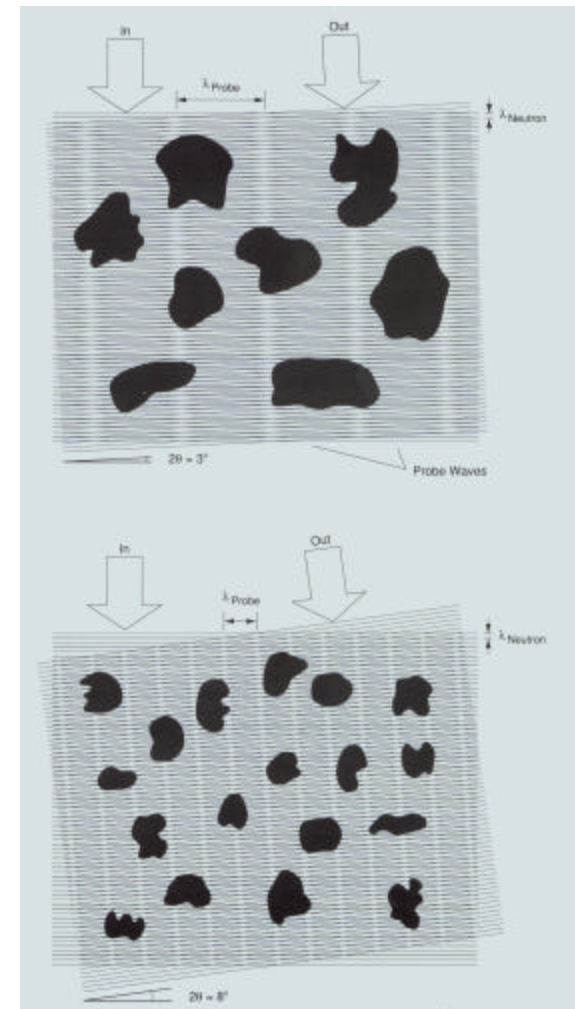
1. What is SANS and what does it measure?
2. Form factors and particle correlations
3. Guinier approximation and Porod's law
4. Contrast and contrast variation
5. Deuterium labelling
6. Examples of science with SANS
 1. Particle correlations in colloidal suspensions
 2. Helium bubble size distribution in steel
 3. Verification of Gaussian statistics for a polymer chain in a melt
 4. Structure of 30S ribosome
 5. The fractal structure of sedimentary rocks

Note: The NIST web site at www.ncnr.nist.gov has several good resources for SANS – calculations of scattering length densities & form factors as well as tutorials

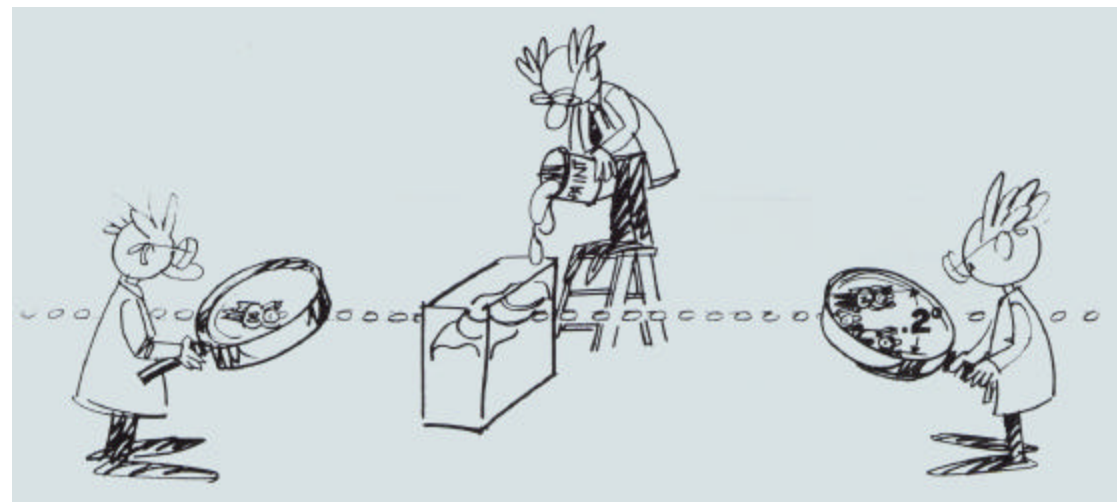
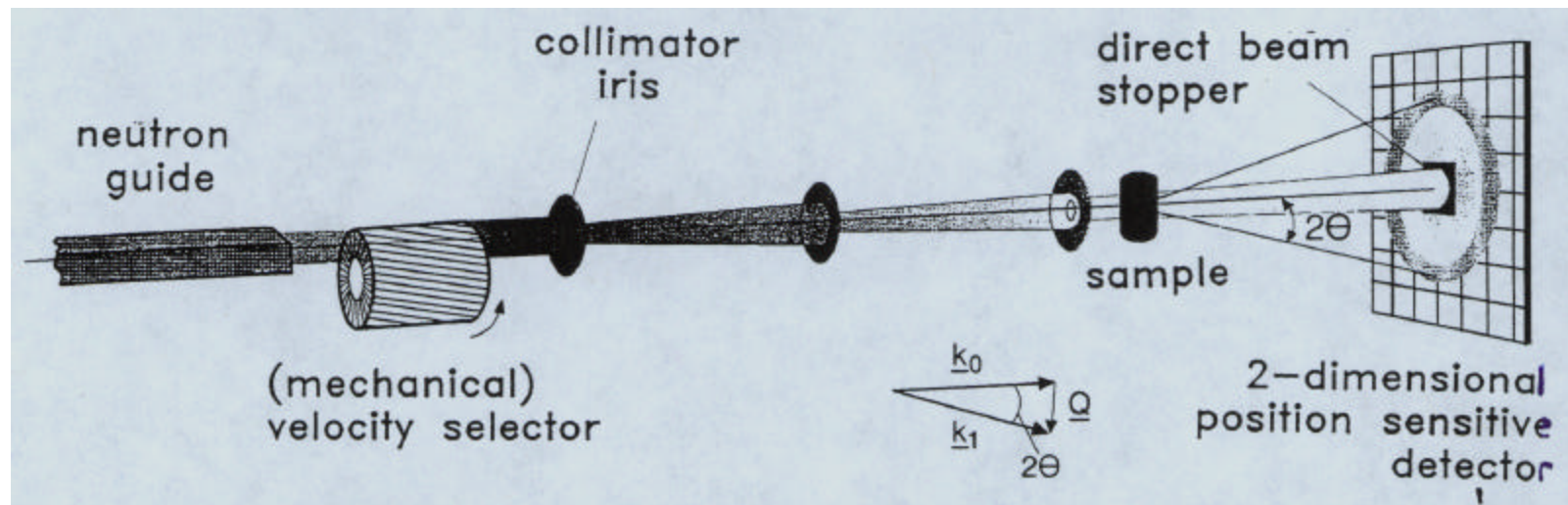
Small Angle Neutron Scattering (SANS) Is Used to Measure Large Objects (~ 1 nm to ~ 1 μm)

- Complex fluids, alloys, precipitates, biological assemblies, glasses, ceramics, flux lattices, long-wavelength CDWs and SDWs, critical scattering, porous media, fractal structures, etc

Scattering at small angles probes large length scales



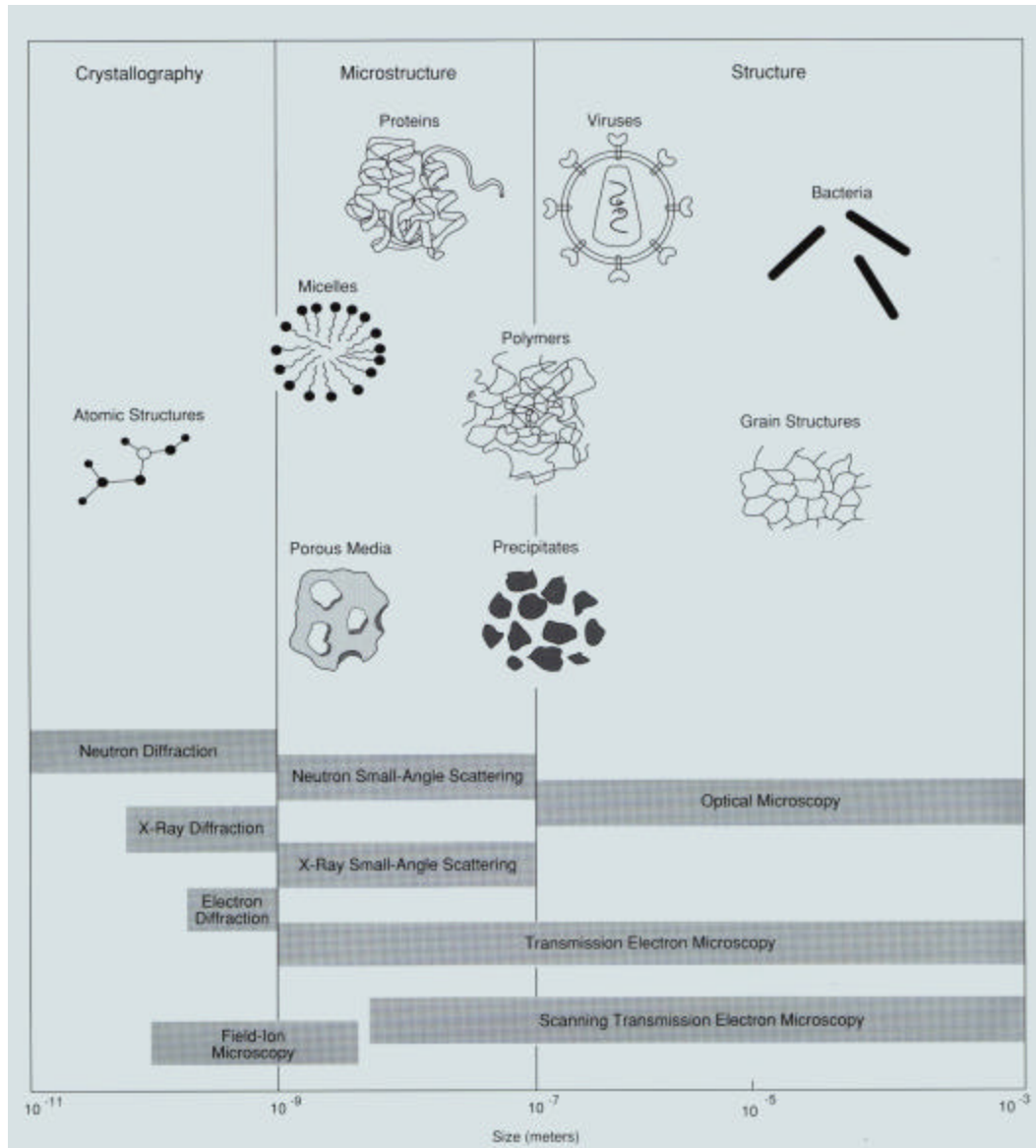
Two Views of the Components of a Typical Reactor-based SANS Diffractometer



The NIST 30m SANS Instrument Under Construction



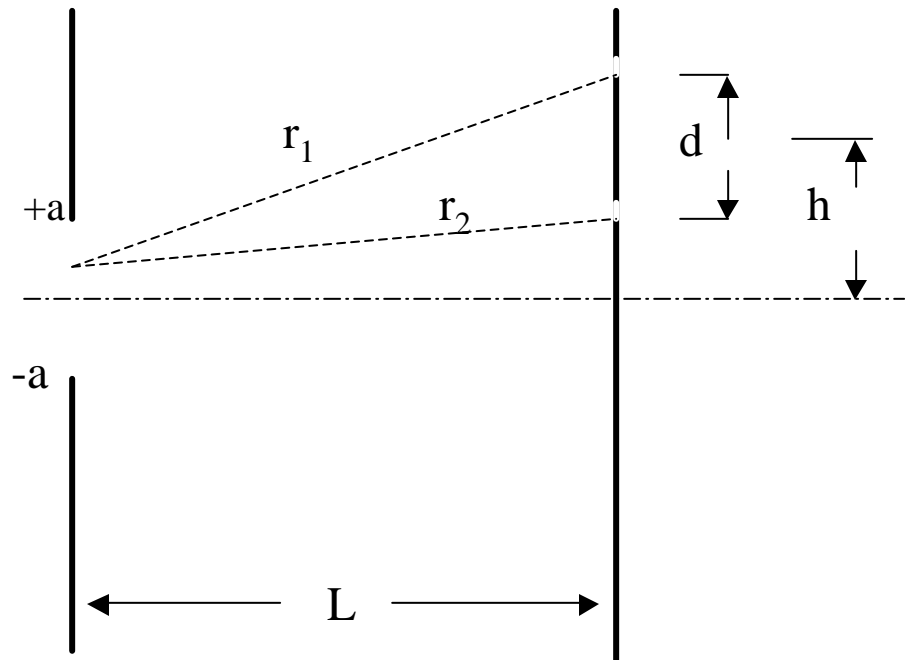
Where Does SANS Fit As a Structural Probe?



- SANS resolves structures on length scales of 1 – 1000 nm
- Neutrons can be used with bulk samples (1-2 mm thick)
- SANS is sensitive to light elements such as H, C & N
- SANS is sensitive to isotopes such as H and D

What Is the Largest Object That Can Be Measured by SANS?

- Angular divergence of the neutron beam and its lack of monochromaticity contribute to finite transverse & longitudinal coherence lengths that limit the size of an object that can be seen by SANS
- For waves emerging from slit center, path difference is hd/L if $d \ll h \ll L$; for waves from one edge of the slit path difference is $(h+a)d/L$
- The variation of path difference, which causes decreased visibility of Young's fringes, is ad/L so the variation in phase difference is $\Delta\psi = kad/L$
- To maintain the visibility of the Young's interference pattern we $\Delta\psi \sim 2\pi$ so the **coherence length**, $d \sim \lambda/\alpha$ where α is the divergence angle a/L
- The coherence length is the maximum distance between points in a scatterer for which interference effects will be observable



Instrumental Resolution for SANS

Traditionally, neutron scatterers tend to think in terms of Q and E resolution

$$Q = \frac{4p}{I} \sin q \Rightarrow \left\langle \frac{dQ^2}{Q^2} \right\rangle = \left\langle \frac{dl^2}{I^2} \right\rangle + \left\langle \frac{\cos^2 q \cdot dq^2}{\sin^2 q} \right\rangle$$

For SANS, $(dl/I)_{rms} \sim 5\%$ and q is small, so $\left\langle \frac{dQ^2}{Q^2} \right\rangle = 0.0025 + \left\langle \frac{dq^2}{q^2} \right\rangle$

For equal source - sample & sample - detector distances of L and equal apertures at source and sample of h, $dq_{rms} = \sqrt{5/12}h/L$.

The smallest value of q is determined by the direct beam size : $q_{min} \sim 1.5h/L$

At this value of q , angular resolution dominates and

$$dQ_{rms} \sim (dq_{rms}/q_{min})Q_{min} \sim dq_{rms} 4p/I \sim (2p/I)h/L$$

The largest observable object is $\sim 2p/dQ_{rms} \sim I h/L$.

This is equal to the transverse coherence length for the neutron and achieves a maximum of about 5 mm at the ILL 40 m SANS instrument using 15 Å neutrons. Note that at the largest values of q , set by the detector size and distance from the sample, wavelength resolution dominates.

The Scattering Cross Section for SANS

$$\text{recall that } \frac{ds}{dO} = \langle b \rangle^2 N S(\vec{Q}) \text{ where } S(\vec{Q}) = \frac{1}{N} \left\langle \left| \int d\vec{r} \cdot e^{-i\vec{Q} \cdot \vec{r}} n_{nuc}(\vec{r}) \right|^2 \right\rangle$$

where $\langle b \rangle^2$ is the coherent nuclear scattering length and $n_{nuc}(\vec{r})$ is the nuclear density

- Since the length scale probed at small Q is \gg inter-atomic spacing we may use the scattering length density (SLD), ρ , introduced for surface reflection and note that $n_{nuc}(r)b$ is the local SLD at position r .
- A uniform scattering length density only gives forward scattering ($Q=0$), thus **SANS measures deviations from average scattering length density.**
- If ρ is the SLD of particles dispersed in a medium of SLD ρ_0 , and $n_p(r)$ is the particle number density, we can separate the integral in the definition of $S(Q)$ into an integral over the positions of the particles and an integral over a single particle. We also measure the particle SLD relative to that of the surrounding medium i.e:

SANS Measures Particle Shapes and Inter-particle Correlations

$$\frac{d\mathbf{S}}{d\Omega} = \langle b \rangle^2 \int_{space} d^3r \int_{space} d^3r' n_N(\vec{r}) n_N(\vec{r}') e^{i\vec{Q} \cdot (\vec{r} - \vec{r}')}}$$

$$= \int_{space} d^3R \int_{space} d^3R' \left\langle n_P(\vec{R}) n_P(\vec{R}') \right\rangle e^{i\vec{Q} \cdot (\vec{R} - \vec{R}')} \left| (\mathbf{r} - \mathbf{r}_0) \int_{particle} d^3x e^{i\vec{Q} \cdot \vec{x}} \right|^2$$

$$\frac{d\mathbf{S}}{d\Omega} = (\mathbf{r} - \mathbf{r}_0)^2 \left| F(\vec{Q}) \right|^2 N_P \int_{space} d^3R G_P(\vec{R}) e^{i\vec{Q} \cdot \vec{R}}$$

where G_P is the particle - particle correlation function (the probability that there is a particle at \vec{R} if there's one at the origin) and $|F(\vec{Q})|^2$ is the particle form factor :

$$\left| F(\vec{Q}) \right|^2 = \left| \int_{particle} d^3x e^{i\vec{Q} \cdot \vec{x}} \right|^2$$

These expressions are the same as those for nuclear scattering except for the addition of a form factor that arises because the scattering is no longer from point-like particles

Scattering for Spherical Particles

The particleform factor $|F(\vec{Q})|^2 = \left| \int_V d\vec{r} e^{i\vec{Q} \cdot \vec{r}} \right|^2$ is determined by the particleshape.

For a sphere of radius R, $F(Q)$ only dependson the magnitude of Q :

$$F_{sphere}(Q) = 3V_0 \left[\frac{\sin QR - QR \cos QR}{(QR)^3} \right] \equiv \frac{3V_0}{QR} j_1(QR) \rightarrow V_0 \text{ at } Q = 0$$

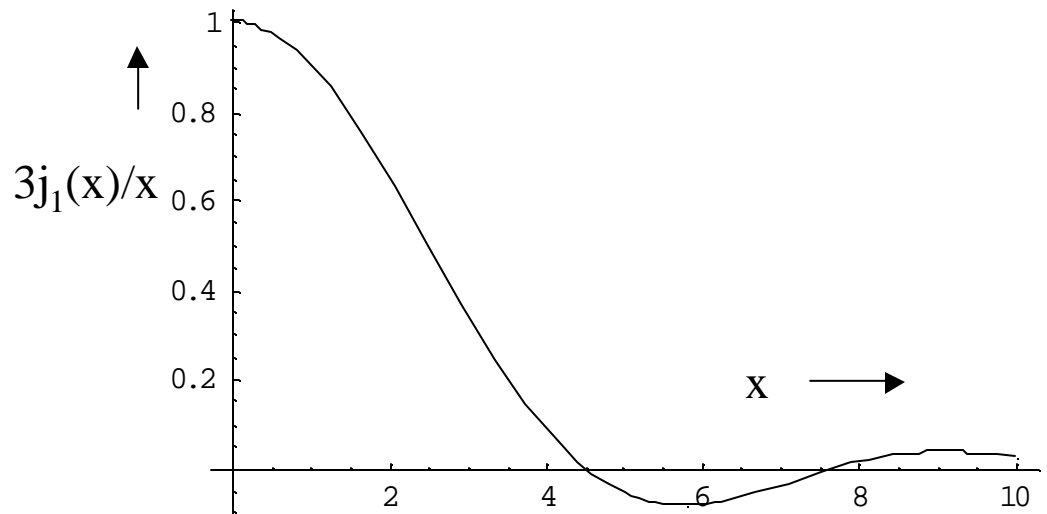
Thus, as $Q \rightarrow 0$, the totalscattering from an assembly of uncorrelated spherical particles[i.e. when $G(\vec{r}) \rightarrow \mathbf{d}(\vec{r})$] is proportional to the square of the particle volume times the number of particles.

For elliptical particles

replace R by :

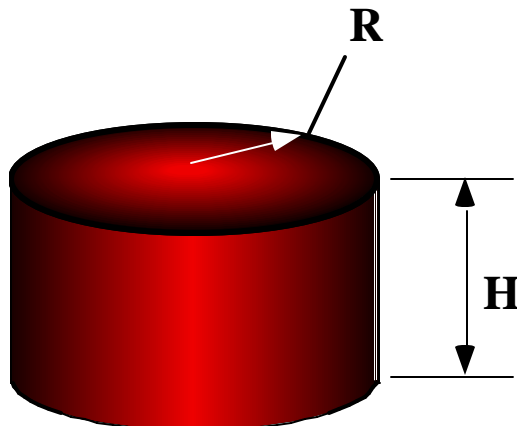
$$R \rightarrow (a^2 \sin^2 J + b^2 \cos^2 J)^{1/2}$$

where J is the angle between
the major axis (a) and \vec{Q}



Examples of Spherically-Averaged Form Factors

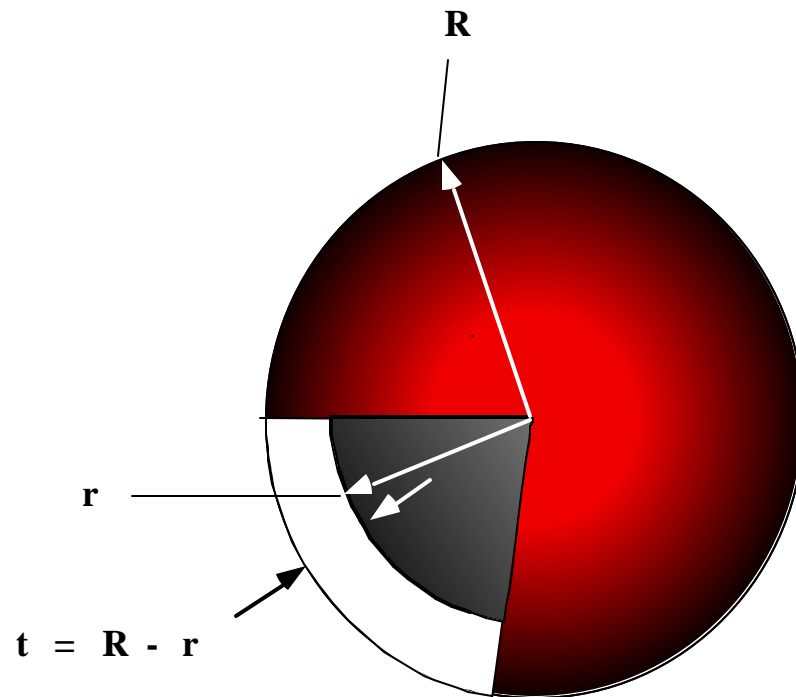
Form Factor for Cylinder with Q at angle q to cylinder axis



$$F(Q, q, H, R) = \frac{4V_0 \sin([QH / 2] \cos q) J_1(QR \sin q)}{QH \cos q (QR \sin q)^2}$$

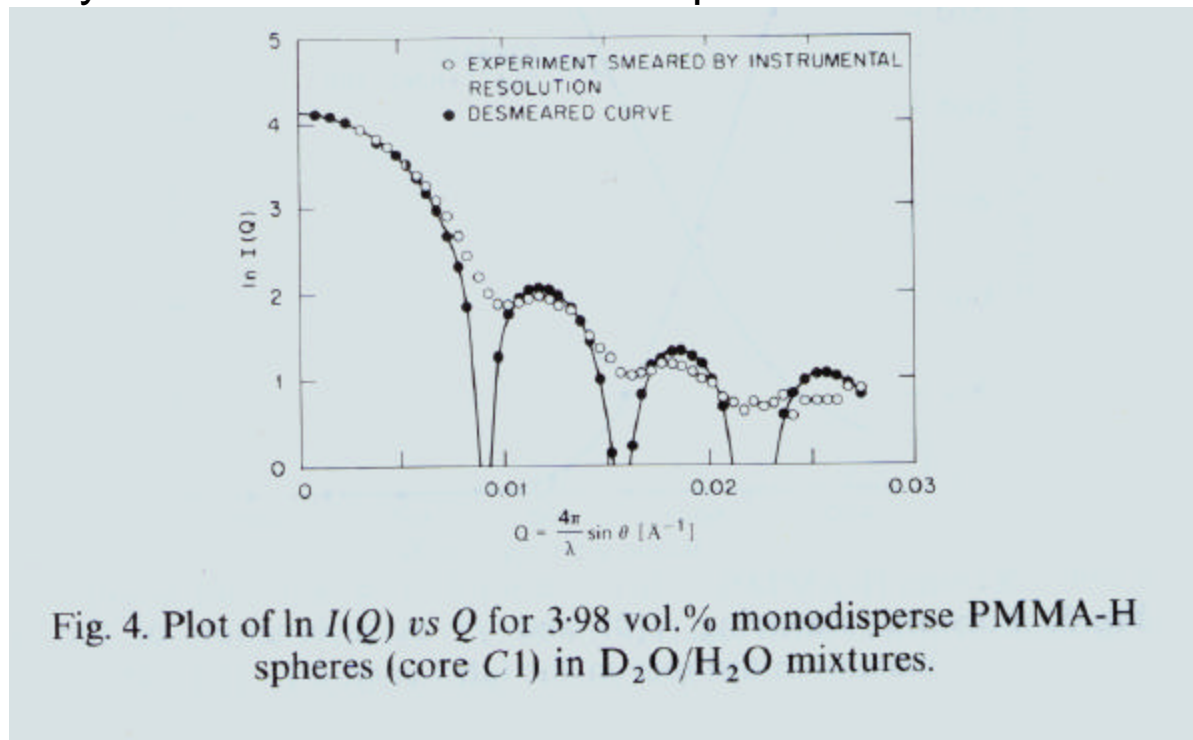
Form Factor for a Vesicle

$$F(Q, R, r) = 3V_0 \frac{R^2 j_1(QR) - r^2 j_1(Qr)}{Q^2 (R^3 - r^3)}$$



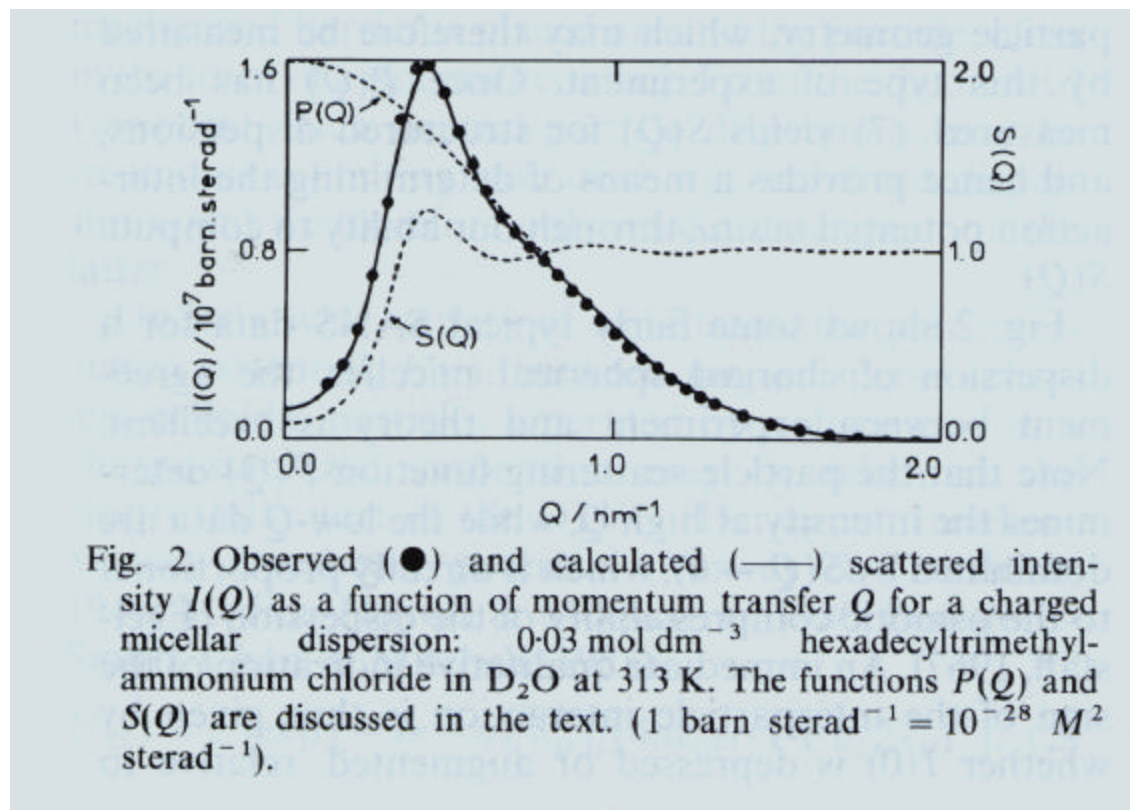
Determining Particle Size From Dilute Suspensions

- Particle size is usually deduced from dilute suspensions in which inter-particle correlations are absent
- In practice, instrumental resolution (finite beam coherence) will smear out minima in the form factor
- This effect can be accounted for if the spheres are mono-disperse
- For poly-disperse particles, maximum entropy techniques have been used successfully to obtain the distribution of particle sizes



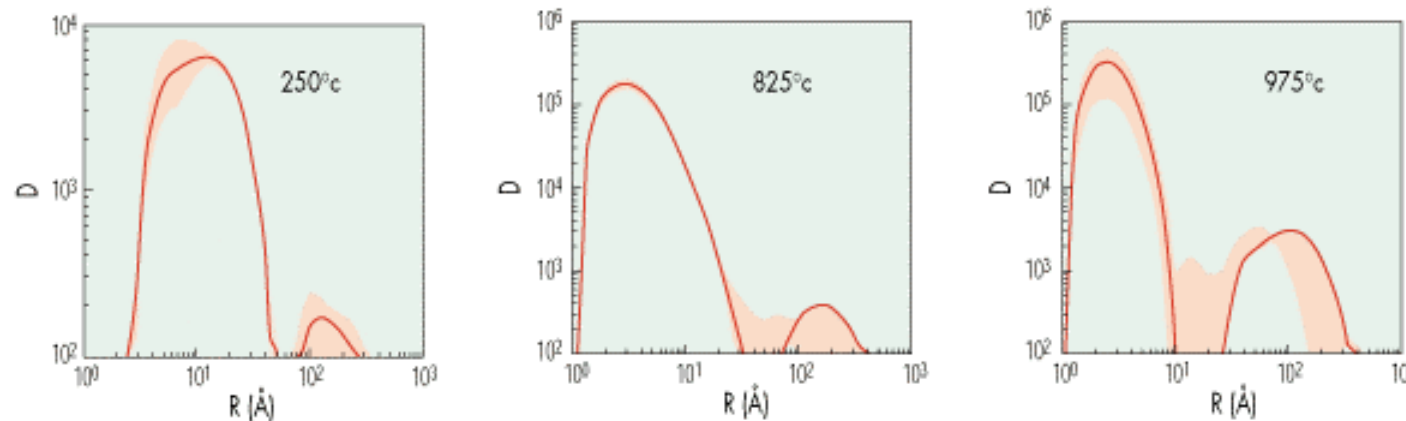
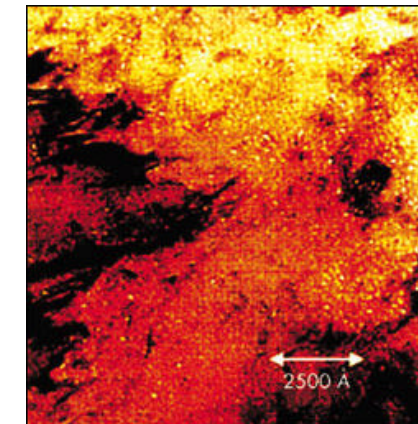
Correlations Can Be Measured in Concentrated Systems

- A series of experiments in the late 1980's by Hayter et al and Chen et al produced accurate measurements of $S(Q)$ for colloidal and micellar systems
- To a large extent these data could be fit by $S(Q)$ calculated from the mean spherical model using a Yukawa potential to yield surface charge and screening length



Size Distributions Have Been Measured for Helium Bubbles in Steel

- The growth of He bubbles under neutron irradiation is a key factor limiting the lifetime of steel for fusion reactor walls
 - Simulate by bombarding steel with alpha particles
- TEM is difficult to use because bubble are small
- SANS shows that larger bubbles grow as the steel is annealed, as a result of coalescence of small bubbles and incorporation of individual He atoms



SANS gives bubble volume (arbitrary units on the plots) as a function of bubble size at different temperatures. Red shading is 80% confidence interval.

Radius of Gyration Is the Particle “Size” Usually Deduced From SANS Measurements

If we measure \vec{r} from the centroid of the particle and expand the exponential in the definition of the form factor at small Q :

$$F(Q) = \int_V d\vec{r} e^{i\vec{Q} \cdot \vec{r}} \approx V_0 + i \cancel{\int_V \vec{Q} \cdot \vec{r} d^3 r} - \frac{1}{2} \int_V (\vec{Q} \cdot \vec{r})^2 d^3 r + \dots$$

$$= V_0 \left[1 - \frac{Q^2}{2} \frac{\int_0^p \cos^2 \mathbf{q} \sin \mathbf{q} \cdot d\mathbf{q} \int_V r^2 d^3 r}{\int_0^p \sin \mathbf{q} \cdot d\mathbf{q} \int_V d^3 r} + \dots \right] = V_0 \left[1 - \frac{Q^2 r_g^2}{6} + \dots \right] \approx V_0 e^{-\frac{Q^2 r_g^2}{6}}$$

where r_g is the radius of gyration is $r_g = \int_V R^2 d^3 r / \int_V d^3 r$. It is usually obtained from a fit to SANS data at low Q (in the so - called Guinier region) or by plotting $\ln(\text{Intensity}) v Q^2$. The slope of the data at the lowest values of Q is $r_g^2/3$. It is easily verified that the expression for the form factor of a sphere is a special case of this general result.

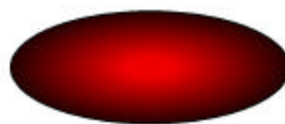
Guinier Approximations: Analysis Road Map

Guinier Law

$$\lim_{Q \rightarrow 0} I(Q) = \Delta M_0 \exp\left(-\frac{R_g^2 Q^2}{3}\right)$$

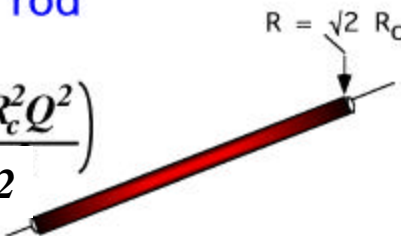
$$\Delta M_0 = V^2 (\bar{\rho}_p - \rho_s)^2$$

$$R_g = \frac{1}{V} \int \rho(r) r^2 dv_r$$



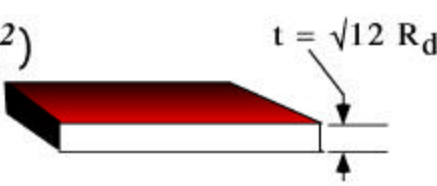
Guinier Law for a rod

$$I(Q) = \frac{\pi}{Q} \Delta m_0 \exp\left(-\frac{R_c^2 Q^2}{2}\right)$$



Guinier Law for a sheet

$$I(Q) = \frac{2\pi}{Q^2} \Delta \mu_0 \exp(-R_d^2 Q^2)$$



Generalized Guinier approximation

$$\langle P(Q) \rangle = \begin{cases} 1; & \alpha = 0 \\ \alpha \pi Q^{-\alpha}; & \alpha = 1, 2 \end{cases} \Delta M_{\alpha 0} \exp\left(-\frac{R_{\alpha}^2 Q^2}{3-\alpha}\right)$$

Derivative-log analysis

$$\frac{d \ln \langle P(Q) \rangle}{d \ln(Q)} = \frac{Q}{\langle P(Q) \rangle} \frac{d \langle P(Q) \rangle}{d Q} = -\alpha - \frac{2}{3-\alpha} R_{\alpha}^2 Q^2$$

- Guinier approximations provide a roadmap for analysis.
- Information on particle composition, shape and size.
- Generalization allows for analysis of complex mixtures, allowing identification of domains where each approximation applies.

* Viewgraph courtesy of Rex Hjelm

Contrast & Contrast Matching

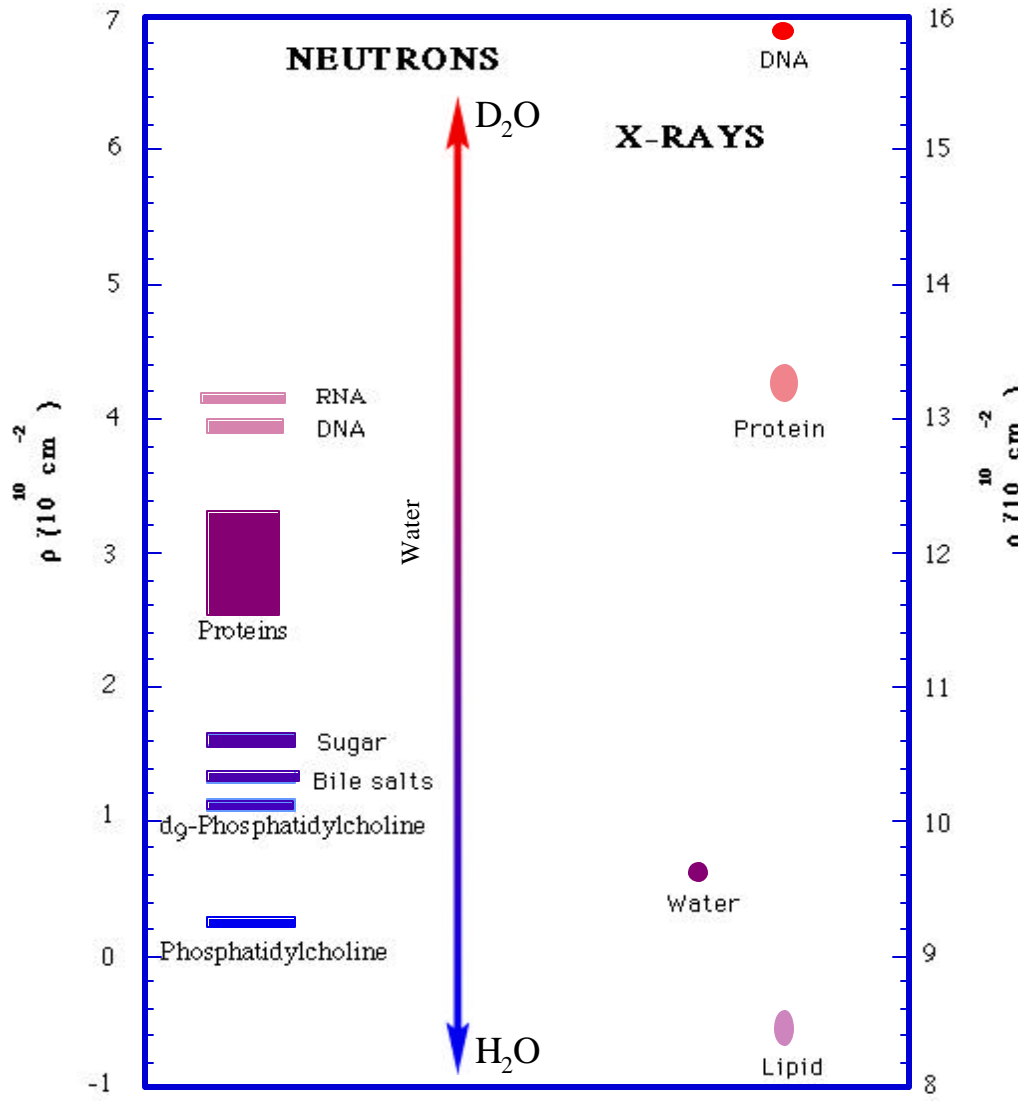
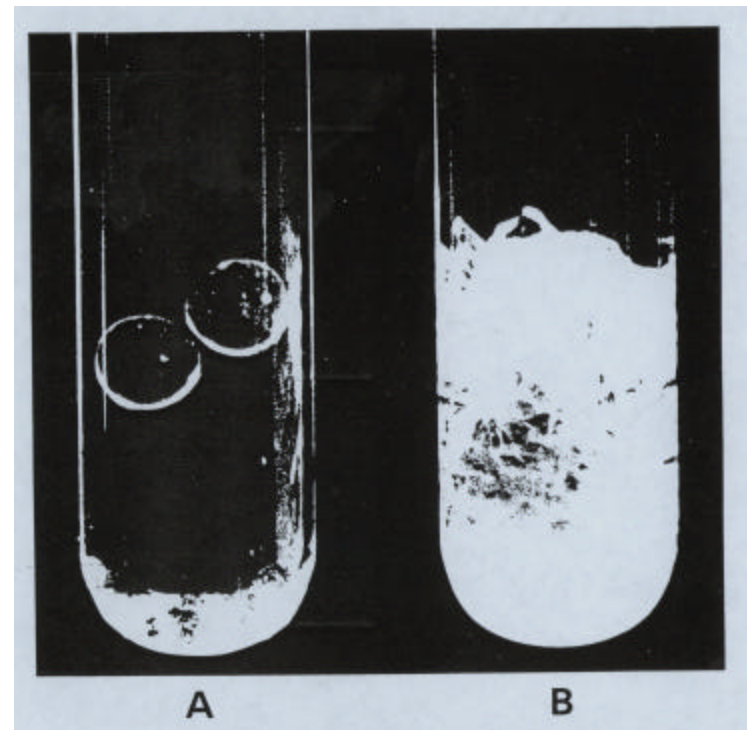


* Chart courtesy of Rex Hjelm



Both tubes contain borosilicate beads + pyrex fibers + solvent. (A) solvent refractive index matched to pyrex;. (B) solvent index different from both beads and fibers – scattering from fibers dominates

Isotopic Contrast for Neutrons

Hydrogen Isotope	Scattering Length b (fm)
¹ H	-3.7409 (11)
² D	6.674 (6)
³ T	4.792 (27)

Nickel Isotope	Scattering Lengths b (fm)
⁵⁸ Ni	15.0 (5)
⁶⁰ Ni	2.8 (1)
⁶¹ Ni	7.60 (6)
⁶² Ni	-8.7 (2)
⁶⁴ Ni	-0.38 (7)

Verification of the Gaussian Coil Model for a Polymer Melt

- One of the earliest important results obtained by SANS was the verification of that $r_g \sim N^{1/2}$ for polymer chains in a melt
- A better experiment was done 3 years later using a small amount of H-PMMA in D-PMMA (to avoid the large incoherent background) covering a MW range of 4 decades

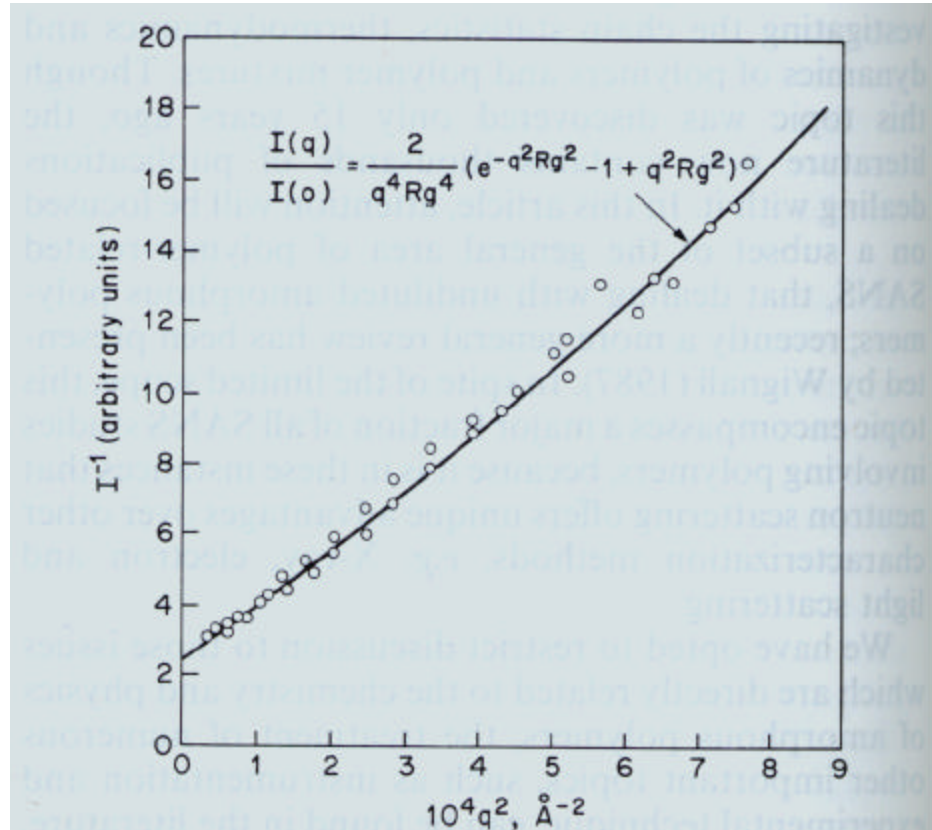


Fig. 1. SANS results obtained by Kirste, Kruse & Schelten (1972) for 1.2% deuterated poly(methyl methacrylate) (PMMA) in normal PMMA (mol. wt of 250 000) plotted in Ornstein-Zernike form. The solid curve represents a Debye function [equation (1)]. This was one of the first quantitative demonstrations of Gaussian coil behavior for bulk polymers.

SANS Has Been Used to Study Bio-machines

- Capel and Moore (1988) used the fact that prokaryotes can grow when H is replaced by D to produce reconstituted ribosomes with various pairs of proteins (but not rRNA) deuterated
- They made 105 measurements of inter-protein distances involving 93 30S protein pairs over a 12 year period. They also measured radii of gyration
- Measurement of inter-protein distances is done by Fourier transforming the form factor to obtain $G(R)$
- They used these data to solve the ribosomal structure, resolving ambiguities by comparison with electron microscopy

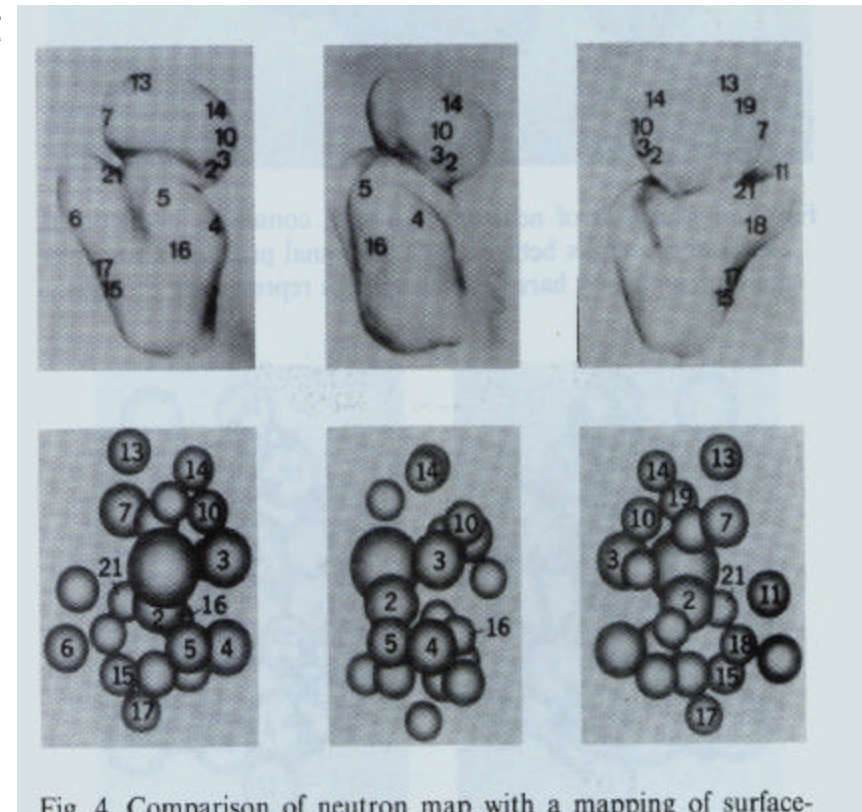


Fig. 4. Comparison of neutron map with a mapping of surface-exposed antigenic sites of ribosomal proteins of the 30S subunit obtained by immune-electron microscopy (Stoeffler & Stoeffler-Meilicke, 1986).

Porod Scattering

Let us examine the behavior of $|F(Q)|^2 (QR)^4$ at large values of Q for a spherical particle (i.e. $Q \gg 1/R$ where R is the sphere radius)

$$\begin{aligned}|F(Q)|^2 (QR)^4 &= 9V^2 \left[\frac{\sin QR - QR \cos QR}{(QR)^3} \right]^2 (QR)^4 = 9V^2 \left[\frac{\sin QR}{QR} - \cos QR \right]^2 \\&\rightarrow 9V^2 \cos^2 QR \text{ as } Q \rightarrow \infty \\&= 9V^2 / 2 \text{ on average (the oscillations will be smeared out by resolution)}\end{aligned}$$

Thus $|F(Q)|^2 \rightarrow \frac{9V^2}{2(QR)^4} = \frac{2pA}{Q^4}$ where A is the area of the sphere's surface.

This is Porod's law and holds as $Q \rightarrow \infty$ for any particle shape provided the particle surface is smooth.

Another way to obtain it is to expand $G(r) = 1 - ar + br^2 + \dots$ [with $a = A/(2pV)$] at small r and to evaluate the form factor with this (Debye) form for the correlation function.

Scattering From Fractal Systems

- Fractals are systems that are “self-similar” under a change of scale I.e. $R \rightarrow CR$
- For a mass fractal the number of particles within a sphere of radius R is proportional to R^D where D is the fractal dimension

Thus

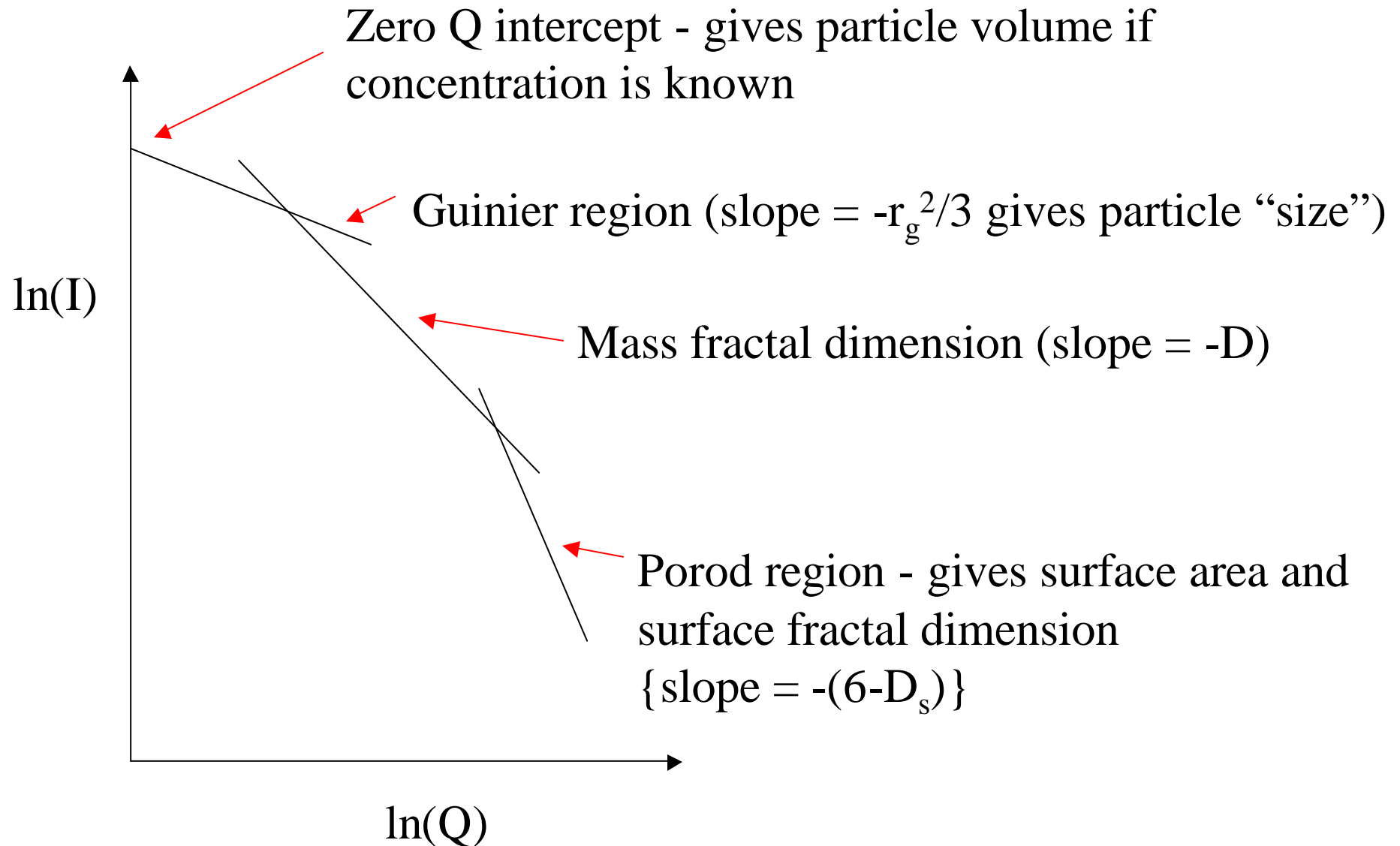
$$4\pi R^2 dR G(R) = \text{number of particles between distance } R \text{ and } R + dR = cR^{D-1} dR$$

$$\therefore G(R) = (c/4\pi) R^{D-3}$$

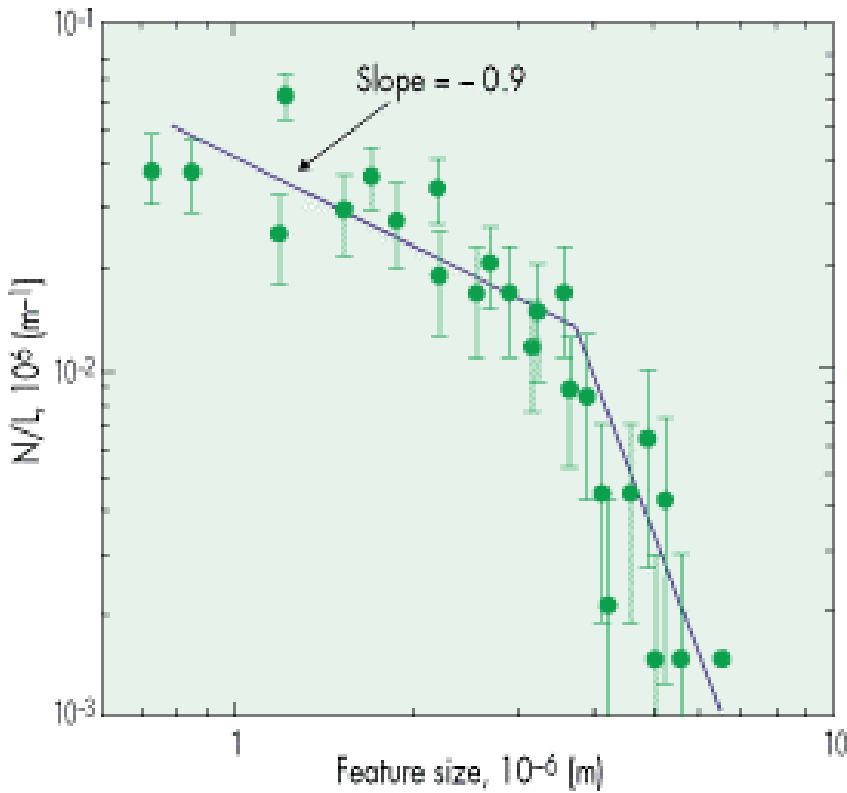
$$\begin{aligned} \text{and } S(\vec{Q}) &= \int d\vec{R} e^{i\vec{Q} \cdot \vec{R}} G(R) = \frac{2\pi}{Q} \int dR R \sin QR (c/4\pi) R^{D-3} \\ &= \frac{c}{2} \frac{1}{Q^D} \int dx x^{D-2} \sin x = \frac{\text{const}}{Q^D} \end{aligned}$$

For a surface fractal, one can prove that $S(Q) \propto \frac{\text{const}}{Q^{6-D_s}}$ which reduces to the Porod form for smooth surfaces of dimension 2.

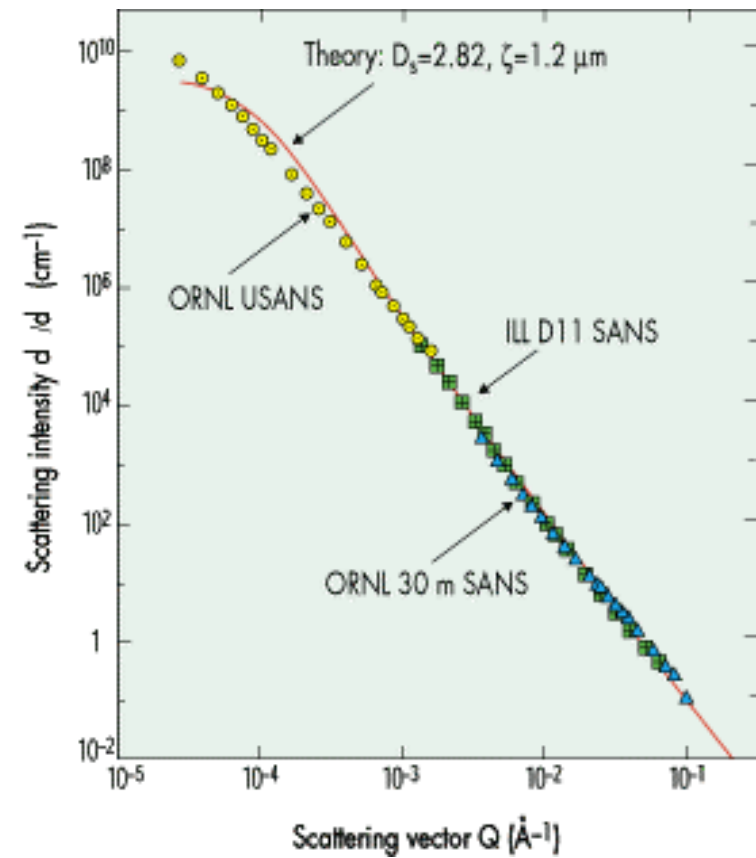
Typical Intensity Plot for SANS From Disordered Systems



Sedimentary Rocks Are One of the Most Extensive Fractal Systems*



Variation of the average number of SEM features per unit length with feature size. Note the breakdown of fractality ($D_s=2.8$ to 2.9) for lengths larger than 4 microns

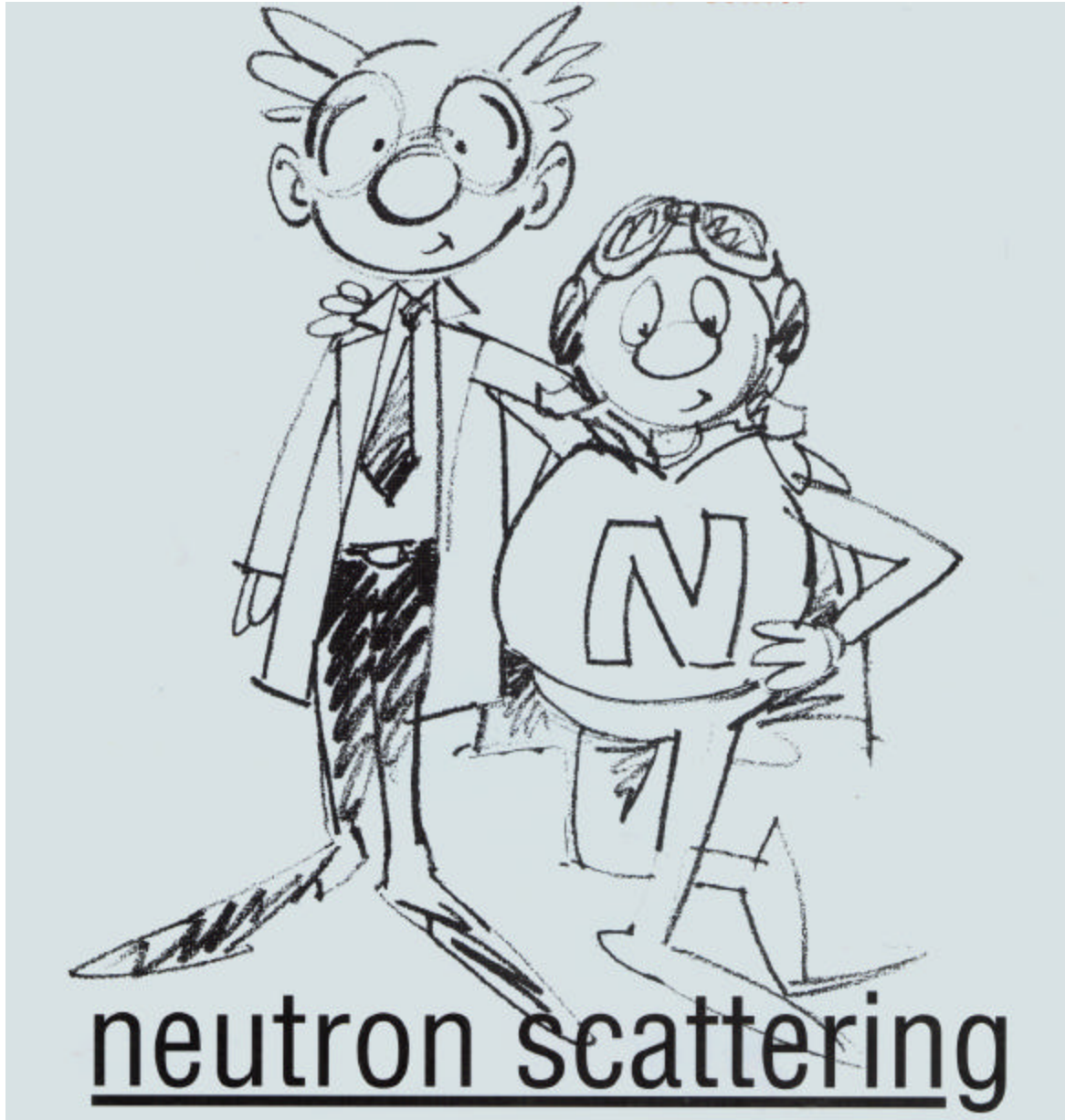


SANS & USANS data from sedimentary rock showing that the pore-rock interface is a surface fractal ($D_s=2.82$) over 3 orders of magnitude in length scale

*A. P. Radlinski (Austr. Geo. Survey)

References

- Viewgraphs describing the NIST 30-m SANS instrument
 - http://www.ncnr.nist.gov/programs/sans/tutorials/30mSANS_desc.pdf



neutron scattering

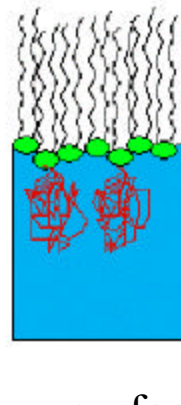
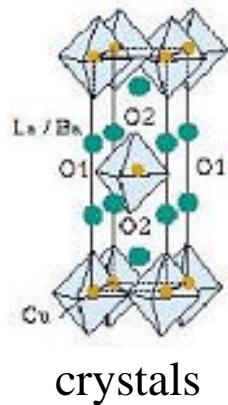
LECTURE 6: Inelastic Scattering

by

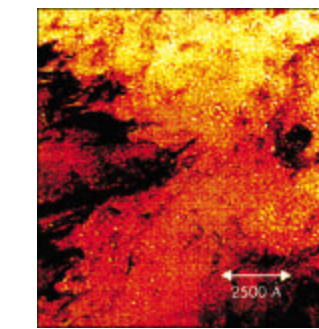
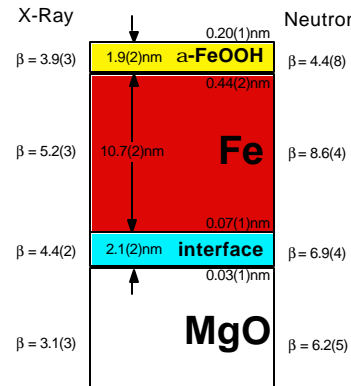
Roger Pynn

Los Alamos
National Laboratory

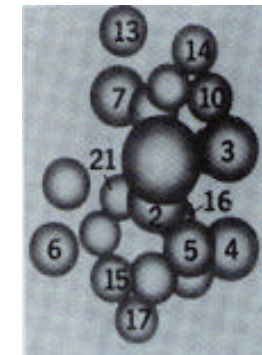
We Have Seen How Neutron Scattering Can Determine a Variety of Structures



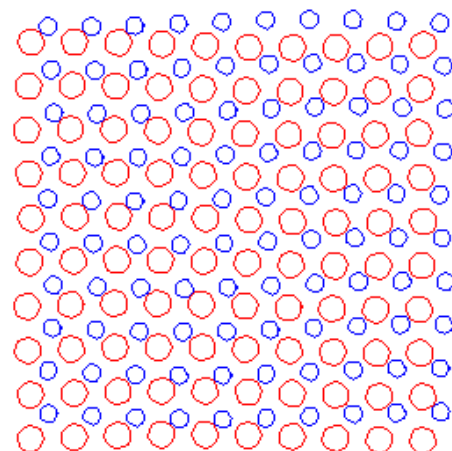
surfaces & interfaces



disordered/fractals



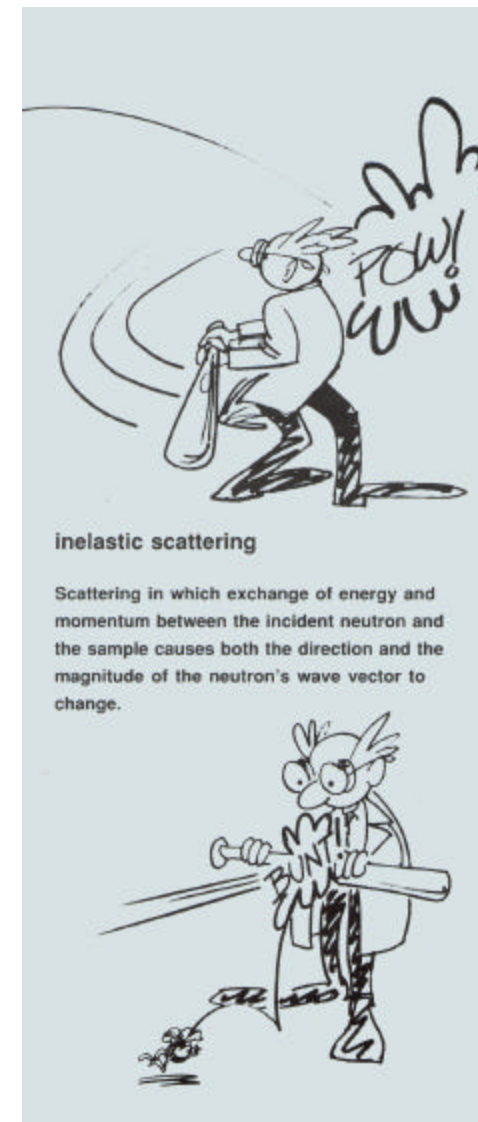
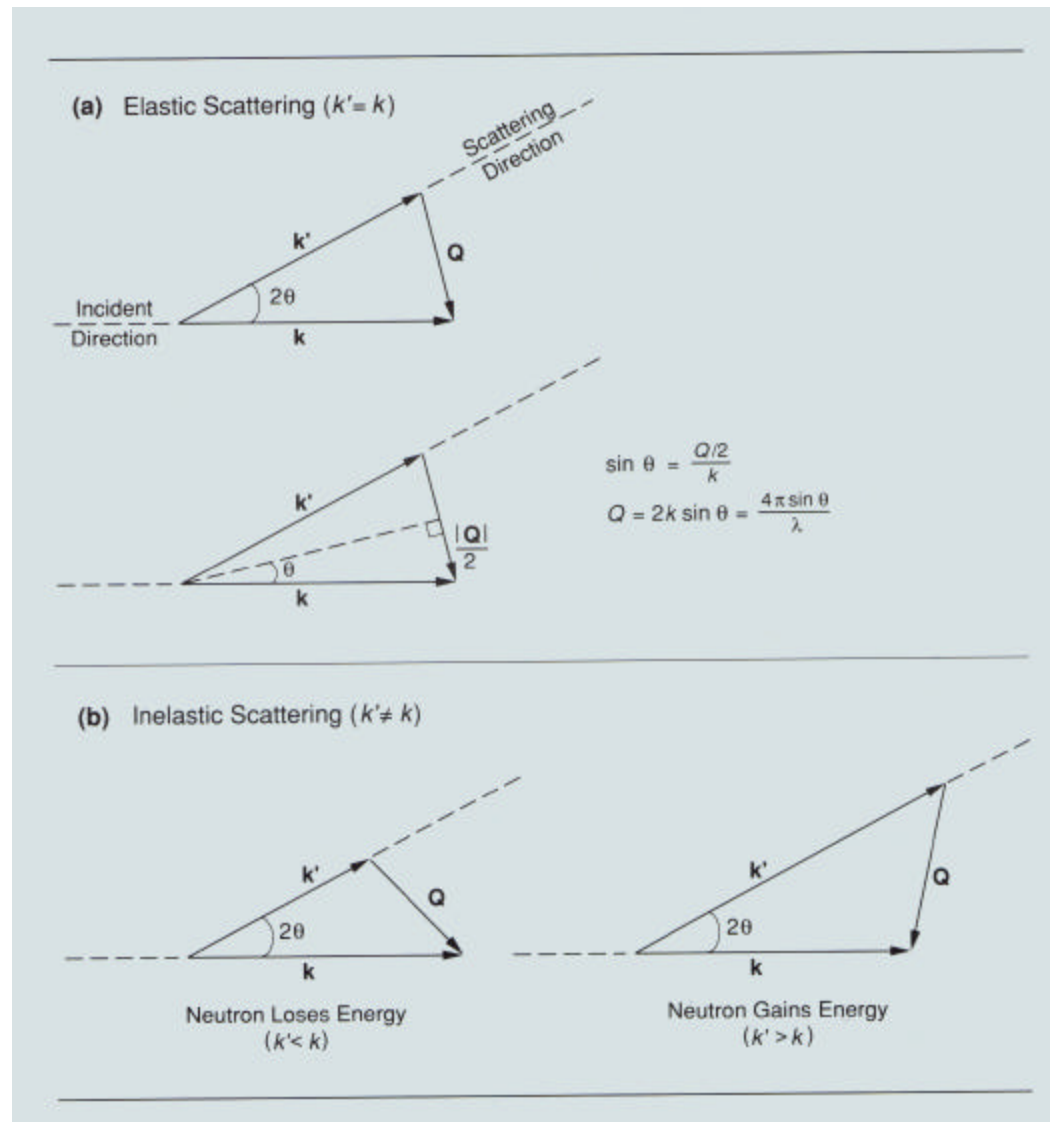
but what happens when the atoms are moving?



Can we determine the directions and time-dependence of atomic motions?
Can we tell whether motions are periodic?
Etc.

These are the types of questions answered by inelastic neutron scattering

The Neutron Changes Both Energy & Momentum When Inelastically Scattered by Moving Nuclei



The Elastic & Inelastic Scattering Cross Sections Have an Intuitive Similarity

- The intensity of **elastic, coherent** neutron scattering is proportional to the **spatial Fourier Transform** of the Pair Correlation Function, $G(r)$ i.e. the probability of finding a particle at position r if there is simultaneously a particle at $r=0$
- The intensity of **inelastic coherent** neutron scattering is proportional to the **space and time Fourier Transforms of the time-dependent** pair correlation function function, $G(r,t)$ = probability of finding a particle at position r at time t when there is a particle at $r=0$ and $t=0$.
- For **inelastic incoherent** scattering, the intensity is proportional to the **space and time Fourier Transforms of the self-correlation** function, $G_s(r,t)$ i.e. the probability of finding a particle at position r at time t when the same particle was at $r=0$ at $t=0$

The Inelastic Scattering Cross Section

Recall that $\left(\frac{d^2\mathbf{S}}{d\Omega.dE} \right)_{coh} = b_{coh}^2 \frac{k'}{k} NS(\vec{Q}, \mathbf{w})$ and $\left(\frac{d^2\mathbf{S}}{d\Omega.dE} \right)_{inc} = b_{inc}^2 \frac{k'}{k} NS_i(\vec{Q}, \mathbf{w})$

where $S(\vec{Q}, \mathbf{w}) = \frac{1}{2p\hbar} \iint G(\vec{r}, t) e^{i(\vec{Q}\cdot\vec{r} - \mathbf{w}t)} d\vec{r} dt$ and $S_i(\vec{Q}, \mathbf{w}) = \frac{1}{2p\hbar} \iint G_s(\vec{r}, t) e^{i(\vec{Q}\cdot\vec{r} - \mathbf{w}t)} d\vec{r} dt$

and the correlation functions that are intuitively similar to those for the elastic scattering case :

$$G(\vec{r}, t) = \frac{1}{N} \int \langle \mathbf{r}_N(\vec{r}, 0) \mathbf{r}_N(\vec{r} + \vec{R}, t) \rangle d\vec{r} \quad \text{and} \quad G_s(\vec{r}, t) = \frac{1}{N} \sum_j \int \langle \mathbf{d}(\vec{r} - \vec{R}_j(0)) \mathbf{d}(\vec{r} + \vec{R} - \vec{R}_j(t)) \rangle d\vec{r}$$

The evaluation of the correlation functions (in which the \mathbf{r} 's and \mathbf{d} - functions have to be treated as non - commuting quantum mechanical operators) is mathematically tedious. Details can be found, for example, in the books by Squires or Marshal and Lovesey.

Examples of $S(Q,\omega)$ and $S_s(Q,\omega)$

- Expressions for $S(Q,\omega)$ and $S_s(Q,\omega)$ can be worked out for a number of cases e.g:
 - Excitation or absorption of one quantum of lattice vibrational energy (phonon)
 - Various models for atomic motions in liquids and glasses
 - Various models of atomic & molecular translational & rotational diffusion
 - Rotational tunneling of molecules
 - Single particle motions at high momentum transfers
 - Transitions between crystal field levels
 - Magnons and other magnetic excitations such as spinons
- Inelastic neutron scattering reveals details of the shapes of interaction potentials in materials

A Phonon is a Quantized Lattice Vibration

- Consider linear chain of particles of mass M coupled by springs. Force on n 'th particle is

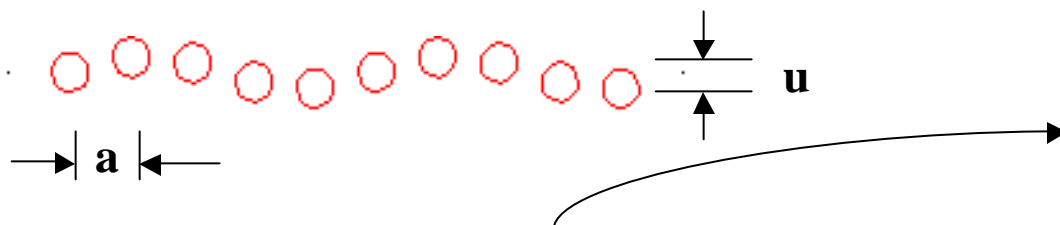
$$F_n = \mathbf{a}_0 u_n + \mathbf{a}_1 (u_{n-1} + u_{n+1}) + \mathbf{a}_2 (u_{n-2} + u_{n+2}) + \dots$$

First neighbor force constant displacements

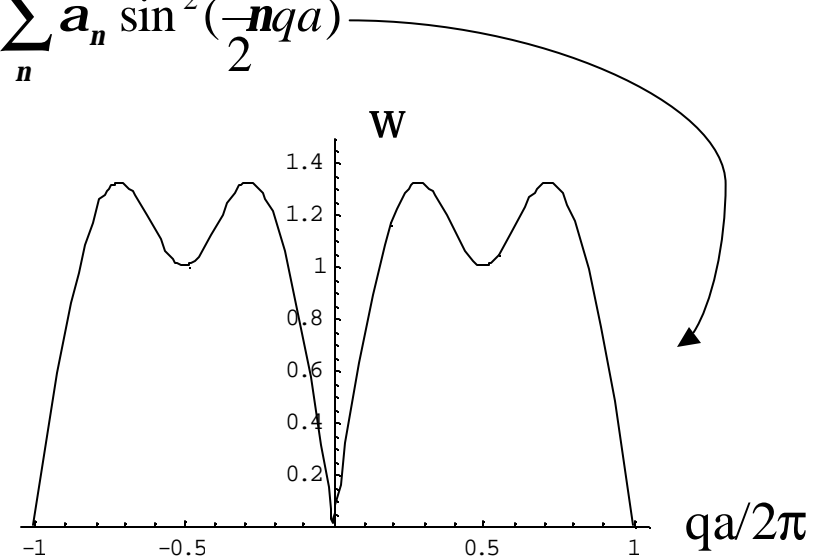
- Equation of motion is $F_n = M\ddot{u}_n$

- Solution is: $u_n(t) = A_q e^{i(qna - \omega t)}$ with $\omega_q^2 = \frac{4}{M} \sum_n \mathbf{a}_n \sin^2(\frac{1}{2} nqa)$

$$q = 0, \pm \frac{2\pi}{L}, \pm \frac{4\pi}{L}, \dots, \pm \frac{N}{2} \frac{2\pi}{L}$$



Phonon Dispersion Relation:
Measurable by inelastic neutron scattering



Inelastic Magnetic Scattering of Neutrons

- In the simplest case, atomic spins in a ferromagnet precess about the direction of mean magnetization

$$H = \sum_{l,l'} J(\vec{l} - \vec{l}') \vec{S}_l \cdot \vec{S}_{l'} = H_0 + \sum_q \hbar w_q b_q^+ b_q$$

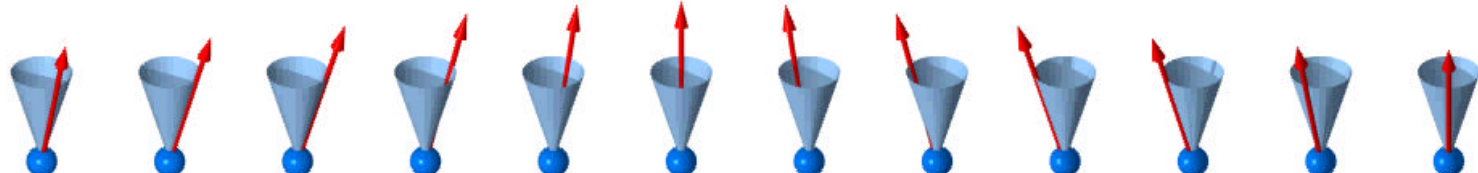
↑
exchange coupling ↑
 ground state energy ↓
 spin waves (magnons)

with

$$\hbar w_q = 2S(J_0 - J_q) \quad \text{where} \quad J_q = \sum_l J(\vec{l}) e^{i\vec{q} \cdot \vec{l}}$$

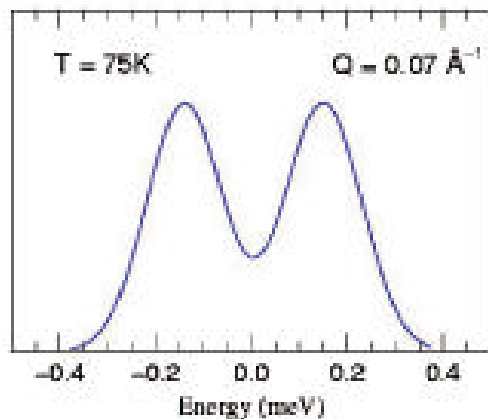
$\hbar w_q = Dq^2$ is the dispersion relation for a ferromagnet

Fluctuating spin is
perpendicular to mean spin
direction => spin-flip
neutron scattering

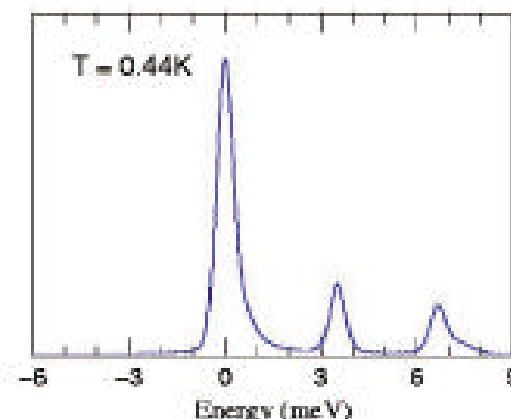


Spin wave animation courtesy of A. Zheludev (ORNL)

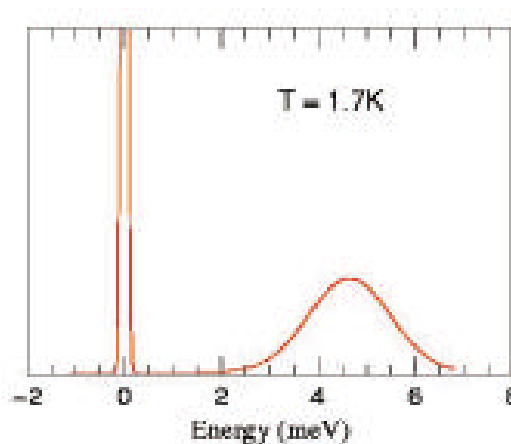
Measured Inelastic Neutron Scattering Signals in Crystalline Solids Show Both Collective & Local Fluctuations*



Spin waves – collective excitations



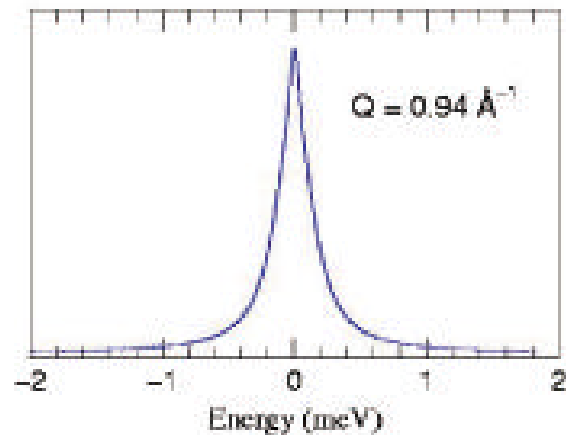
Crystal Field splittings
(HoPd₂Sn) – local excitations



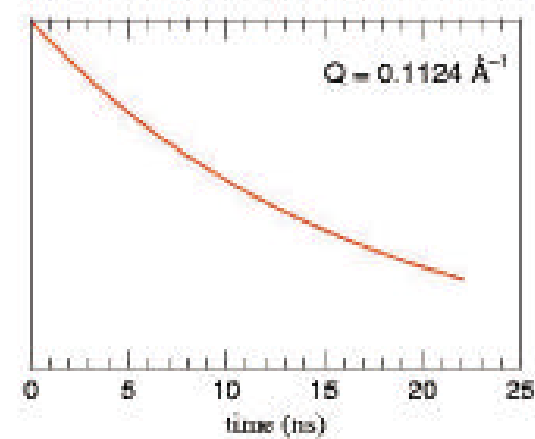
Local spin resonances (e.g. ZnCr₂O₄)

* Courtesy of Dan Neumann, NIST

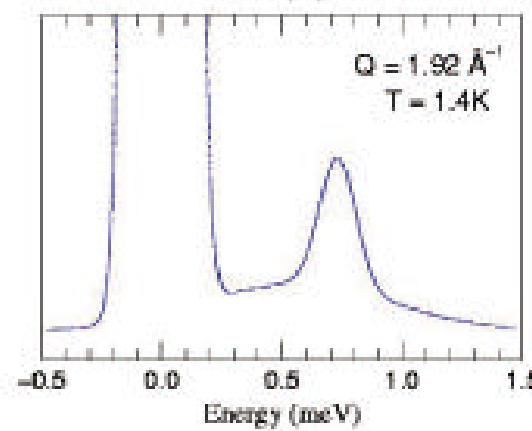
Measured Inelastic Neutron Scattering Signals in Liquids Generally Show Diffusive Behavior



“Simple” liquids (e.g. water)

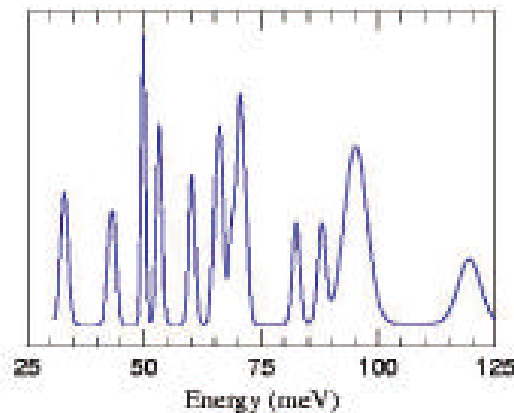


Complex Fluids (e.g. SDS)

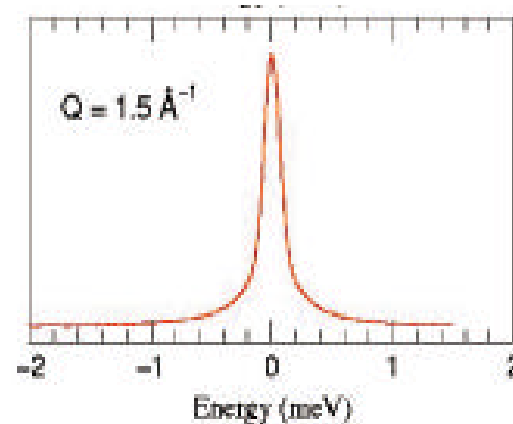


Quantum Fluids (e.g. He in porous silica)

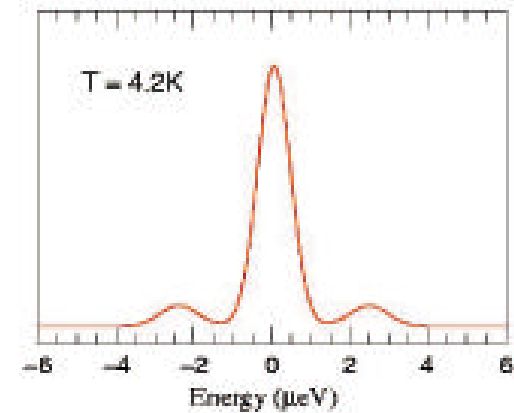
Measured Inelastic Neutron Scattering in Molecular Systems Span Large Ranges of Energy



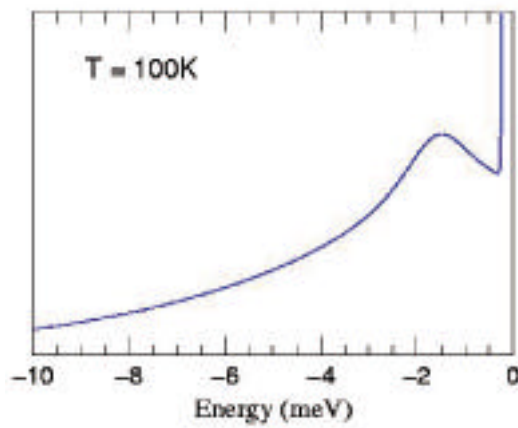
Vibrational spectroscopy
(e.g. C_{60})



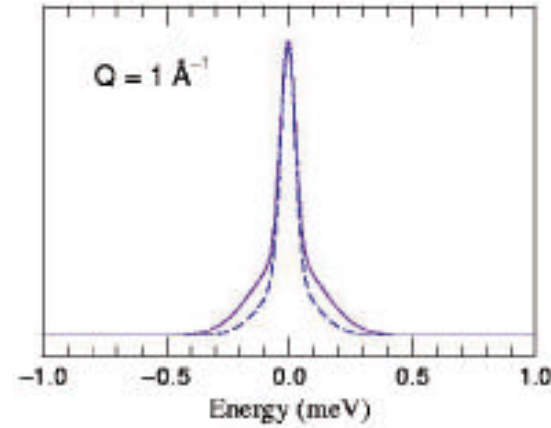
Molecular reorientation
(e.g. pyrazine)



Rotational tunneling
(e.g. CH_3I)

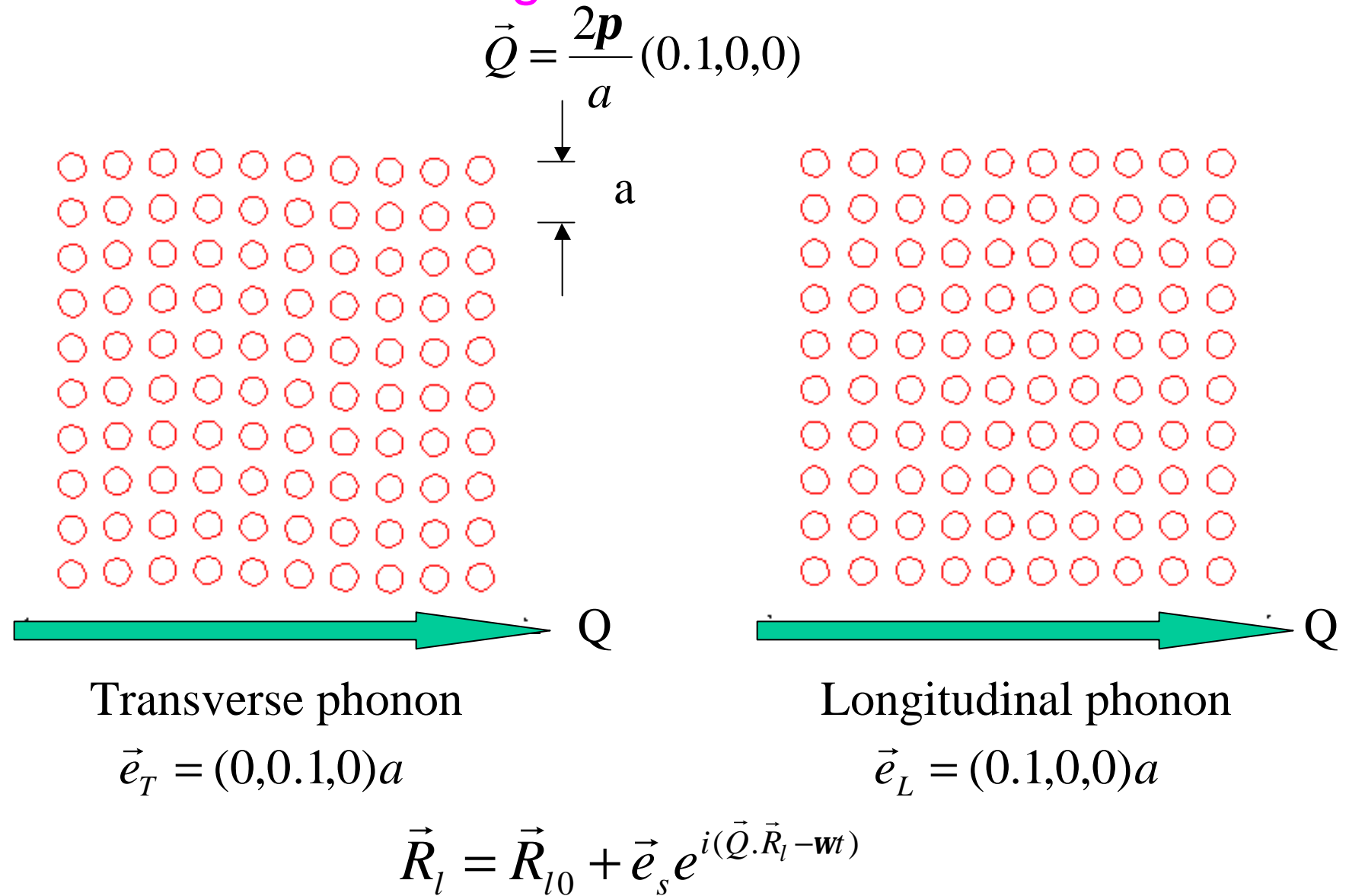


Polymers

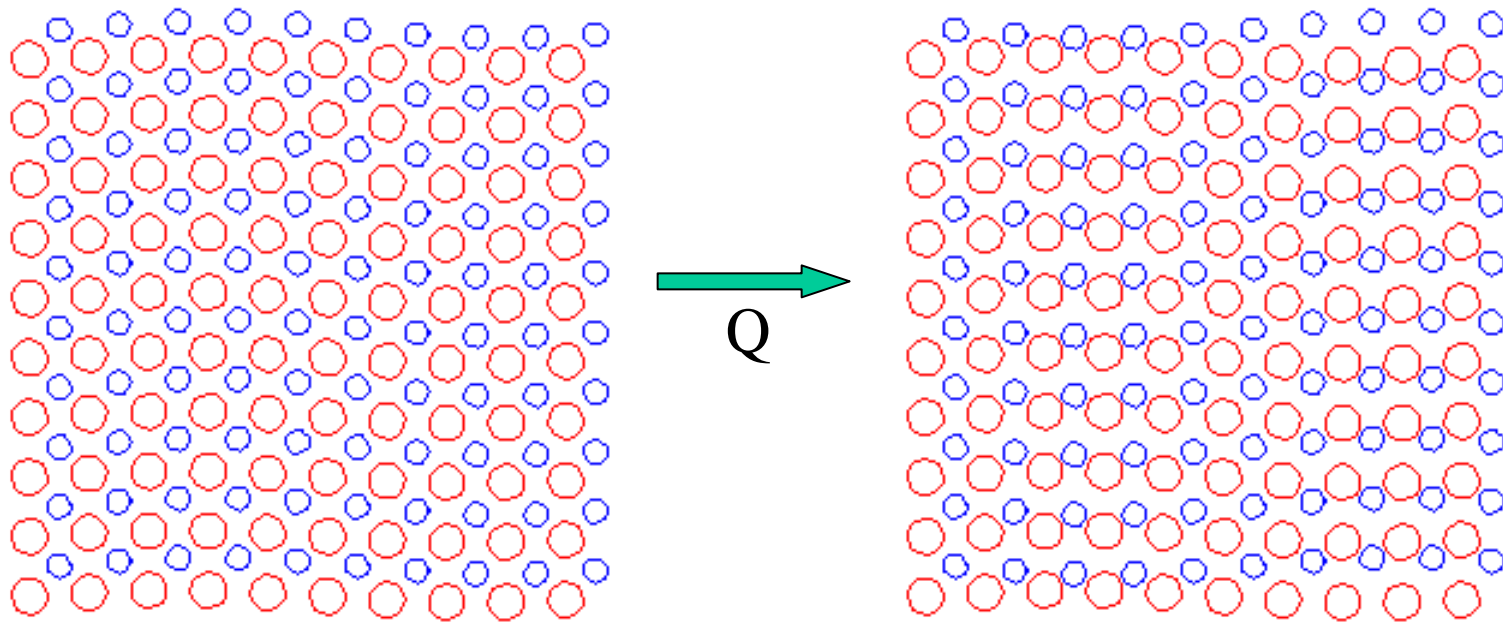


Proteins

Atomic Motions for Longitudinal & Transverse Phonons



Transverse Optic and Acoustic Phonons



Acoustic

$$\vec{e}_{red} = (0, 0.1, 0)a$$

$$\vec{e}_{blue} = (0, 0.14, 0)a$$

Optic

$$\vec{e}_{red} = (0, 0.1, 0)a$$

$$\vec{e}_{blue} = (0, -0.14, 0)a$$

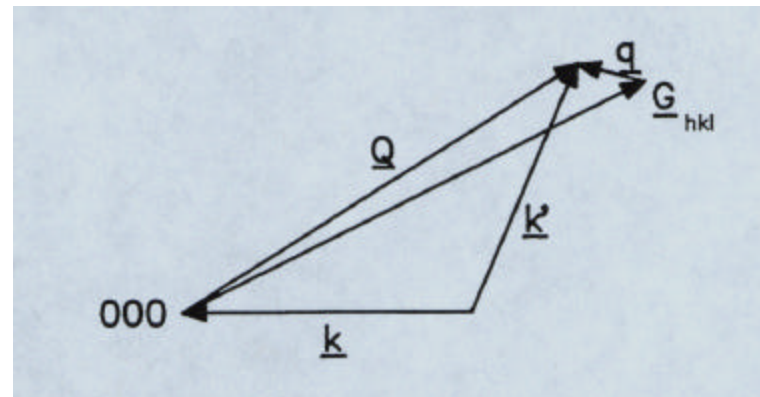
$$\vec{R}_{lk} = \vec{R}_{lk}^0 + \vec{e}_s e^{i(\vec{Q} \cdot \vec{R}_l - \omega t)}$$

Phonons – the Classical Use for Inelastic Neutron Scattering

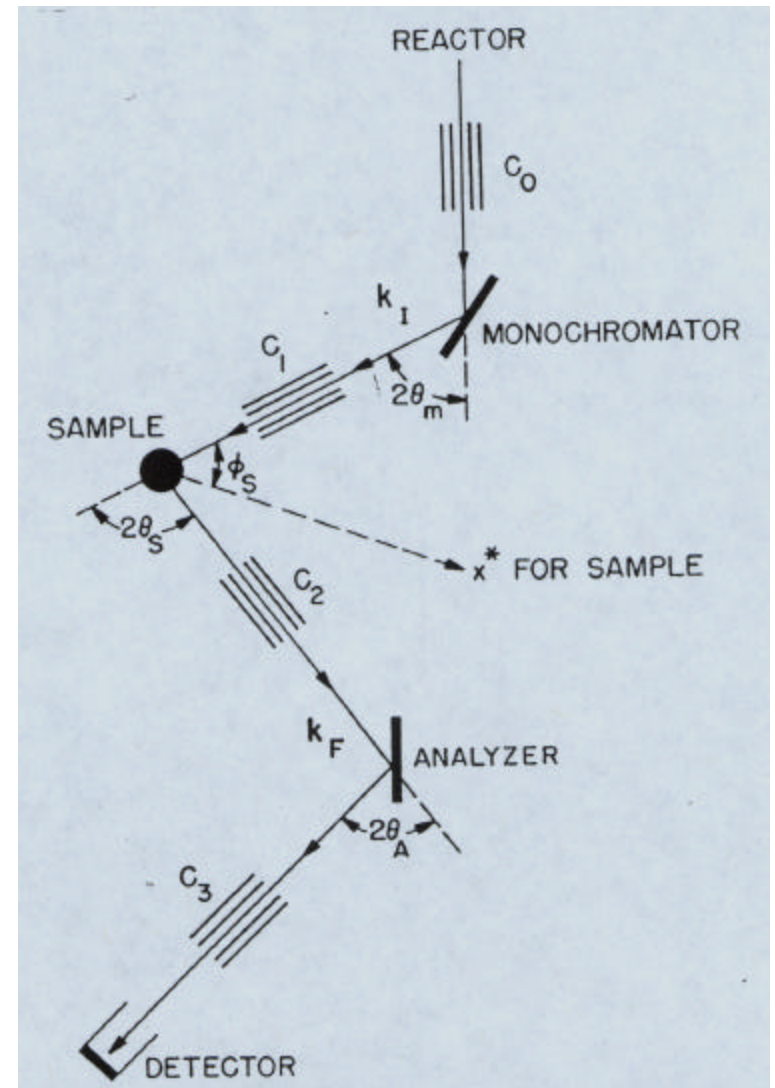
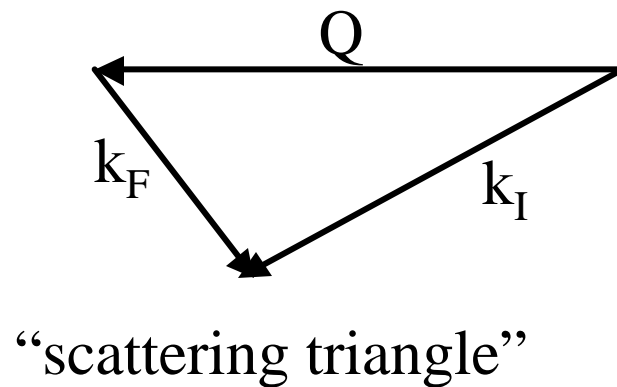
- Coherent scattering measures scattering from single phonons

$$\left(\frac{d^2\mathbf{s}}{d\Omega dE} \right)_{coh\pm 1} = \mathbf{s}_{coh} \frac{k'}{k} \frac{\mathbf{p}^2}{MV_0} e^{-2W} \sum_s \sum_G \frac{(\vec{Q} \cdot \vec{e}_s)^2}{\mathbf{w}_s} \left(n_s + \frac{1 \pm 1}{2} \right) \mathbf{d}(\mathbf{w} \mp \mathbf{w}_s) \mathbf{d}(\vec{Q} - \vec{q} - \vec{G})$$

- Note the following features:
 - Energy & momentum delta functions => see single phonons (labeled s)
 - Different thermal factors for phonon creation ($n_s + 1$) & annihilation (n_s)
 - Can see phonons in different Brillouin zones (different recip. lattice vectors, \mathbf{G})
 - Cross section depends on relative orientation of \mathbf{Q} & atomic motions (\mathbf{e}_s)
 - Cross section depends on phonon frequency (ω_s) and atomic mass (M)
 - In general, scattering by multiple excitations is either insignificant or a small correction (the presence of other phonons appears in the Debye-Waller factor, W)

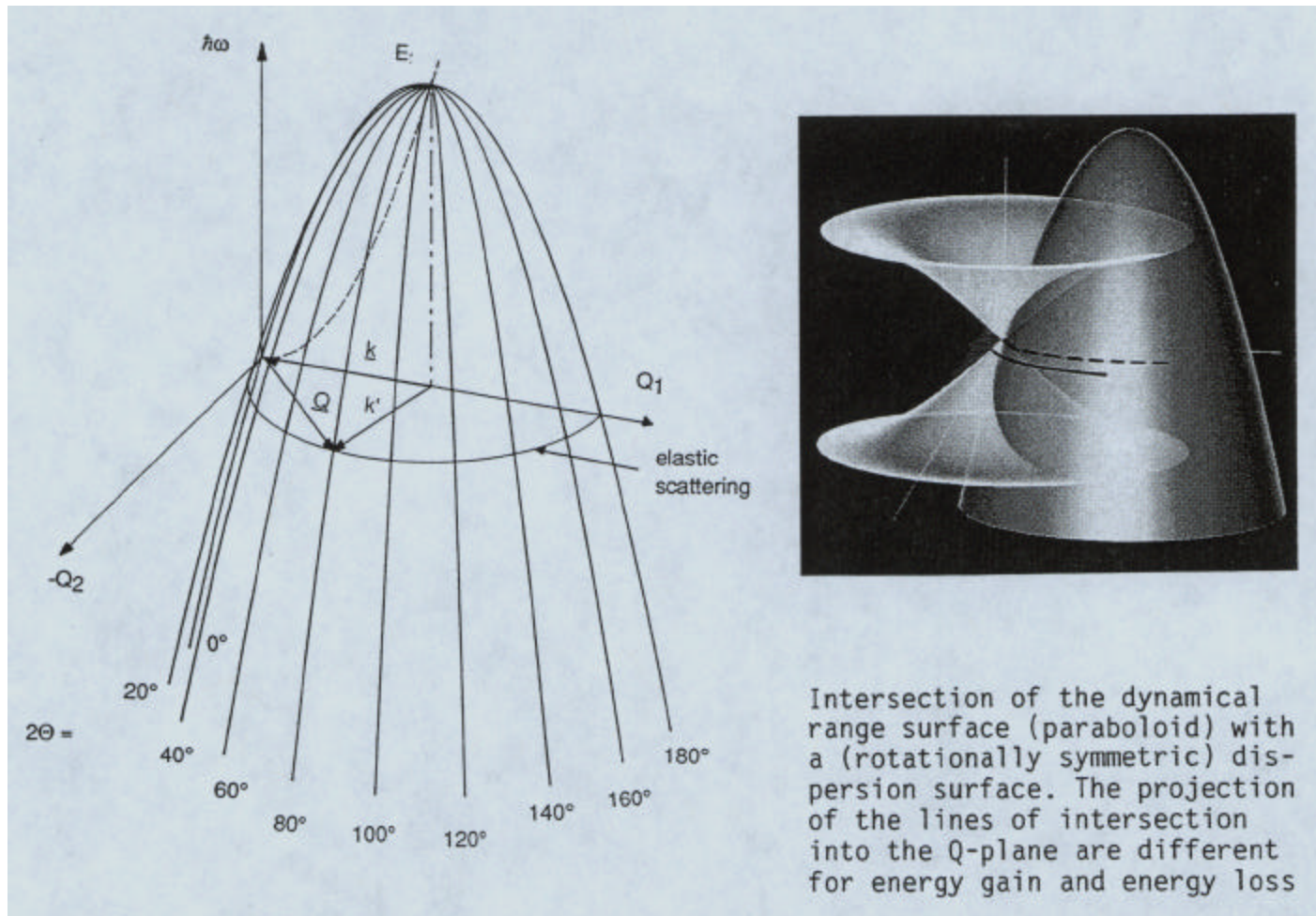


The Workhorse of Inelastic Scattering Instrumentation at Reactors Is the Three-axis Spectrometer



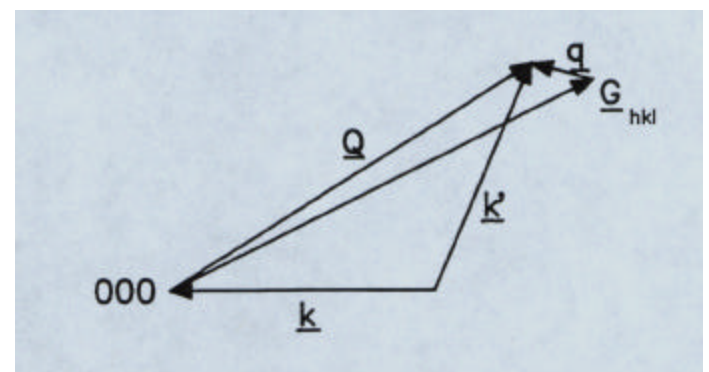
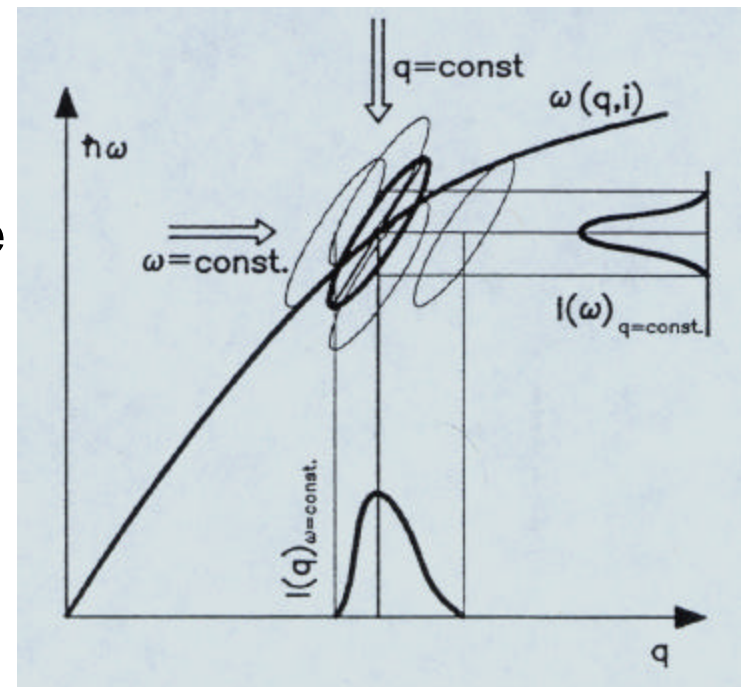
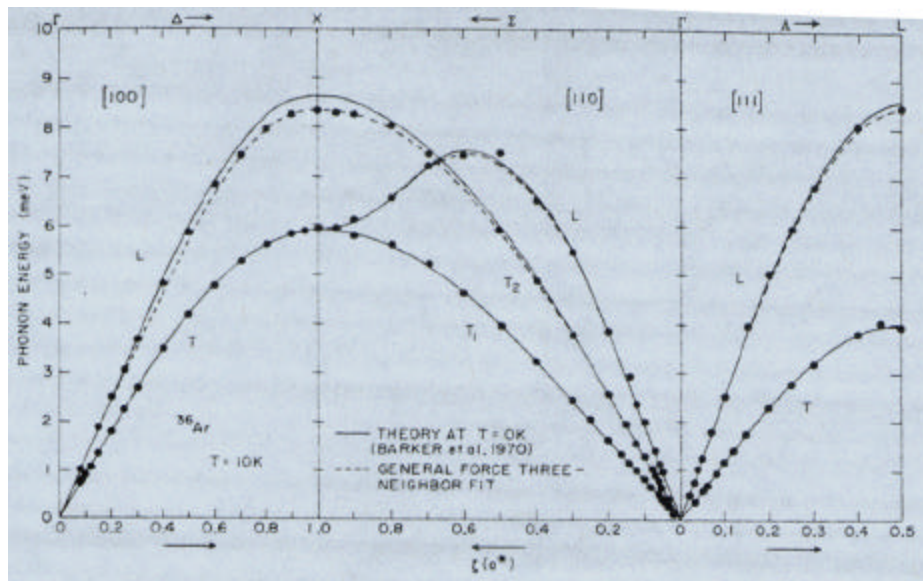
The Accessible Energy and Wavevector Transfers Are Limited by Conservation Laws

- Neutron cannot lose more than its initial kinetic energy & momentum must be conserved



Triple Axis Spectrometers Have Mapped Phonons Dispersion Relations in Many Materials

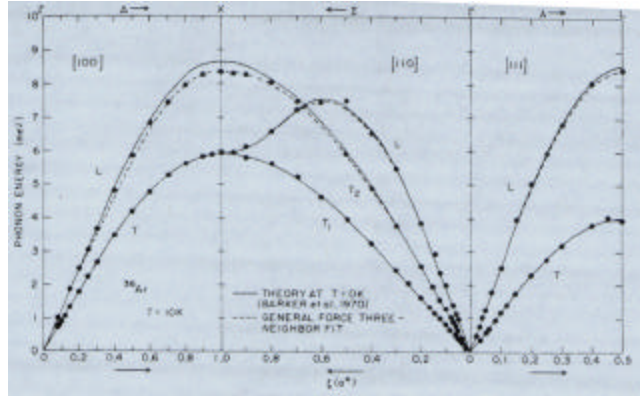
- Point by point measurement in (Q, E) space
- Usually keep either k_i or k_F fixed
- Choose Brillouin zone (i.e. G) to maximize scattering cross section for phonons
- Scan usually either at constant- Q (Brockhouse invention) or constant- E



What Use Have Phonon Measurements Been?

- Quantifying interatomic potentials in metals, rare gas solids, ionic crystals, covalently bonded materials etc
- Quantifying anharmonicity (I.e. phonon-phonon interactions)
- Measuring soft modes at 2nd order structural phase transitions
- Electron-phonon interactions including Kohn anomalies
- Roton dispersion in liquid He
- Relating phonons to other properties such as superconductivity, anomalous lattice expansion etc

Examples of Phonon Measurements



Phonons in ^{36}Ar – validation of LJ potential

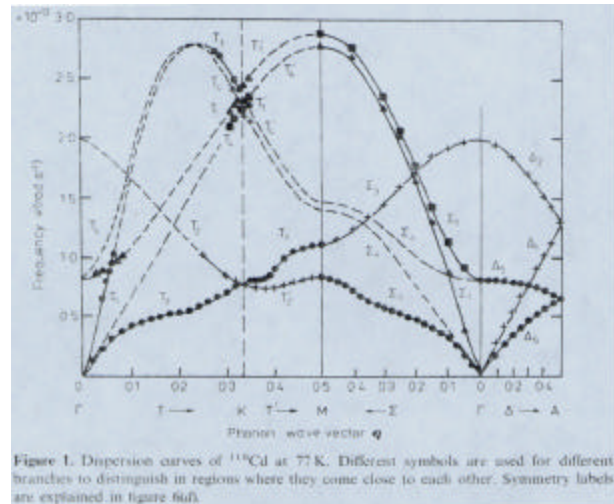
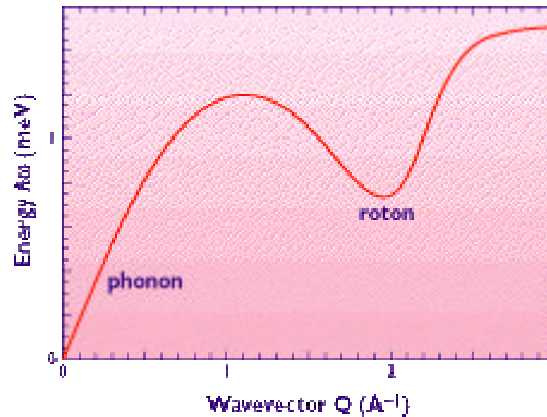


Figure 1. Dispersion curves of ^{110}Cd at 77 K. Different symbols are used for different branches to distinguish regions where they come close to each other. Symmetry labels are explained in figure 6(a).

Phonons in ^{110}Cd



Roton dispersion in ^4He

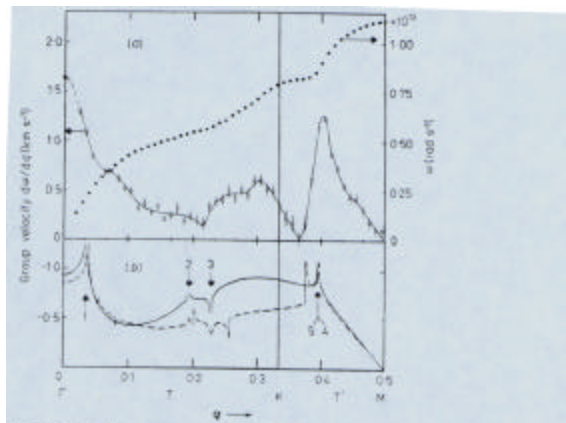
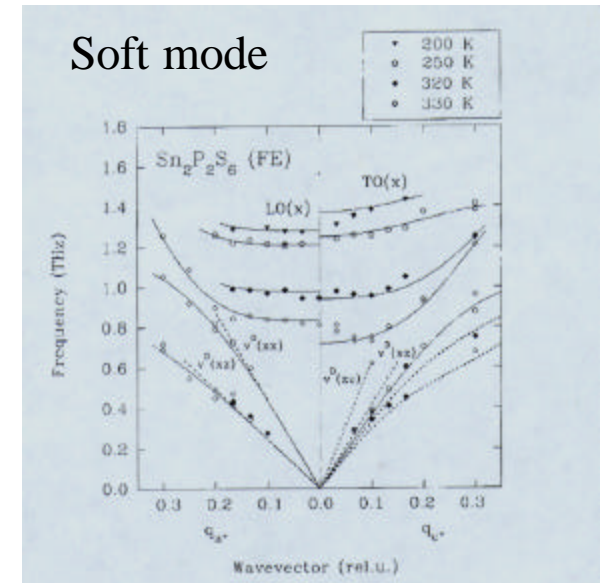
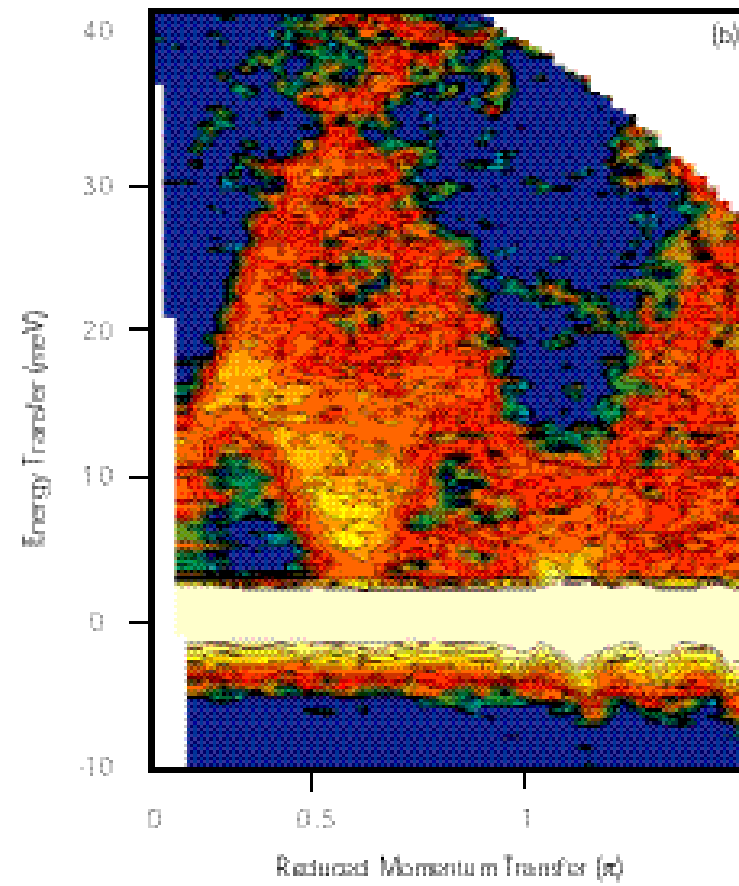
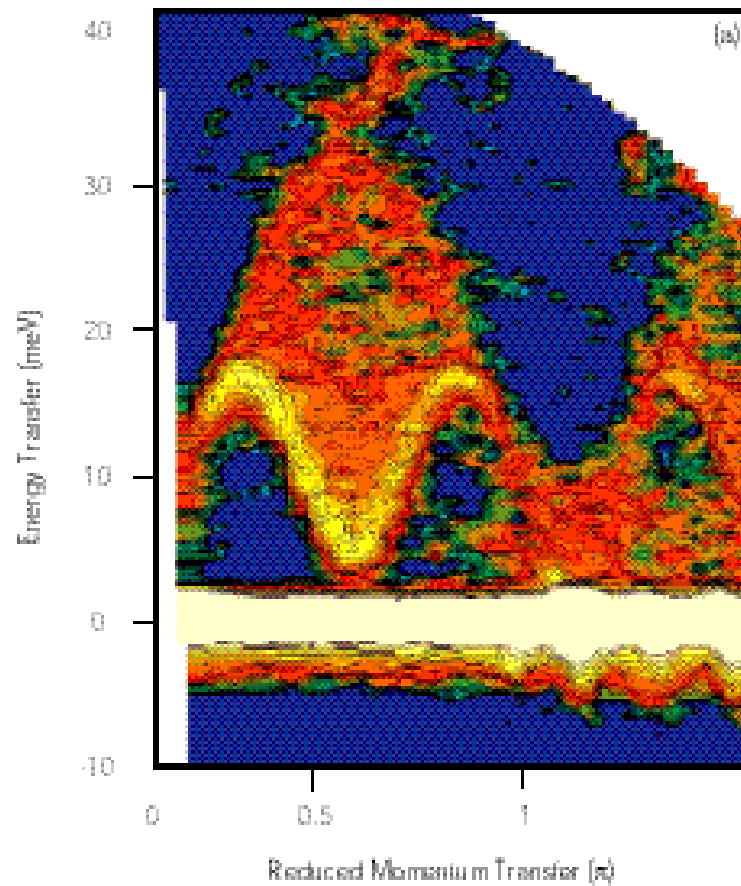


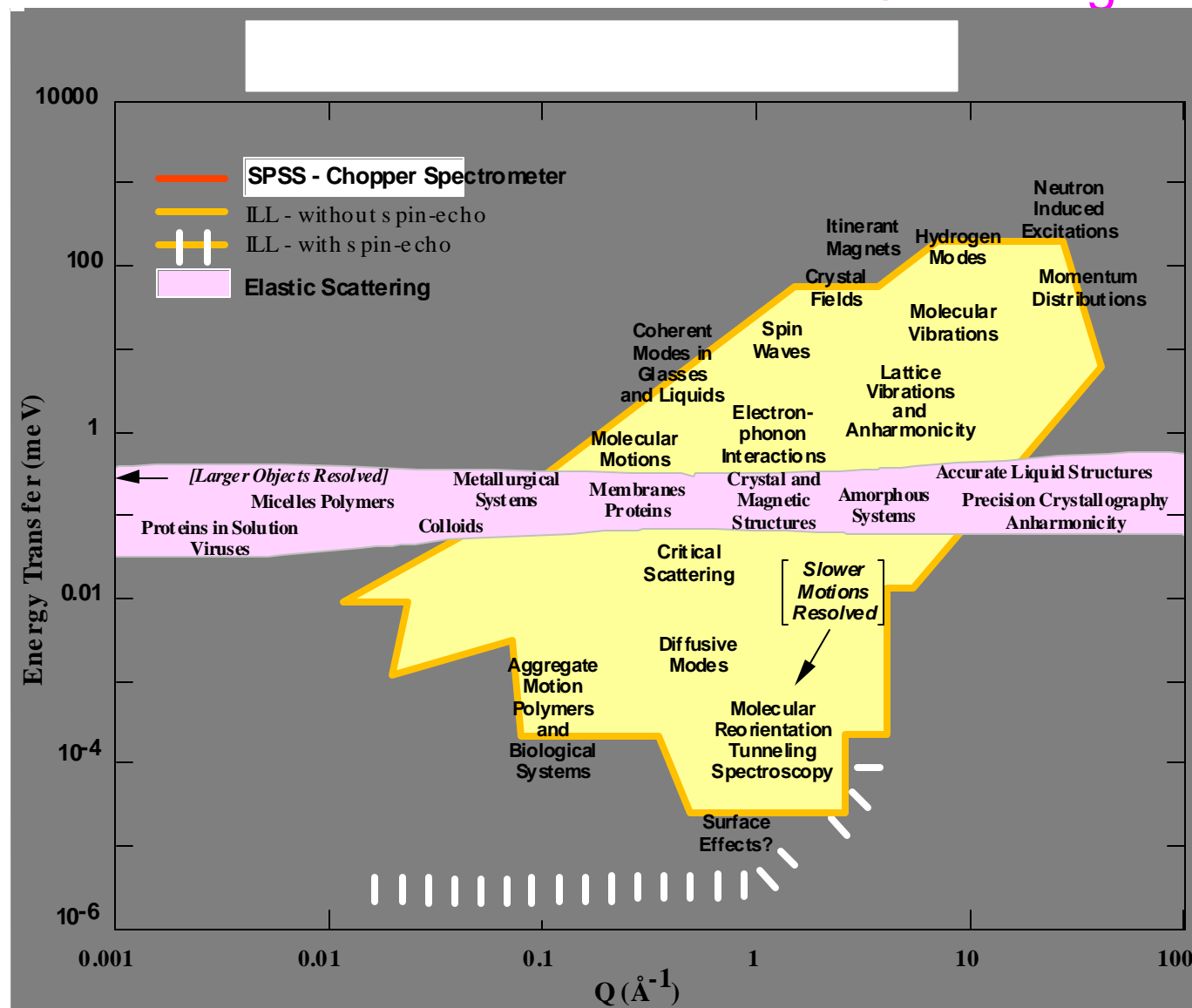
Figure 2. (i) dispersion curves (full circles) and group velocity v/ω (open circles) for the T_1-T_2 branch at 77 K. At $q=0$ the group velocity obtained from the elastic constants (Garland and Silverman 1960) is represented by a full circle. The line is a guide to the eye. (ii) theoretical predictions of the group velocity for the T_3-T_1 direction. The full line is calculated in perturbation theory including second-order terms in the potential; the broken line including third-order terms in the potential. The numbers refer to the anomalies listed in table 2.

Time-of-flight Methods Can Give Complete Dispersion Curves at a Single Instrument Setting in Favorable Circumstances



CuGeO_3 is a 1-d magnet. With the unique axis parallel to the incident neutron beam, the complete magnon dispersion can be obtained

Much of the Scientific Impact of Neutron Scattering Has Involved the Measurement of Inelastic Scattering



Energy & Wavevector Transfers accessible to Neutron Scattering

Neutron Spin Echo

By

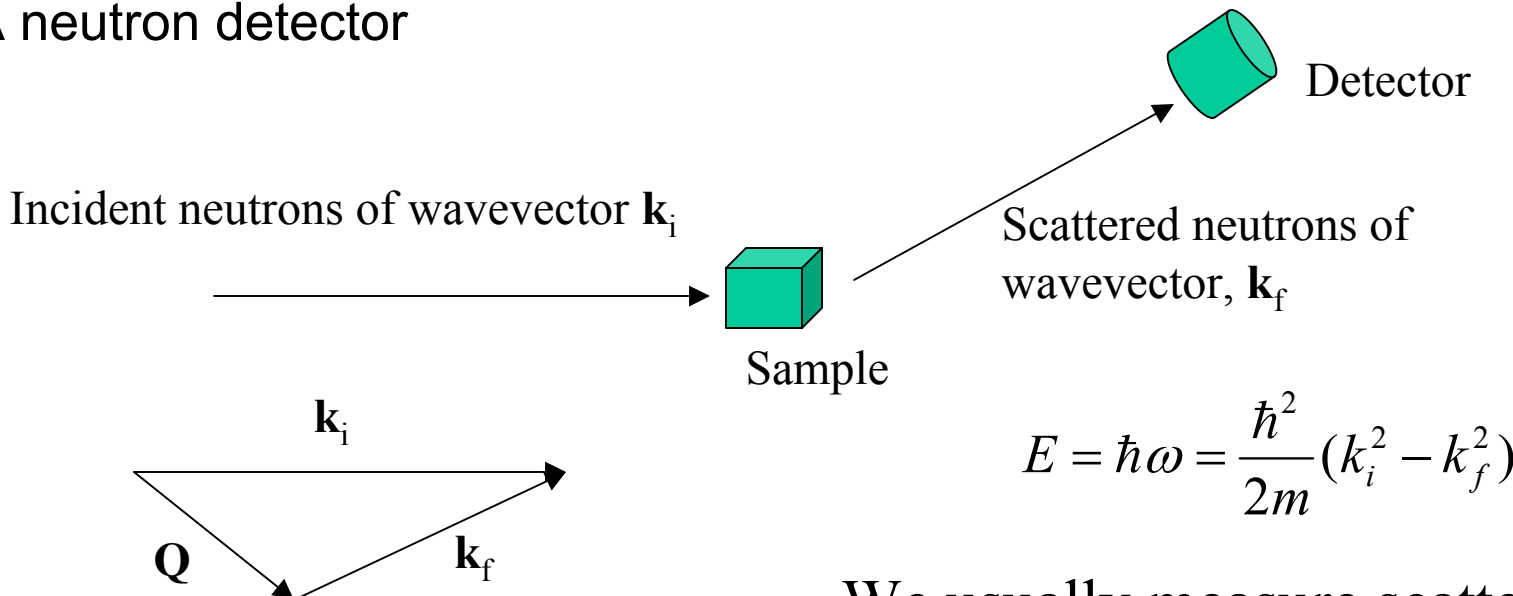
Roger Pynn*

Los Alamos National Laboratory

*With contributions from B. Farago (ILL), S. Longeville (Saclay),
and T. Keller (Stuttgart)

What Do We Need for a Basic Neutron Scattering Experiment?

- A source of neutrons
- A method to prescribe the wavevector of the neutrons incident on the sample
- (An interesting sample)
- A method to determine the wavevector of the scattered neutrons
- A neutron detector

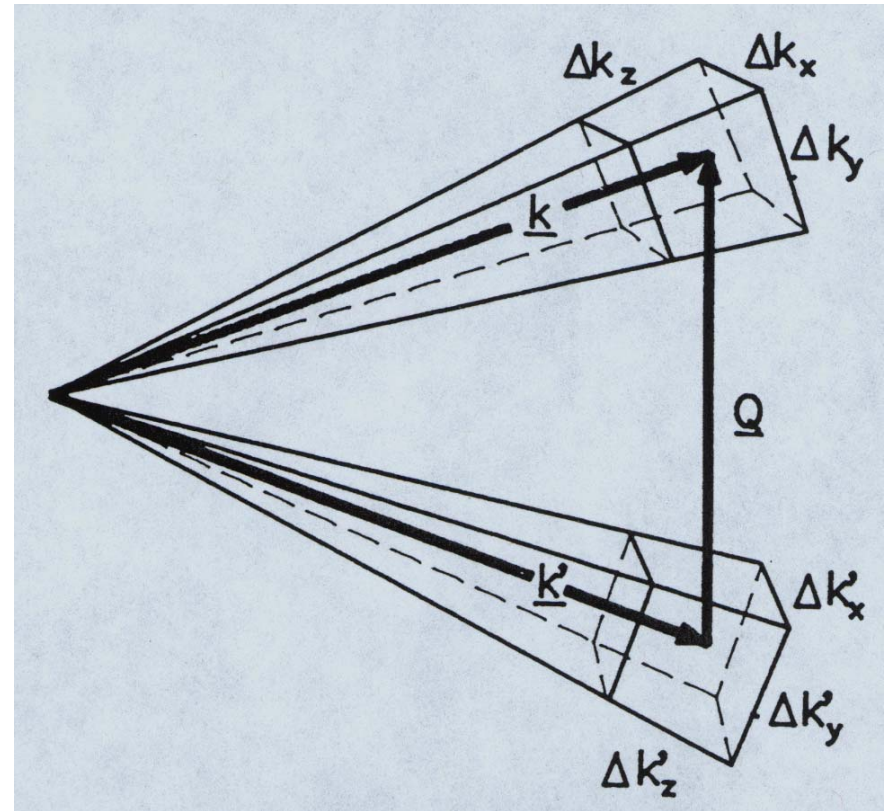


$$E = \hbar\omega = \frac{\hbar^2}{2m} (k_i^2 - k_f^2)$$

We usually measure scattering as a function of energy (E) and wavevector (\mathbf{Q}) transfer

Instrumental Resolution

- Uncertainties in the neutron wavelength & direction of travel imply that Q and E can only be defined with a certain precision
- When the box-like resolution volumes in the figure are convolved, the overall resolution is Gaussian (central limit theorem) and has an elliptical shape in (Q, E) space
- The total signal in a scattering experiment is proportional to the phase space volume within the elliptical resolution volume – **the better the resolution, the smaller the resolution volume and the lower the count rate**



The Goal of Neutron Spin Echo is to Break the Inverse Relationship between Intensity & Resolution

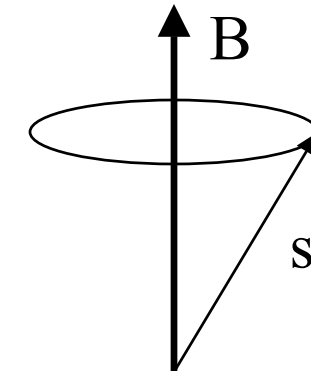
- Traditional – define *both* incident & scattered wavevectors in order to define E and \mathbf{Q} accurately
- Traditional – use collimators, monochromators, choppers etc to define both \mathbf{k}_i and \mathbf{k}_f
- NSE – measure as a function of the *difference* between appropriate components of \mathbf{k}_i and \mathbf{k}_f (original use: measure $\mathbf{k}_i - \mathbf{k}_f$ i.e. energy change)
- NSE – use the neutron's spin polarization to encode the difference between components of \mathbf{k}_i and \mathbf{k}_f
- NSE – can use large beam divergence &/or poor monochromatization to increase signal intensity, while maintaining very good resolution

The Underlying Physics of Neutron Spin Echo (NSE) Technology is Larmor Precession of the Neutron's Spin

- The time evolution of the expectation value of the spin of a spin-1/2 particle in a magnetic field can be determined classically as:

$$\frac{d\vec{s}}{dt} = \gamma \vec{s} \wedge \vec{B} \quad \Rightarrow \quad \omega_L = |\gamma| B$$

$$\gamma = -2913 * 2\pi \text{ Gauss}^{-1} \cdot s^{-1}$$



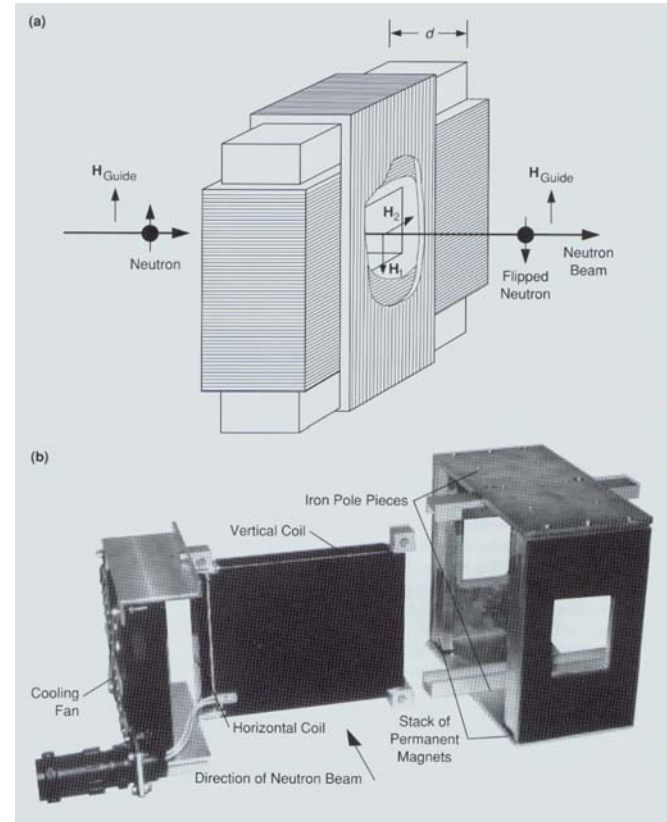
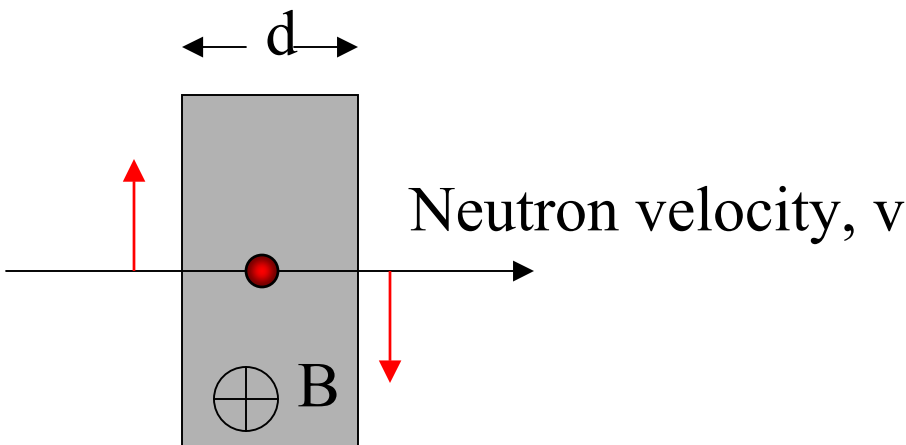
- The total precession angle of the spin, ϕ , depends on the time the neutron spends in the field: $\phi = \omega_L t$

B(Gauss)	ω_L (10^3 rad.s $^{-1}$)	N (msec $^{-1}$)	Turns/m for 4 Å neutrons
10	183	29	~29

Larmor Precession allows the Neutron Spin to be Manipulated using π or $\pi/2$ Spin-Turn Coils: Both are Needed for NSE

- The total precession angle of the spin, ϕ , depends on the time the neutron spends in the B field

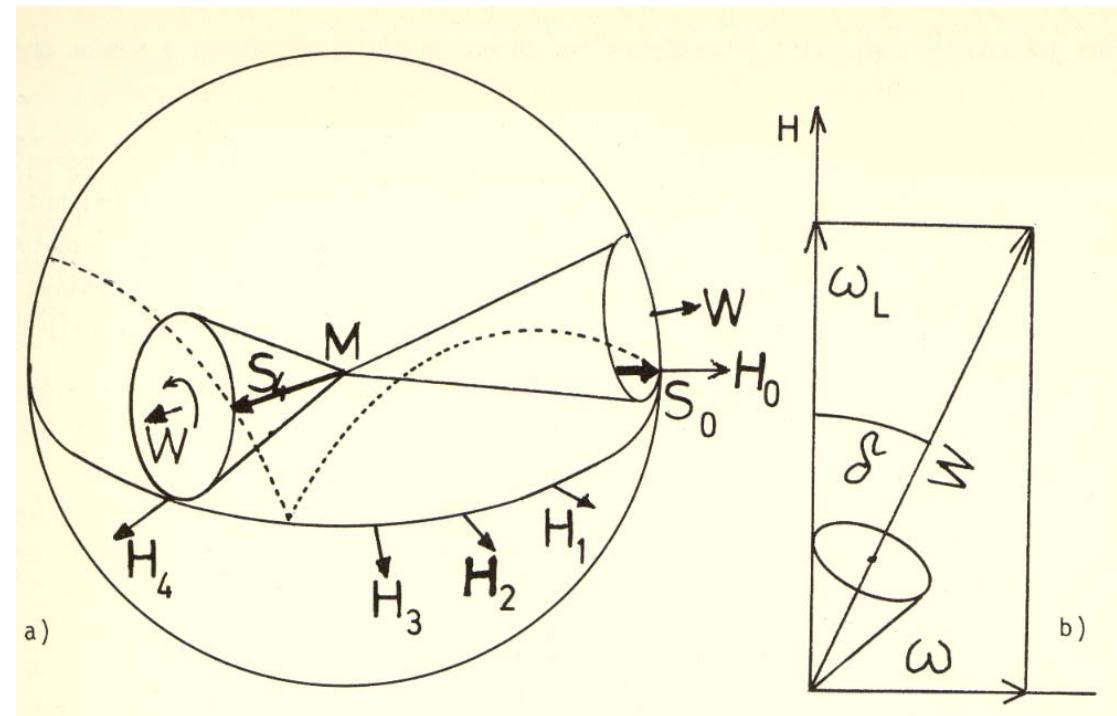
$$\phi = \omega_L t = \gamma B d / v$$



$$\text{Number of turns} = \frac{1}{135.65} \cdot B[\text{Gauss}] \cdot d[\text{cm}] \cdot \lambda[\text{Angstroms}]$$

How does a Neutron Spin Behave when the Magnetic Field Changes Direction?

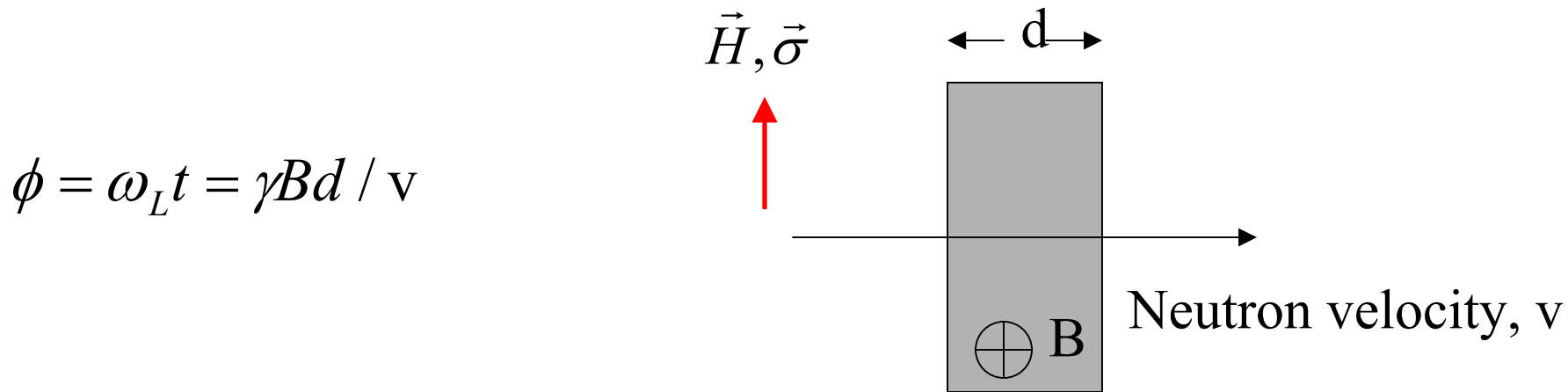
When H rotates with frequency ω , $H_0 \rightarrow H_1 \rightarrow H_2 \dots$, and the spin trajectory is described by a cone rolling on the plane in which H moves



- Distinguish two cases: adiabatic and sudden
- *Adiabatic* – $\tan(\delta) \ll 1$ – large B or small ω – spin and field remain co-linear – this limit used to “guide” a neutron spin
- *Sudden* – $\tan(\delta) \gg 1$ – large ω – spin precesses around new field direction – this limit is used to design spin-turn devices

Neutron Spin Echo (NSE) uses Larmor Precession to “Code” Neutron Velocities

- A neutron spin precesses at the Larmor frequency in a magnetic field, B . $\omega_L = \gamma B$
- The total precession angle of the spin, ϕ , depends on the time the neutron spends in the field



$$\phi = \omega_L t = \gamma B d / v$$

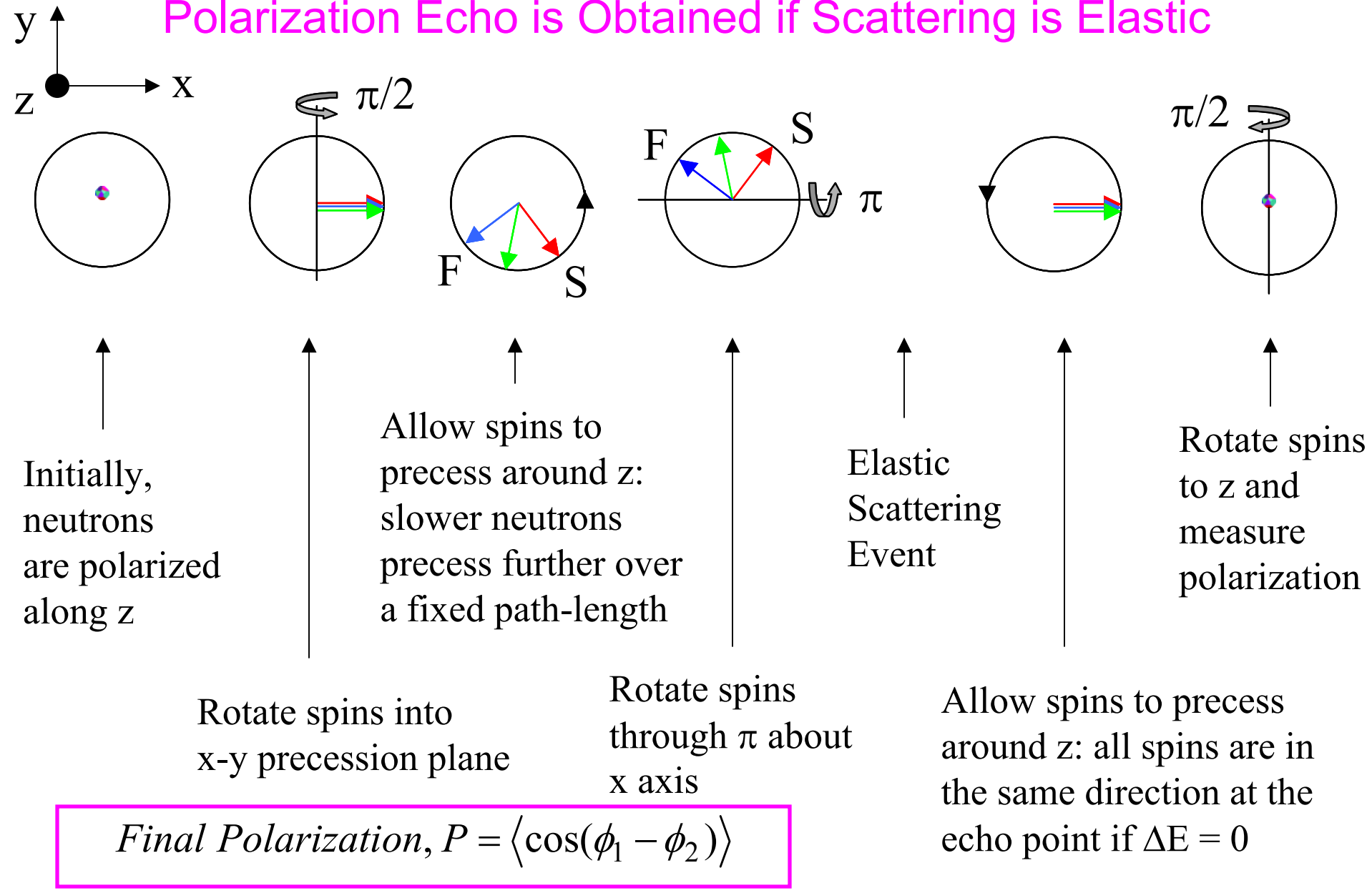
$$\text{Number of turns} = \frac{1}{135.65} \cdot B[\text{Gauss}] \cdot d[\text{cm}] \cdot \lambda[\text{Angstroms}]$$

The precession angle ϕ is a measure of the neutron's speed v

The Principles of NSE are Very Simple

- If a spin rotates anticlockwise & then clockwise by the same amount it comes back to the same orientation
 - Need to reverse the direction of the applied field
 - Independent of neutron speed provided the speed is constant
- The same effect can be obtained by reversing the precession angle at the mid-point and continuing the precession in the same sense
 - Use a π rotation
- If the neutron's velocity, v , is changed by the sample, its spin will not come back to the same orientation
 - The difference will be a measure of the change in the neutron's speed or energy

In NSE*, Neutron Spins Precess Before and After Scattering & a Polarization Echo is Obtained if Scattering is Elastic



$$Final\ Polarization,\ P = \langle \cos(\phi_1 - \phi_2) \rangle$$

For Quasi-elastic Scattering, the Echo Polarization depends on Energy Transfer

- If the neutron changes energy when it scatters, the precession phases before & after scattering, ϕ_1 & ϕ_2 , will be different:

using $\hbar\omega = \frac{1}{2}m(v_1^2 - v_2^2) \approx mv\delta\nu$

$$\phi_1 - \phi_2 = \gamma Bd \left(\frac{1}{v_1} - \frac{1}{v_2} \right) \approx \frac{\gamma Bd}{v^2} \delta\nu \approx \frac{\gamma Bd\hbar\omega}{mv^3} = \frac{\gamma Bdm^2\lambda^3\omega}{2\pi\hbar^2}$$

- To lowest order, the difference between ϕ_1 & ϕ_2 depends only on ω (i.e. $v_1 - v_2$) & not on v_1 & v_2 separately
- The measured polarization, $\langle P \rangle$, is the average of $\cos(\phi_1 - \phi_2)$ over all transmitted neutrons i.e.

$$\langle P \rangle = \frac{\iint I(\lambda)S(\vec{Q},\omega) \cos(\phi_1 - \phi_2) d\lambda d\omega}{\iint I(\lambda)S(\vec{Q},\omega) d\lambda d\omega}$$

Neutron Polarization at the Echo Point is a Measure of the Intermediate Scattering Function

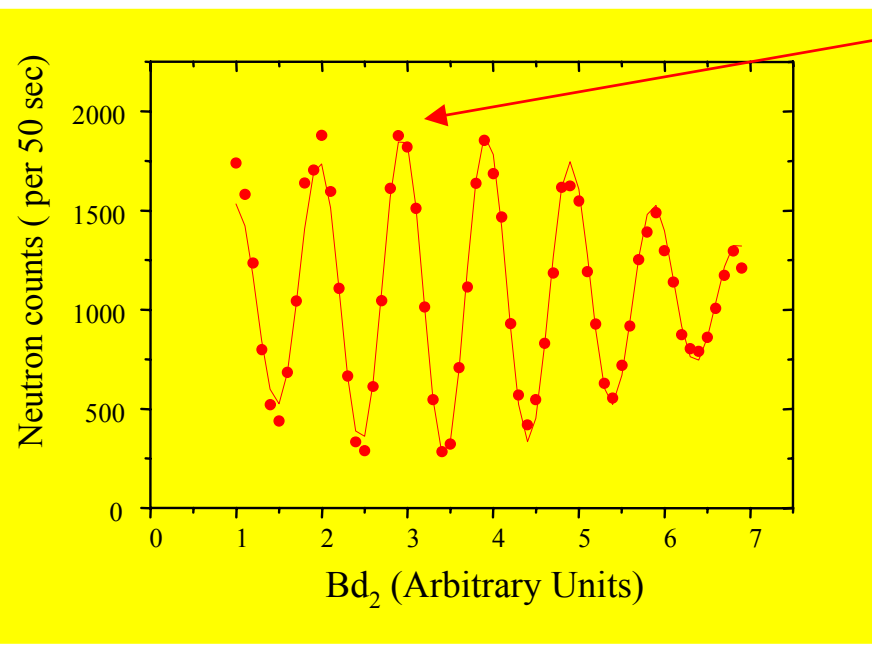
$$\langle P \rangle = \frac{\iint I(\lambda) S(\vec{Q}, \omega) \cos(\phi_1 - \phi_2) d\lambda d\omega}{\iint I(\lambda) S(\vec{Q}, \omega) d\lambda d\omega} \approx \left\langle \int S(\vec{Q}, \omega) \cos(\omega\tau) d\omega \right\rangle = I(\vec{Q}, \tau)$$

where the "spin echo time" $\tau = \gamma Bd \frac{m^2}{2\pi h^2} \lambda^3$

Bd (T.m)	λ (nm)	τ (ns)
1	0.4	12
1	0.6	40
1	1.0	186

- $I(\vec{Q}, t)$ is called the intermediate scattering function
 - Time Fourier transform of $S(\vec{Q}, \omega)$ or the \vec{Q} Fourier transform of $G(\vec{r}, t)$, the two particle correlation function
- NSE probes the sample dynamics as a function of time rather than as a function of ω
- The spin echo time, τ , is the “correlation time”

Neutron Polarization is Measured using an Asymmetric Scan around the Echo Point



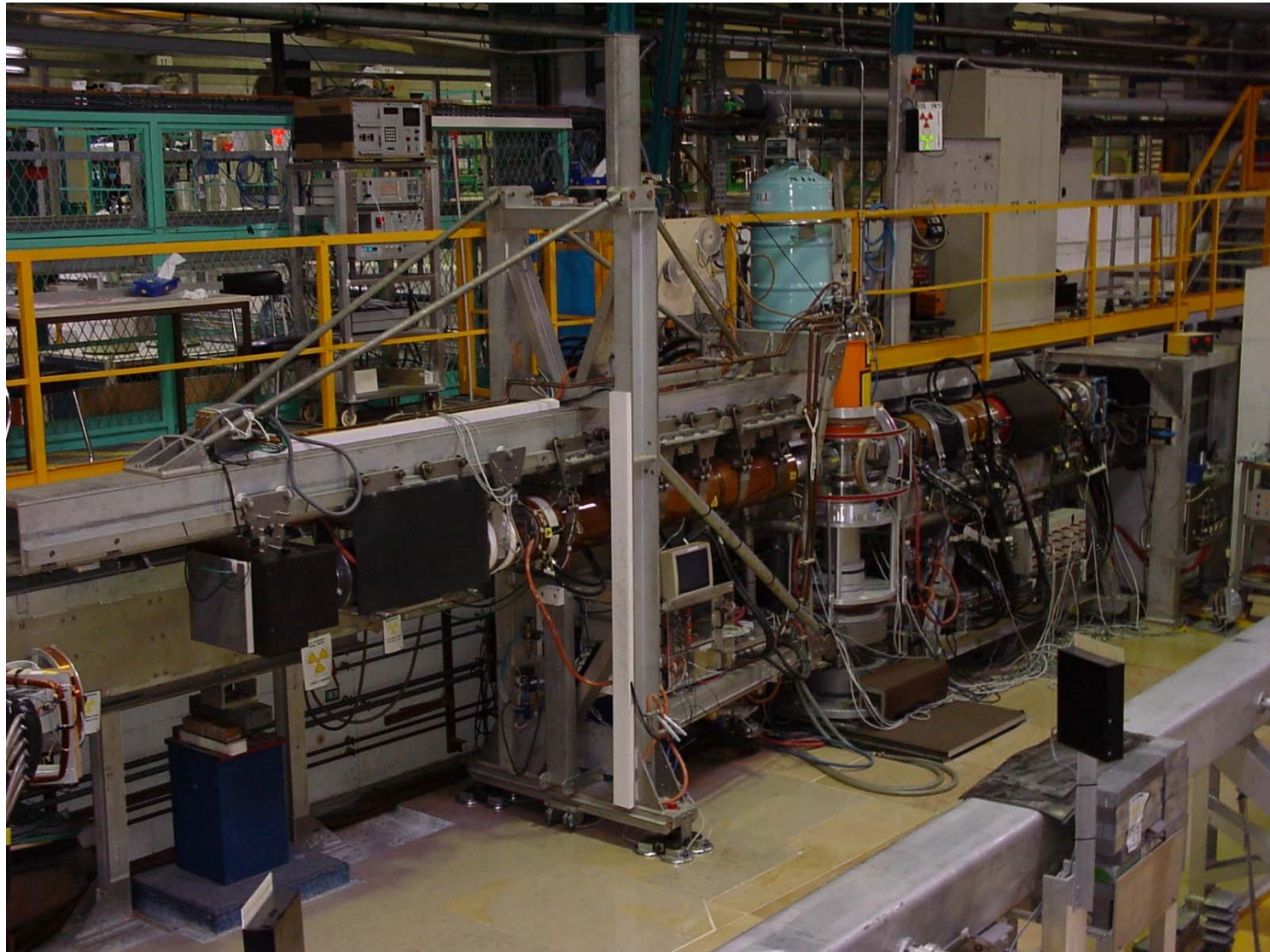
Echo Point

The echo amplitude decreases when $(Bd)_1$ differs from $(Bd)_2$ because the incident neutron beam is not monochromatic.
For elastic scattering:

$$\langle P \rangle \sim \int I(\lambda) \cos \left[\frac{m}{h} \{(Bd)_1 - (Bd)_2\} \lambda \right] d\lambda$$

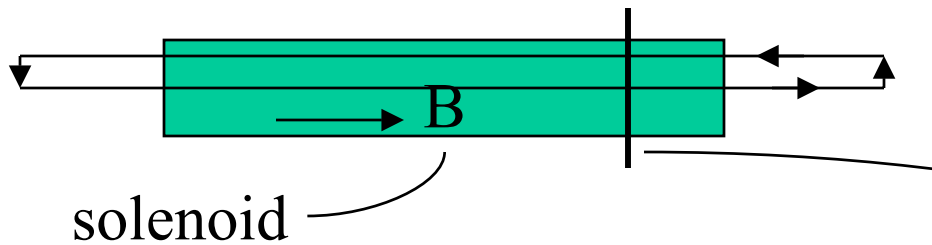
Because the echo point is the same for all neutron wavelengths, we can use a broad wavelength band and enhance the signal intensity

What does a NSE Spectrometer Look Like? IN11 at ILL was the First



Field-Integral Inhomogeneities cause τ to vary over the Neutron Beam: They can be Corrected

- Solenoids (used as main precession fields) have fields that vary as r^2 away from the axis of symmetry because of end effects ($\text{div } \mathbf{B} = 0$)



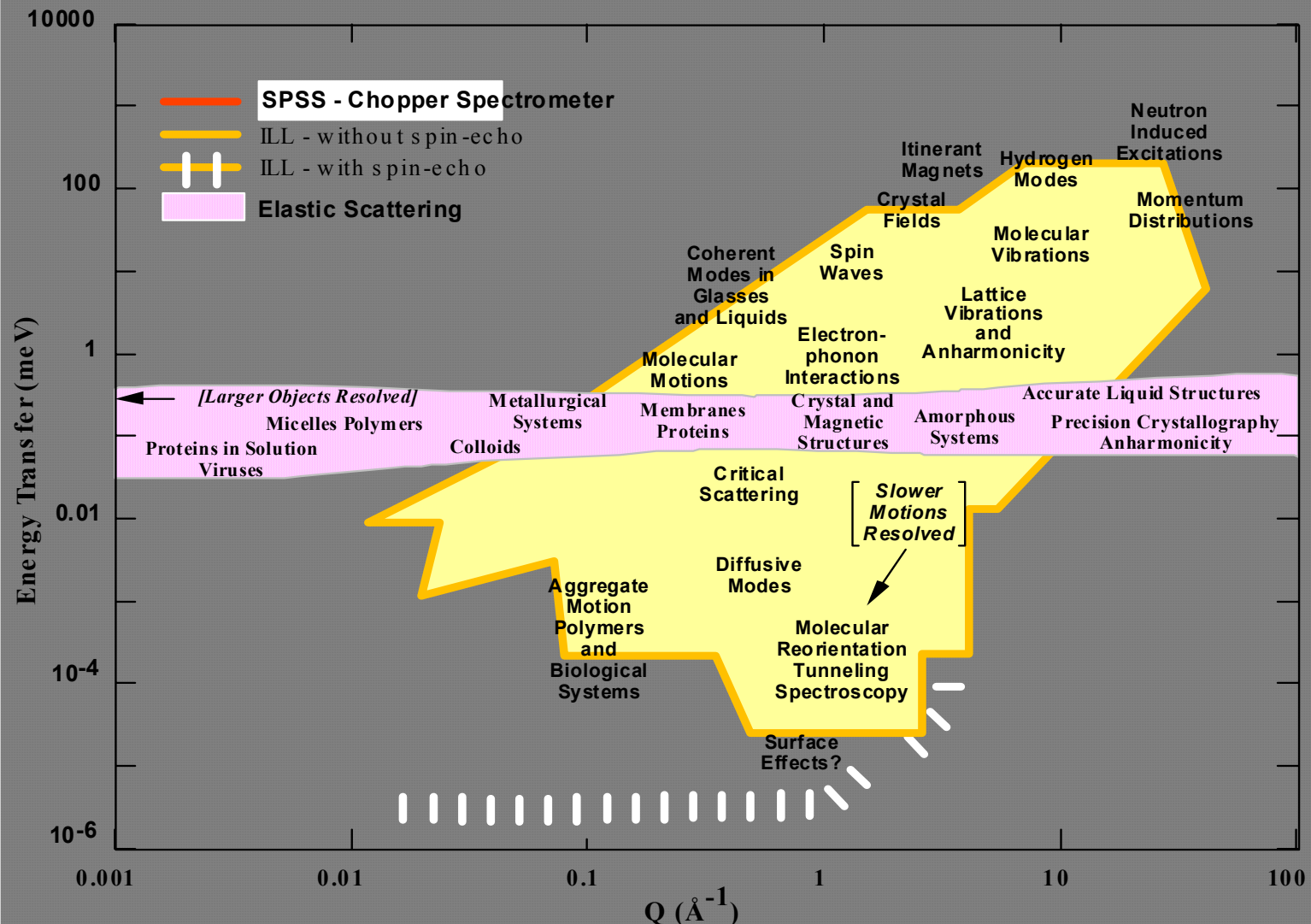
solenoid

- According to Ampere's law, a current distribution that varies as r^2 can correct the field-integral inhomogeneities for parallel paths
- Similar devices can be used to correct the integral along divergent paths



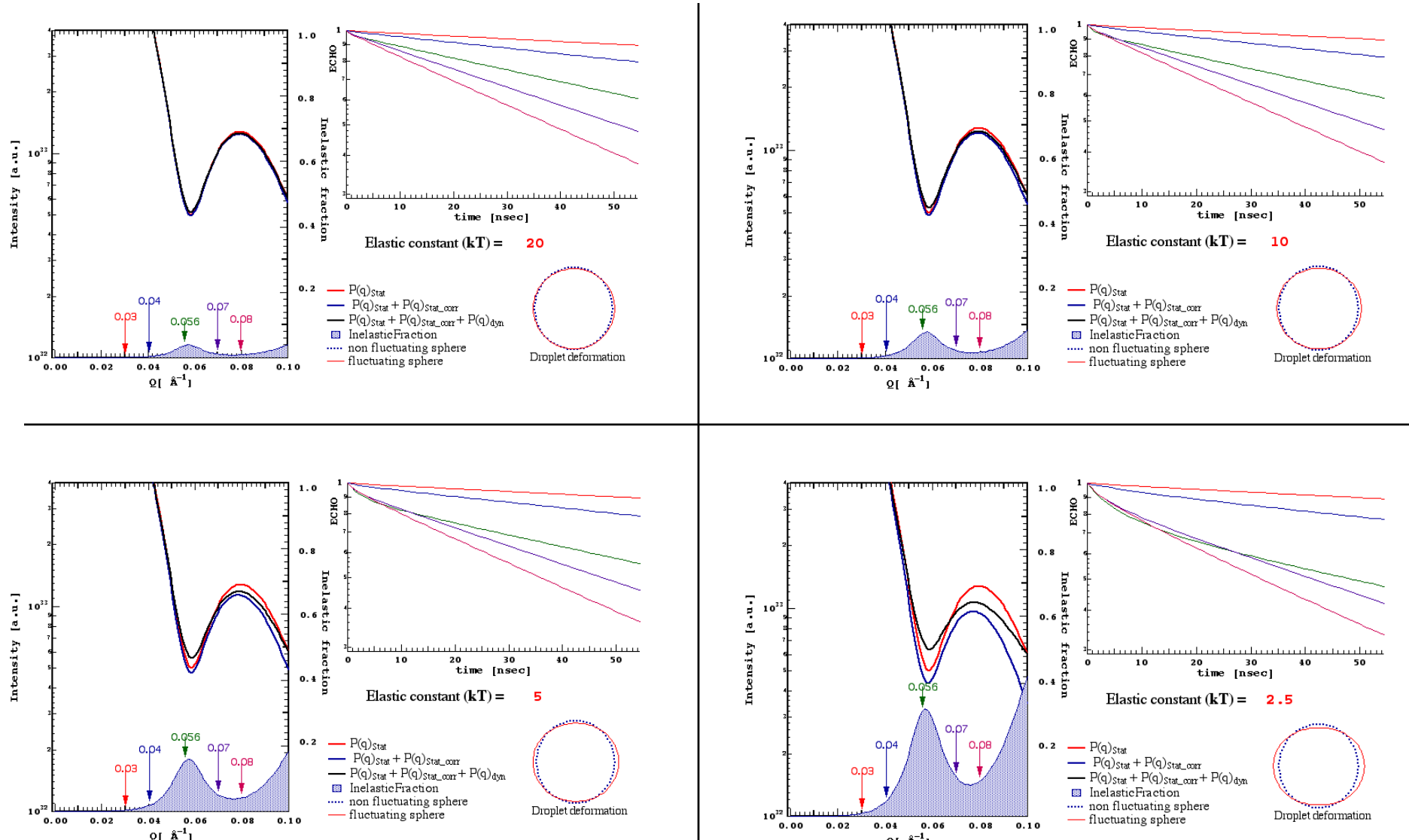
Fresnel correction coil for IN15

Neutrons in Condensed Matter Research



Neutron Spin Echo has significantly extended the (Q, E) range to which neutron scattering can be applied

Neutron Spin Echo study of Deformations of Spherical Droplets*

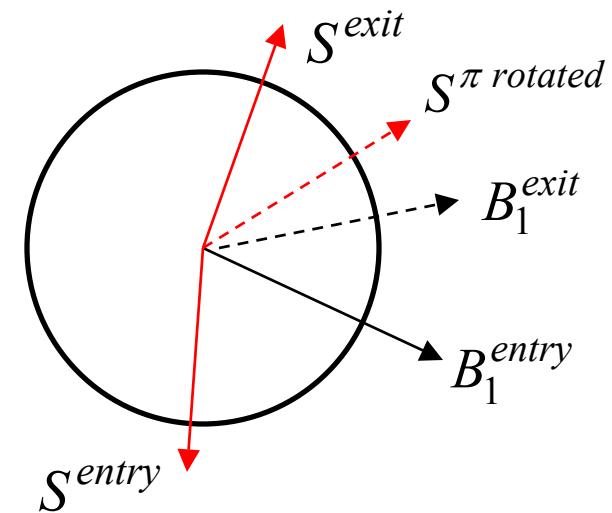
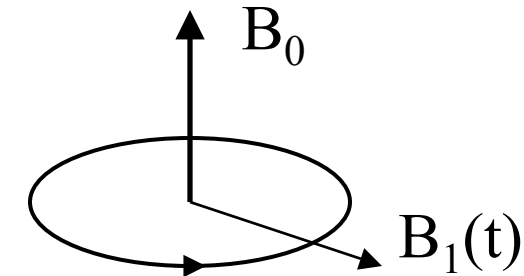


* Courtesy of B. Farago

The Principle of Neutron Resonant Spin Echo

- Within a coil, the neutron is subjected to a steady, strong field, B_0 , and a weak rf field $B_1 \cos(\omega t)$ with a frequency $\omega = \omega_0 = \gamma B_0$
 - Typically, $B_0 \sim 100$ G and $B_1 \sim 1$ G
- In a frame rotating with frequency ω_0 , the neutron spin sees a constant field of magnitude B_1
- The length of the coil region is chosen so that the neutron spin precesses around B_1 thru an angle π .
- The neutron precession phase is:

$$\begin{aligned}\phi_{neutron}^{exit} &= \phi_{RF}^{exit} + (\phi_{RF}^{entry} - \phi_{neutron}^{entry}) \\ &= 2\phi_{RF}^{entry} - \phi_{neutron}^{entry} + \omega_0 d / v\end{aligned}$$



Neutron Spin Phases in an NRSE Spectrometer*

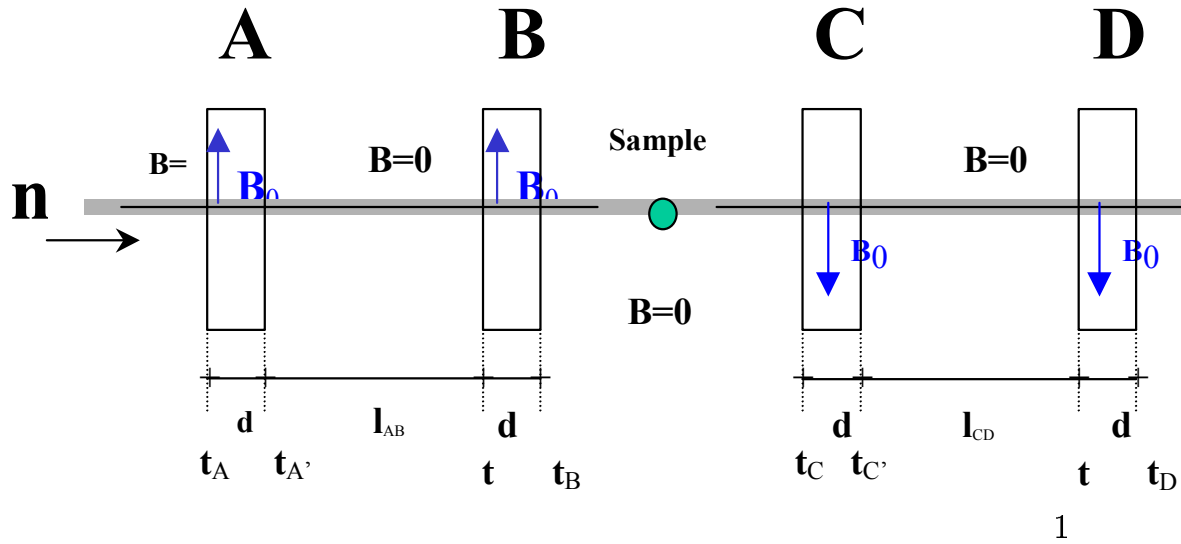
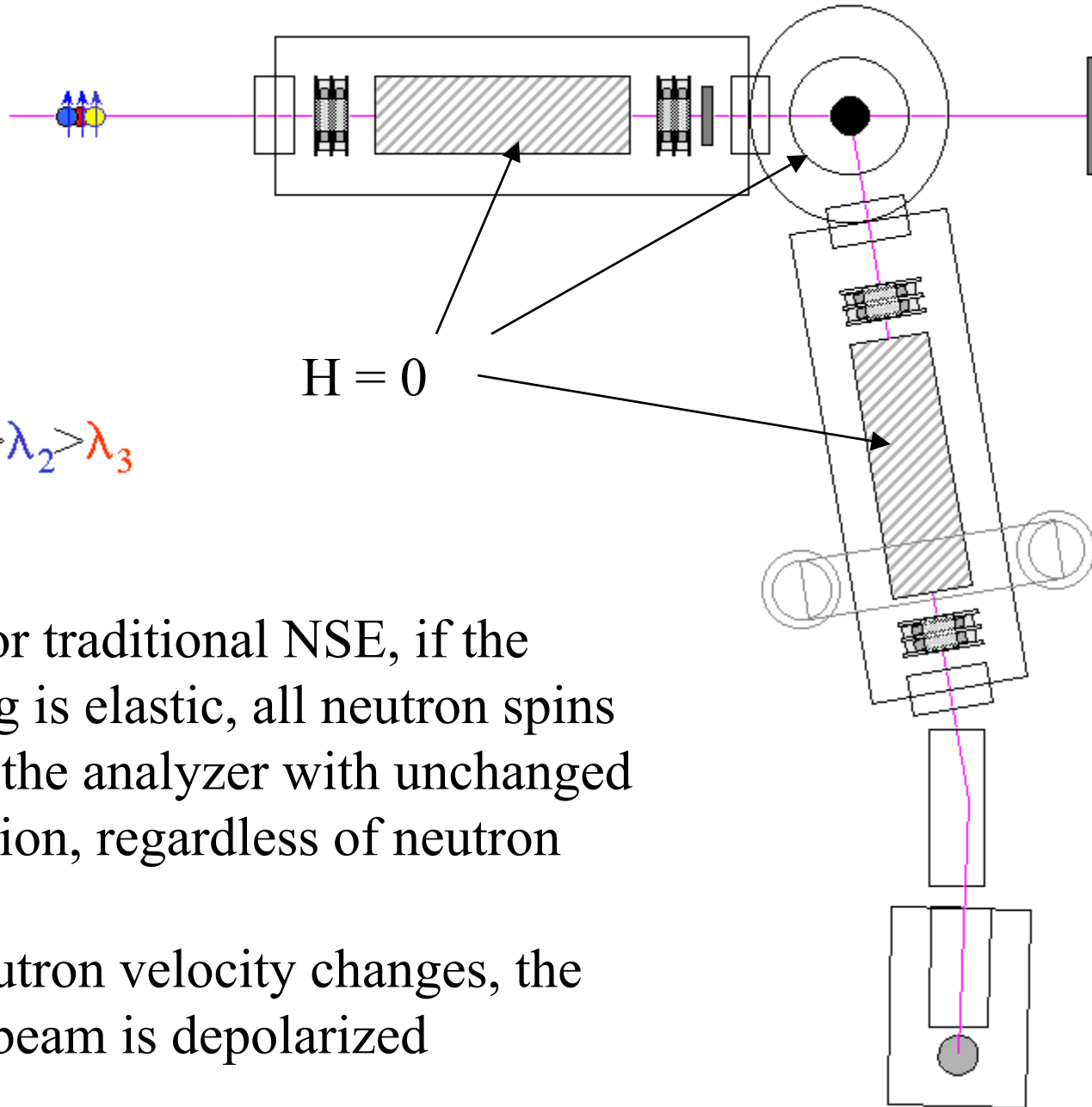


Table 1. Spin orientation

Time t	Phase field B_r	neutron Spin phase S
A t_A	ωt_A	0
A' $t_{A'} = t_A + \frac{d}{v}$	$\omega t_{A'}$	$2\omega t_A + \omega \frac{d}{v}$
B $t_B = t_A + \frac{l_{AB}+d}{v}$	ωt_B	$2\omega t_A + \omega \frac{d}{v}$
B' $t_{B'} = t_A + \frac{l_{AB}+2d}{v}$	$\omega t_{B'}$	$2\omega \frac{l_{AB}+d}{v}$
C t_C	$-\omega t_C$	$2\omega \frac{l_{AB}+d}{v}$
C' $t_{C'} = t_C + \frac{d}{v'}$	$-\omega t_{C'}$	$-\omega \frac{d}{v'} - 2\omega t_C - 2\omega \frac{l_{AB}+d}{v}$
D $t_D = t_C + \frac{l_{CD}+d}{v'}$	$-\omega t_D$	$-\omega \frac{d}{v'} - 2\omega t_C - 2\omega \frac{l_{AB}+d}{v}$
D' $t_{D'} = t_C + \frac{l_{CD}+2d}{v'}$	$-\omega t_{D'}$	$2\omega \left(\frac{l_{AB}+d}{v} - \frac{l_{CD}+d}{v'} \right)$

Echo occurs for elastic scattering when
 $l_{AB} + d = l_{CD} + d$

* Courtesy of S. Longeville



Just as for traditional NSE, if the scattering is elastic, all neutron spins arrive at the analyzer with unchanged polarization, regardless of neutron velocity.

If the neutron velocity changes, the neutron beam is depolarized

The Measured Polarization for NRSE is given by an Expression Similar to that for Classical NSE

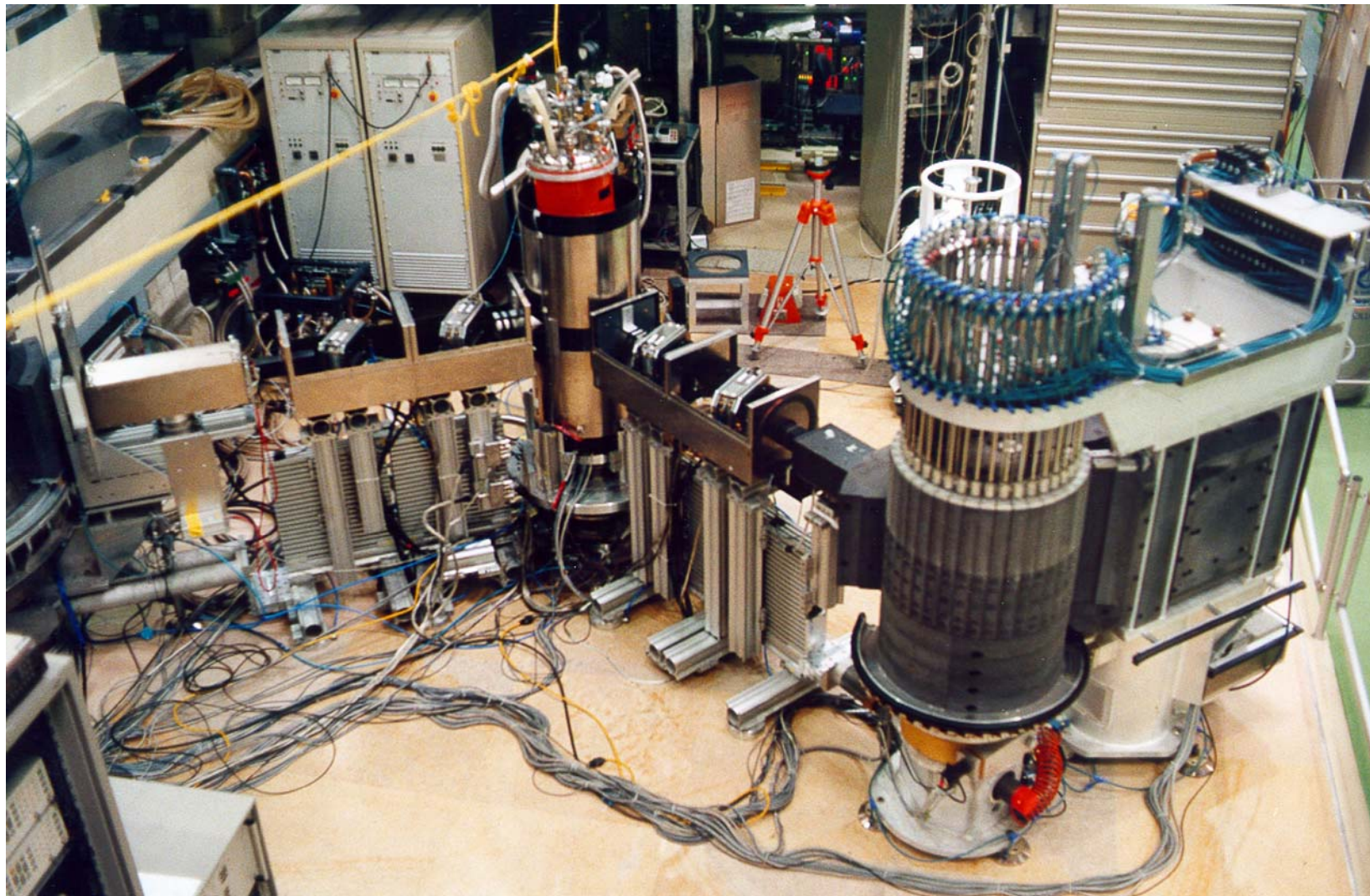
- Assume that $v' = v + \delta v$ with δv small and expand to lowest order, giving:

$$\langle P \rangle = \frac{\iint I(\lambda) S(\vec{Q}, \omega) \cos(\omega \tau_{NRSE}) d\lambda d\omega}{\iint I(\lambda) S(\vec{Q}, \omega) d\lambda d\omega}$$

where the "spin echo time" $\tau_{NRSE} = 2\gamma B_0(l + d) \frac{m^2}{2\pi h^2} \lambda^3$

- Note the additional factor of 2 in the echo time compared with classical NSE (a factor of 4 is obtained with “bootstrap” rf coils)
- The echo is obtained by varying the distance, l , between rf coils
- In NRSE, we measure neutron velocity using fixed “clocks” (the rf coils) whereas in NSE each neutron “carries its own clock” whose (Larmor) rate is set by the local magnetic field

An NRSE Triple Axis Spectrometer at HMI: Note the Tilted Coils



Measuring Line Shapes for Inelastic Scattering

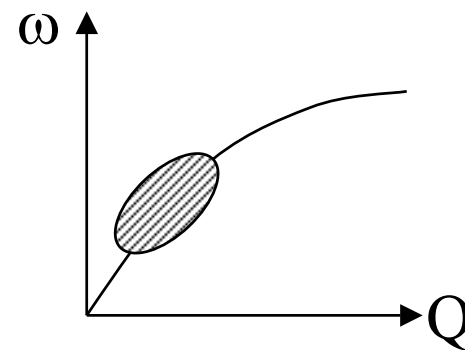
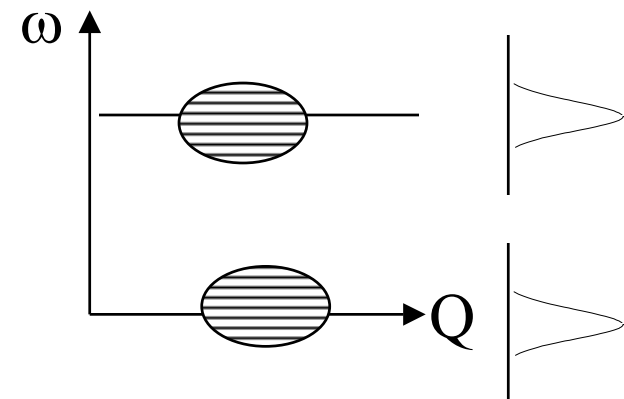
- Spin echo polarization is the FT of scattering within the spectrometer transmission function

- An echo is obtained when

$$\frac{d}{dk_1} \left[\frac{(Bd)_1}{k_1} - \frac{(Bd)_2}{k_2} \right] = 0 \Rightarrow \frac{N_1}{k_1^2} = \frac{N_2}{k_2^2}$$

- Normally the lines of constant spin-echo phase have no gradient in Q, ω space because the phase depends only on $|k|$

- The phase lines can be tilted by using “tilted” precession magnets



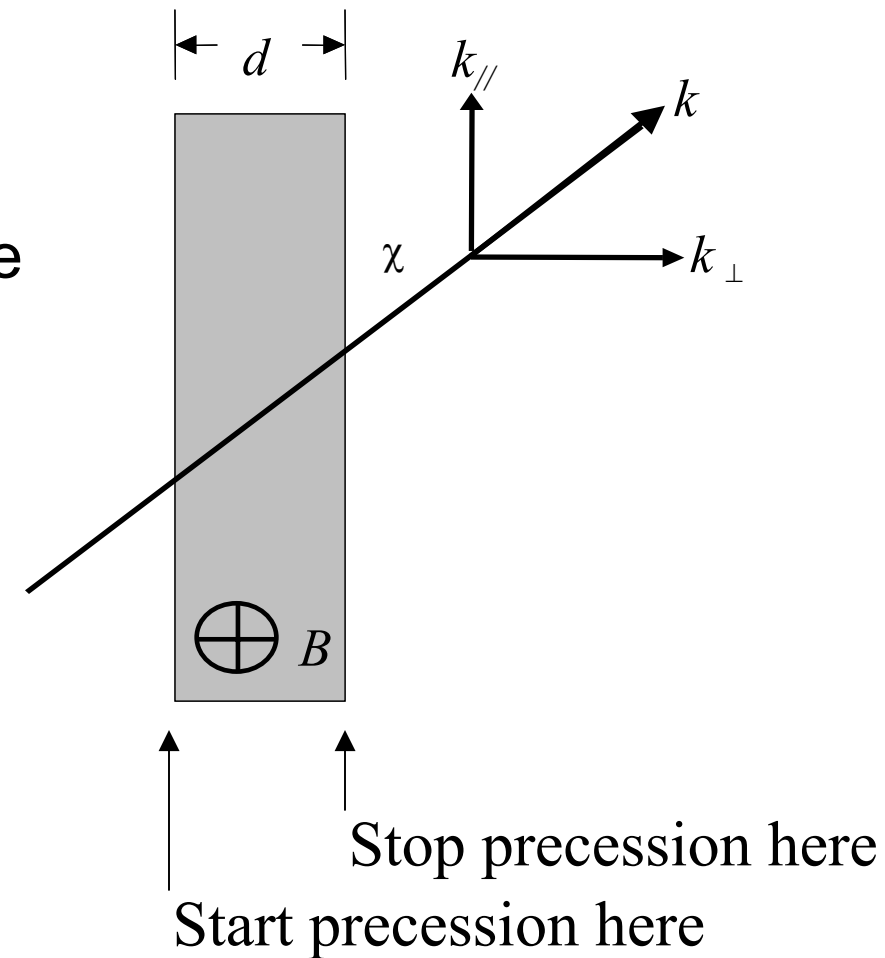
By “Tilting” the Precession-Field Region, Spin Precession Can Be Used to Code a Specific Component of the Neutron Wavevector

If a neutron passes through a rectangular field region at an angle, its total precession phase will depend only on k_{\perp} .

$$\omega_L = \gamma B$$

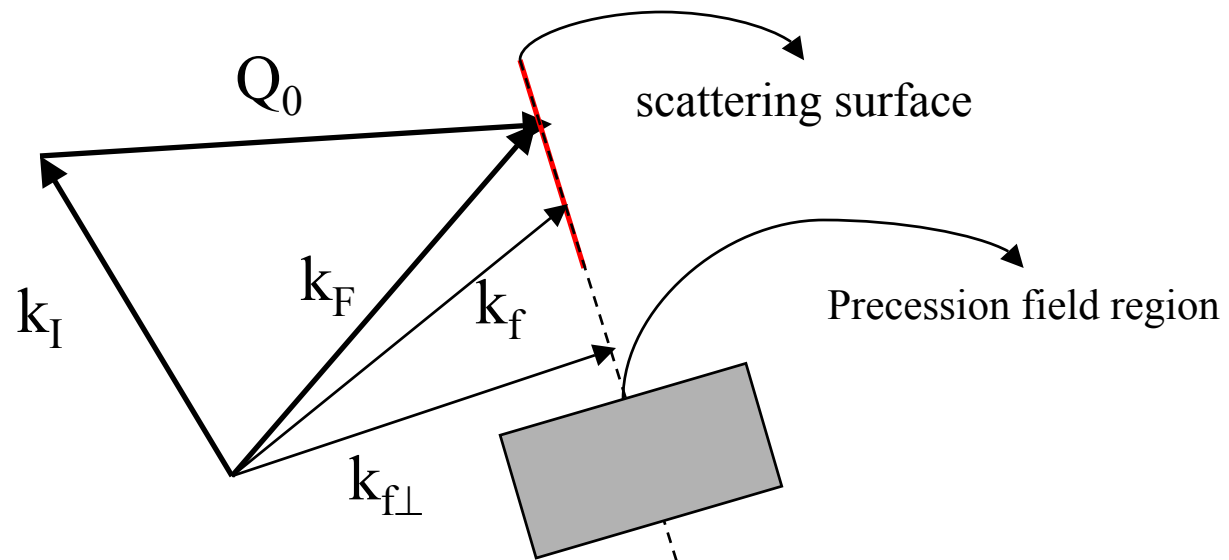
$$\phi = \omega_L t = \gamma B \frac{d}{v \sin \chi} = \frac{KBd}{k_{\perp}}$$

with $K = 0.291 \text{ (Gauss.cm.Å)}^{-1}$



“Phonon Focusing”

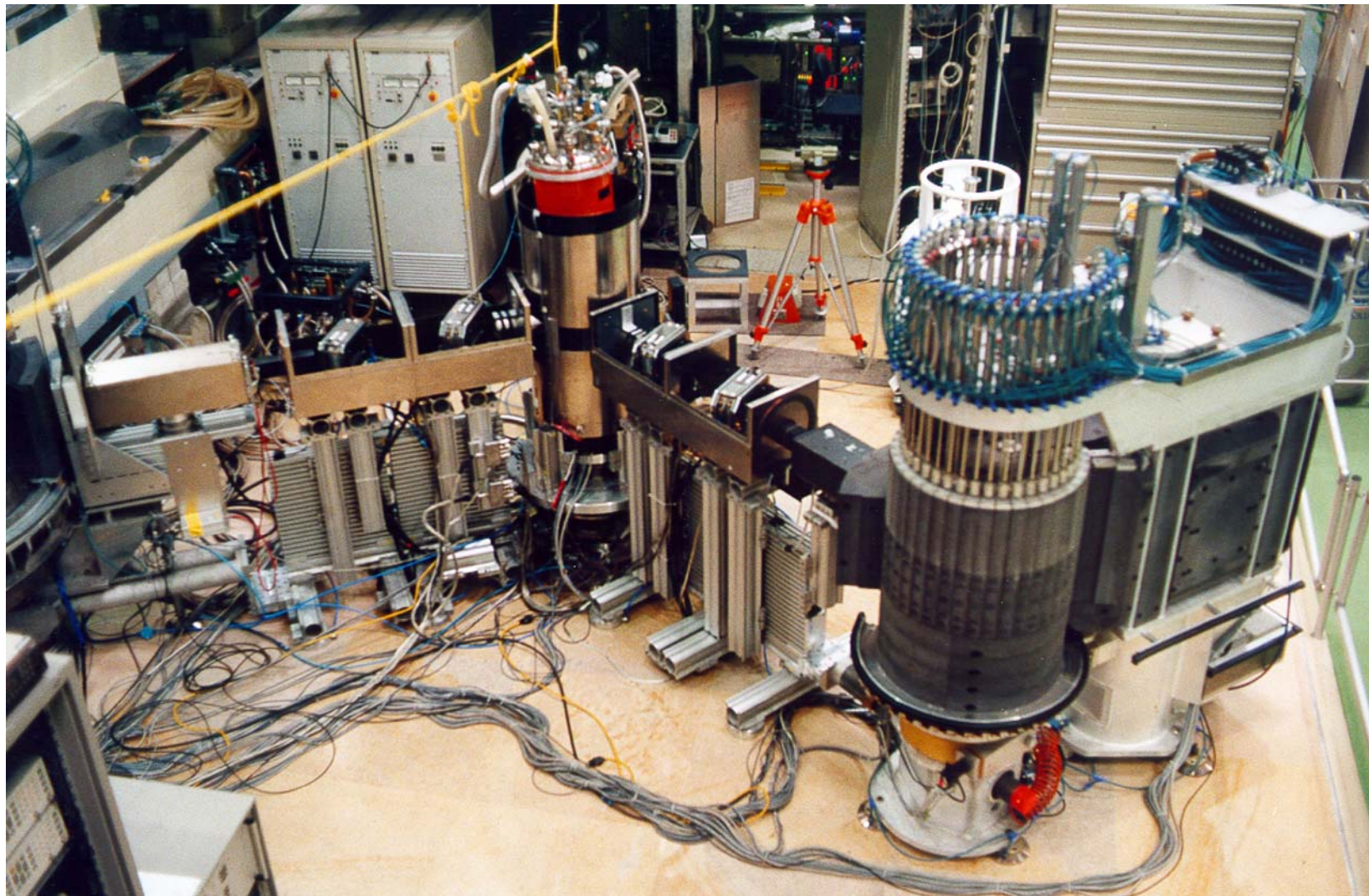
- For a single incident neutron wavevector, \mathbf{k}_I , neutrons are scattered to \mathbf{k}_F by a phonon of frequency ω_0 and to \mathbf{k}_f by neighboring phonons lying on the “scattering surface”.
 - The topology of the scattering surface is related to that of the phonon dispersion surface and it is locally flat
- Provided the edges of the NSE precession field region are parallel to the scattering surface, all neutrons with scattering wavevectors on the scattering surface will have equal spin-echo phase



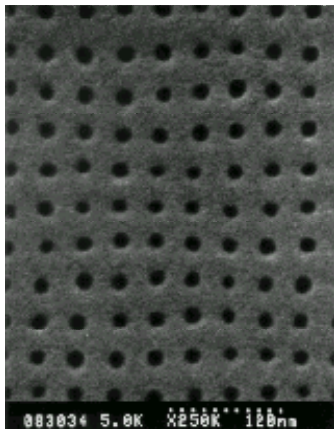
“Tilted Fields”

- Phonon focusing using tilted fields is available at ILL and in Japan (JAERI)....however,
- The technique is more easily implemented using the NRSE method and is installed as an option on a 3-axis spectrometers at HMI and at Munich
- Tilted fields can also be used can also be used for elastic scattering and may be used in future to:
 - Increase the length scale accessible to SANS
 - Separate diffuse scattering from specular scattering in reflectometry
 - Measure in-plane order in thin films
 - Improve Q resolution for diffraction

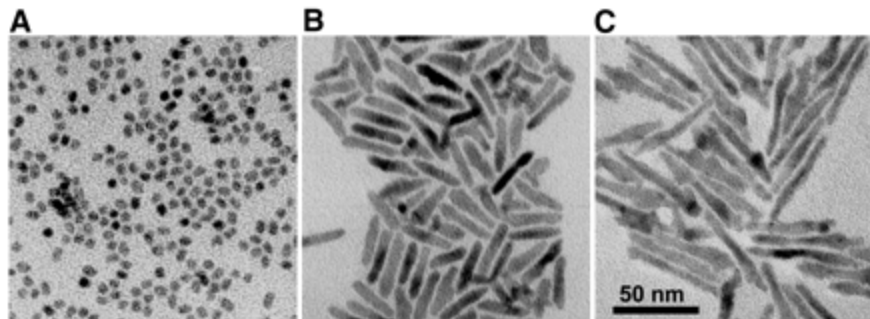
An NRSE Triple Axis Spectrometer at HMI: Note the Tilted Coils



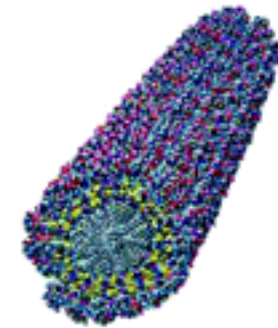
Nanoscience & Biology Need Structural Probes for 1-100 nm



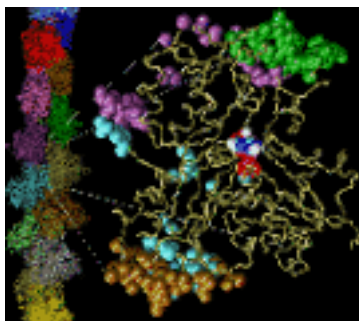
10 nm holes in PMMA



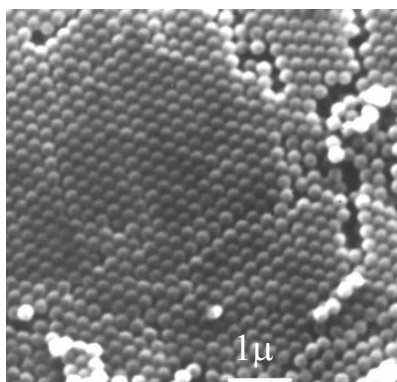
CdSe nanoparticles



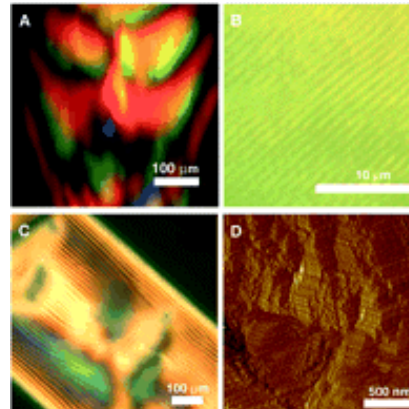
Peptide-amphiphile nanofiber



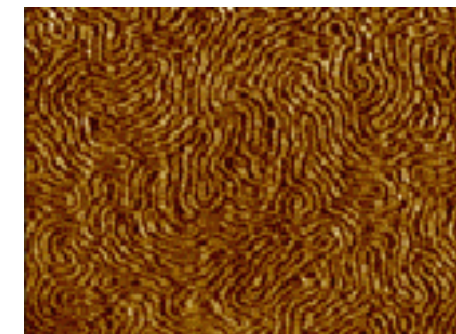
Actin



Si colloidal crystal

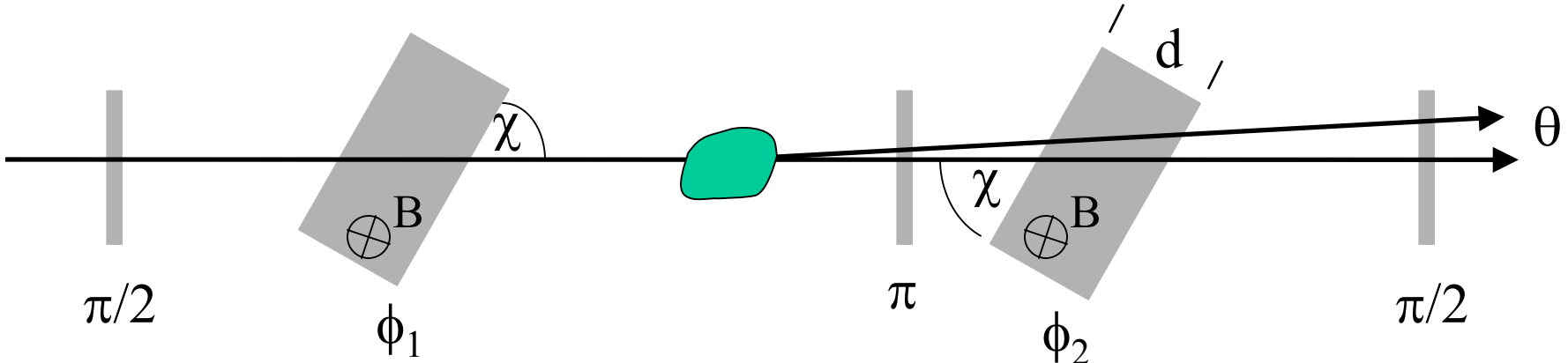


Structures over many length scales in self-assembly of ZnS and cloned viruses



Thin copolymer films

“Tilted” Fields for Diffraction: SANS



- Any unscattered neutron ($\theta=0$) experiences the same precession angles (ϕ_1 and ϕ_2) before and after scattering, whatever its angle of incidence
- Precession angles are different for scattered neutrons

$$\phi_1 = \frac{KBd}{k \sin \chi} \text{ and } \phi_2 = \frac{KBd}{k \sin(\chi + \theta)} \Rightarrow \cos(\phi_1 - \phi_2) \approx \cos\left[\frac{KBd \cos \chi}{k \sin^2 \chi} \theta\right]$$

$$P = \int dQ S(Q) \cdot \cos\left[\frac{KBd \cos \chi}{k^2 \sin^2 \chi} Q\right]$$

Polarization proportional to Fourier Transform of $S(Q)$

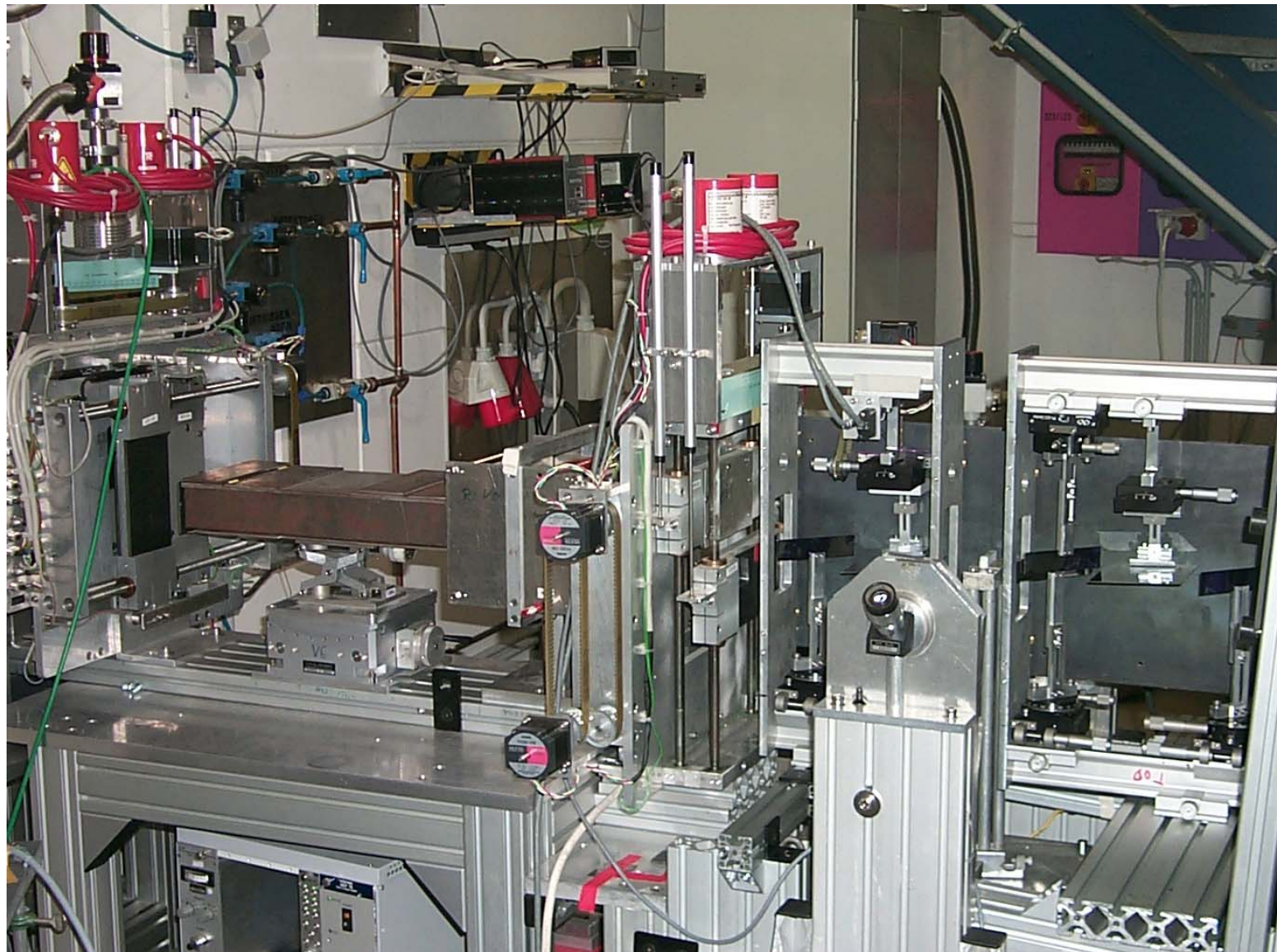
Spin Echo Length, $r = KBd \cos \chi / (k \sin \chi)^2$

How Large is the Spin Echo Length for SANS?

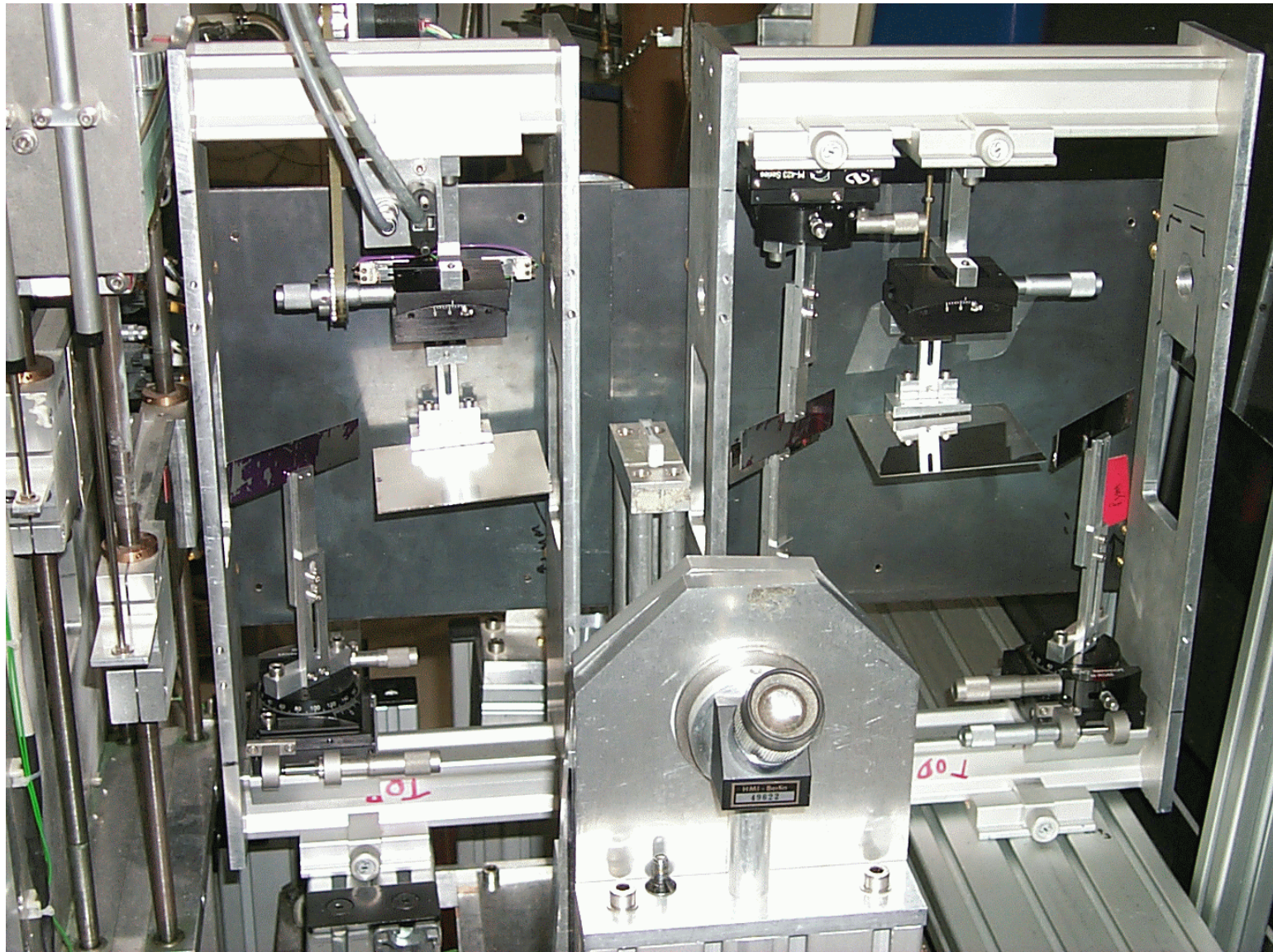
Bd/sin χ (Gauss.cm)	λ (Angstroms)	χ (degrees)	r (Angstroms)
3,000	4	20	1,000
5,000	4	20	1,500
5,000	6	20	3,500
5,000	6	10	7,500

It is relatively straightforward to probe length scales of ~ 1 micron

Spin Echo SANS using Magnetic Films: 200 nm Correlation Distance Measured



Close up of SESAME (Spin Echo Scattering Angle Measurement) Apparatus



Conclusion:

NSE Provides a Way to Separate Resolution from Monochromatization & Beam Divergence

- The method currently provides the best energy resolution for inelastic neutron scattering (\sim neV)
 - Both classical NSE and NRSE achieve similar energy resolution
 - NRSE is more easily adapted to “phonon focusing” I.e. measuring the energy line-widths of phonon excitations
- The method is likely to be used in future to improve (Q) resolution for elastic scattering
 - Extend size range for SANS (SESANS)
 - May allow 100 – 1000 x gain in measurement speed for some SANS exps
 - Separate specular and diffuse scattering in reflectometry
 - Measure in-plane ordering in thin films (SERGIS)